

PROCEEDINGS

PST  
BANGKOK 2019 THAILAND

# The International Conference and Exhibition on Pharmaceutical Sciences and Technology 2019

“Pharmaceutical Engineering and Pharmaceutical Sciences for Human Health”

18-19 June 2019 ■ The Ambassador Bangkok Hotel, Bangkok, Thailand

# PST

BANGKOK 2019 THAILAND

The International Conference and Exhibition on  
Pharmaceutical Sciences and Technology 2019  
“Pharmaceutical Engineering and Pharmaceutical Sciences for Human Health”

18-19 June 2019 ■ The Ambassador Bangkok Hotel, Bangkok, Thailand



# Committee

---

## International Advisory Board

Prof. Chomchin Chantaraskul TIPA, Thailand	Asst. Prof. Chaichan Thavaravej Silpakorn University, Thailand	Assoc. Prof. Tanasait Ngawhirunpat Silpakorn University, Thailand
Col. Isada Sirimontree TIPA, Thailand	Prof. Sompol Prakongpan AFPS/TIPA Thailand	Asst. Prof. Thanapat Songsak Rangsit University, Thailand
Ms. Sorada Wangmethukul TIPA, Thailand Official representative TPMA, Thailand Official representative TCEB, Thailand	Mr. Totsapon Santitewagun ISPE Thailand Prof. Pornsak Sriamornsak TIPA, Silpakorn University, Thailand Prof. Narong Sarisuta Thammasart University, Thailand	Asst. Prof. Wimon phuntuwate Srinakharinwirot University, Thailand Assoc. Prof. Chalerm Sri Pummangura Siam University, Thailand Asst. Prof. Wichan Janwitayanuchit Huachiew Chalermprakiet University, Thailand

## Organizing Committee

Assoc. Prof. Tanasait Ngawhirunpat <i>Chairman</i> Silpakorn University, Thailand	Asst. Prof. Surasit Lochid-amnuay <i>Venue</i> Silpakorn University, Thailand	Dr. Purin Charoensuksai <i>Hospitality/Social function</i> Silpakorn University, Thailand
Assoc. Prof. Suchada Piriyaprasarth <i>Scientific</i> Silpakorn University, Thailand	Dr. Sineenart Krichanchai <i>Venue/Registration</i> Silpakorn University, Thailand	Assoc. Prof. Narisa Kamkaen <i>Hospitality/Social function</i> Rangsit University, Thailand
Assoc. Prof. Sontaya Limmatvapirat <i>Scientific</i> Silpakorn University, Thailand	Ms. Pattana Mangjak <i>Finance</i> TIPA, Thailand	Dr. Prasopchai Patrojanasophon <i>Secretariat/Sponsor contact</i> Silpakorn University, Thailand
Asst. Prof. Perayot Pamonsinlapham <i>Registration</i> Silpakorn University, Thailand	Mr. Chaisan Sriwichupong <i>Finance</i> TIPA, Thailand	Dr. Pawaris Wongprayoon <i>Assistant Secretariat</i> Silpakorn University, Thailand

# Committee (continued)

---

## Scientific Committee

Prof. Mont Kumpugdee-Vollrath  
Beuth Hochschule für Technik Berlin,  
Germany  
Prof. Kunikazu Moribe  
Chiba University,  
Japan  
Prof. Vitaliy Khutoryanskiy  
University of Reading,  
United Kingdom  
Prof. Young-Joon Surh  
Seoul National University,  
South Korea  
Prof. Mao Shirui  
Shenyang Pharmaceutical University,  
China  
Prof. Pornanong Aramwit  
Chulalongkorn University,  
Thailand  
Prof. Praneet Opanasopit  
Silpakorn University,  
Thailand  
Assoc. Prof. Theerasak Rojanarata  
Silpakorn University,  
Thailand

Prof. Pawinee Piyachaturawat  
Mahidol University,  
Thailand  
Prof. Varaporn Junyaprasert  
Mahidol University,  
Thailand  
Prof. Waraporn Putalun  
Khon Kaen University,  
Thailand  
Prof. Thaned Pongjanyakul  
Khon Kaen University,  
Thailand  
Assoc. Prof. Rakesh K. Sindhu  
Chitkara University,  
India  
Prof. Leena Suntornsuk  
Mahidol University,  
Thailand  
Dr. Nawinda Chinatangkul  
Siam University,  
Thailand  
Dr. Parapat Sobharaksha  
Huachiew Chalermprakiet  
University,  
Thailand

Assoc. Prof. Prasert akkaramongkolporn  
Silpakorn University,  
Thailand  
Assoc. Prof. Penpun Wetwitayaklung  
Silpakorn University,  
Thailand  
Asst. Prof. Sathaporn Nimkulrat  
Mahidol University,  
Thailand  
Asst. Prof. Jirapornchai Sokseree  
Rangsit University,  
Thailand  
Dr. Duangratana Shuwisitkul  
Srinakharinwirot University,  
Thailand  
Dr. Prasopchai Patrojanasophon  
Silpakorn University,  
Thailand  
Assoc. Prof. Suchada Piriyaprasarth  
Silpakorn University,  
Thailand  
Assoc. Prof. Sontaya Limmatvapirat  
Silpakorn University,  
Thailand

# Solubility enhancement, solution and solid-state characterization of asiaticoside/sulfobutyl-ether- $\beta$ -cyclodextrin

Hay Man Saung Hnin Soe<sup>1,a</sup>, and Phatsawee Jansook<sup>1,b\*</sup>

<sup>1</sup>Department of Pharmaceutics and Industrial Pharmacy,  
Faculty of Pharmaceutical Sciences, Chulalongkorn University, Thailand

<sup>a</sup>haymansaunghninsoe@gmail.com, <sup>b</sup>phatsawee.j@chula.ac.th

**Keywords:** asiaticoside, cyclodextrin, solubility, characterization

**Abstract.** Asiaticoside (AS) is triterpenoid glycoside, which is one of the four major constituents of *Centella asiatica*. It has been attracted much for its significant wound healing activity but its application was limited due to its poor solubility. Hence, the aim of the study was to improve AS solubility via complexation with  $\beta$ -cyclodextrin ( $\beta$ CD) and its derivatives i.e., carboxy-methyl- $\beta$ -cyclodextrin (CM $\beta$ CD) and sulfobutyl-ether- $\beta$ -cyclodextrin (SBE $\beta$ CD). The complexation in solution-state was evaluated by phase-solubility technique and <sup>1</sup>H nuclear magnetic resonance (<sup>1</sup>HNMR). The enhanced solubility was obtained with linear (A<sub>L</sub>) type phase solubility profile with all CDs tested which represented 1:1 stoichiometry inclusion complex. SBE $\beta$ CD exhibited the better complexation efficiency for AS than CM $\beta$ CD and selected for further studies whereas  $\beta$ CD was excluded because of its limited aqueous solubility. The mode of inclusion was supported by <sup>1</sup>H-NMR and indicated that true inclusion complex was formed between AS and SBE $\beta$ CD. The solid AS/SBE $\beta$ CD complex was prepared by freeze-drying (FD) method and formation of complexation was determined by solid-state characterizations that were Fourier transform infra-red spectroscopy (FT-IR) and powder X-ray diffraction (PXRD) techniques. FT-IR showed the presence of interaction in the complex whereas PXRD revealed that binary complex was in amorphous state and/or presence of inclusion AS/SBE $\beta$ CD complex. Thus, the formation of AS/SBE $\beta$ CD complex could be beneficial to enhance the solubilization of AS.

## Introduction

*Centella asiatica*, also known as Indian pennywort is perennial creeping herb, which is plenty in many Asian countries and also has common name as ‘Buabok’ in Thailand. It has been reported that the plant extract contains major pentacyclic triterpene derivatives such as madecassoside, madecassic acid, asiaticoside (AS), and asiatic acid [1]. One of the main components of the plant named AS is well known in modulating the inflammatory response by inhibiting nitric oxide and tumor necrosis factor- $\alpha$  secretion from macrophages [2]. AS has also been shown to enhance periodontal tissue healing and promote osteogenic differentiations in human periodontal ligament cells [3]. These properties of AS suggested that it could be useful in the treatment of periodontal wound healing. However, AS has low aqueous solubility (0.67 mg/ml) and it may hamper the bioavailability. The most popular approach to improve the solubility of water-insoluble drug is the complexation with cyclodextrins (CDs). CDs represent the family of cyclic oligosaccharides and parent cyclodextrins are known as  $\alpha$ ,  $\beta$ ,  $\gamma$ -CD which consist of 6,7,8 glucopyranose units, respectively [4]. The main interest possesses cone-shape with outer hydrophilic surface and inner lipophilic cavity. Its characteristic structure can modulate the lipophilic moiety of the drug to increase the aqueous solubility [5]. Since the natural CDs have rather limited aqueous solubility, CD derivatives were modified [6]. Of these, SBE $\beta$ CD is polyanionic  $\beta$ CD derivative with average degree of substitutions of seven. It has much higher aqueous solubility and ability to enhance the solubility of lipophilic drugs [7].

Hence, the present work was conducted to observe the solubility enhancement as well as the formation of binary system and mode of interaction of complexes by nuclear magnetic resonance (NMR) spectroscopy. Besides, solid binary complex was prepared by freeze-drying method and was examined by Fourier transform infra-red spectroscopy (FT-IR) and powder X-ray diffractometry.

## Materials and methods

### Materials

Asiaticoside (AS) was purchased from Xi'an Haoxuan Bio-Tech Co., Ltd (Xi'an, China).  $\beta$ -cyclodextrin ( $\beta$ CD), and carboxy methyl  $\beta$ -cyclodextrin (CM $\beta$ CD) from Wacker Chemie (Germany), sulfobutylether- $\beta$ -cyclodextrin MS 0.9 (SBE $\beta$ CD) (MW 2163 Da) from Roquette (France). All other chemicals used were of analytical reagent grade purity. Milli-Q (Millipore, Billerica, MA, USA) water was used for the preparation of all solutions.

### Methods

#### 1. Solubility determination

The solubility of AS was determined by heating method. An excess amount of drug was added in aqueous solutions containing  $\beta$ CD (0-1.5% w/v), CM $\beta$ CD and SBE $\beta$ CD (0-10% w/v). The drug suspensions were placed in sealed vials and heated in ultrasonic bath at 60°C for 30 min and allowed to cool to room temperature. The suspensions were equilibrated for 5-7 days at room temperature under constant agitation. After equilibrium was reached, the suspensions were filtered through 0.45 $\mu$ m nylon filter, the filtrate was diluted with methanol:water (70:30 v/v) and analyzed by HPLC. The phase-solubility diagrams were constructed by plotting the total dissolved AS concentration (M) against CD concentrations (M).

#### 2. Quantitative analysis

Quantitative determination of AS was performed on a reversed-phase HPLC component system from Agilent 1260 Infinity II consisting of Liquid chromatography pump (quaternary pump, G7111A), UV-VIS detector (G7115A), auto sampler (G7129A) with Chem Station software, and Shiseido<sup>TM</sup> Capcell Pack C18 MG II S-5, C18, 250x4.5 mm ID with C18 guard cartridge column MGII 5 $\mu$ m, 4x10 mm. The HPLC condition was as follows; mobile phase: acetonitrile: water (28:72 v/v); flow rate: 0.9 ml/min; oven temperature: ambient; UV detector wavelength: 220 nm; injection volume: 20  $\mu$ L; and run time: 15 minutes. The HPLC method was compiled to the method validation which showed system suitability, precision and accuracy.

#### 3. Preparation and characterization of the binary complexes

##### 3.1 Solution-state characterization (<sup>1</sup>H-NMR)

The pure solid samples of AS, SBE $\beta$ CD as well as AS/SBE $\beta$ CD complexes were dissolved in 10% v/v D<sub>2</sub>O in DMSO-d<sub>6</sub>. <sup>1</sup>H-NMR spectroscopy measurements were performed using a 500 MHz <sup>1</sup>H-NMR spectrometer (BRUKER model AVANCE III HD, USA). The spectrum and chemical shift values were recorded. <sup>1</sup>H-NMR chemical shifts were referred to DMSO-d<sub>6</sub> (2.50 ppm) as internal standard and calculated according to the formula:  $\Delta\delta^* = \delta(\text{complex}) - \delta(\text{free})$ .

## 3.2 Solid-state characterization

### Sample preparations

Aqueous solutions containing binary AS/SBE $\beta$ CD (1:1 molar ratio) complex was prepared by heating in an ultrasonic bath at 60°C for 30 min. The samples were equilibrated at 30 $\pm$ 1°C for 7 days under constant agitation. After centrifugation (Thermo Fisher Scientific, MA, USA) at 13000 rpm for 20 min, the supernatant was withdrawn, frozen at -80°C for 2 hr and then lyophilized at -52°C for 48 hr in a freeze-dryer (Labconco Lyophilizer, MO, USA), yielding a solid complex powder (FD). Identical physical mixture (PM) was prepared by careful blending of AS/SBE $\beta$ CD in a mortar with pestle. The samples were characterized in solid-state as follows: pure AS, SBE $\beta$ CD, PM and FD of binary AS/SBE $\beta$ CD complexes.

#### 3.2.1 Powder X-ray diffraction (PXRD) studies

The PXRD patterns were recorded using Powder X-ray diffractometer (Rigaku model MiniFlex II, Japan) and operated at a voltage of 30 kV and a current of 15 mA. The samples were analyzed as the 2 $\theta$  angle range of 3°–40° and process parameters were set as follows: step size of 0.020° (2 $\theta$ ) and scan speed of 2° per minute.

#### 3.2.2 Fourier transform infra-red (FT-IR) spectroscopy

The samples were measured in a FT-IR spectrometer (Thermo Scientific model Nicolet iS10, USA) using Attenuated Total Reflectance (ATR) technique. The data was obtained in the range of 400–4500 cm<sup>-1</sup>. The analyses were performed at room temperature.

## Result and discussion

### 1. Solubility determinations

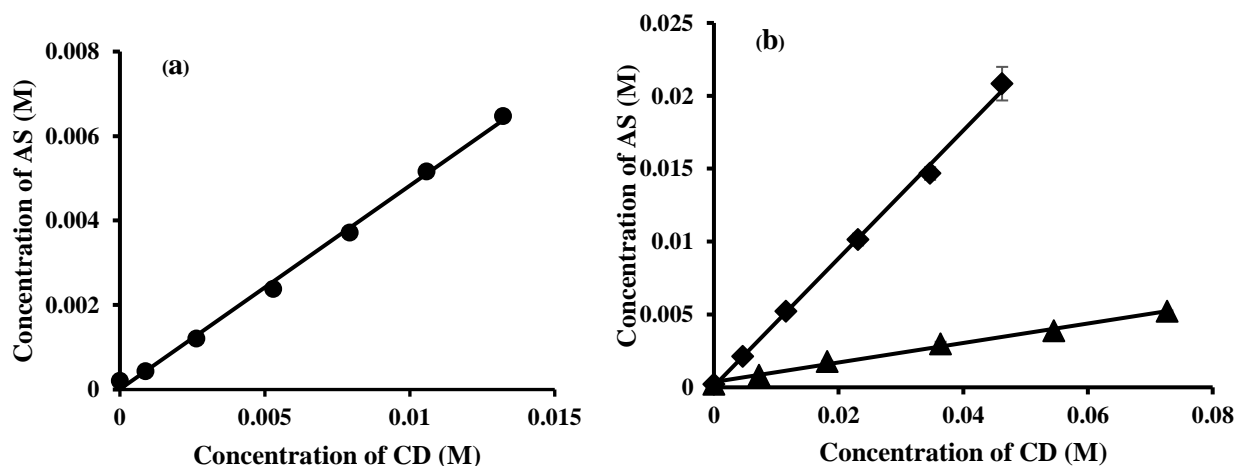


**Fig. 1** Phase-solubility profiles of asiaticoside in aqueous CD solutions (a)  $\beta$ CD, (b) SBE $\beta$ CD ( $\blacklozenge$ ) and CM $\beta$ CD ( $\blacktriangle$ )

Figure 1a and 1b displayed the phase-solubility diagrams of AS in aqueous CD solutions i.e.,  $\beta$ CD, SBE $\beta$ CD, and CM $\beta$ CD. All of the phase-solubility profiles represented the A<sub>L</sub>-type according to Higuchi and Connors (1965) [8]. The solubility of AS increased linearly as the concentration of CD increased, indicating that 1:1 AS:CD complex was formed. The apparent stability constant ( $K_{1:1}$ ) and complexation efficiency (CE) were calculated from slope of the phase-solubility diagram and shown in Table 1. The highest CE was obtained with  $\beta$ CD followed by SBE $\beta$ CD in complexing medium. It was suggested that neutral CD has the higher affinity to complex with AS while the negatively charged CDs (i.e., SBE $\beta$ CD and CM $\beta$ CD)

have relatively lower CE. This may be due to the position of charged groups which were located on or around the CDs cavity and causing the changes in hydrophobicity of inner cavity as well as geometry of inclusion complexation [9]. In comparison of charged CDs, SBE $\beta$ CD has greater binding capacity which may be due to that the significant separation of charged sulfonate moiety from the CD cavity and butyl moiety also act as supplementary binding site for substrates [10]. Owing to the limited aqueous solubility of  $\beta$ CD, it was excluded for further studies. SBE $\beta$ CD was selected for complex formation with AS and was then characterized in solution and solid-state.

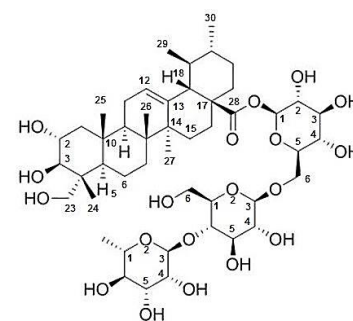
**Table 1.** The values of the apparent stability constant ( $K_{1:1}$ ) and the complexation efficacy (CE) of AS/CD complexes in pure aqueous CD solutions at  $30\pm 1^\circ\text{C}$ .

Cyclodextrin	Type	$K_{1:1}$ ( $\text{M}^{-1}$ )	CE
$\beta$ CD	AL	$3.84 \times 10^3$	0.94
CM $\beta$ CD	AL	$2.95 \times 10^2$	0.07
SBE $\beta$ CD	AL	$3.19 \times 10^3$	0.78

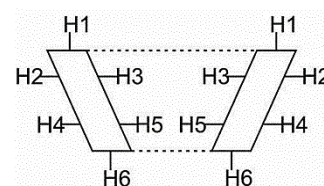
## 2. Solution-state characterization ( $^1\text{H}$ -NMR)

**Table 2.** The  $^1\text{H}$ -chemical shifts of AS alone and in the presence of SBE $\beta$ CD

$^1\text{H}$		$\delta_{\text{free}}$	$\delta_{\text{complex}}$	$\Delta\delta^* = (\delta_{\text{complex}} - \delta_{\text{free}})$
<i>AS</i>	H-12	5.264	5.219	- 0.045
	H-1	5.174	5.125	- 0.049
	CH3-18	2.050	2.043	- 0.007
	CH3-27	1.151	1.066	- 0.085
	CH3-25	0.931	0.854	- 0.077
	CH3-29	0.854	0.752	- 0.102
	CH3-24	0.656	0.598	- 0.058
	Rha-5	3.898	3.864	- 0.034
<i>SBE<math>\beta</math>CD</i>	H-1	4.880	4.858	- 0.022
	H-2	3.400	3.368	- 0.032
	H-3	3.784	3.822	+0.038
	H-4	3.286	-*	-*
	H-5	3.611	3.531	- 0.080
	H-6	3.674	3.684	+0.010
	(CH <sub>2</sub> ) <sub>4</sub> SO <sub>3</sub> -	2.733	2.744	+0.011
	(CH <sub>2</sub> ) <sub>4</sub> SO <sub>3</sub> -	1.583	1.591	+0.008



asiaticoside



cyclodextrin

\*overlapping of chemical shifts

The information brought about by  $^1\text{H}$ -NMR spectroscopy could be used to establish the inclusion modes of AS/SBE $\beta$ CD complex. Herein, the chemical shifts of protons in AS/SBE $\beta$ CD were shown in Table 2. It is well-known that H-3 and H-5 protons of CDs are located in the inner cavity of CDs and prominent chemical shifts of H-3 and H-5 are major factors for possible complex formations of drug and CDs [11]. For binary complexes of AS/SBE $\beta$ CD, downfield shift of H-3 and upfield shift of H-5 in AS/SBE $\beta$ CD were +0.038 and -0.080 ppm, respectively. According to the literature, in case of  $\Delta\delta^*$  values of H-5 of CDs were higher than that of H-3, it indicated that totally inclusion complex of drug was formed in CD



cavities. From the results suggested that AS embedded to SBE $\beta$ CD cavity deeper and exhibited the stable inclusion complex formation. In comparison of proton shift of AS molecules in binary complex, CH<sub>3</sub>-24 CH<sub>3</sub>-25 CH<sub>3</sub>-27 and CH<sub>3</sub>-29 proton of AS were significantly upfield shifted. Panichpakdee and Supaphol (2011) [12] reported the <sup>1</sup>H-NMR of AS complexation with HP $\beta$ CD and revealed that the cyclohexane ring of AS containing active binding sites (lipophilic moiety of AS molecule) was well fitted into the inner cavity of HP $\beta$ CD while the glucose moieties were outside the CD cavity. In this present study, the most chemical shift of CH<sub>3</sub>-29 was observed in AS/SBE $\beta$ CD complex. This evidence emphasized that AS molecule was almost totally included into SBE $\beta$ CD cavity.

### 3. Solid-state characterization

#### 3.1 Fourier transform infra-red (FT-IR) spectroscopy

FT-IR spectroscopy is the widely used technique to determine the interaction between CDs and guest molecules in solid state and the complexation of guest molecules can be observed from changes or shifts in absorption spectrums. Fig. 3 shows the FT-IR spectra of pure AS, SBE $\beta$ CD and their binary PM and FD samples. The FT-IR spectrum of pure AS displayed the typical absorption bands of C=C stretching vibration at 1027.49 cm<sup>-1</sup>, C-O-C stretching at 1448.60 cm<sup>-1</sup>, C-C stretching at 1734.22 cm<sup>-1</sup>, C-H stretching at 2905.64 cm<sup>-1</sup> and broad peak of O-H stretching at 3355.71 cm<sup>-1</sup> (Fig. 3a) [13]. The FT-IR spectrum of AS in PM indicated that there was less interaction of AS and SBE $\beta$ CD and only simple superimposition of individual components (Fig. 3c). In FD of AS/SBE $\beta$ CD, the prominent characteristic peaks of AS i.e., C=C, C-H, and O-H stretching were shifted to 1078.95, 2921.75, 3373.48 cm<sup>-1</sup> respectively (Fig. 3d). These results served to confirm the presence of interactions between the AS and SBE $\beta$ CD binary complexation.

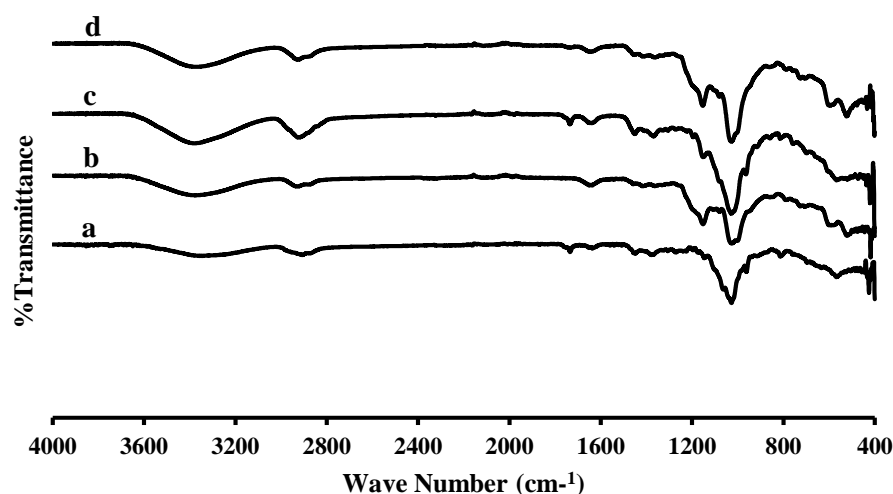


**Fig. 3** FTIR spectra of (a) pure AS, (b) pure SBE $\beta$ CD, (c) PM AS/SBE $\beta$ CD, (d) FD AS/SBE $\beta$ CD

### 3.2 Powder X-ray diffraction (PXRD)

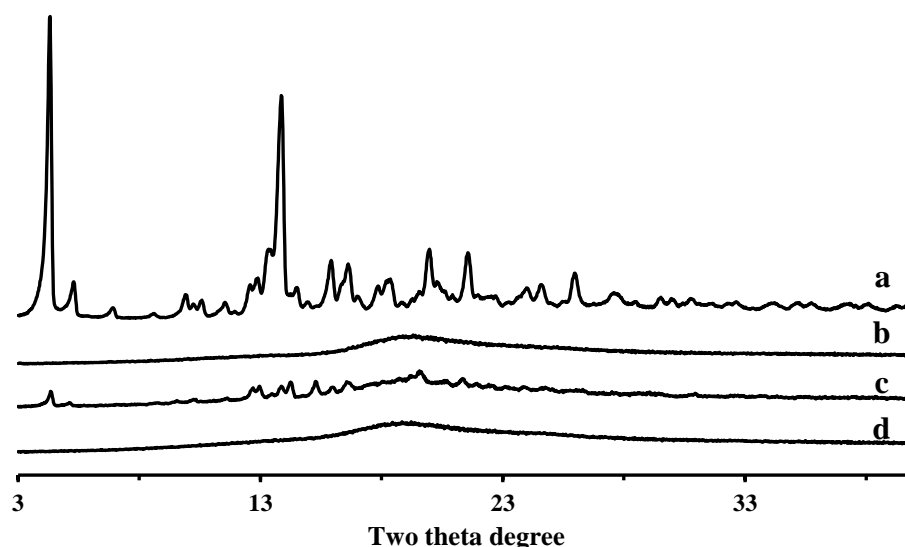


**Fig. 4** PXRD spectra of (a) pure AS, (b) pure SBE $\beta$ CD, (c) PM AS/SBE $\beta$ CD, (d) FD AS/SBE $\beta$ CD

PXRD is the powerful method to detect CD complexation of compound in powder or crystalline state. Figure 4 depicted the diffraction patterns of intact, PM and FD of AS/SBE $\beta$ CD. The X-ray spectrum of AS represented the numerous sharp diffractions indicating the high degree of crystallinity (Fig. 4a). For SBE $\beta$ CD, the diffractogram did not show any sharp peak and only halo pattern was obtained because of practically amorphous material (Fig. 4b) [14]. Simple overlapping of native patterns was observed in PM AS/SBE $\beta$ CD and the sharp crystalline peaks of AS were still be existed (Fig. 4c). In case of FD sample of binary complexes, the corresponding AS peaks were completely disappeared (Fig. 4d). It was suggested that AS was in amorphous state or formed binary complex with SBE $\beta$ CD.

### Conclusion

In this study, the solubility of AS was significantly enhanced through CD complexation. It demonstrated that SBE $\beta$ CD was able to totally include AS in the hydrophobic cavity. The binary AS/SBE $\beta$ CD complexation was characterized in solid-state and confirmed that there were interactions between AS and SBE $\beta$ CD. This observation provided the data for further studies.

### References

- [1] H.A. Azis, M. Taher, A.S. Ahmed, W.M.A.W. Sulaiman, D. Susanti, S.R. Chowdhury, Z.A. Zakaria, *In vitro* and *in vivo* wound healing studies of methanolic fraction of *Centella asiatica* extract, *South African Journal of Botany*, 108 (2017) 163-174.
- [2] N.X. Nhiem, B.H. Tai, T.H. Quang, P.V. Kiem, C.V. Minh, N.H. Nam, J.H. Kim, L.R. Im, Y.M. Lee, Y.H. Kim, A new ursane-type triterpenoid glycoside from *Centella asiatica* leaves modulates the production of nitric oxide and secretion of TNF- $\alpha$  in activated RAW 264.7 cells, *Bioorganic & Medicinal Chemistry Letters*, 21 (2011) 1777-1781.
- [3] N. Nowwarote, T. Osathanon, P. Jitjaturunt, S. Manopattanasoontorn, P. Pavasant, Asiaticoside induces type I collagen synthesis and osteogenic differentiation in human periodontal ligament cells, *Phytotherapy Research*, 27 (2013) 457-462.
- [4] T. Loftsson, M.E. Brewster, Cyclodextrins as functional excipients: methods to enhance complexation efficiency, *Journal of Pharmaceutical Sciences*, 101 (2012) 3019-3032.

- [5] L. Hovgaard, H. Brøndsted, Drug delivery studies in Caco-2 monolayers. IV. Absorption enhancer effects of cyclodextrins, *Pharmaceutical Research*, 12 (1995) 1328-1332.
- [6] T. Loftsson, M.E. Brewster, Pharmaceutical applications of cyclodextrins. 1. Drug solubilization and stabilization, *Journal of Pharmaceutical Sciences*, 85 (1996) 1017-1025.
- [7] V. Zia, R.A. Rajewski, V.J. Stella, Effect of cyclodextrin charge on complexation of neutral and charged substrates: comparison of (SBE)7M- $\beta$ -CD to HP- $\beta$ -CD, *Pharmaceutical Research*, 18 (2001) 667-673.
- [8] T. Higuchi, K.A. Connors, Phase-solubility techniques, *Advances in Analytical Chemistry and Instrumentation*, 4 (1965) 117-212.
- [9] K. Shiotani, K. Uehata, T. Irie, F. Hirayama, K. Uekama, Characterization of the inclusion mode of beta-cyclodextrin sulfate and its effect on the chlorpromazine-induced hemolysis of rabbit erythrocytes, *Chemical & Pharmaceutical Bulletin*, 42 (1994) 2332-2337.
- [10] V. Zia, R.A. Rajewski, E.R. Bornancini, E.A. Luna, V.J. Stella, Effect of alkyl chain length and degree of substitution on the complexation of sulfoalkyl ether- $\beta$ - cyclodextrins with steroids, *Journal of Pharmaceutical Sciences*, 86 (1997) 220-224.
- [11] P. Mura, Analytical techniques for characterization of cyclodextrin complexes in aqueous solution: a review, *Journal of Pharmaceutical and Biomedical Analysis*, 101 (2014) 238-250.
- [12] J. Panichpakdee, P. Supaphol, Use of 2-hydroxypropyl- $\beta$ -cyclodextrin as adjuvant for enhancing encapsulation and release characteristics of asiaticoside within and from cellulose acetate films, *Carbohydrate Polymers*, 85 (2011) 251-260.
- [13] Y. Meliana, S. B. Harmami, W. K. Restu, Characterization of nanoencapsulated *Centella asiatica* and *Zingiber officinale* extract using combination of malto dextrin and gum arabic as matrix, *Materials Science and Engineering*, 172 (2017) 1-7.
- [14] Y. Deng, Y. Pang, Y. Guo, Y. Ren, F. Wang, X. Liao, B. Yang, Host-guest inclusion systems of daidzein with 2-hydroxypropyl- $\beta$ -cyclodextrin (HP- $\beta$ -CD) and sulfobutyl ether- $\beta$ -cyclodextrin (SBE- $\beta$ -CD): preparation, binding behaviors and water solubility, *Journal of Molecular Structure*, 1118 (2016) 307-315.

# Production and structural characterization of polysaccharides from marine actinomycetes

Pornpun Aramsangtienchai<sup>1,a\*</sup>, Titapa Kongmon<sup>1,b</sup> and Janjarus Watanachote<sup>2,c</sup>

<sup>1</sup> Department of Biochemistry, Faculty of Science, Burapha University, Chonburi, 20131, Thailand

<sup>2</sup>Institute of Marine Science, Burapha University, Chonburi, 20131, Thailand

<sup>a</sup>pornpun.ar@go.buu.ac.th, <sup>b</sup>58030229@go.buu.ac.th, <sup>c</sup>janjarus@buu.ac.th

**Keywords:** Microbial polysaccharides, Actinomycetes, Fructan, Levan

**Abstract.** Microbial polysaccharides are biopolymers produced from different microorganisms. Due to their interesting bioactivities with low toxicity, microbial polysaccharides have been widely applied in pharmaceutical and cosmetics industries. Nowadays, exploring new microbial strains for better polysaccharide producers have been increasing continuously. Herein, we investigated the ability of different actinomycetes screened from different mangrove areas in Thailand for polysaccharide production, in particular fructan. These isolates were initially grown in ISP2 (International Streptomyces Project2) media containing 20% (w/v) sucrose at 30 °C for seven days. The polysaccharides in the supernatant were then precipitated by adding two volumes of cold absolute ethanol. The types and components of polysaccharide were analyzed by acid hydrolysis and thin layer chromatography. We found that one of the isolates, PL-4-6, was able to produce fructan. After structural characterization by FT-IR and NMR techniques, the fructan from PL-4-6 had a similar structure to levan. Without an optimization of the culture condition, the obtained yield of levan from PL-4-6 was 2 g.L<sup>-1</sup>. Taken together, this study suggested that PL-4-6 might be used as another microbial source of levan production for pharmaceutical applications in the future.

## Introduction

Microbial polysaccharides are natural and biodegradable polymers produced from a variety of microorganisms and secreted out the cells called exopolysaccharides (EPS). Up until now, several studies have reported for interesting bioactivities of polysaccharides such as antioxidant, antitumor, and immunomodulatory activities [ 1]. Levan is one type of fructan consisting of beta-2,6 fructofuranoside residues. Levan has been reported for its potential in pharmaceutical applications, for example, using levan as a nanocarrier system for peptide and protein drug delivery [ 2]. Also, the development of levan produced from *Halomonas smyrnensis* AAD6T as microparticles to encapsulate antibiotics drug, vancomycin, was recently revealed [ 3]. Several strains of bacteria were reported for levan production such as *Bacillus subtilis*, *Zymomonas mobilis*, *Erwinia herbicola*, *Pseudomonas syringae* and so on [ 4]. However, among these levan producers rarely are actinobacteria. Actinobacteria, in particular actinomycetes, are well known as a source of bioactive secondary metabolite production such as antibiotics, vitamins, enzymes, and antitumour agents [ 5]. In this study, different actinomycetes isolated from mangrove forest in Thailand were investigated for polysaccharide production, in particular fructan. The precipitated polysaccharides from these isolates were initially investigated by TLC, and further characterized for their functionality and structure by FT-IR and NMR, respectively.

## Methods

### Microorganisms, growth medium and culture method

Different actinomycetes (NS2-5, CP58-7-4, CP15-9-6, A1-3, CP15-9-6, A16-1, A3-3, PL-4-6, Ry3-37, Ry3-32, Cp58-4-21, Ry3-43) were grown in ISP2 agar containing 4 g.L<sup>-1</sup> yeast extract, 10 g.L<sup>-1</sup> malt extract, 4 g.L<sup>-1</sup> dextrose and 17 ppt sea water, pH 6.0 at 30 °C for 4 days. A single colony was subsequently inoculated into ISP2 broth supplemented with 2 %0(w/v) sucrose and incubated at 37 °C, 110 rpm for 7 days. Cells were then removed by centrifugating and filtering through Whatman no.1 filter paper, and the supernatant was kept at -20 °C.

### Polysaccharide precipitation

To obtain polysaccharide products, two volumes of cold absolute ethanol was added into the cell-free supernatant of each isolate. The precipitated polysaccharides were separated by centrifugation at 4,000 rpm for 20 min. The pellet was then washed twice with 80% (v/v) ethanol, dissolved in distilled water and kept at -20 °C until the next experiment.

### Thin-layer chromatography (TLC)

The mixtures were analyzed on silica gel G-60 (MERCK) using butanol: acetic acid: water (50:30:15, V/V/V) as a mobile phase. The ketose-containing compound was visualized by dipping the TLC plate into the solution containing 5 g of urea in 2 M hydrochloric acid and incubated at 120 °C for 10 min [6]. To detect carbohydrate compound, the TLC plate was dipped into the solution containing 20 mg of orcinol in 8 ml of absolute ethanol, and subsequently added 1 mL of H<sub>2</sub>SO<sub>4</sub>. The plate was incubated at 120 °C for 10 min.

### Analysis of monosaccharide components by acid hydrolysis

To analyze the sugar compositions of the mixture, acid hydrolysis was performed by incubating each sample with 2 M of hydrochloric acid and heating at 95 °C for 20 min. The sugar components were then analyzed by TLC.

### Structural characterization by FT-IR and NMR

The polysaccharide colloidal solution was put in a dialysis tubing cellulose membrane (Sigma#D9652) and dialyzed through distilled water at 4 °C for 3-4 days. The samples were then lyophilized and kept in a silica gel desiccator until completely dried. The structural functionality of partial purified fructan was analyzed by using an ATR-FTIR spectrometer (PerkinElmer-Frontier) with 250 scans per sample at a wave number range of 4000-400 cm<sup>-1</sup> and a resolution of 4 cm<sup>-1</sup>. For NMR analysis, <sup>1</sup>H and <sup>13</sup>C-NMR of D<sub>2</sub>O-dissolved samples were measured with a Bruker AVANCE Ultrashield 400 MHz spectrometer.

## Results

### Screening for polysaccharide production from different isolates

Different actinobacteria isolated from the different mangrove areas of Thailand were grown in ISP2 containing 20% (w/v) sucrose. To obtain the crude polysaccharide products, two volumes of cold absolute ethanol were added in to each cell-free supernatant. The polysaccharide pellets were dissolved in distilled water and analyzed for the type of polysaccharide by TLC. To detect for ketose-containing polysaccharide, urea-HCl was used as a staining reagent [6]. From the result, the fructan polysaccharide product was observed at the origin spot of the isolate PL-4-6 (Fig1A). We, therefore, chose the isolate PL-4-6 (Fig1B) for further studies of fructan production.

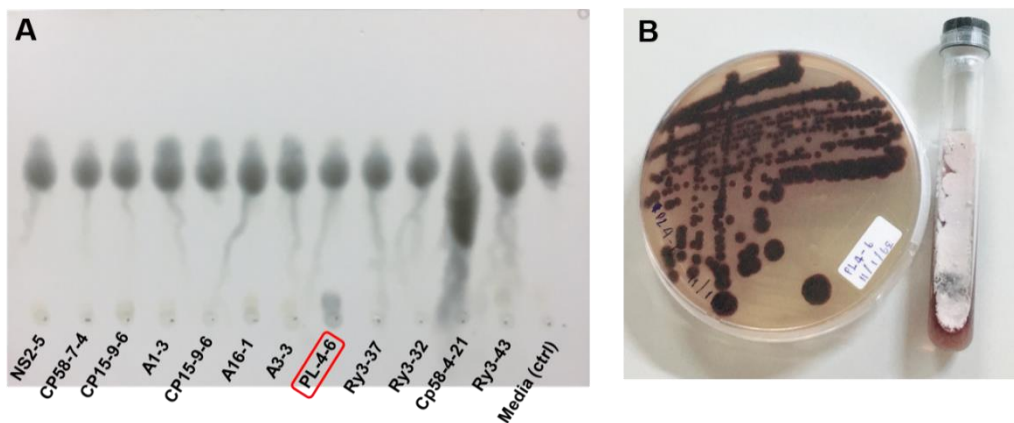


**Fig. 1,** Screening for fructan polysaccharide production. (A) Thin layer chromatogram of precipitated polysaccharides from different isolates dipped into urea-HCl staining reagent. (B) The morphology of PL-4-6 on ISP2 agar and slant agar.

The culture of actinomycete PL-4-6 was scaled up for polysaccharide production. The precipitated polysaccharide was water soluble in a hydrocolloid form. This product was further confirmed as a fructan by comparing to other standard sugars. From Fig2A, the orcinol:H<sub>2</sub>SO<sub>4</sub> was used as a staining reagent to detect all carbohydrate compounds. We observed polysaccharides at the origin spot of TLC in both lanes of levan standard and polysaccharide product from PL-4-6. We also used urea-HCl staining solution to detect ketose-containing compound as shown in Fig2B. Since glucose and maltoheptose (G7) did not react to this staining reagent, they did not show up on the TLC. On the other hand, the spots of both fructose-containing standards such as fructose, sucrose, and levan, and the polysaccharide from PL-4-6 were existed on the TLC, suggesting that the product from PL-4-6 was indeed a fructan. Moreover, we performed acid hydrolysis by treating each sample with 2 M of hydrochloric acid and heating at 95 °C for 20 minutes, respectively. The result demonstrated that after acid hydrolysis the fructan from PL-4-6 was disappeared from the origin spot with an increase in the intensity of fructose spot in the lane PL4-6+HCl (Fig2C). From these results, it implied that the major PL-4-6 polysaccharide component was fructose molecules.

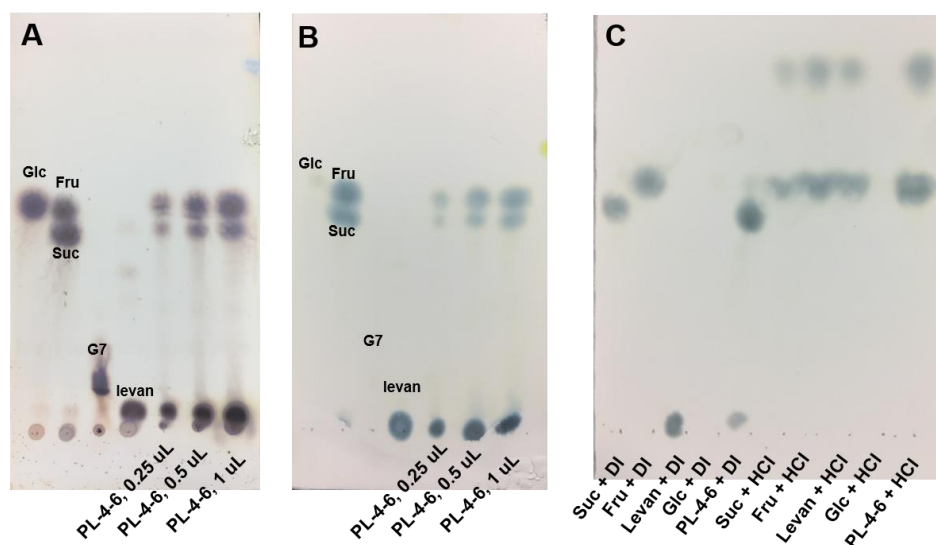


**Fig. 2,** Thin layer chromatogram of fructan polysaccharide isolated from PL-4-6. (A)

Different standard sugars: Glc(Glucose), Fru(Fructose), Suc(Sucrose), G7(maltoheptaose), levan(levan) and different volume of polysaccharide precipitated from PL-4-6. The plate was dipped into orcinol-H<sub>2</sub>SO<sub>4</sub> solution (B) The same samples as (A) but the plate was dipped into urea-HCl staining reagent. (C) Different standard sugars and polysaccharide from PL-4-6 were treated with either distilled water (DI) or 2 M of hydrochloric acid solution (HCl) and the plate was stained with urea-HCl reagent.

The structure of fructan from PL-4-6 was further characterized by FT-IR and NMR measurements, respectively. From the FT-IR spectrum, the functional groups in the fructan were revealed as following. The strong band of O-H stretching was observed at 3,271 cm<sup>-1</sup>, and the C-H stretching vibrations were approximately at 2,881 and 2,934 cm<sup>-1</sup>, representing the presence of fructose molecule [7]. Moreover, the band around 1,647 cm<sup>-1</sup> exhibited the C=O stretching vibration [8]. The stretching vibrations from glycosidic linkages of C-O-C and the side groups C-OH were also observed between 1,123 and 1,013 cm<sup>-1</sup> [9-10]. The band around 924 cm<sup>-1</sup> indicated the stretching vibration of a pyran ring.

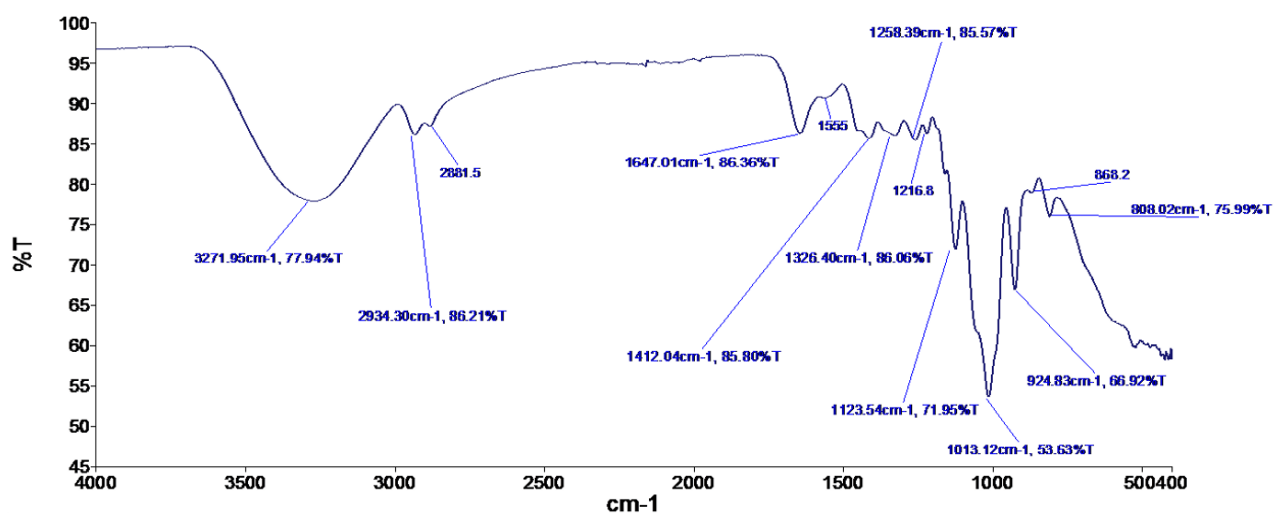


**Fig. 3,** FT-IR spectrum of fructan polysaccharides produced by the isolate PL-4-6.

For the NMR analysis, the spectra of <sup>1</sup>H and <sup>13</sup>C NMR were shown in Fig3A and 3B, respectively. From the <sup>1</sup>H spectrum of fructan from PL-4-6, the chemical shifts were observed at 3.670 ppm (H1a), 3.599 ppm (H1b), 4.093 ppm (H3), 4.009 ppm (H4), 3.862 ppm (H5), 3.801 ppm (H6a), and 3.467 ppm (H6b), respectively. All of the proton signals were between 3.40-4.20 ppm suggesting no existence of anomeric protons (5.40 to 4.20 ppm) in this fructan [11]. According to the <sup>13</sup>C NMR spectrum, the signals were at 59.92 ppm (C1), 104.19 ppm (C2), 76.31 ppm (C3), 75.20 ppm (C4), 80.28 ppm (C5), 63.38 ppm (C6), corresponding to the resonance signals from beta-2,6 fructofuranose or levan from the previous reports as shown in Table 1.

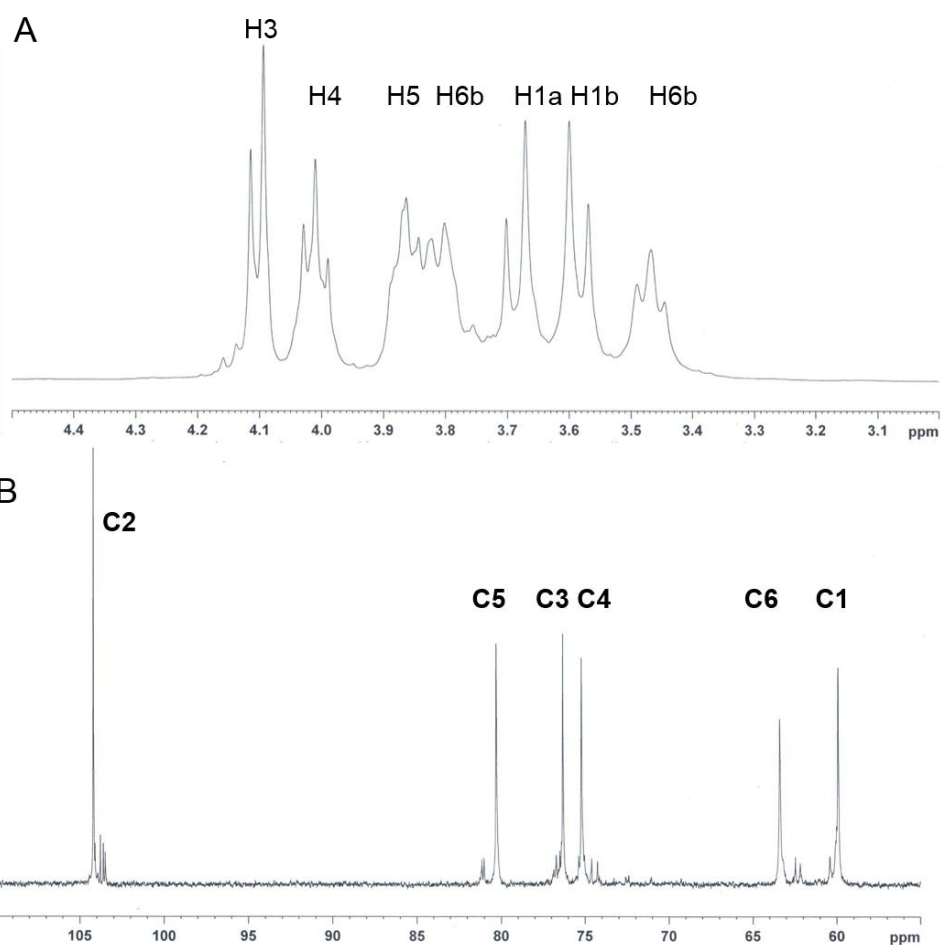


**Fig. 4,** NMR spectra of fructan polysaccharides produced by the isolate PL-4-6. (A)  $^1\text{H}$ -NMR spectra (B)  $^{13}\text{C}$ -NMR spectra.

**Table 1** Comparison of chemical shifts of  $^{13}\text{C}$ -NMR from different sources of levan polymer

Carbon atom	Chemical shift [ppm] from				
	PL-4-6	<i>Brenneria goodwinii</i>	<i>Bacillus megaterium</i> GJT321	<i>Pseudomonas fluorescens</i>	<i>Leuconostoc citreum</i> BD1707
C-1	59.92	60.953	59.86	60.435	60.234
C-2	104.19	104.568	104.14	104.696	104.537
C-3	76.31	77.273	76.25	76.770	76.628
C-4	75.20	75.914	75.15	75.784	75.532
C-5	80.28	80.675	80.23	80.880	80.622
C-6	63.38	63.830	63.31	63.978	63.716
Reference	This study	[13]	[12]	[10]	[11]

### Summary

We found that PL-4-6, the actinomycetes isolated from mangrove area in Thailand and grown in ISP2 media containing 20% (v/v) sucrose, was able to produce fructan polysaccharide. From TLC analysis and structural characterization by FT-IR and NMR, the hydrocolloidal solution of polysaccharide product had the similar structure to levan. Without an optimization of the culture condition, the yield of levan obtained from this experiment was  $2 \text{ g}\cdot\text{L}^{-1}$ . The results from this study suggested that actinomycete might be used as another source for



microbial levan production. The optimization for culture condition will be further investigated to obtain a higher yield and the levan product will be evaluated for using as a drug delivery system.

## References

- [1] N.H. Ahmad, S. Mustafa, Y.B. Che Man, Microbial Polysaccharides and Their Modification Approaches: A Review, *International Journal of Food Properties*, 18 (2015) 332-347.
- [2] A.D. Sezer, H. Kazak, E.T. Öner, J. Akbuğa, Levan-based nanocarrier system for peptide and protein drug delivery: Optimization and influence of experimental parameters on the nanoparticle characteristics, *Carbohydrate Polymers*, 84 (2011) 358-363.
- [3] A.D. Sezer, H. Kazak Sarilmiser, E. Rayaman, A. Cevikbas, E.T. Oner, J. Akbuga, Development and characterization of vancomycin-loaded levan-based microparticulate system for drug delivery, *Pharm Dev Technol*, 22 (2017) 627-634.
- [4] E.T. Oner, L. Hernandez, J. Combie, Review of Levan polysaccharide: From a century of past experiences to future prospects, *Biotechnol Adv*, 34 (2016) 827-844.
- [5] A. Raja, P. Prabakaran, Actinomycetes and Drug-An Overview, *Am. J. Drug Discovery Dev*, 1 (2011) 75-84.
- [6] R. Dedonder, [The glucides of the Jerusalem artichoke. I. Evidence of a series of glucofructosanes in the tubers; the isolation, analysis and structure of the least polymerized members of the series], *Bull Soc Chim Biol (Paris)*, 34 (1952) 144-156.
- [7] J. Liu, J. Luo, H. Ye, Y. Sun, Z. Lu, X. Zeng, Medium optimization and structural characterization of exopolysaccharides from endophytic bacterium *Paenibacillus polymyxa* EJS-3, *Carbohydrate Polymers*, 79 (2010) 206-213.
- [8] R. Srikanth, G. Siddartha, C.H. Sundhar Reddy, B.S. Harish, M. Janaki Ramaiah, K.B. Uppuluri, Antioxidant and anti-inflammatory levan produced from *Acetobacter xylinum* NCIM2526 and its statistical optimization, *Carbohydr Polym*, 123 (2015) 8-16.
- [9] M. Wu, Y. Wu, J. Zhou, Y. Pan, Structural characterisation of a water-soluble polysaccharide with high branches from the leaves of *Taxus chinensis* var. *mairei*, *Food Chemistry*, 113 (2009) 1020-1024.
- [10] N. R. Jathore, M. Bule, A. Deore, U. Annapure, Microbial levan from *Pseudomonas fluorescens*: Characterization and medium optimization for enhanced production, 2012.
- [11] J. Han, X. Xu, C. Gao, Z. Liu, Z. Wu, Levan-Producing *Leuconostoc citreum* Strain BD1707 and Its Growth in Tomato Juice Supplemented with Sucrose, *Appl Environ Microbiol*, 82 (2015) 1383-1390.
- [12] X. Yu, L. Li, J. Zhang, Z. Shen, C. Zhu, P. Wang, X. Jiang, Structural analysis of macromolecular levan produced by *Bacillus megaterium* GJT321 based on enzymatic method, *Int J Biol Macromol*, 93 (2016) 1080-1089.
- [13] Q. Liu, S. Yu, T. Zhang, B. Jiang, W. Mu, Efficient biosynthesis of levan from sucrose by a novel levansucrase from *Brenneria goodwinii*, *Carbohydr Polym*, 157 (2017) 1732-1740.

# Development of value added organic rice for commercialization: food and cosmetic products

Sureewan Duangjit<sup>1, a\*</sup>, Jintana Napaporn<sup>1, b</sup>, Nattapatt Phitsorat<sup>1, c</sup>,  
Ekasit Onsaard<sup>2, d</sup>, Wiriya Onsaard<sup>2, e</sup>, Sureeporn Kate-ngam<sup>2, f</sup> and  
Sureewan Bumrunghai<sup>3, g</sup>

<sup>1</sup>Faculty of Pharmaceutical Sciences, Ubon Ratchathani University, Ubon Ratchathani 34190, Thailand

<sup>2</sup>Faculty of Agriculture, Ubon Ratchathani University, Ubon Ratchathani 34190, Thailand

<sup>3</sup>Department of Microbiology and Parasitology, School of Medical Sciences,  
University of Phayao, Phayao 56000 Thailand

<sup>a</sup>sureewan.d@ubu.ac.th, <sup>b</sup>jintana.n@ubu.ac.th, <sup>c</sup>nattapat.ph.58@ubu.ac.th, <sup>d</sup>ekasit.o@ubu.ac.th,  
<sup>e</sup>wiriya.p@ubu.ac.th, <sup>f</sup>sureeporn.k@ubu.ac.th, <sup>g</sup>sureewan.b@windowslive.com,

\* corresponding author

**Keywords:** Rice bran oil, Oryzanol, Facial cleansing, Scrub, Bead, Nanocosmetic

**Abstract.** Thailand is well known for the last 3 decades as the world's largest rice exporter. Therefore, rice production has played an important role in the economic and social development of the nation. However, the rice-farmers are typically faced with several problems about the uncertainties of their crop. The drought in summer with insufficient rain destroyed a great amount of rice. Nevertheless, the excessive rain could also do the same. This problem significantly affects the price of Thai rice. Open learning developing local-level of knowledge in connection with 'research' may overcome the farmer's solution. The aim of this study was to develop value added organic rice for commercialization. Rice procured from Ubon Ratchathani province was used in this study. The chemical compositions of rice bran, defatted rice bran and rice bran protein from different sources were studied in order to apply for food and pharmaceutical products. Organic rice bran oil (O-RBO) encapsulated beads, organic rice bran (O-RB)-facial cleansing scrub and O-RBO loaded nanovesicles were designed and developed. The finding indicated that the by-product from organic rice can be used as a potential protein source for food and pharmaceutical product. Moreover, the encapsulated O-RBO beads and O-RB facial cleansing scrub and O-RBO loaded nanovesicles can be used as potential ingredients for cosmetic industries.

## Introduction

In Asian countries, rice consumption per capita is 84.9 kg during the year 2012-2014 (total world consumption is 156.1 kg), and it is expected to rise up to 86.8 kg by the year 2024. The growth is expected to be higher in developing countries (about 1.2% mean per annum (p.a.)) than in developed countries at (approximately 0.4% p.a.). The Asian countries account for almost 80% of the global consumption increase [1]. However, the world rice production (494 Mt) was reported to have the same amount as the world rice consumption (488.8 Mt) during 2012-2014. Rice is a major food crop of the world, particularly in Asian and Pacific countries. However, the rice-farmers are typical faced with several problems about the uncertainties of their crop. The droughts in summer, too little rain destroyed much of rice, the excessive rain could do the same. This result, much affecting the uncertainties price of world's price. To overcome the world farmer's problem, there are massive of research studying and learning to develop the local-level knowledge with regard to 'organic' production method. The quality of rice grain production was improved by improving rice breeding as well as improving rice properties by using food technology approaching.

Organic rice bran oil (O-RBO) and rice bran (RB) obtained from Agriculture Cooperative Co., Ltd., Ubon Ratchathani province are byproducts of the milling process of organic rice. The O-RBO and RB is now considered a valuable natural compound following the publication of its several bioactive activities. O-RBO extracted from organic RB consists of g-oryzanol (sterols and triterpene alcohol ferulates) and a-, b-, g-tocopherols. O-RBO can be used as anti-aging raw materials as it is composed of a variety of antioxidants.  $\gamma$ -oryzanol (OZ) is an ester mixture of ferulic acid and phytic acid. O-RBO can also be used as nutraceutical product that can protect our body from several diseases (e.g., cardio-vascular disease), maintain bone mineral density, reduce menopausal symptoms, and also decrease the risk of osteoporosis [2-7]. Various products from O-RBO and RB have been developed using advanced technology including nanotechnology. Recently, nanotechnology played an important role in drug and cosmetic delivery. Therefore, the demand for the nanotechnology in drug and cosmetic industries increased by more than 12 percent per year since 2007, and it has now reached 2.5 billion sales [8]. Therefore, the development of O-RBO and RB products using nanotechnology may improve the value of the crop from the organic rice agriculture cooperative Ltd. Ubon Ratchathani province.

Thus, the aim of this study was to increase the value of organic rice for commercialization both in the form of foods and cosmetics. The chemical compositions of rice bran, defatted rice bran and rice bran protein from different sources were studied. In addition, organic rice bran oil (O-RBO) encapsulated beads, organic rice bran (O-RB) facial cleansing scrub, and O-RBO loaded nanovesicles were designed and developed.

## Materials

Organic rice bran oil (O-RBO) obtained from the organic rice agriculture cooperative Ltd. Ubon Ratchathani province. Rice bran (RB) sample were purchased from a local milling at Phibun Mangsahan District (RB-P) and Det Udom District (RB-D), Ubon Ratchathani province. Phosphatidylcholine (PC) was generously supplied by Lipoid GmbH (Ludwigshafen, Germany). Cholesterol (Chol) was purchased from Wako Pure Chemical Industries (Osaka, Japan). All other chemicals used were of reagent grade and were purchased from Wako Pure Chemical Industries.

## Study of Chemical Composition of Defatted Rice Bran at Different Sources

**Preparation of Defatted Rice Bran (DRB).** RB was steamed at 85 °C for 20 min to inactivate enzyme and then was dried at 60 °C for 3 hrs. The RB samples were defatted using hexane solution in a ratio 1:4 (w/v) and stirring at room temperature for 30 min. A new hexane solution was applied again (twice) and the fat was decanted and removed using forced air oven at 60 °C for 1 hr. The DRB (or rice flour) was ground to pass through 40 mesh and kept in aluminum foil bag at 4 °C. The DRBP samples from Phibun Mangsahan District and Det Udom District were named DRB-P and DRB-D, respectively.

**Preparation of Rice Bran Protein (RBP).** RBP samples were prepared by alkali solution and isoelectric precipitation [9]. The DRB samples were dispersed in distilled water in a ratio of 1:9 (w/v). The mixture was adjusted to pH 9 using 2.0 N NaOH, and continuously stirred for 1 h to extract the protein and the insoluble material was removed by centrifugation for 15 min at 14,120 x g at 4 °C. The protein in the soluble phases was adjusted to pH 4.5 using 2 N HCl, and the precipitated protein was obtained by centrifugation for 15 min at 14,120g at 4 °C. The protein slurry was neutralized to pH 7.0 using 1.0 N NaOH and then freeze-drying was conducted. The RBP samples from Phibun Mangsahan District and Det Udom District were titled as RBP-P and RBP-D, respectively.

**Chemical Composition Analysis of DRB and RBP.** The DRB and RBP were analyzed for protein, fat, moisture, ash and fiber content using AOAC method (1999).

## **Formulation of the Cosmetics Product**

### **Encapsulated O-RBO Beads and O-RB into a Facial Cleansing Scrub Preparation.**

First, encapsulation by coacervation technique was utilized in this study to improve stability of rice bran oil prior to incorporate into a facial cleansing scrub product. The preparation of rice bran bead was conducted by Encapsulator B-395 Pro (Buchi, Thailand) with 200- $\mu\text{m}$  nozzle. Beading polymers were composed of sodium alginate, pectin, and gelatin. Gelling agent (cellulose derivatives) was studied for compatibility with anionic and amphoteric surfactants used in gel base to achieve an optimal viscosity and cleansing property. Second, accelerated stability test (heating-cooling cycle) was performed under  $4\pm 2^\circ\text{C}$  for 24 hrs. and  $45\pm 2^\circ\text{C}$  for 24 hrs. for 6 cycles. Then, the formulation was examined for physical and microbiological stability.

**O-RBO Loaded Nanocosmetic Preparation.** O-RBO loaded nanovesicles (niosomes) were prepared using the sonication method. The nanovesicles containing a constant amount of nonionic surfactant and cholesterol (1:1). The mixture was dissolved in organic solvent and evaporated by using nitrogen stream. The dried lipid film loaded O-RBO was hydrated with a phosphate buffer solution (PBS; pH 7.4). All nanovesicles formulations were subsequently sonicated for 30 min. The O-RBO loaded nanovesicles were freshly prepared and stored in airtight containers at  $4^\circ\text{C}$  prior to use. Then, the vesicle size, size distribution and zeta potential of the O-RBO loaded nanovesicles were determined by photon correlation spectroscopy (PCS) (Zetasizer Nano series, Malvern Instruments, U.K.) All samples were taken at room temperature ( $25^\circ\text{C}$ ). At least three independent measurements were recorded. The  $\gamma$ -OZ content in the O-RBO loaded nanovesicle was determined after nanovesicle disruption with Triton<sup>®</sup> X-100 (0.1% w/v) at a 1:1 volume ratio and appropriate dilution with PBS. The vesicles/Triton<sup>®</sup> X-100 solution was centrifuged at 10,000 rpm at  $4^\circ\text{C}$  for 10 min. The supernatant was filtered through a 0.45  $\mu\text{m}$  nylon syringe filter, and then analyzed by a HPLC. The stability of O-RBO loaded nanovesicles was evaluated by the accelerated stability test. The heating-cooling cycle was performed under  $4\pm 2^\circ\text{C}$  for 24 hrs. and  $45\pm 2^\circ\text{C}$  for 24 hrs. for 6 cycles. The physicochemical properties of nanovesicles e.g., vesicle size, size distribution and zeta potential were measured by PCS.

## **Data analysis**

The data were reported as the means  $\pm$  standard deviation (SD) ( $n=3$ ). A  $p$ -value of less than 0.05 was considered to be significant.

## **Results and Discussion**

### **Chemical Composition of Defatted Rice Bran at Different Sources**

The chemical composition of defatted rice bran samples (DRB-P and DRB-D) and rice bran protein samples (RBP-P and RBP-D) were shown in Table 1. It was found that RB-P, RB-D, DRP-D and DRB-D contained protein content of 12.23%, 13.39%, 16.20% and 13.69%, respectively. The high fat content was observed for RBP-P (25.07%) comparing with RBP-D (7.88%). In contrast, the highest protein content was found in RBP-D compared to RBP-P. Noptana, R. and Onsaard, E. reported that rice bran protein contained 76.09% of protein, 7.92% of fat, 5.25% of ash, 0.65% of fiber and 8.63% of carbohydrate [9]. Differences in chemical composition of the rice bran protein due to a variation of raw materials, plantation conditions and different preparation methods. However, high protein content of RBP-P and RBP-D could be an alternative ingredients as a potential protein source for food and pharmaceutical product.

### **Encapsulated O-RBO beads and O-RB into a Facial Cleansing Scrub.**

The results demonstrated that rice bran oil was successfully encapsulated and spherical beads were formed by coacervation technique using 3 main bead polymers; sodium alginate, pectin, and gelatin. Spherical shaped beads were fashioned by total bead polymer concentration of 7 % w/v with proportion 1.5:1:1 (sodium alginate: pectin: gelatin). Beads were found to

have even size distribution (mean = 237 nm), uniform color with optimal hardness. Stability test (72 hrs. in phosphate buffers at room temperature) revealed that beads were most stable in pH 6.0-8.0 which is a suitable pH range for a facial cleansing scrub product. Gel base formulation, composed of 15% w/v surfactants (Zohareric D2, Dehyton KT, Texapon N70, and Texapon N8000) and 4% w/v coconut diethanolamine as a foam booster, was demonstrated to have an optimal cleansing property without irritation after rinse. Desired viscosity was then obtained by adding HPMC 5% w/v without incompatibility. Size selected and washed rice bran (as scrub material) and encapsulated rice bran oil beads were added in the gel base formulation in a concentration of 3% w/v and 10% w/v, respectively (Figure 1). This formulation was pH adjusted to 6.5 to achieve suitable pH and stability. The appearance, pH, and viscosity of the formulation remained unchanged after the accelerated stability test. Microbiological stability test, according to t cps.261/2554 and t cps.173/2554 for facial scrub products and facial cleansing products, respectively, was shown that the total colony count did not exceed  $1 \times 10^3$  CFU/ml. Moreover, no *Staphylococcus aureus*, *Pseudomonas aeruginosa*, and *Candida albicans* was found. It could be concluded that organic rice bran oil has a potential as a raw material for cosmetic preparation, illustrating a good chemical component quality with good anti-oxidant property. Furthermore, it can be accountable for anti-oxidant activity and moisturizing effect once it is incorporated into the cosmetic products.

**Table 1.** Chemical composition of rice bran samples (RB-P and RB-D), defatted rice bran samples (DRB-P and DRB-D) and rice bran protein samples (RBP-P and RBP-D) from Phibun Mangsahan District and Det Udom District

Chemical composition <sup>1</sup> (%)	RB-P	RB-D	DRB-P	DRB-D	RBP-P	RBP-D
Moisture	5.93±0.22	7.38±0.09	4.56±0.19	3.50±0.23	2.80±0.05	2.75±0.05
Protein <sup>2</sup>	12.23±0.69	13.39±1.86	16.20±0.20	13.69 ±1.86	58.24±1.59	77.31 ±0.39
Fat	18.41±0.06	17.18±0.72	3.26±0.11	0.84 ± 0.03	25.07±0.68	7.88 ± 0.06
Ash	11.54±0.74	6.04±0.02	12.38±0.02	7.41±0.05	2.98±0.15	7.59±0.10
Fiber	41.26±3.35	41.17±1.27	15.24±0.41	12.76±2.58	32.0±37.0	08.0±23.0
Carbohydrate <sup>3</sup>	51.90±0.16	56.00±0.35	63.59±0.14	74.56±2.06	54.10±70.1	24.4±0.47

<sup>1</sup> Values are given as mean ± standard from triplicate determination

<sup>2</sup> 6.25 was used as the nitrogen conversion factor

<sup>3</sup> Estimated by difference



**Figure 1.** Facial Cleansing Scrub derived from organic jasmine rice bran

### O-RBO Loaded Nanovesicles

The vesicle size of O-RBO loaded nanovesicle was 77-151 nm with size distribution (PDI) of 0.1-0.4 (Figure 2). Previous studies reported that the vesicle smaller than 600 nm were able to penetrate into deep skin [10, 11]. The zeta potential was 5-23 with a negative charge.

This result indicated that the negative nanovesicle may be stable due to the sedimentation have prevented through inter-vesicle attractive and repulsive forces. The O-RBO loaded nanovesicles were stable under the incubation period of 120 days at  $5\pm 1^{\circ}\text{C}$ . In the development of cosmetics the efficacy, safety and stability were the prime factors that should be considered. Considering the basic physicochemical properties of the nanovesicle, we successful in showing the feasibility of O-RBO loaded nanovesicle preparation. Thus, the O-RBO loaded nanovesicle in this study may properly utilize as a nanocosmetics. The approach high value added to the natural product from organic rice agriculture cooperative Ltd. Ubon Ratchathani province as nanocosmetic may be selected.

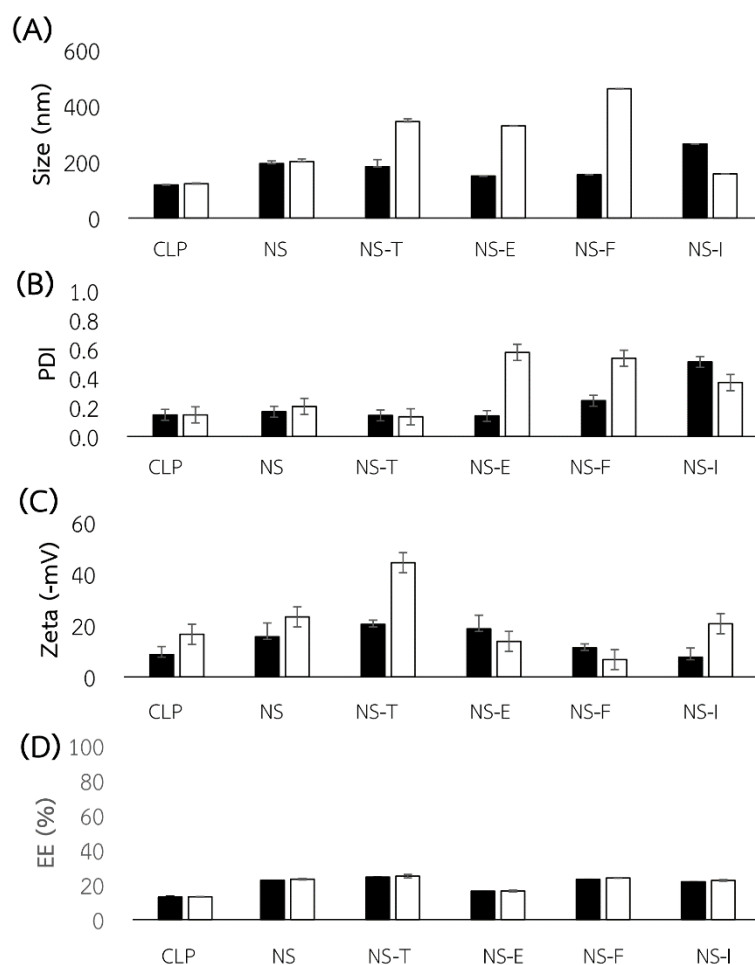


**Figure 2.** The physicochemical properties of O-RBO loaded nanovesicle; ■ initial □ after 6 cycle stability test: (A) vesicle size, (B) size distribution, (C) zeta potential and (D) entrapment efficiency

## Summary

In the development of food and cosmetic products, the key to success is to optimize the dietary reference values of foods, the efficacy, stability and safety of cosmetics. In this study, the difference sources affected the chemical composition of rice bran oil and rice bran protein (RB, DRB and RBP). The defatted rice bran and rice bran protein can be used as a potential protein source for food and pharmaceutical product. Moreover, the O-RBO have been formulated and developed as a potential as a raw material for cosmetic including encapsulated O-RBO beads, O-RB as a facial cleansing scrub and O-RBO loaded nanovesicles. The efficacy and stability were also studied. The finding cosmetic product can be illustrated a good chemical component quality with good anti-oxidant property. The protein source for food and pharmaceutical and the cosmetic products from the organic rice were selected as the approach

high value added of the rice from organic rice agriculture cooperative Ltd. Ubon Ratchathani province.

### **Acknowledgement**

The authors gratefully acknowledge Thailand Research Fund through the Royal Golden Jubilee Advanced Program (Grant No. RAP59K0019) and the National Research Council of Thailand (NRCT) for the financial support. Grateful thanks also go to Faculty of Pharmaceutical Sciences, Ubon Ratchathani University for supporting facilities and equipment. In addition, the authors would like to thank the the Queen Saovabha Memorial Institute, Thai Red Cross Society, Bangkok, Thailand for kindly providing the shed snake skin used in the pre-formulation study.

### **References**

- [1] OECD/FAO. OECD-FAO Agricultural Outlook 2015-2024. OECD Publishing, Paris (2015).
- [2] Chotimarkorn C, Ushio H, The effect of trans-ferulic acid and gamma-oryzanol on ethanol-induced liver injury in C57BL mouse. *Phytomedicine*, 15, 951-958 (2008).
- [3] Islam MS, Murata T, Fujisawa M, Nagasaka R, Ushio H, Bari AM, Hori M, Ozaki H, Anti-inflammatory effects of phytosteryl ferulates in colitis induced by dextran sulphate sodium in mice. *Br J Pharmacol*, 154, 812-824 (2008).
- [4] Oka T, Fujimoto M, Nagasaka R, Ushio H, Hori M, Ozaki H, Cycloartenyl ferulate, a component of rice bran oil- derived gamma- oryzanol, attenuates mast cell degranulation. *Phytomedicine*, 17, 152-156 (2010).
- [5] Kahlon TS, Saunders RM, Sayre RN, Chow FI, Chill MM, Betschart AA, Cholesterol lowering effect of rice bran and rice bran oil fraction in hypercholesterolemic hamsters. *Cereal Chem*, 69, 485–489 (1992).
- [6] Xu Z, Hua N, Godber JS, Antioxidant activity of tocopherols, tocotrienols and  $\gamma$  -oryzanol components from rice bran against cholesterol oxidation accelerated by 2,2'-azobis(2-methylpropionamide) dichloride. *J Agri Food Chem*, 49, 2077-2081 (2001).
- [7] Wang JF: Effect of Acupuncture Combined With TDP on Estrogen and Bone Metabolism in Postmenopausal Patients With Deficiency of Liver and Kidney Syndrome. *Zhongguo Zhen Jiu*, 29, 623–625 (2009).
- [8] Kaur IP, Agrawal R, Nanotechnology: a new paradigm in cosmeceuticals. *Recent Patents on Drug Deliv Formul*, 1, 171-182 (2007).
- [9] Onsaard E, Noptana R, Enhanced Physical Stability of Rice Bran Oil-in-Water Emulsion by Heat and Alkaline Treated Proteins from Rice Bran and Soybean. *Sci & Technol Asia*, 23, 9-16 (2018).
- [10] Jennings V, Gysler A, Schafer-Korting M, Gohla SH, Vitamin A loaded solid lipid nanoparticles for topical use: occlusive properties and drug targeting to the upper skin. *Eur J Pharm Biopharm*, 49, 211-218 (2000).
- [11] Abdel-Mottaleb MM, Mortada ND, El-Shamy AA, Awad GA, Physically cross-linked polyvinyl alcohol for the topical delivery of fluconazole. *Drug Dev Ind Pharm*, 35, 311-320 (2009).

# Development of nanogels using gamma radiation induced crosslinking of inter-polymer complexes

Pattra Lertsarawut<sup>1,2 a</sup>,  
Sujimon Tunvichien<sup>1,b</sup>, Thitirat Rattanawongwiboon<sup>2,c</sup>,  
Kasinee Hemvichian<sup>2,d</sup> and Duangratana Shuwisitkul<sup>1,e\*</sup>

<sup>1</sup>Department of pharmaceutical technology, Srinakharinwirot University, Thailand.

<sup>2</sup>Thailand Institute of Nuclear Technology (Public Organization), Thailand

<sup>a</sup>pattra@tint.or.th, <sup>b</sup>sujimon@g.swu.ac.th, <sup>c</sup>smc.cuu@hotmail.com, <sup>d</sup>kasineeh@yahoo.com,  
<sup>e\*</sup>duangrats@g.swu.ac.th

**Keywords:** nanogels, gamma radiation, chitosan, hyaluronic acid, polyvinyl pyrrolidone.

**Abstract.** Nanogels is a dosage form that can deliver a drug to a specific target. Optimal choices of polymers are good beginning to prepare nanogels. The objective of this study was to select appropriate polymers for preparing nanogels by radiation-induced crosslinking. The inter-polymer complexes (IPCs) of chitosan with polyvinyl pyrrolidone (CS-PVP), sodium hyaluronic acid with polyvinyl pyrrolidone (HA-PVP) and chitosan with sodium hyaluronic acid (CS-HA) were chosen to prepare nanogels using gamma radiation-induced crosslinking. IPCs were irradiated at 1 kGy of the different polymer concentrations (0.10 - 0.50 mg/ml). The particle size was measured by a zetasizer. Stability of the nanogels was taken into consideration. Only CS-HA IPCs could form suitable nanogels with the particles size of approximately 150 nm. Increasing CS and HA concentrations resulted in the increase in size of the particles. CS-HA nanogels was stable up to 7 days in the aspects of particles size, polydispersity index, pH and zeta potential. It is possible to load a drug to the CS-HA nanogels used as a delivery system. However, a further drug loading and release study are required.

## Introduction

Nanogels are the nanosized particles (in the range of 20-200 nm) by three-dimensionally crosslinked polymer network that exhibits high capability to adsorb water, drug, protein or the other molecule and maintaining their structure. They are highly biocompatibility, flexibility when prepared using appropriate carriers and can be manipulated to avoid clearance by phagocytic cell [1, 2]. Chemical and physical crosslinking are used to prepare nanogels. Chemical crosslinking can be done using initiator, catalyst and crosslinker, which all chemicals are toxic. Physical crosslinking can also occur by self-assembly of the polymeric chains through either Van der Waals force or electrostatic interaction. Physical crosslinking by the self-assembly can lead to the weakness of nanogels structure that influence the stability of the nanogels [1, 2].

Radiation-induced crosslinking has been considered as an another excellent way to prepare nanogels, because they are the convenient method and can be carried out at room temperature without using initiator and catalyst [3]. It has been considered as green technology due to its additive-free initiation and easy control procedure. Radiation can induce covalent bonding that are strong binding between polymer chains of inter-polymer complexes (IPCs) resulting in more stable nanogels.

The objective of this study was to select appropriate polymers for preparing nanogels by radiation-induced crosslinking. Chitosan (CS), polyvinyl pyrrolidone (PVP) and sodium hyaluronic acid (HA) were chosen to form nanogels using gamma radiation-induced



crosslinking. Different concentrations of the polymers were investigated. The stability of the particle after preparation was monitored.

## Materials and Method

**Materials.** Chitosan (molecular weight of 500 kDa and 85% degree of deacetylation) was purchased from Seafresh chitosan (Lab Co., LTD, Thailand). Polyvinyl pyrrolidone (PVP, molecular weight of 360 kDa) was purchased from Fluka (US). Sodium Hyaluronic acid (HA, molecular weight of 1.3 MDA) was obtained from Soliance (France).

**Preparation of inter-polymer complex nanogels using gamma radiation.** HA, CS and PVP solutions was prepared at the concentration ranging from 0.10-0.50 mg/ml. HA and PVP were dissolved in sterile water while CS was dissolved in 1% acetic acid. The CS-PVP IPCs was prepared by mixing CS solution and PVP solution (having a similar concentration) at 1:1 ratio using dropping method. The PVP solution was dropped into the CS solution via hypodermic syringe no.21 under continuous magnetic stirring for 30 minutes. The CS-PVP IPCs was placed into a glass vial and deoxygenated by purging with N<sub>2</sub>O for 10 minutes. After that, the sample were irradiated using a Co-60 gamma irradiator (Gamma chamber 5000, BRIT, India) at 1 kGy. The HA-PVP and CS-HA nanogels were prepared using the same method as mentioned above.

**pH measurement.** The pH of the IPCs and the nanogels were measured using a pH meter (Mettler Toledo, Switzerland).

**Particle size, polydispersity index and zeta potential analysis.** Zetasizer Nano ZS (Malvern Instruments Ltd., UK) was used for determining the size, polydispersity index (PDI) and zeta potential of the particles. The samples were diluted to 0.5x from the initial concentration before 750  $\mu$ L of the diluted solution were transferred to a disposable zeta cell. The particle size, polydispersity index (PDI) value and zeta potential of the IPCs and the nanogels were averaged from 3 runs.

**Stability study of nanogels.** The nanogels were stored at room temperature and at 4°C for 2 weeks. The pH value, particles size, PDI and zeta potential of the nanogels were measured at different time points (0, 1, 3, 5, 7 and 14 days).

## Results and discussion

Types of polymer has an impact on the nanogel formation. There were two peaks in the spectra of the CS-PVP and the HA-PVP IPCs after radiation and measuring particle size using zetasizer (Fig. 1a and 1b). The peak above 10000 nm indicated large particles caused by the aggregation of the CS-PVP and the HA-PVP nanogels. The PDI value of the CS-PVP and the HA-PVP nanogels were  $0.406 \pm 0.03$  and  $0.573 \pm 0.04$ , respectively.

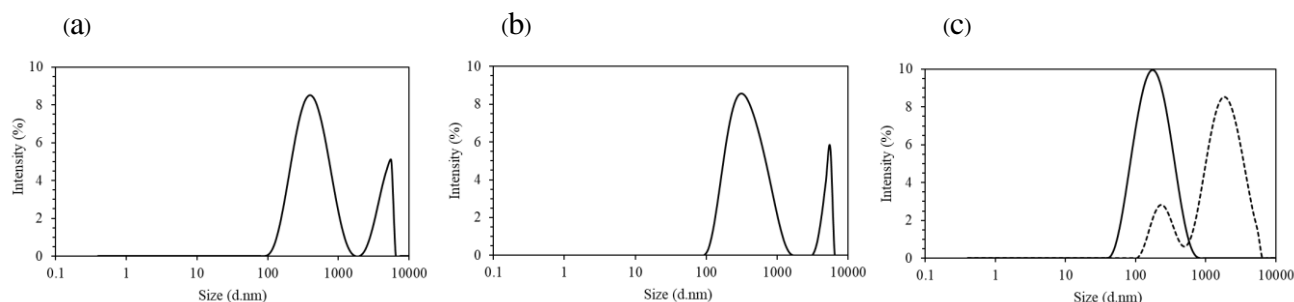
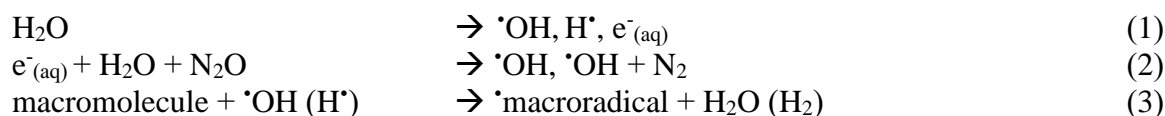


**Fig. 1.** Spectrums of the CS-PVP nanogels (a), the HA-PVP nanogels (b) and the CS-HA nanogels (c) from Zetasizer Analysis using 0.10 mg/ml of each polymer solutions.

The CS-HA IPCs can form nanogels after radiation. The average particles size (Fig. 1c) was about  $155.87 \pm 0.84$  nm and the PDI value was  $0.228 \pm 0.01$ . Before radiation, the spectrum was shown as the dash line in Fig. 1c. It demonstrated two-separate peaks, one peak at 260 nm and another peak at approximate 2100 nm. It indicated that polymerization of the CS-HA IPCs could not formed completely without radiation. Therefore, the CS-HA IPCs was the suitable polymer for nanogels preparation in this study.

The CS-HA IPCs could firstly form weak nanogels by ionic interaction between  $\text{NH}_3^+$  (cationic) of CS and  $\text{COO}^-$  (anionic) of HA. Radiation helped the nanogels to form completely and firmly. When the diluted aqueous solution is subjected to ionizing radiation (gamma rays or electrons beam), the most of radiation energy is adsorbed by water. The decomposition of water molecule could be done as the following reaction (1)



The hydroxyl radicals ( $\cdot\text{OH}$ ) and hydrogen radicals ( $\text{H}\cdot$ ) are initiators of reactions. The  $\cdot\text{OH}$  could to convert from the solvate electrons ( $\text{e}^-_{\text{aq}}$ ) by saturating the solution with  $\text{N}_2\text{O}$  (reaction (2)). ( $\cdot\text{OH}$  and  $\text{H}\cdot$  are capable of abstracting hydrogen atoms from macromolecules, generating react sensitively molecule or macroradicals (reaction (3)) that can induce crosslinking of the polymers [4, 5] and leading to nanogel formation.

Polymer concentrations had an impact on the particles size of the CS-HA nanogels. It was found that the particles size increased as the polymer concentration was increased (Fig. 2). At high concentrations of CS and HA, coalescence can occur resulting in the larger particles [6]. The concentration of the polymers higher than 0.25 mg/ml of the polymer solutions was not appropriate to form nanogels due to the formation of large particles ( $> 200$  nm).

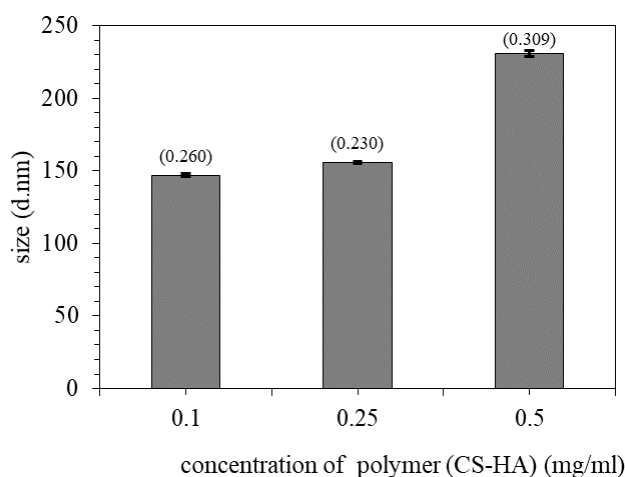


**Fig. 2.** Relationship between the concentration of CS-HA IPCs nanogels and their particle sizes.

The stability of the CS-HA nanogels was evaluated when preparing the nanogels using 0.25 mg/ml of CS and HA solutions. It was found that the CS-HA nanogels had particles sizes of  $154.20 \pm 1.27$  nm after 7 days of storage. The particle size was nearly similar to the initial time (Fig. 3). The storage of the CS-HA nanogels at room temperature (RT) and in the refrigerator ( $4^\circ\text{C}$ ) provided no statistically significant differences ( $P < 0.01$ ) in the particles size (Fig. 3), zeta potential (Table 1) and pH value (data not shown).

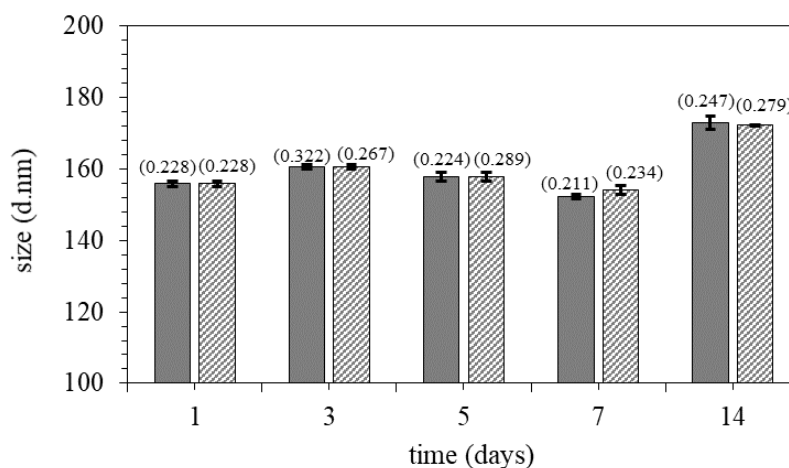


**Fig. 3.** Relationship of the particles size of the CS-HA IPCs nanogels at different time points after storage at room temperature (■) and 4°C (▨).

**Table 1.** zeta potential of the CS-HA nanogels at different time points after storage at room temperature and 4°C.

Conditions of preservation	Zeta potential [mV]		
	1 days	7 days	14 days
RT	26.07 ± 0.50	25.15 ± 1.06	25.97 ± 1.10
4°C	26.07 ± 0.50	23.27 ± 1.27	25.40 ± 1.14

The minimum desirable zeta potential value of nanogels of about  $\pm 20$  mV helps prevent aggregation of the nanogels in colloidal solution [7, 8]. For the CS-HA nanogels, the positive zeta potential value above  $\pm 20$  mV indicated that the nanogels had the good colloidal stability due to electrostatic repulsion of the particles with the similar electrical charge.

### Summary

The CS-HA IPCs was successfully employed to prepare nanogels by gamma radiation induced crosslinking, whereas the CS-PVP and HA-PVP IPCs were unfeasible to form nanogels. The particles size of the CS-HA nanogels was under 200 nm when using CS and HA at the concentration less than 0.25 mg/ml. From particles size, PDI value, zeta potential and pH value, the CS-HA nanogels was stable until 7 days after storage at room temperature and 4°C. Therefore, crosslink by gamma radiations is a practical and feasible method used to prepare crosslinked nanogels from the CS-HA IPCs.

### Acknowledgments

This work was partly supported by Pharmaceutical Technology Department of Srinakharinwirot University and Thailand Institute of Nuclear Technology (Public Organization), Thailand

## References

- [1] F. Sultana, M. Manirujjaman, M.A. Imran-UI-Haque, S. Sharmin, An overview of nanogel drug delivery system, *J Appl Pharm Sci* 3(8) (2013) 95-105.
- [2] H. Zhang, Y. Zhai, J. Wang, G. Zhai, New progress and prospects: The application of nanogel in drug delivery, *Materials Science and Engineering: C* 60 (2016) 560-568.
- [3] T. Rattanawongwiboon, M. Ghaffarlou, S.D. Sütekin, W. Pasanphan, Preparation of multifunctional poly (acrylic acid)-poly (ethylene oxide) nanogels from their interpolymer complexes by radiation-induced intramolecular crosslinking, *Colloid and Polymer Science* 296(9) (2018) 1599-1608.
- [4] S. Kadlubowski, Radiation-induced synthesis of nanogels based on poly (N-vinyl-2-pyrrolidone)-A review, *Radiation Physics and Chemistry* 102 (2014) 29-39.
- [5] P. Ulański, I. Janik, J. Rosiak, Radiation formation of polymeric nanogels, *Radiation Physics and Chemistry* 52(1-6) (1998) 289-294.
- [6] D.C. Priyanka Saharan, S.P.S. Bhatt, K. Bahmani, The study the effect of polymer and surfactant concentration on characteristics of nanoparticle formulations *Der Pharmacia Lettre* 12(7) (2015) 365-371
- [7] P. Islam, J. J Water, A. Bohr, J. Rantanen, Chitosan-Based Nano-Embedded Microparticles: Impact of Nanogel Composition on Physicochemical Properties, 2016.
- [8] S. Honary, F. Zahir, Effect of zeta potential on the properties of nano-drug delivery systems-a review (Part 2), *Tropical Journal of Pharmaceutical Research* 12(2) (2013) 265-273.

# Development of transdermal patch from *Centella asiatica* crude extract

Teerarat Pummarin<sup>1,a</sup>, Chanai noysang<sup>2,b</sup>, Sujimon Tunwichien<sup>1,c</sup> and Duangratana Shuwisitkul<sup>1,d\*</sup>

<sup>1</sup>Department of Pharmaceutical Technology, Faculty of Pharmacy, Srinakharinwirot University, Nakhon Nayok, Thailand

<sup>2</sup>Thai Traditional Medicine College, Rajamangala University of Technology Thanyaburi, Pathumthani, Thailand

<sup>a</sup> teeraratpum@gmail.com, <sup>b</sup> chanai\_n@rmutt.ac.th, <sup>c</sup> sujimon@swu.ac.th, <sup>d</sup> duangrats@swu.ac.th

**Keywords:** *Centella asiatica* extract, asiaticoside, transdermal patch, Eudragit RS, Eudragit RL

**Abstract.** *Centella asiatica* has been widely used for treatment of scar. The duration of action can be prolonged by preparing the *Centella asiatica* crude extract in the form of transdermal patches. The objective of the study was to select suitable polymers and sources of crude extract for preparing transdermal patches containing *Centella asiatica* crude extract and to study the effect of extract on mechanical and bioadhesive properties of the transdermal patches. The active compound, asiaticosides, was analyzed using HPTLC. The quantitative determination of asiaticosides from three companies found that the extract of *C. asiatica* from two companies contained asiaticosides. The transdermal patches containing 5% by weight of chosen *C. asiatica* extract were prepared by solvent casting method using Eudragit RS, RL and the blend of Eudragit RS and RL in the ratio of 1:1. The transdermal patches were evaluated for mechanical, bioadhesive properties and extract release. The results from tensile strength showed that the transdermal patches containing *C. asiatica* extract had higher strength and Young's Modulus than the film without *C. asiatica* extract. The elongation of transdermal patches decreased with the addition of *C. asiatica* extract. It was similar to mechanical properties. The bioadhesive property of patches would be decreased with the addition of *C. asiatica* extract. After adding 5% by weight of *C. asiatica* extract, the mechanical and bioadhesive properties of transdermal patches prepared by Eudragit RL and the polymer blend would be better than the patches prepared by Eudragit RS. However, the release of extract from the patches prepared by Eudragit RS would be faster than those prepared by Eudragit RL and polymer blend. In conclusion, *C. asiatica* extract had an impact on mechanical and bioadhesive properties of transdermal patches prepared by Eudragit RS, RL and their blend. Eudragit RL and the polymer blend were chosen for further development of transdermal patches containing 5% by weight of *C. asiatica* extract due to the mechanical and bioadhesive properties with improvement of extract release.

## Introduction

Transdermal patches are recognized as one of potential dosage forms for local and systemic delivery of drugs. It offers many advantages over conventional administration, such as enhanced efficacy, avoiding problems of gastric irritation, improved patient compliance and avoiding hepatic first pass metabolism [1, 2]. Drug level from transdermal patches can be maintained within the therapeutic window for prolonged periods. Thus, duration of drug action following a single administration of the drug can be extended and the frequency of dosing is reduced. Patient compliance and acceptability of the drug therapy can be improved. Another

advantage is that the drug therapy can be terminated by simply removing the patch from the skin [3].

*Centella asiatica* (L) Urban is belonging to the plant family of Apiaceae. It is used as a medicinal herb to treat a wide variety of conditions, such as improving memory and blood flow, wound healing agent. The active chemical compounds of *C. asiatica* were asiatic acid, asiaticoside, madecassic acid and madecassoside [4]. Nowadays, *C. asiatica* extract has been available in the form of gel and cream. Transdermal patches containing *C. asiatica* extract has not been launched to the drug market in Thailand.

The objective of the study was to select suitable polymers and source of crude extract for preparing transdermal patches containing *Centella asiatica* crude extract and to study effect of the extract on mechanical and bioadhesive properties of the transdermal patches. Transdermal patch formulations were developed by using synthetic and pH independent polymer, Eudragit RL100, Eudragit RS100 and the blend between Eudragit RS with RL in the ratio of 1:1.

## Materials and Methods

### Materials

*Centella asiatica* extract were purchased from AP Operations Co., Ltd. (Lot No. CTL60060132-4, Thailand), Chemipan Corporation co., Ltd. (Batch 20170629, Bangkok, Thailand), Specialty Natural Products Co., Ltd. (Lot No. TS64CEA71A, Chonburi, Thailand), Eudragit RS100 and Eudragit RL100 (Evonik Röhm Pharma, Germany) were donated by Jebsen & Jessen Ingredients (T) Ltd (Bangkok, Thailand), Triethylcitrate (TEC) were purchased from Sigma Chemical Co (St. Louis, USA), and isopropyl alcohol (IPA) was used as received.

### Methods

#### HPTLC Studies

Extract powder was dissolved in methanol in the concentration of 10 mg/ ml. Chromatography was performed on HPTLC precoated silica gel 60<sub>F254</sub> plates (20×10 cm, with 0.2 mm thickness; Merck, Germany). Methanolic solution of the sample and standard asiaticosides of known concentrations were applied to layers as 6 mm-wide bands positioned 10 mm from the bottom and 15 mm from side of plate using Camag Linomat 5. The injection volume for all the samples was 10 µL. The mobile phase consisted of chloroform : methanol : water (15:7:1 by volume) [5]. The plate was developed to distance of 80 mm in Camag automatic developing chamber. After development, anisaldehyde reagent (0.5 mL anisaldehyde, 10 mL acetic acid, 85 mL methanol, and 10 mL sulphuric acid) was sprayed onto the plates and heated at 100 °C for 5-10 min. Densitometric scanning was performed using TLC scanner 3 (Camag, Switzerland) using the WinCATS software. The wavelength of detection was 210 nm.

#### Transdermal patch preparation

The formulations of transdermal patch with *C. asiatica* extract showed in Table 1. The preparation was prepared by dissolving the polymer or the polymer blend in isopropyl alcohol: water mixture in the ratio of 1:1. Then, TEC was added as a plasticizer and stirred for 2h at room temperature. The polymer solution (10 g) was casted into Teflon dish (7×7 cm) and allowed evaporation of the solvent under the fume hood for 12 h. Finally, transdermal patch was dried in hot air oven at 50 °C for 1 h.

**Table 1** Codes and Formulation of transdermal patch

Ingredients	Formulation (% w/w)		
	F1	F2	F3
Eudragit® RS100	5		2.5
Eudragit® RL100		5	2.5
TEC	1	1	1
Isopropyl Alcohol : Water (1:1)	qs	qs	qs
Extract	5	5	5
Total	100	100	100

### Mechanical properties

Mechanical Properties of transdermal patches were measured using texture analyzer (TA 500, LLOYD instrument, UK). The patches were cut into  $10 \times 50 \text{ mm}^2$  and stretched at a rate of 100 mm/min until breaking. Tensile strength (TS) and percentage of elongation (%) at break were evaluated in nine replicates.

$$\text{Tensile Strength (N/mm}^2\text{)} = \frac{\text{Breaking Force (N)}}{\text{Cross-sectional area of sample (mm}^2\text{)}}$$

$$\text{Elongation at break (\%)} = \frac{\text{Increase in length at breaking point (mm)}}{\text{Initial length (mm)}}$$

### In vitro bioadhesive studies

Bioadhesive strength of the patches was evaluated by the modified method from Wong et al [6]. The measurement was conducted with texture analyzer (TA 500, LLOYD instrument, UK) The patches were stretched at a rate of 100 mm/min. Pig skin, as a model tissue, purchased from the market after the removal of all fats and wax on the surface. The skin and films were cut into  $10 \times 50 \text{ mm}^2$ . The patch and pig skin were overlapped in the area of  $1 \times 1.5 \text{ cm}^2$ . The work of adhesion was calculated from area under the force-distance curve, whereas the peak detachment force was the maximum force needed for detaching the patch from the tissue. Each measurement was repeated for six times.

### In vitro release studies

Extract release of transdermal patch containing *C. asiatica* extract was evaluated using a paddle type USP dissolution apparatus 5 (paddle over disk). It was performed using dissolution tester (708-DS, Agilent, Malaysia) equipped with dissolution sampling machine (850-DS, Agilent, Malaysia). The dissolution medium was 400 ml of phosphate buffer pH 7.4 at  $37 \pm 0.5 \text{ }^\circ\text{C}$  and stirring rate of 50 rpm under sink condition. 5 mL of samples were withdrawn and replaced by the fresh medium. The sample were analyzed using spectrophotometer (UV-1601, Shimadzu, Japan) at 278 nm. The cumulative extract release at various time intervals were calculated and plotted against time.

### Statistical analysis

The result was expressed as the mean  $\pm$  standard deviation. Analysis of variance (ANOVA) was used to test the statistical significance of the differences between groups.

## Result and discussion

### HPTLC Studies

Asiaticosides were quantified using calibration analysis. Linear regression was  $y = 46.844x - 169.9$  with coefficient of determination ( $R^2$ ) of 0.9991. The result of quantitative determination of asiaticoside from *C. asiatica* crude extract found that *C. asiatica* extract from AP Operations Co., Ltd. and Specialty Natural Products Co., Ltd. had the content of asiaticosides of 489.4041 mg/g crude extract and 500.1812 mg/g of crude extract respectively. However, asiaticosides in crude extract from Chemipan Corporation co., Ltd could not be detected. In Thai Pharmacopoeia, the chromatogram should demonstrate purple spot of asiaticosides with  $R_f$  of 0.27-0.28 [5], which was nearly similar to the purple spots from *C. asiatica* extract with  $R_f$  of 0.30-0.33 (Fig.1). The extract from Specialty Natural Products Co., Ltd. was chosen for preparing transdermal patches.

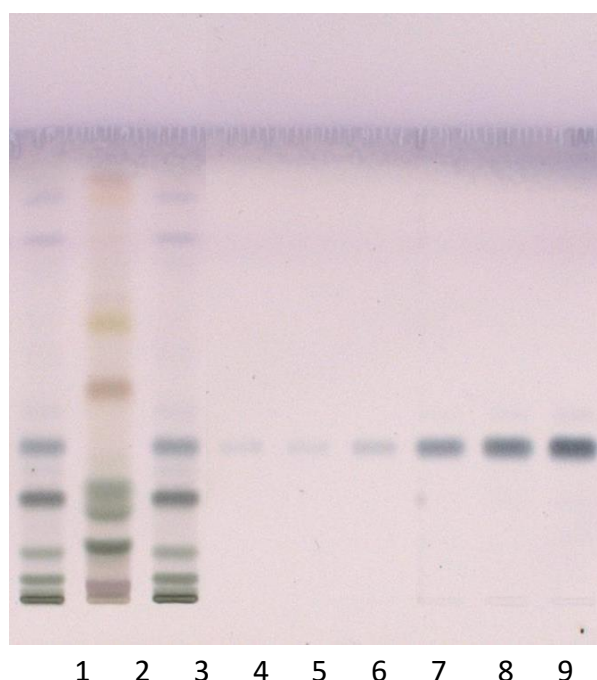


**Fig. 1** HPTLC of *C. asiatica* crude extract after detecting with anisaldehyde-sulphuric reagent. 1: crude extract from AP Operations Co., Ltd.; 2: crude extract from Chemipan Corporation co., Ltd.; 3: crude extract from Specialty Natural Products Co., Ltd.; 4-9: standard of asiaticoside

### Mechanical properties

Tensile strength and Young's Modulus of film bases were less than the patches containing *C. asiatica* extract (Table 2). The patches containing *C. asiatica* extract were more strengthen and less flexibility than those of film bases. Elongation and pH also decreased with the addition of *C. asiatica* extract (Table 2). In addition of 5% *C. asiatica* extract, the mechanical properties of transdermal patches prepared by Eudragit RL and the polymer blend would be better than the patched prepared by Eudragit RS.

### In vitro bioadhesive studies

The result of bioadhesive was shown in Table 3. The maximum load of the film bases would be more than the transdermal patches containing *C. asiatica* extract and the work of failure were not so much different. The bioadhesive property of patches would be decreased with the addition of *C. asiatica* extract. (Table 3).



**Table 2** Characterization of transdermal patches

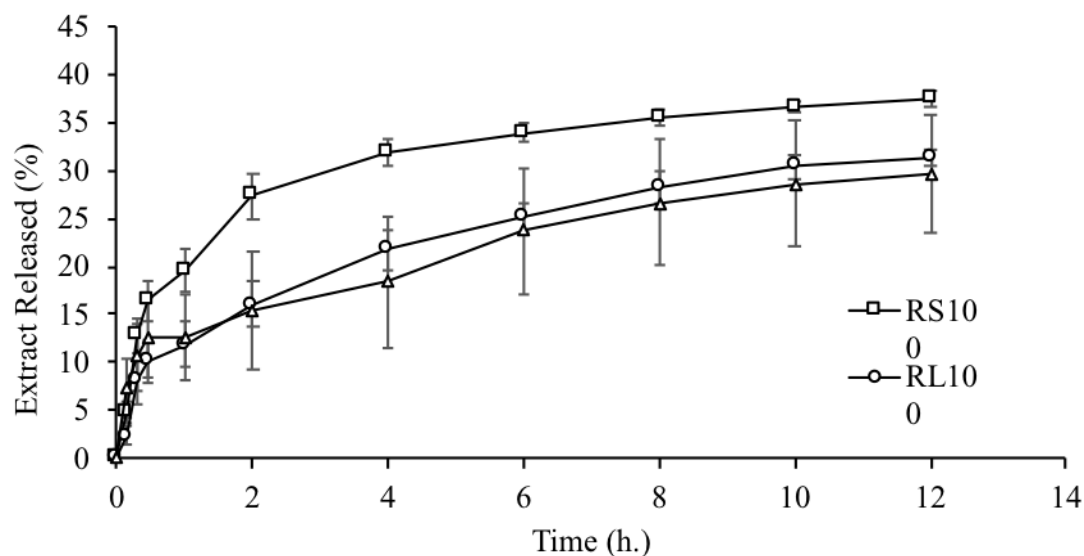
Formulations	Weight (g) <sup>a</sup>	Thickness (mm) <sup>a</sup>	pH <sup>b</sup>	Tensile strength (MPa) <sup>a</sup>	Elongation (%) <sup>a</sup>	Young's Modulus (Mpa) <sup>a</sup>
Films base	RS100	0.61 ± 0.01	0.098 ± 0.01	6.67 ± 0.31	1.853 ± 0.13	263.09 ± 50.19
	RL100	0.61 ± 0.01	0.093 ± 0.01	6.86 ± 0.08	1.959 ± 0.19	202.54 ± 27.26*
	MIX	0.61 ± 0.01	0.104 ± 0.01	6.74 ± 0.08	1.858 ± 0.29	264.89 ± 48.83
5%Extract	RS100	1.03 ± 0.02	0.144 ± 0.02	5.14 ± 0.07	7.239 ± 1.23	20.31 ± 10.65
	RL100	1.02 ± 0.02	0.132 ± 0.03	5.31 ± 0.07	7.486 ± 1.68	48.16 ± 8.75
	MIX	1.09 ± 0.08**	0.151 ± 0.03	5.08 ± 0.03	7.344 ± 0.85	33.76 ± 10.76

<sup>a</sup> Mean ± SD, n=6<sup>b</sup> Mean ± SD, n=3\* Compare different between of patch without 5% *C. asiatica* extract (P>0.05)\*\* Compare different between of patch containing 5% *C. asiatica* extract (P>0.05)**Table 3** Bioadhesive strength of transdermal patches

Formulations	Work of Failure (N/mm <sup>2</sup> )	Load at Maximum Load (N)
Films base	RS100	0.2937 ± 0.08
	RL100	0.4784 ± 0.21
	MIX	0.4282 ± 0.10
5%Extract	RS100	0.6881 ± 0.22
	RL100	0.4150 ± 0.15
	MIX	0.5838 ± 0.29

**In vitro release studies**

The extract release profile was shown in Fig 2. The release of *C. asiatica* from the patches prepared by Eudragit RS would be faster than those prepared by Eudragit RL and the Eudragit RS/RL blend. This finding was opposite to other studies. There was the study of transdermal patches containing stavudine. Formulations using Eudragit RS100:RL100 in ratio 1:9, 2:8, 3:7, 4:6 and 1:1. The drug release was increased when concentration of Eudragit RL100 increased [7]. The finding from the result could be possibly explained by hydrophobic and hydrophilic properties of *C. asiatica* extract and Eudragit RL. The extract preferred to be in Eudragit RL patch due to more similar properties than Eudragit RS patch.

**Fig. 2** Extract release profile of transdermal patches containing *C. asiatica* extract.

## Conclusions

*C. asiatica* extract from only two companies contained asiaticosides. *C. asiatica* extract had an impact on mechanical and bioadhesive properties of transdermal patches prepared by Eudragit RS, RL and their blend. The mechanical and bioadhesive properties would be decreased with the addition of *C. asiatica* extract. Eudragit RL and the polymer blend were chosen to further development of transdermal patches containing 5% by weight of *C. asiatica* extract due to the mechanical and bioadhesive properties. Improvement of extract release should be done to reach a good transdermal patch containing *C. asiatica* extract.

## Acknowledgement

This work was partly supported by Thai Traditional Medicine College, Rajamangala University of Technology Thanyaburi, Thanyaburi, Pathumthani, Thailand

## References

- [1] M. Bharkatiya, R. K. Nema, M. Bhatnagar, Development and characterization of transdermal patches of metoprolol tartrate, *Asian J. Pharm. Clin. Res.* 3(2) (2010) 130-134.
- [2] B. Rasool, U. Aziz, O. Sarheed, A. Rasool, Design and evaluation of a bioadhesive film for transdermal delivery of propranolol hydrochloride, *Acta Pharm.* 61(3) (2011) 271-282.
- [3] K. Suwannachote, G. C. Ritthidej, Development of transdermal patch comprising *Centella asiatica* extract, *Advanced Materials Research, Trans Tech Publ*, 2010, pp. 389-392.
- [4] B. Brinkhaus, M. Lindner, D. Schuppan, E.G. Hahn, Chemical, pharmacological and clinical profile of the East Asian medical plant *Centella asiatica*, *Phytomedicine* 7(5) (2000) 427-448.
- [5] Thai Pharmacopoeia Committee, BUA BOK-*Centella asiatica* Herbs, Supplement to Thai Herbal Pharmacopoeia2004.
- [6] C. Wong, K. Yuen, K. Peh, Formulation and evaluation of controlled release Eudragit buccal patches, *Int. J. Pharm.* 178(1) (1999) 11-22.
- [7] S.S. Kumar, B. Behury, P. Sachinkumar, Formulation and evaluation of transdermal patch of Stavudine, *Dhaka Univ. j. pharm. sci.* 12(1) (2013) 63-69.

# Physicochemical Properties of Rice Flour at Different Ripening Stages as Potential Excipients for Food and Pharmaceutical Products

Wiriya Onsaard<sup>1, a\*</sup>, Wachirapan Boonyaputthipong<sup>1, b</sup>, Apinya Ekpong<sup>1, c</sup>, Panchaporn Tadpitchayangkul Promchote<sup>1, d</sup> and Ekasit Onsaard<sup>1, e</sup>

<sup>1</sup> Department of Agro-Industry, Faculty of Agriculture, Ubon Ratchathani University  
85 Sathollamrk Rd., Warinchumrab, Ubon Ratchathani, Thailand

<sup>a</sup>wiriya.p@ubu.ac.th, <sup>b</sup> wachirapan.b@ubu.ac.th, <sup>c</sup>apinya.e@ubu.ac.th, <sup>d</sup>pan.p@ubu.ac.th,

<sup>e</sup> ekasit.o@ubu.ac.th

\* corresponding author

**Keywords:** Rice Flour; Ripening stages; Physicochemical Properties

**Abstract.** The physiochemical properties of rice flour were determined using a high amylopectin rice comparing between two stages: dough and mature stages as aimed to apply the flour for suitable food or pharmaceutical product development. Proximate analysis, amylose content, total starch content and thermal properties of flour were conducted with triplication. It was found that most of chemical components did not differ, exception of lipid content. However, the pasting properties of mature ripening flour provided a harder texture than the dough stage flour despite of the swollen starch granule was found less than the dough stage. It could be suggested that some complex chemical interaction may occur during heating and cooling of dough stage flour.

## Introduction

In Asian countries, the rice consumption per capita is 84.9 kg during year 2012-2014 (156.1 kg of total world consumption) and is expected to rise up to 86.8 kg by year 2024. The growth is expected to be higher in developing countries (1.2% p.a.) than in developed countries (0.4% p.a.) with Asian countries accounting for almost 80% of global consumption increase (OECD/FAO, 2015). However, a world rice production (494 Mt) was reported to have the same amount as the world rice consumption (488.8 Mt) during year 2012-2014. It can be confirmed that rice is a staple food of the world in particularly Asian and Pacific countries. Thus there are massive of research studying a rice grain quality by improving rice breeding as well as improving rice properties by using food technology approaching. However, most of all have been researched for rice grain at maturity stage but a few research works have been found to study on the other stage of rice grain (Singh and Juliano, 1977, Arai and Itani, 2000 and Ekasit and Jiraporn, 2013). The ripening stage of rice grain begins at fertilization and continues, through grain filling and ripening, approximately 25-35 days regardless of variety. Grain filling occurs as nutrients and water are transported from one part of the plant to another; the process is affected by the availability of water and nutrients, and by temperature. Formation of grain results mainly from accumulation of carbohydrates in the pistils of the florets. The primary source of the carbohydrate is from photosynthesis occurring in the uppermost three to four leaves and the stem. The carbohydrate that accumulates in grain is stored in the form of starch. The starchy portion of the grain is the endosperm. Initially, the starch is white and milky in consistency which is called milk stage. The following dough stage begins where the milky consistency of the starch in the endosperm changes as it loses moisture leading the milky liquid begins to solidify resulted that the endosperm becomes firm and has a chalky texture. Lastly, maturity stage is obtained where the physiological processes associated with grain filling cease

and the lost the moisture content occurs resulting of the endosperm becomes hard and opaque (Dunand and Saichuk, 1999). The immature rice stage was reported to have high sugar content than a maturity stage (Singh and Juliano, 1977) providing a different characteristic of rice product both texture and sensory. Arai and Itani (2000) found that the amylose content and protein content decreased during the maturity stage comparing between early-harvest (10 days earlier) and ordinary-harvest of Japanese rice grain but the value was not significant. Moreover, hardness value of the mature cooked rice became higher compared to the early-harvested cooked rice. On the other hand, the stickiness of the ordinary-harvested cooked rice was lower than the immature cooked rice. It could be suggested that different ripening stages of rice grain containing different chemical compositions would provide different pasting properties of rice flour which finally effect to the application for food and pharmaceutical product. Thus, this study was attempted to compare the physiochemical properties of rice flour at different ripening stage correlated to proximate compositions for Thai rice variety in order to apply for food and pharmaceutical products.

## **Methodology**

### **1. Raw material**

The dough and mature paddies (Lee Nok Var.) were obtained from a local farm at Trakan Phuet Phon district, Ubon ratchathani province which dough stage paddy was harvested at the 19-21 days after flower blooming on March 2017 and the mature paddy was also obtained on April 2017 the same rice field. The rice grain was packed in aluminum bag and stored at -18°C before analysis.

### **2. Proximate analysis and amylose content**

The proximate compositions were analyzed by using official methods of Association of Official Analytical Chemists (AOAC, 2000) as followed: moisture content, protein content, carbohydrate content, ash content, fat content, fiber content. The starch content of dough stage and mature rice flour were performed using amyloglucosidase/ $\alpha$ -amylase method (AOAC Method 996.11 and AACC Method 76-13.01, Megazyme kits). The amylose content analysis was conducted using method of starch-iodine colorimetry using a UV-spectrophotometer at 610 nm (Juliano, 1971). Triplication of analysis was conducted.

### **3. Pasting properties**

The pasting properties of rice flour were measured using Rapid Visco Analyzer (RVA) (RVA-4, NEWPORT, USA.). The pasting curve recorded Peak viscosity, Breakdown, Final viscosity, Setback, Pasting temperature, Trough and Peak Time. All the measurements were performed in triplicated.

### **4. Gelatinization temperature**

The rice flour was mixed with distilled water and was left overnight at 4°C in order to obtain 7% (wet basis) moisture content using 40  $\mu$ l aluminum pan. The Differential Scanning Colorimeter (DSC1, METTLER TOLEDO, Switzerland) was performed using the heating rate at 10°C/min and the heating temperature range was set as 20–110°C (Fan et al, 1999). Onset temperature ( $T_o$ ) peak temperature ( $T_p$ ), conclusion temperature ( $T_c$ ) and the endothermic energy of gelatinization ( $\Delta H$ , J/g) were recorded.

## **Results and discussion**

The rice flour was obtained by wet milling and was dried at temperature of 45°C for 6-8 hr until the moisture content less than 13% (wet basis). The grinding was conducted and passed through 80 mesh sieve. The proximate compositions of rice flour both dough and mature stages of Lee Nok var. were shown in Table 1. It can be found that most of chemical

compositions are not different between dough and mature stage, exception for fat content which decreased after the mature stage. Moreover, amylose and amylopectin content as well as total starch content were similar for both dough and mature rice flour.

**Table 1.** Proximate compositions, starch and amylose content of rice flour (Lee Nok var.) between dough and mature stage

<b>Compositions (%, wet basis)</b>	<b>Dough stage</b>	<b>Mature stage</b>
<b>Moisture content</b>	9.68 ± 0.02	9.77 ± 0.03
<b>Fat</b>	1.84 ± 0.03 <sup>a</sup>	1.68 ± 0.01 <sup>b</sup>
<b>Ash</b>	1.28 ± 0.02	1.23 ± 0.01
<b>Crude protein</b>	5.45 ± 0.12	5.69 ± 0.12
<b>Crude fiber</b>	0.78 ± 0.02	0.77 ± 0.01
<b>Carbohydrate</b>	80.95 ± 0.11	80.84 ± 0.08
<b>Amylose</b>	2.57 ± 0.08	2.55 ± 0.13
<b>Amylopectin</b>	97.42 ± 0.09	97.44 ± 0.13
<b>Total starch</b>	52.91±10.90	51.19±9.96

Note: Means±SD values with different letters in the same row are significantly different at \* $P < 0.05$

This result agreed with Arai and Itani (2000) which the protein content and amylose content were similar for both the ordinary-harvest and the early-harvest Japanese rice (harvested 10 days earlier). However, the hardness of Japanese cooked rice increased for the ordinary harvesting compared to the 10 days earlier harvesting. The result of Arai and Itani (2000) was compatible with this study as the final viscosity of mature rice flour was higher than the dough rice flour after cooling. It could be suggested that the dough ripening stage was reported to have high sugar content than a maturity stage (Singh and Juliano, 1977), thus a texture of cooked rice become softer than the mature ripening stage. However, peak viscosity of dough stage rice flour consisting of immature starch (data not shown) and various compositions was higher than that of the mature rice flour (Table 1) and the viscosity dropped rapidly after swelling compared to the mature rice flour (Fig. 1). Moreover, the lower initial temperature and the higher enthalpy of gelatinization were more observed in the mature rice flour (Table 2) as the mature amylopectin of rice which is mainly in glutinous rice would be occurred. Therefore, the result of physiochemical properties of rice flour at two different ripening stages could be considered as potential excipients for food, drug and cosmetic products by applying the appropriated rice flour stage for food and pharmaceutical product development.

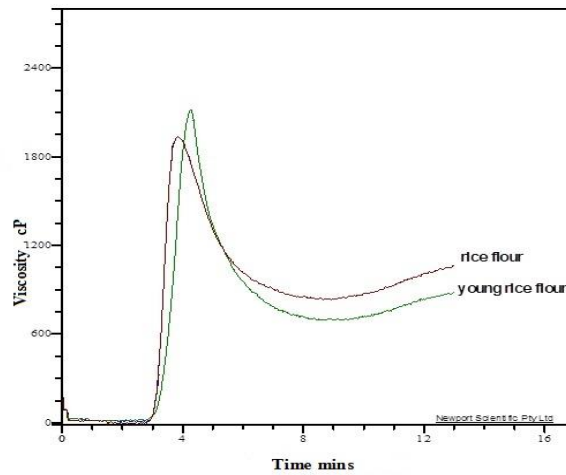


**Figure 1.** Pasting properties of rice flour (Lee Nok var.) between dough and mature stage

**Table 2.** Gelatinization temperature and enthalpy of rice flour (Lee Nok var.) between dough and mature stage using DSC

Rice stage	T <sub>o</sub> (°C)	T <sub>p</sub> (°C)	T <sub>c</sub> (°C)	T <sub>c</sub> -T <sub>o</sub> (°C)	ΔH (J/g)
<b>Dough</b>	66.40 ± 0.38 <sup>a</sup>	72.44 ± 0.24 <sup>a</sup>	79.85 ± 0.19 <sup>b</sup>	13.45 ± 0.28 <sup>b</sup>	2.32 ± 0.12 <sup>a</sup>
<b>Mature</b>	62.11 ± 0.05 <sup>b</sup>	71.05 ± 0.08 <sup>b</sup>	80.94 ± 0.07 <sup>a</sup>	18.83 ± 0.04 <sup>a</sup>	3.06 ± 0.04 <sup>b</sup>

Note: Means with different letters in the same column are significantly different at \**P*<0.05

### Summary

Proximate compositions of high amylopectin flour were similar for both dough and mature ripening stages. However, the pasting properties of dough rice flour were found higher in peak viscosity than the mature rice flour and the viscosity dropped rapidly after swelling compared to the mature rice flour which could be due to higher swollen starch. It could be due to some complex interaction between chemical compositions of dough rice flour during heating and cooling.

## References

- [1] AOAC. Official of Association of Analytical Chemist (17th Ed.), Association of Analytical Chemist, Washington D.C. (2000).
- [2] E.Arai and T.Itani. Effect of early harvesting of grains on taste characteristics of cooked rice. *Food Sci. Technol. Res.* 6(4) (2000) 252-256.
- [3] R. Dunan and J. Saichuk. Rice growth and development. In *Luisiana Rice Production Handbook*. Ed. Saichuk, J.LSU AgCenter Research and Extension, LSU AgCenter publication 2270, Louisian, (1999) 34-45.
- [4] O. Ekasit, and B. Jiraporn. Some physical characteristics and bioactive compounds of young flattern rice (Khao-Mao). *Int. Food Res. J.* 20(3) (2013) 1627-1632.
- [5] J. Fan , B.P. Marks, M.J. Daniels, T. J. Siebenmorgen. Effect of postharvest operations on the gelatinization and retrogradation properties of long-grain rice. *Trans. ASAE.* 42(3) (1999) 727-731.
- [6] Juliano, B.O. A simplified assay milled rice amylase. *J.Cereal Sci.* 16:334-338.
- [7] OECD/FAO. 2015. *OECD-FAO Agricultural Outlook 2015-2024*. OECD/Food and Agriculture Organization of the United Nations, OECD Publishing, Paris. [http://dx.doi.org/10.1787/agr\\_outlook-2015-en](http://dx.doi.org/10.1787/agr_outlook-2015-en) (1971).
- [8] R.Singh, and B.O. Juliano, B.O. Free sugar in relation to starch accumulation in developing rice grain. *Plant Physiol.* 59 (1977) 417-421.

## Formulation and evaluation of ginger lozenges

Pirapun Tangkittiwat<sup>1, a</sup>, Suwimon Kreuafan<sup>1, b</sup>, Ratana Indranupakorn<sup>2, c</sup>  
and Chawalinee Asawahame<sup>3, d \*</sup>

<sup>1</sup>Pharmaceutical Sciences students, Faculty of Pharmaceutical Sciences,  
Huachiew Chalermprakiet University, Thailand

<sup>2</sup>Department of Pharmacognosy, Faculty of Pharmaceutical Sciences,  
Huachiew Chalermprakiet University, Thailand

<sup>3</sup>Department of Industrial Pharmacy, Faculty of Pharmaceutical Sciences,  
Huachiew Chalermprakiet University, Thailand

<sup>a</sup>pirapuntangkittiwat@gmail.com, <sup>b</sup>fufukey.23138@gmail.com, <sup>c</sup>nong2indra@gmail.com,  
<sup>d</sup>chawalinee\_a@hotmail.com

**Keywords:** ginger, molded lozenges, compressed lozenges, wet granulation

**Abstract.** The aim of this study was to formulate herbal lozenges containing ginger extract to presented as an alternative oral dosage form to be used as an effective and safe treatment for nausea and vomiting. The lozenges were formulated by molding method and wet granulation method for producing candy lozenges and compressed lozenges containing ginger extract, respectively. Ginger rhizomes were extracted with 95% ethanol by simple maceration process. The extract was identified by using high performance liquid chromatography (HPLC) method to analyze for 6-gingerol, which is the major chemical composition that act as the active compound. The physical properties of formulated lozenges such as appearance, hardness, friability and organoleptic properties were carried out for the optimization of the formulation. The result show that 6-gingerol content in the ginger extract that used in this study was found to be 12.59% w/w. Ginger extract can be formulated into lozenges. The formulation of candy lozenges (3.4 g per lozenge) containing 13.5 mg of ginger extract with liquid glucose, sucrose, citric acid, propylene glycol and the formulation of compressed lozenges (500 mg per tablet) containing 6.75 mg of ginger extract with sugar free based excipients as mannitol, corn starch, starch gel, sodium stearyl fumarate, aspartame and citric acid were the optimized formulations that successfully formulated and evaluated.

### Introduction.

Ginger (*Zingiber officinale* Roscoe, Zingiberaceae) has been traditionally used both as the herb for food ingredient and a medicinal herb for treatment in many illness conditions. There are many evidences showed that ginger has antiemetic effect in many ways such as morning sickness, motion sickness or nausea and vomiting after chemotherapy. The most active chemical compounds of ginger are gingerols and shogaols that show biological activity as antiemetic agents [1, 2].

Lozenges are solid preparation that are intended to dissolve or disintegrate in mouth or pharynx. It can be given to patients who have difficulty in swallowing. Thus, lozenge is the dosage form of choice that can be chosen for patient who feel nauseous or vomiting. Commercially lozenges are made by molding or compression techniques [3, 4]. The aim of this study was to extract ginger and to formulate the lozenges containing ginger extract by molding method and wet granulation method for producing candy lozenges and compressed lozenges, respectively.



## Material and Methods

### Material.

Fresh gingers were purchased from Number one market (Samutprakarn, Thailand). Chemical substances were procured from commercial sources. Other chemicals for analytical studied were of analytical grade.

### Preparation of ginger extract.

Fifteen kilograms of ginger rhizomes were cleaned, washed and sliced to small pieces, then dried in the hot air oven at 60°C and ground to powder. The dried powder of ginger was macerated in 95% ethanol for 7 days then filtered through a membrane filter. The filtrate was concentrated by rotary evaporator (BUCHI Rotavapor R-205). Maceration was repeated twice on each residue. Percentage yield of ginger extract was calculated.

### Determination of 6-gingerol as active compound in ginger extract using HPLC.

The study for determine the content of 6-gingerol as active compound in ginger extract was carried out by HPLC system. 6-gingerol (Sigma, USA) was used as standard substance. The content of 6-gingerol in the sample was determined by using standard curve constructed by using several concentrations of standard solution. The RP-HPLC system was used for 6-gingerol analysis. The UV absorbance was measured at 280 nm. Chromatographic conditions were as follows: The mobile phase was acetonitrile (solvent A) and water (solvent B). The gradient elution was: 0 min, 40:60 (solvent A:B v/v); 6 min, 55:45; 13 min, 90:10; 30 min, 90:10. The flow rate was set at 1 mL/min and the sample volume injected was 20 µL.

### Preparation of ginger extract lozenges.

*By molding technique (Candy Molded Lozenges):* Sugar bases (sucrose and liquid glucose) and deionized water as solvent were weighed and heated up to 143°C. Propylene glycol and flavoring agent were added to the mixture of the sugar bases. After the temperature of the mixture was cooled down to 50 – 60°C, the ginger extract which was dissolved in small amount of ethanol and flavoring agent (if needed) were added and mixed together. The mixture was poured into the lubricated mold. The molded lozenges were hardened when the temperature of the mixture decreased to room temperature. The ginger molded lozenges were sealed and wrapped in aluminum foil sheet as a unit packaging. Visual inspection of ginger molded lozenges for physical properties were tested.

*By wet granulation technique (Compressed Lozenges):* Three different fillers were chosen to study for suitable filler when combined with mannitol as sugar-free filler bases for wet granulation method. Ginger extract, fillers (corn starch or microcrystalline cellulose or dicalcium phosphate, binder (pregelatinized starch), sweetening agent (aspartame), flavor (citric acid) and other flavoring agent (if needed) were weighed and form to be the damp mass. The damp mass was sieved with sieve no.10 and dried at 50 – 60°C for 1.5 hours. The dried granule mass was through sieve no.16. Dried granules were analyzed for moisture content, flow properties as angle of repose and percent compressibility. The granules were then mixed with lubricant and compressed into tablets by single stroke tableting machine. Used 15 mm flat-faced punch and 13 mm concaved punch for tablet weight 1000 mg/tablet and 500 mg/tablet, respectively. The physical properties of tablets were evaluated for hardness, thickness, friability and weight uniformity of tablets.

## Results and Discussion

### Preparation of ginger extraction and determination of active compound as 6-gingerol.

In this study, we employed maceration technique by using 95% ethanol as solvent for the extraction of ginger. After the extraction followed by concentration process, the dark brown

resin of ginger extract was collected. The percentage yield was calculated as 10.81% of ginger extract. The HPLC analysis of ginger extract was carried out with standard compound of 6-gingerol. HPLC chromatograms of standard 6-gingerol and representative ginger extract are showed in Fig. 1. Six concentrations of standard 6-gingerol (0.05, 0.075, 0.100, 0.150, 0.200 and 0.250 mg/mL) were used to established the calibration curve. The linear regression equation was  $y = 5E+07x + 425129$ , where  $y$  is peak area,  $x$  is amount of 6-gingerol and  $r^2$  is 0.9984. The content of active compounds was dependent on method and solvent that we used in the extraction. From HPLC analysis of the ginger extract from this study showed the same retention time (RT = 12.157 min) and had the active compound of 12.59% (w/w) of 6-gingerol.

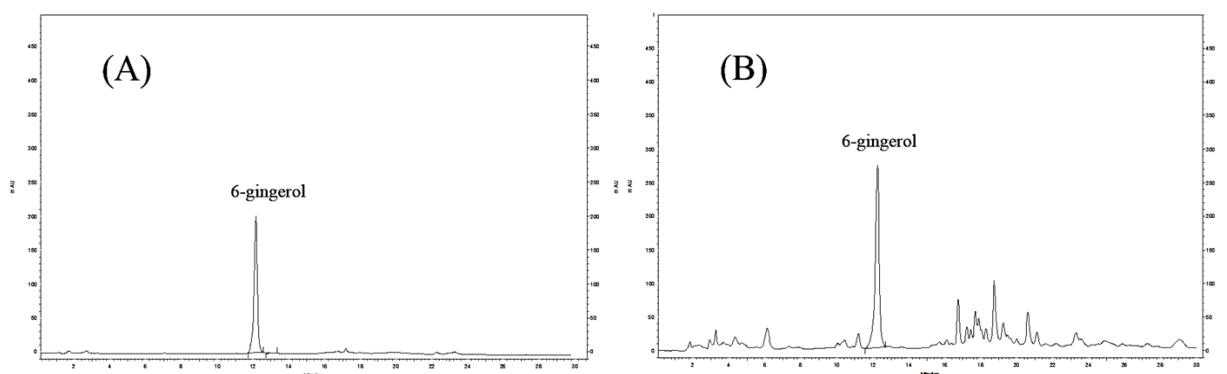


**Fig. 1** (A) HPLC chromatogram of 6-gingerol standard solution (B) HPLC chromatogram of ethanol ginger extract

### Preparation of ginger extract lozenges; by candy molding technique.

The formulations of ginger extract molded lozenges were showed in Table 1. The result showed that the suitable amount of candy base as mixture that poured into the mold to form a candy with appropriate size and shape was 3.4 g per lozenge. By using sucrose, liquid glucose, propylene glycol, citric acid and deionization can be produced candy molded lozenges with good appearances. Ginger extract as active ingredient which was added into the mixture of candy base tended to decrease the hardness of lozenges. Added propylene glycol from 0.24 to 2.4% in the ginger extract lozenge formulations can improve the strength of the lozenges. Various amounts of ginger extract were incorporated in the formulations (A<sub>2</sub> – A<sub>5</sub>) that equivalented with the active ingredient as dried ginger powder between 125 – 350 mg/ lozenge. It was found that, the formulations that comprising with the high amount of ginger extract gave a very dominant flavor and very spicy taste. Thus, decreased the amount of ginger extract to 13.5 mg/ lozenges (A<sub>5</sub>) was the suitable amount of ginger extract that the sweeteners in candy base can mask the spicy taste of ginger. Lozenges are usually hygroscopic in nature hence ginger molded lozenges should be kept in single unit packaging and then placed in water resistant container.

**Table 1.** Composition of ginger molded lozenges

Ingredients	A <sub>1</sub>	A <sub>2</sub>	A <sub>3</sub>	A <sub>4</sub>	A <sub>5</sub>
Ginger extract [mg/lozenge]	-	37	27	18.5	13.5
Sucrose [%]	53 – 57				
Liquid glucose [%]	30				
Propylene glycol [%]	0.24		2.4		
Citric acid [%]	0.1				
Menthol [%]	0.1	-	-	-	-
Purified water	qs				

### Preparation of ginger extract lozenges; by wet granulation technique.

Wet granulation method was used for making ginger compressed lozenges. Three fillers; corn starch, microcrystalline cellulose and dicalcium phosphate were studied for chosen as suitable filler which was combined with mannitol to use as sugar- free filler in the formulations (B<sub>1</sub> – B<sub>3</sub>). The results showed that using corn starch with mannitol as filler could be produced the tablets with good physical properties and had better mouth feel when compared with other fillers. Four different formulations of ginger compressed lozenges were formulated to varied the amount of ginger extract in the lozenges between 37 – 6.75 mg/tablets (B<sub>4</sub> – B<sub>7</sub>).

The prepared ginger extract granules for compression were evaluated for moisture content and flow properties. The results revealed that all of the formulation showed good flow property in term of angle of repose (35.3 – 36.1°), compressibility index (14 – 16%) and the moisture content of the granules was not excess 2%. The ginger compressed lozenges were evaluated for various parameters. All the formulations showed acceptable results for weight uniformity test. The hardness of the tablets was found in the range 5.36 ± 0.59 – 10.07 ± 0.91 kp. The friability of ginger compressed lozenges was found to be within 1% except in the formulation B<sub>5</sub> that failed in friability test. The thickness of the thin tablets in formulations B<sub>1</sub> – B<sub>5</sub> (total weight 1000 mg/tablet, diameter of tablet; 15 mm) were in the range of 3.19 ± 0.17 – 3.31 ± 0.11 mm that made the dissolving time in the mouth so quickly. Formulation B<sub>5</sub> and B<sub>6</sub> which decreased the amount of ginger extract in the lozenges to 9.25 and 6.75 mg/tablets, respectively and total weight of tablet was reduced to 500 mg/tablet (diameter of tablet; 13 mm) possessed good mechanical strength with suitable thickness in the range of 5.31 ± 0.11 - 5.30 ± 0.18 mm and passed friability test. The spicy taste of ginger was reduced by decreasing in the amount of ginger extract that comprised in the compressed tablets. By using only sugar-free fillers and sweetening agent, the spicy taste of ginger still remained in the compressed lozenges. The prepared ginger compressed lozenges were found to be pale yellow in color. The formulations of ginger compressed lozenges were showed in Table 2.

**Table 2.** Composition of ginger compressed lozenges

Ingredients	B <sub>1</sub>	B <sub>2</sub>	B <sub>3</sub>	B <sub>4</sub>	B <sub>5</sub>	B <sub>6</sub>	B <sub>7</sub>
Ginger extract [mg/lozenge]	-	-	-	37	18.5	9.25	6.75
Corn starch [%]	30	-	-	30			
Microcrystalline cellulose [%]	-	30	-	-	-	-	-
Dicalcium phosphate [%]	-	-	30	-	-	-	-
Mannitol [%]	qs						
Starch gel [%]	3				5		
Aspartame [%]	1					1.5	
Citric acid [%]	1						
Sodium stearyl fumarate [%]	0.5						

\* Total weight of tablets: Formulation B<sub>1</sub> – B<sub>5</sub> were 1000 mg/tablet, Formulation B<sub>6</sub> – B<sub>7</sub> were 500 mg/tablet

Hence based on good physical properties and the satisfaction of taste and mouthfeel of ginger lozenges amongst all formulations, the formulation A<sub>5</sub> and B<sub>7</sub> were selected as the best formulations for ginger molded lozenges and ginger compressed lozenges, respectively.

## Summary

Ginger extract obtained from maceration method that used in this study contained the active compound of 6-gingerol which has antiemetic effect. Both of molded lozenges and compressed lozenges of ginger extract can be prepared successfully. The taste of the ginger lozenges was sweet with mild pungent taste of ginger and acceptable physical properties. Ginger lozenges provide easy administration that can be use as an alternative dosage form for treatment nausea and vomiting.

## References

- [1] D. Bhowmik, C. Pankaj, K.K. Tripathi, M.R. Chandira, K.P.S. Kumar, *Zingiber officinale* the herbal and traditional medicine and its therapeutically importance, Res J Pharmacognos Phytochem. 2 (2010) 102-110.
- [2] I. Lete, J. Allue, The effectiveness of ginger in the prevention of nausea and vomiting during pregnancy and chemotherapy, Integr Med Insights. 11 (2016) 11-17.
- [3] R. Pothu, M.R. Yamasani, Lozenges formulation and evaluation: A review, JAPR. 5 (2014) 290-298.
- [4] R.B. Semwal, D.K. Semwal, S. Combrinck, A.M. Viljoen, Gingerols and shogaols: Important nutraceutical principles from ginger, Phytochemical. 117 (2015) 554-568.

# Formulation and *in-vitro* evaluation of fast dissolving tablets using superdisintegrant blend with effervescent material

Noppadol Chongcherdsak<sup>1, a</sup>, Chutima Limmatvapirat<sup>2, b</sup> and Sontaya Limmatvapirat<sup>3, c\*</sup>

<sup>1</sup>Department of Pharmaceutical Care, Faculty of Pharmacy, Siam University, Bangkok, 10160 Thailand

<sup>2</sup>Department of Pharmaceutical Chemistry, Faculty of Pharmacy, Silpakorn University, Nakhon- Pathom, 73000, Thailand

<sup>3</sup>Department of Pharmaceutical Technology, Faculty of Pharmacy, Silpakorn University, Nakhon- Pathom, 73000, Thailand

<sup>a</sup>Noppadol.cho@siam.edu, <sup>b</sup>Limmatvapirat\_C@su.ac.th, <sup>c</sup>Limmatvapirat\_S@su.ac.th

\*Corresponding author

**Keywords:** Fast Dissolving Tablets, Direct Compression, Superdisintegrants, Effervescent

**Abstract.** The objective of this study was to formulate fast dissolving tablets (FDTs) using superdisintegrant and effervescent material. The tablets were prepared by direct compression method. The effect of superdisintegrant content was studied. The weight and hardness were controlled within the range of  $500\pm 20$  mg and  $50\pm 10$  N, respectively. Tableting properties including weight, thickness, diameter, friability, hardness, wetting time, water absorption ratio and *in-vitro* dispersion time were evaluated. As a result, the physical properties of tablets were within the required limit. As increasing the amount of sodium starch glycolate, the water absorption ratio had a tendency to increase. However, the wetting and dispersion time took more longer. By effect of adding effervescent material (tartaric acid and sodium bicarbonate), the wetting and dispersion time were lower. The time showed less than 3 min that represented a good characteristic of FDTs. This study showed that, among the designed formulations, the formulation containing effervescent material emerges as the overall best formulation based on drug dissolving characteristics.

## Introduction

The tablet is the most preferred dosage form due to its common and convenience. However, geriatric, pediatric and mentally ill patients experiences difficulty in swallowing conventional tablets, which lead to poor patient compliance [1]. To solve this problem, the developed drug delivery system known as fast dissolving/disintegrating tablets (FDTs) is introduced. These tablets are dissolved/disintegrated in saliva within few seconds without water. To fabricate FDTs, various techniques are used such as lyophilization, direct compression method, melt granulation, etc [2]. Therefore the objectives of this research were to formulate FDTs by using combination technique (direct compression method and gas generating system) to enhance the properties of FDTs.

## Experimental

### Materials

Microcrystalline cellulose, sodium starch glycolate and spray dried lactose were purchased from DFE Pharma (Netherlands). Talcum, citric acid, tartaric acid and sodium bicarbonate were obtained from Vidhyasom (Thailand). Aspartame and magnesium stearate were purchased from Srichand (Thailand).

## Preparation of tablets

The formula with different amount of excipient were compressed by direct compression method as show in **Table 1**. All ingredient were grounded into fine particles and passed through screen number 40 mesh before used. The first steps, tablets without drug were prepared to find out the optimum formula and then selected the best formula to further investigation with drug. The excipients were mixed for 5 min and then magnesium stearate was subsequently added to powder mixture and mixed for another 5 min. The total time of mixing was 10 min. The powder mixture was then compressed with flat-faced single punch tableting machine. The weight and hardness of tablets were controlled within  $500\pm 20$  mg and  $50\pm 10$  N, respectively. All tablets were kept in the ambient temperature before evaluated.

**Table 1.** Formulation of blank tablets (% by weight)

Ingredient	F1	F2	F3	F4
Microcrystalline cellulose	20	20	20	20
Sodium starch glycolate	10	20	30	10
Citric acid	1	1	1	1
Talcum	1	1	1	1
Aspatame	1	1	1	1
Magnesium stearate	1	1	1	1
Tartaric acid	-	-	-	2
Sodium bicarbonate	-	-	-	3.4
Spray dried lactose	66	56	46	60.6

## Tablet evaluation

Weight variation was measured by analytical balance (Sartorius CP224S, Germany). Hardness, diameter and thickness were comparatively evaluated by digital thickness guage (Mitutoyo, Japan) and hardness tester (Pharmatest PTB311, Germany), respectively. Friability was measured by USP-type Roche friabilitor. Wetting time, water absorbtion ratio and *in-vitro* dispersion time were determined by Gohel *et al.* (2004) method [3]. Water absorbtion ratio (R) was calculated by using Eq.1. Where  $W_b$  was the weight of tablet before study and  $W_a$  was the weight of tablet after study.

$$R = 100 \times (W_a - W_b) / W_b \quad (1)$$

## Result and Discussion

### Physical properties of blank tablets

The powder mixture has a good free flowing by considering Carr's index and Hausners's ratio. The blank tablets were successfully fabricated by direct compression method. The weight and hardness of blank tablets were within the the required range. All formulation passed % friability limit. All data are represented in Table 2.

**Table 2.** Physical properties of blank tablets

Formulation	Weight variation (mg)	Thickness (mm)	Diameter (mm)	Hardness (N)	Friability (%)
F1	505.26±10.98	3.01±0.09	12.01±0.02	53.17±8.65	0.94
F2	503.67±8.53	3.04±0.05	12.10±0.01	57.37±5.04	0.83
F3	509.81±13.49	2.99±0.05	12.06±0.01	58.83±7.85	0.67
F4	500.83±7.95	2.93±0.05	12.02±0.01	55.43±4.02	0.75

**Absorption ratio.**

The blank tablets were evaluated in water and artificial saliva. The percentage of absorption ratio is show in **Fig.1**. The result revealed that the amount of superdisintegrant increased (F1-F3), the absorption ratio had tendency to increase proportionally. This might be the effect of sodium starch glycolate allowing rapid water uptake. In case of tablet containing effervescent material (F4), the absorption ratio was lower than the earlier formulation. After F4 contacted with solution, the solution could penetrate and react with effervescent material to generate gas [4,5]. The weight of tablet was lost after the reaction resulting in reduction of absorption ratio.

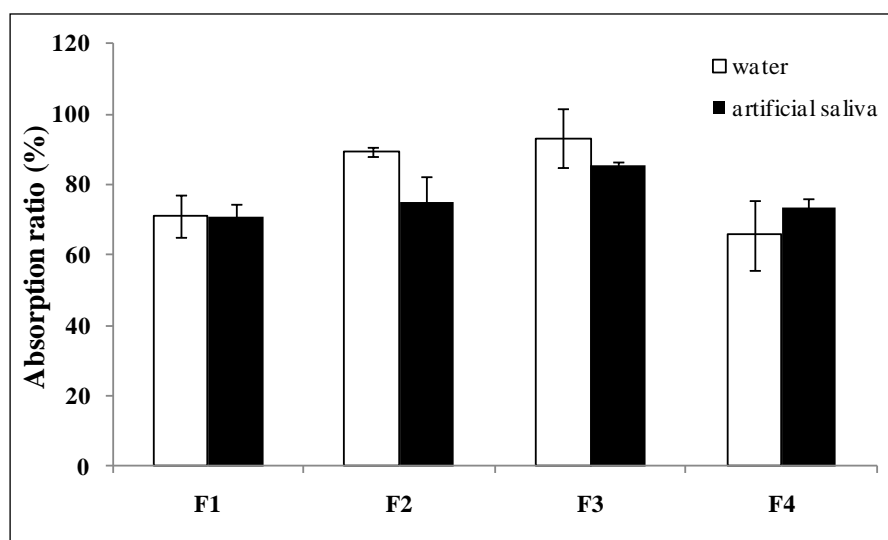


**Figure 1.** Absorption ratio

**Table 3.** Wetting time and dispersion time

Formulation	Wetting time (sec.)		Dispersion time (sec.)	
	water	artificial saliva	Water	artificial saliva
F1	99.17±19.69	323.35±12.13	71.67±1.52	213.35±5.93
F2	178.42±23.20	468.35±32.72	90.12±2.32	275.35±3.62
F3	219.67±21.17	693.73±6.70	167.33±3.76	482.73±7.50
F4	31.97±3.05	213.12±18.29	31.37±1.79	102.12±11.24

### Wetting time and dispersion time.

The most important parameter that needs to be optimized in the development of FDTs are wetting and dispersion time. The tablets were evaluated in water and artificial saliva. The data are showed in **Table 3**. The result showed that as the amount of superdisintegrant increased, the wetting and dispersion time also increased. This might be the property of sodium starch glycolate in terms of less tendency toward gel formation [6]. In case of tablet containing effervescent, the wetting and dispersion time were reduced.

### Summary

In the present work, fast dissolving tablets were prepared by direct compression method. The low values of the standard deviation of average weight, thickness, diameter and hardness of tablets indicated uniformity within the batches prepared. The reduced dispersion time of formulation containing effervescent material showed the characteristic advantages of FDTs over conventional dosage form.

### References

- [1] V. Parkash, S. Maan, Deepika, S.K. Yadav and V. Jogpai, Fast disintegrating tablets: Opportunity in drug delivery system, *J Adv Pharm Technol Res.* 2 (2011) 223-235.
- [2] V. Dave, R.B. Yadav, R. Ahuja and S. Yadav, Formulation design and optimization of novel fast dissolving tablet of chlorpheniramine maleate by using lyophilization techniques, *B-FOPCU.* 55 (2017) 31-39.
- [3] M. Gohel, M. Patel, A. Amin, R. Agrawal, R. Dave and N. Bariya, Formulation design and optimization of mouth dissolve tablets of nimesulide using vacuum drying technique, *AAPS PharmSciTech.* 5 (2004) 10-15.
- [4] F. Stops, J.T. Fell, J.H. Collett, H.L. Sharma and L.G. Martini, Floating dosage forms to prolong gastro-retention – The characterisation of calcium alginate beads, *Int. J. Pharm.* 350 (2008) 301-311.
- [5] N. Chongcherdsak, D. Aekthammarat, C. Limmatvapirat and S. Limmatvapirat, Fabrication of shellac-based effervescent floating matrix tablet as a novel carrier for controlling of drug release, *Adv. Mat. Res.* 747 (2013) 135-138.
- [6] R. Santanu, S.D. Hussan, V. Pooja, S. Devina and S. Sonam, A concise review on novel aspects of superdisintegrants, *Int. Res J Pharm. App Sci.* 2 (2012) 207-213.



# Chemical constituents and antioxidant activities of *Curcuma roscoeana* Wall. rhizomes

Orawan Theanphong<sup>1,a\*</sup>, Thaya Jenjittikul<sup>2,b</sup> and Withawat Mingvanish<sup>3,c</sup>

<sup>1</sup> Department of Pharmacognosy, College of Pharmacy, Rangsit University, Pathumthani, 12000, Thailand.

<sup>2</sup> Department of Plant Science, Faculty of Science, Mahidol University, Bangkok, 10400, Thailand.

<sup>3</sup> Organic Synthesis, Electrochemistry & Natural Product Research Unit, Department of Chemistry, Faculty of Science, King Mongkut's University of Technology Thonburi, Bangkok 10140, Thailand.

\*[orawan.t@rsu.ac.th](mailto:orawan.t@rsu.ac.th), <sup>b</sup>[thaya.jenjtit@gmail.com](mailto:thaya.jenjtit@gmail.com), <sup>c</sup>[withawat.min@kmutt.ac.th](mailto:withawat.min@kmutt.ac.th)

**Keywords:** *Curcuma roscoeana*, antioxidant activity, Zingiberaceae

**Abstract.** The hydrodistilled essential oil and crude ethanolic extract from the fresh rhizomes of *Curcuma roscoeana* were investigated for their chemical constituents and antioxidant activities. The major component of the essential oil was found to be tricyclene (45.18%). Preliminary phytochemical screening results of the crude ethanolic extract revealed the presence of triterpenoids. Antioxidant activities were evaluated using five different methods including DPPH radical scavenging, hydroxyl radical scavenging, superoxide anion radical scavenging, ferrous ion chelating and ferric reducing power assays. *L*-ascorbic acid and ethylenediaminetetraacetic acid (EDTA) were used as a positive control. The essential oil and crude ethanolic extract showed strong hydroxyl radical scavenging and superoxide anion radical scavenging activities as well as high ferric reducing power.

## Introduction

Reactive oxygen species (ROS), byproducts of cellular redox processes, include free radicals such as superoxide anion radicals ( $O_2^{\cdot-}$ ), hydroxyl radicals ( $OH^{\cdot}$ ), and non-free radical species such as hydrogen peroxide ( $H_2O_2$ ) and singlet oxygen ( $^1O_2$ ) [1]. ROS can generate oxidative stress that is a major cause of several chronic and degenerative diseases such as cancer, cardiovascular and neurodegenerative diseases [2].

Naturally occurring antioxidants exhibit their antioxidant activities by various mechanisms including breakup of chain reactions by donation of hydrogen atoms or electrons that convert free radicals into more stable species and decomposition of lipid peroxides into more stable final products [3].

Several essential oils and crude extracts from rhizomes of *Curcuma* species such as *C. aeruginosa*, *C. amada*, *C. aromatic*, *C. longa* and *C. zedoaria*, have been reported for their antioxidant activities [4-19].

*C. roscoeana* or Jewel of Burma is a rhizomatous herb in the family Zingiberaceae. It is cultivated as an ornamental plant. However, there have been no reports on chemical constituents and antioxidant activities of the fresh rhizomes of *C. roscoeana*. Thus, the aims of this study were to investigate chemical compositions of the essential oil and crude ethanolic extract obtained from the fresh rhizomes of *C. roscoeana* and to evaluate their *in vitro* antioxidant activities.

## **Material and Methods**

### **Plant material**

The fresh rhizomes of *C. roscoeana* were collected in November-December, 2015 from Prachin Buri provinces, Thailand and identified by Assist. Prof. Dr. Thaya Jenjittikul. The voucher specimen of this plant sample was deposited at College of Pharmacy, Rangsit University, Thailand.

### **Preparation of plant extract**

The fresh rhizomes of *C. roscoeana* (750 g) were washed with tap water, air dried, cut into small pieces and ground with the blender. The ground plant sample was divided into two portions for hydrodistillation and solvent extraction.

### **Extraction procedure**

The crude ethanolic extract was prepared by macerating 350 g of ground plant sample with ethanol (500 ml x 3 times x 3 day each). The extract was collected and filtered and the filtrate was concentrated to afford the crude extract under reduced pressure at 40°C.

### **Isolation of essential oil**

The ground rhizomes (350 g) were subjected to water distillation using Clevenger apparatus for 3 hr. The essential oil was collected and stored at 4°C in air-tight containers before analyzed by GC-MS technique.

### **GC-MS Analysis**

Essential oil was diluted in ethanol (HPLC grade, Merck, Germany) with the oil:ethanol ratio of 1:25 by volume. GC-MS analysis was performed using an Agilent Technologies 7890A GC system equipped with a 5975C inert XL EI/CI MAD with Triple-Axis detector. The DB-5MS (Phenyl Arylene polymer virtually equivalent to a (5%-Phenyl)-methylpolysiloxane) capillary column (30 m in length, 0.25 mm i. d., and 0.25 μm in thickness) was used for GC analysis. Helium gas was used as a carrier gas with the flow rate of 1 ml/min. One microliter of the diluted essential oil was injected using GC sampler 80 autosampler (splitless). The operating conditions for GC oven started by being held at 60°C for 1 min, ramped at the rate of 3°C/min to 240°C and held for 5 min. The GC injector and GC-MSD interface temperatures were set at 180°C and 290°C, respectively. Electron impact ionization positive mode at 70 eV was acquired over the mass range of 40-650 m/z at the scanning rate of 2.42 amu / second.

### **Identification of essential oil components**

Essential oil components were identified by comparing their mass fragmentation patterns with the mass fragmentation patterns from Adams Essential Oil Mass Spectral Library and NIST05 Mass Spectral Library. The amount of each essential oil component was determined based on peak area measurement.

### **Preliminary phytochemical screening**

Preliminary phytochemical screening of the crude extract, i. e. alkaloids, anthraquinones, saponins, cardiac glycosides flavonoids and tannins, was performed by following the methods of Evans, 2009 [20] with a few modifications. The phytosterols and triterpenoids were screened by method of Tiwari *et al.*, 2011[21] with a few modifications.

### **Antioxidant activities**

The antioxidant activities of the essential oil and crude ethanolic extract were evaluated by five difference methods including DPPH radical scavenging [22], hydroxyl radical scavenging [22], ferrous ion chelating [22], superoxide anion radical scavenging [1] and ferric

reducing power assays [23]. *L*-ascorbic acid and ethylenediaminetetraacetic acid (EDTA) were used as a positive control.

### Statistical analysis

All experiments were performed in triplicate. The experimental results were reported as mean  $\pm$  SD. The Duncan test and one-way analysis of variance (ANOVA) were used for multiple comparisons (SPSS Statistics version 18).

## Results and discussion

### Chemical constituents of essential oil

The essential oil obtained from water distillation of the fresh rhizomes of *C. roscoeana* was clear and pale yellow oil with the percent yield of 0.23% v/w. Twenty eight compounds corresponding to 99.08% of total oil content were identified. The chemical compositions of the essential oil, their peak area percentages and Kovats Indices (KIs) are tabulated in Table 1.

The essential oil of *C. roscoeana* rhizomes was mainly dominated by monoterpene hydrocarbons (73.71%), which was represented by tricyclene. Three major components included tricyclene (45.18%), camphene (25.95%) and camphor (11.61%).

**Table 1.** Essential oil components of the fresh rhizomes of *C. roscoeana*

Chemical constituents	KI <sup>a</sup>	Content(%)
<b><u>Monoterpene hydrocarbons</u></b>		
Tricyclene	926	<b>45.18</b>
$\alpha$ -Pinene	939	0.87
$\beta$ -Pinene	979	0.17
Myrcene	990	0.12
Camphene	990	25.95
Limonene	1029	1.42
<b><u>Oxygenated monoterpenes</u></b>		
Camphor	1146	11.61
Borneol	1169	0.16
Isobornyl acetate	1285	0.27
<b><u>Sesquiterpene hydrocarbon</u></b>		
$\alpha$ -Cubebene	1348	0.34
Cyclosativene	1371	0.80
$\alpha$ -Copaene	1376	3.10
Sativene	1391	0.20
Caryophyllene	1419	0.48
Aristolene	1433	0.10
Aromadendrene	1441	0.10
$\alpha$ -Muurolene	1479	0.36
<i>trans</i> -Calamenene	1522	0.18
Epizonarene	1529	0.17
Alloaromadendrene	1641	1.29
6- $\alpha$ -Cubebene	-	0.18
(+)- <i>epi</i> -Bicyclosesquiphellandrene	-	0.16
Cubenene	-	1.19
<b><u>Oxygenated sesquiterpene</u></b>		
Carvenone	1258	2.44
Caryophyllene oxide	1583	0.54
Ledol	1602	1.23
7- $\alpha$ -Eudesmol	1663	0.37
<b><u>Hydrocarbons</u></b>		
2-Undecanone	1294	0.10

<b>Compound class</b>	
<i>Terpenoids</i>	
- Monoterpene hydrocarbons	73.71
- Oxygenated monoterpenes	12.04
- Sesquiterpene hydrocarbons	8.65
- Oxygenated sesquiterpenes (	4.58
<i>Hydrocarbons</i>	0.10
<b>Total identified</b>	<b>99.08</b>

<sup>a</sup>: Kovats index is determined relative to n-alkanes (C6–C24) on a DB-5 MS column

### Preliminary phytochemical screening

The preliminary phytochemical screening results of the crude ethanolic extract showed the presence of triterpenoids. (Table 2). This result was also in agreement with the previous reports. Triterpenoids have been found in the crude extracts from the rhizomes of several *Curcuma* species such as *C. aeruginosa*, *C. aromatica*, *C. caesia*, *C. longa* and *C. xanthorrhiza* [6, 24-26].

**Table 2.** Phytochemical constituents of the fresh rhizome of *C. roscoeana*

<b>Test</b>	<b>Result</b>
Alkaloids	-
Anthraquinones	-
Saponins	-
Cardiac glycosides	-
Flavonoids	-
Tannins	-
Phytosterols	-
Triterpenoids	+

+ : Present - : Absent

### Antioxidant activities

The antioxidant activities of the essential oil and crude ethanolic extract were investigated by using DPPH radical scavenging assay, hydroxyl radical scavenging assay, superoxide anion radical scavenging assay, ferrous ion chelating assay and ferric reducing power assay. The DPPH radical scavenging and ferrous ions chelating activities of both essential oil and crude ethanolic extract were significantly less than those of *L*-ascorbic acid and EDTA, respectively. The crude ethanolic extract exhibited stronger activity for scavenging superoxide anion radicals as compared with *L*-ascorbic acid. Furthermore, it was found that the effectiveness of scavenging superoxide anions was in the decreasing order: crude ethanolic extract > essential oil = *L*-ascorbic acid. The hydroxyl radical scavenging activity of crude ethanolic extract was significantly higher than essential oil. However, the EC<sub>50</sub> of crude ethanolic extract and essential oil were insignificantly different from those of *L*-ascorbic acid. In addition, the essential oil and crude ethanolic extract exhibited strong ferric reducing power as compared with *L*-ascorbic acid. The EC<sub>50</sub> values of the essential oil, crude ethanolic extract and positive controls were shown in Table 3.

The results were similar to those previously reported. Several essential oils and crude extracts from rhizomes of *Curcuma* species have been reported for their antioxidant activities such as *C. aeruginosa*, *C. aromatica* and *C. leucorrhiza* [4, 12, 28-31].

**Table 3.** The EC<sub>50</sub> values of the fresh rhizome of *C. roscoeana*

Test	EC <sub>50</sub> (µg/ml)*		
	Essential oil	Crude ethanolic extract	Positive control**
DPPH radical scavenging assay	51.68 ± 1.63 <sup>a</sup>	14.32 ± 1.44 <sup>b</sup>	10.77 ± 0.97 <sup>c</sup>
OH Scavenging assay	19.99 ± 1.14 <sup>a</sup>	16.92 ± 1.37 <sup>b</sup>	18.27 ± 1.54 <sup>a,b</sup>
Superoxide anion radical scavenging assay	32.72 ± 1.87 <sup>a</sup>	30.14 ± 1.02 <sup>b</sup>	35.21 ± 1.10 <sup>a</sup>
Ferrous ion chelating assay	247.97 ± 3.74 <sup>a</sup>	193.44 ± 4.56 <sup>b</sup>	154.19 ± 2.45 <sup>c</sup>
Ferric reducing power assay	0.10 ± 0.01 <sup>a</sup>	0.09 ± 0.01 <sup>a</sup>	0.11 ± 0.02 <sup>a</sup>

\* Data are expressed as means ± SD (n = 3)

\*\* *L*-ascorbic acid was used as a positive control in DPPH radical scavenging assay, OH• radical scavenging assay,

Superoxide anion radical scavenging assay and Ferric reducing power assay.

EDTA was used as a positive control in Ferrous ion chelating assay

Means ± SD followed by the same letter for each experiment, within a row, are not significantly different (P > 0.05).

### Conclusion

This is the first report on the chemical compositions of the fresh rhizomes of *C. Roscoeana*. The results obtained might be used as additional information for further phytochemical and chemotaxonomic studies of plants in genus *Curcuma*.

It can be concluded that the essential oil and crude ethanolic extract from the fresh rhizomes of *C. roscoeana* might be a potential source of natural antioxidants that could be used as a natural additive in food and pharmaceutical industries. Thus, it is value added for an ornamental plant or cutting flower i.e. *C. roscoeana*. In addition, other biological activities and toxicities from the essential oil and crude ethanolic extract of this plant material should be further studied.

### Acknowledgments

The authors would like to acknowledge the Research Institute of Rangsit University for financial support (Grant no. 28/2559).

### References

- [1] M.A. Hussein, A convenient mechanism for the free radical scavenging activity of resveratrol, *Int J Phytomed*, 3(2011) 459-469.
- [2] L.A. Pham-Huy, H. He, C. Pham-Huy, Free radicals, antioxidants in disease and health, *Int J Biomed Sci*, 4(2008) 89-96.
- [3] T. Iqbal, A.I. Hussain, S.A.S. Chatha, S.A.R. Naqvi, T.H. Bokhari, Antioxidant activity and volatile and phenolic profiles of essential oil and different extracts of wild mint (*Mentha longifolia*) from the Pakistani Flora, *J Anal Methods Chem*, 2013. doi.org/10.1155/2013/536490.
- [4] M. George, S.J. Britto, Phytochemical and antioxidant studies on the essential oil of the rhizome of *Curcuma aeruginosa* Roxb., *Int Res J Pharm*, 6(2015) 573-579.
- [5] O. Theanphong, W. Mingvanish, C. Kirdmanee, Chemical constituents and biological activities of essential oil from *Curcuma aeruginosa* Roxb. rhizome, *Bull Health Sci Tech*, 13(2015) 6-16.
- [6] N. Waras, K. Nurul, S. Muhamad, B. Maria, I.D.A.A.C. Ardyani, Phytochemical screening, antioxidant and cytotoxic activities in extracts of different rhizome parts from *Curcuma aeruginosa* Roxb., *Int J Res Ayurveda Pharm*, 6(2015) 634-637.
- [7] R.S. Policegoudra, S.M. Aradhya, Biochemical changes and antioxidant activity of mango ginger (*Curcuma amada* Roxb.) rhizomes during postharvest storage at different temperatures, *Postharvest Biol Technol* 46(2007) 189-194.
- [8] G. Nahak, R.K. Sahu, Evaluation of antioxidant activity in ethanolic extracts of five *Curcuma* species, *Int Res J Pharm*, 2 (2011) 243-248.

- [9] M. Vishnupriya, S. Nishaa, J.M. Sasikumar, P.D.D. Teepica, H. Christabel, V.K. Gopalakrishnan, Chemical composition and antioxidant activity of essential oil from *Curcuma amada* Roxb., *Int Res J Pharm*, 3(2012) 99-103.
- [10] S. Singh, A.K. Gupta, Evaluation of phenolics content, flavonoids and antioxidant activity of *Curcuma amada* (mango ginger) and *Zingiber officinale* (ginger), *Res & Rev J Chem*, 2(2013) 32-35.
- [11] A.R. Srvidya, A.K. Yadav, S.P. Dhanbal, Antioxidant and antimicrobial activity of rhizome of *Curcuma aromatica* and *Curcuma zeodaria*, leaves of *Abutilon Indicum*, *Arch Pharm Sci & Res*, 1(2009) 14-19.
- [12] S.M. Al-Reza, A. Rahman, M.A. Sattar, M.O. Rahman, H.M. Fida, Essential oil composition and antioxidant activities of *Curcuma aromatica* Salisb., *Food Chem Toxicol*, 48(2010) 1757-1760.
- [13] S. Tsai, S. Huang, C. Chyau, C. Tsai, C. Weng, J. Mau, Composition and antioxidant properties of essential oils from *Curcuma* rhizome, *Asian J Arts Sci*, 2(2011) 57-66.
- [14] D. Shahwar, M.A. Raza, S. Bukhari, G. Bukhari, Ferric reducing antioxidant power of essential oils extracted from *Eucalyptus* and *Curcuma* species, *Asian Pac J Trop Biomed*, (2012) S1633-S1636.
- [15] V.B. Liju K. Jeena, R. Kuttan, An evaluation of antioxidant, anti-inflammatory, and antinociceptive activities of essential oil from *Curcuma longa* L., *Indian J Pharmacol*, 43(2011) 526-531.
- [16] D.K. Gounder, J. Lingamallu, Comparison of chemical composition and antioxidant potential of volatile oil from fresh, dried and cured turmeric (*Curcuma longa*) rhizomes, *Ind Crops Prod*, 38(2012) 124-131.
- [17] J. Mau, E.Y.C. Lai, N. Wang, C. Chena, C. Chang, D. Chyau, Composition and antioxidant activity of the essential oil from *Curcuma zedoaria*, *Food Chem*, 82(2003) 583-591.
- [18] R. Lobo, K.S. Prabhu, A. Shirwaikar, A. Shirwaikar, *Curcuma zedoaria* Rosc. (white turmeric): a review of its chemical, pharmacological and ethnomedicinal properties, *J Pharm Pharmacol*, 61(2009) 13-21.
- [19] A. Rahman, M. Afroz, R. Islam, K.D. Islam, M.A. Hossain, M. Na, *In vitro* antioxidant potential of the essential oil and leaf extracts of *Curcuma zedoaria* Rosc., *J Appl Pharm Sci*, 4(2014) 107-111.
- [20] W.C. Evans, *Trease and Evana Pharmacognosy*, 15<sup>th</sup> edition, Saunders Ltd., United States, 2009.
- [21] P. Tiwari, B. Kumar, M. Kaur, G. Kaur, H. Kaur, Phytochemical screening and extraction: A review. *Inter Pharm Scientia*. 1(2011) 98-106.
- [22] G. Sudha, M.S. Priya, R.I. Shree, S. Vadivukkarasi, *In vitro* free radical scavenging activity of raw Pepino fruit (*Solanum muricatum* Aiton). *Int J Curr Pharm Res*, 3(2011) 137-140.
- [23] P. Dey, D. Chaudhuri, S. Tamang, T. Chaudhuri, N. Mandal, *In vitro* antioxidant and free radical scavenging potential of *Clerodendrum viscosum*. *Int J Pharma Bio Sci*, 3(2012) 454-471.
- [24] S. Anjusha, A. Gangaprasad, Phytochemical and antibacterial analysis of two important *Curcuma* species, *Curcuma aromatica* Salisb. and *Curcuma xanthorrhiza* Roxb. (Zingiberaceae), *J Pharmacogn Phytochem*, 3 (2014) 50-53.
- [25] P. Donipati, S.H. Sreeramulu, Preliminary phytochemical screening of *Curcuma caesia*, *Int J Curr Microbiol App Sci*, 4(2015) 30-34.
- [26] P. Chauhan, K. Keni, R. Patel, Investigation of phytochemical screening and antimicrobial activity of *Curcuma longa*, *Int J Adv Res Biol Sci*, 4(2017) 153-163.

- [27] N. Kodjio, S.S. Atsafack, S.P.C. Fodouop, J. Kuate, D. Gatsing, *In vitro* antisalmonellal and antioxidant activities of extracts and fractions of *Curcuma longa* L. rhizomes (Zingiberaceae), *Int J Biochem Res Rev*, 11(2016) 1-14.
- [28] W. Nurcholis, N. Khumaida, M. Syukur, M. Bintang, Evaluation of free radical scavenging activity of ethanolic extract from promising accessions of *Curcuma aeruginosa* Roxb., *Molekul*, 12(2017) 133-138.
- [29] Y.L. Lee, C.C. Weng, J.L. Mau, Antioxidant properties of ethanolic and hot water extracts from the rhizome of *Curcuma aromatic*, *J Food Biochem*, 31(2007) 757-771.
- [30] W. Linthoingambi, D.A. Satyavama, M.S. Singh, W.S. Laitonjam, Antioxidant and antimicrobial activities of different solvent extracts of the rhizomes of *Curcuma leucorrhiza* Roxb., *Indian J Nat Prod Resour*, 4(2013) 375-379.
- [31] O. Theanphong, W. Mingvanish, T. Jenjittikul, Chemical constituents and *in vitro* antioxidant activities of essential oil from *Curcuma leucorrhiza* Roxb. rhizome, *Bull Health Sci Tech*, 14(2016) 86-96.

# Screening of the content of polyamines in bird pepper by TLC and HPLC methods

Panadda Phattanawasin<sup>1, a</sup>, Jankana Burana-Osot<sup>1, b</sup>, Lawan Siangjong<sup>2, c</sup>  
and Auayporn Apirakaramwong<sup>2, d</sup>\*

<sup>1</sup>Department of Pharmaceutical Chemistry, Faculty of Pharmacy, Silpakorn University, Thailand

<sup>2</sup>Department of Biopharmacy, Faculty of Pharmacy, Silpakorn University, Thailand

<sup>a</sup>phattanawasin\_p@su.ac.th, <sup>b</sup>buranaosot\_j@su.ac.th, <sup>c</sup>siangjong\_l@su.ac.th,

<sup>d</sup>apirakaramwong\_a@su.ac.th

**Keywords:** polyamine, TLC, image analysis, food

**Abstract.** The abundant biologically active polyamines, putrescine (PUT), spermidine (SPD), and spermine (SPM), are found in almost every organism. These biogenic amines are important for cell growth and viability. Intracellular polyamines are supplied by biosynthesis and by the intake from diet. Polyamines have been gaining much attention due to their effects on health and diseases, especially in aging pathology. Unfortunately, the available polyamine contents data in foods are still insufficient. Normally, high-performance liquid chromatography (HPLC) is the most used technique for polyamine determination but HPLC-based methods are expensive and time-consuming. In the present study, the determination of polyamine contents in Bird pepper or Phrik-khi-nu (*Capsicum annuum* L.), frequently used ingredient in Thai cuisine, was attempted by TLC-densitometry and TLC-image analysis as well as HPLC. The amount of PUT, SPD, and SPM in Bird pepper analyzed by TLC and HPLC were in a comparable concentration range approximately at 300-405 nmol/g of fresh weight (FW). Bird pepper exhibited to be rich in SPM, PUT and SPM, respectively.

## Introduction

The biologically active polyamines (Fig. 1), putrescine (PUT), spermidine (SPD), spermine (SPM), are abundant in almost every organism. These biogenic amines are crucial for cell growth and viability [1]. Intracellular polyamines are supplied by biosynthesis and by dietary intake [2]. Polyamines have become increasingly attractive due to their effect on health and diseases, especially in aging pathology [3-4].

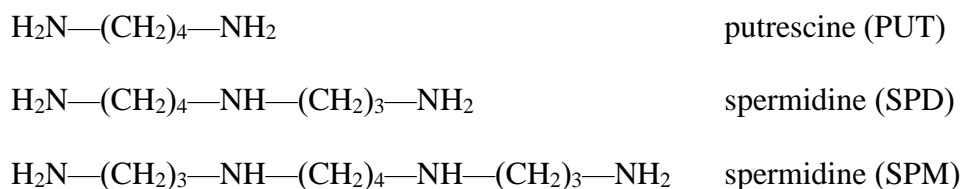


**Fig. 1** Chemical structures of main polyamines

Intracellular polyamine level decreases with age [5]. It is well known that maintaining polyamine level obtained from the diet is important to keep the functioning of various organs in the elderly. Polyamines are present in variable amount in different foods. Unfortunately, there is limited relevant information on their contents in foods [6], including in Bird pepper. The standard analysis technique for polyamines is high-performance liquid chromatography (HPLC) method, but HPLC-based methods are expensive and time-consuming. There is a good



correlation between polyamine determination by thin layer chromatography (TLC) and HPLC. Due to more simplicity and lower operation cost of TLC, therefore, the aim of this study was to determine the levels of polyamine contents in frequently consumed vegetable, Bird pepper or Phrik-khi-nu (*Capsicum annuum* L., Family Solanaceae), by TLC–image analysis and TLC–densitometry as well as HPLC.

## **Experimental**

### **Chemicals and Reagents.**

Standard polyamines, PUT (hydrochloride salt,  $\geq 99\%$ ), SMD (hydrochloride salt,  $\geq 98\%$ ) and SPM ( $\geq 99\%$ ) were obtained from Sigma (St. Louis, USA). Silica gel 60 F254 aluminium plate, 0.25-mm thickness, was purchased from Merck (Darmstadt, Germany). The HPLC-grade acetonitrile was purchased from Merck (Darmstadt, Germany). Other chemicals were of analytical grade. High purity water was prepared by Milli-Q RO system.

### **Sample**

Fresh Bird pepper sample was purchased from Nakhon Pathom fresh market, Amphoe Mueang, Nakhon Pathom Province during February 2019. Identification of the sample was based on morphological and macroscopic characteristics as described in the monograph of PHRIK KHINU in Thai Herbal Pharmacopoeia 2018 [7]. The sample was stored in plastic bag at 4°C before analysis. The voucher specimen (PK-1) was deposited at the Department of Biopharmacy, Silpakorn University, Thailand.

### **Preparation of Stock and Standard Solutions.**

Stock solutions of three standard polyamines, PUT, SMD, and SPM, in 5% (v/v) trichloroacetic acid (TCA) were prepared at a concentration of 5 mg/ml, individually. A standard mixture solution was prepared by the appropriate dilution of the stock standard solutions with 5% (v/v) TCA to the concentration range of 0.5-50  $\mu\text{g/mL}$  for all standards.

### **Extraction of Polyamines in Bird pepper Sample.**

Fresh Bird pepper sample was washed and dried at room temperature for an hour. Polyamine extraction is commonly performed by acid extraction either TCA or perchloric acid. Briefly, they were weighed and homogenized for 10 min in 1/5 volumes of 5% (v/v) TCA according to sample weight. After centrifugation (10,000 x g, 25 min at 4°C), the supernatant was collected, the pellet was further extracted twice with 5% (v/v) TCA. The final concentration of the extract was 70-80% (w/v). All supernatant was kept at -20°C until use.

### **Direct Dansylation.**

The Smith and Best method [7] was used to dansylate the sample with some modification. A 0.2 ml of saturated solution of sodium carbonate (22 g in 100 ml water) and 0.4 ml of dansyl chloride (5 mg/ml in acetone) were added to 0.2 ml of the polyamine-extracted sample and the standard polyamines prepared as described above. After mixing by vortex, the tubes were incubated at 45°C in a heat block for 45 min in the dark. 0.1 ml of proline (100 mg/ml in water) was then added and kept in dark at room temperature for 30 min to destroy the excess dansyl chloride. The dansylated samples were finally adjusted to 1 ml with acetonitrile. All samples were centrifuged at 15,000 x g. An aliquot supernatant was filtered through a 0.45  $\mu\text{m}$  nylon membrane filter and subjected onto TLC plates and into HPLC column.

## **Instrumentation and Chromatographic Conditions.**

### **1. Chromatographic conditions for TLC analysis**

TLC analysis was performed on TLC silica gel 60 F254 aluminium plates (20 cm x 10 cm). 5  $\mu$ L of standard solutions (1-20  $\mu$ g/mL) and a sample solution were applied manually as a 5 mm band onto a TLC plate using Nanomat 3 (Camag, Switzerland). A distance between each band was 1.5 cm. The plate was developed to a distance of 8.5 cm in a TLC chamber previously saturated with chloroform-diethyl ether-triethylamine (5:0.5:0.5, v/v/v) for analysis of PUT, and (6:4:1, v/v/v) for analysis of SMD and SPM. After developments the plate was dried and scanned at wavelength of 360 nm for densitometric analysis. The fluorescence emission of dansyl amine bands was measured using a K400 optical filter. For TLC-image analysis, the TLC plate was photographed under 366 nm by TLC Visualizer (Camag, Switzerland). The color image of the plate was saved as a joint photographic experts group (JPEG) file and resized at a resolution of 640 pixels in height with preserved aspect ratio by using PhotoScape V3.6 for further processing with image analysis software, Sorbfil TLC Videodensitometer (Sorbpolymer, Russia) and UN-SCAN-IT (Silk scientific, USA), ImageJ (NIH, USA) and JustTLC (Sweday, Sweden).

### **2. Chromatographic conditions for HPLC analysis**

The HPLC-Fluorescence system consisted of an Agilent 1100 series pump, an on-line solvent degasser, an autosampler, a fluorescence detector and a Chemstation software Version A.08.01 (Agilent Technologies, USA). A reversed-phase column, 250 mm x 4.6 mm packed with 5  $\mu$ m, Symmetry® C18 modified silica (Water, USA) and a guard column, 20 mm x 3.9 mm packed with 5  $\mu$ m, C18 were used. The separation was carried out under isocratic elution with acetonitrile: water (80:20, v/v). The flow rate was 1.0 ml/min and, the column was operated at ambient temperature. A fluorescence detector was set at excitation and emission wavelengths of 340 nm and 523 nm, respectively. The injection volume was 20  $\mu$ l.

### **Data Analysis.**

The sample was analyzed in triplicates. The amount of PUT, SMD and SPM obtained from these methods was expressed in  $\mu$ g/ml of extracted sample solution and then calculated to nmol/g of fresh weight (FW). One-way ANOVA was used to compare the differences between PUT, SPD and SPM among measuring methods. The significance level was set up at  $p < 0.05$ . All data are presented as a mean  $\pm$  standard error (S.E.M).

## **Results and Discussion**

### **Analysis of dansylated sample by TLC**

Fig.2 showed TLC chromatograms of standards and a Bird pepper sample. Two solvent systems were used in this study. PUT, SMD and SPM were well separated by using chloroform-diethyl ether-triethylamine (6:4:1, v/v/v). However, in a Bird pepper sample, a band of interference was observed closely to the band of PUT. In order to resolve the bands between interferences and PUT in the sample, the solvent system in a ratio of 5:0.5:0.5, v/v/v, was employed. However, SMD and SPM were moved too close to the solvent front. Thus, chloroform-diethyl ether-triethylamine (5:0.5:0.5, v/v/v) was used successfully for analysis of PUT whereas chloroform-diethyl ether-triethylamine (6:4:1, v/v/v) was used for analysis of SMD and SPM in a Bird pepper sample.

The chromatogram and the amount of PUT, SMD and SPM in the sample obtained from TLC-densitometry and TLC-image analysis was shown in Fig.3 and Table 1, respectively. The polynomial regression data showed good relationship ( $r^2 > 0.99$ ) over the concentration range of (1-20  $\mu$ g/mL) for the calibration plot between the area and concentration of each standard.

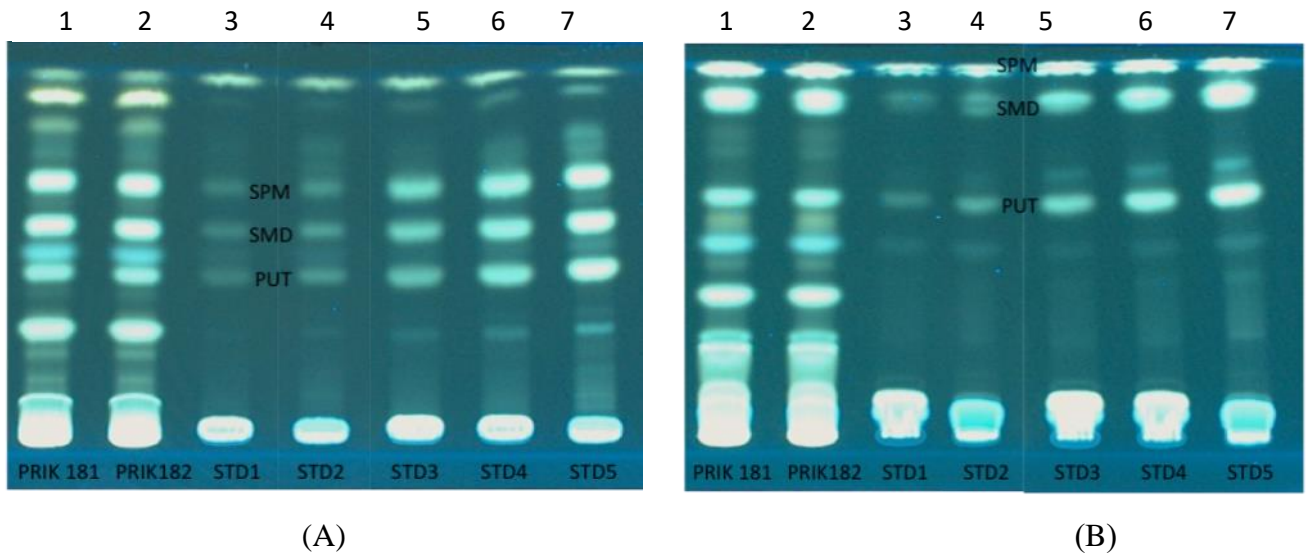
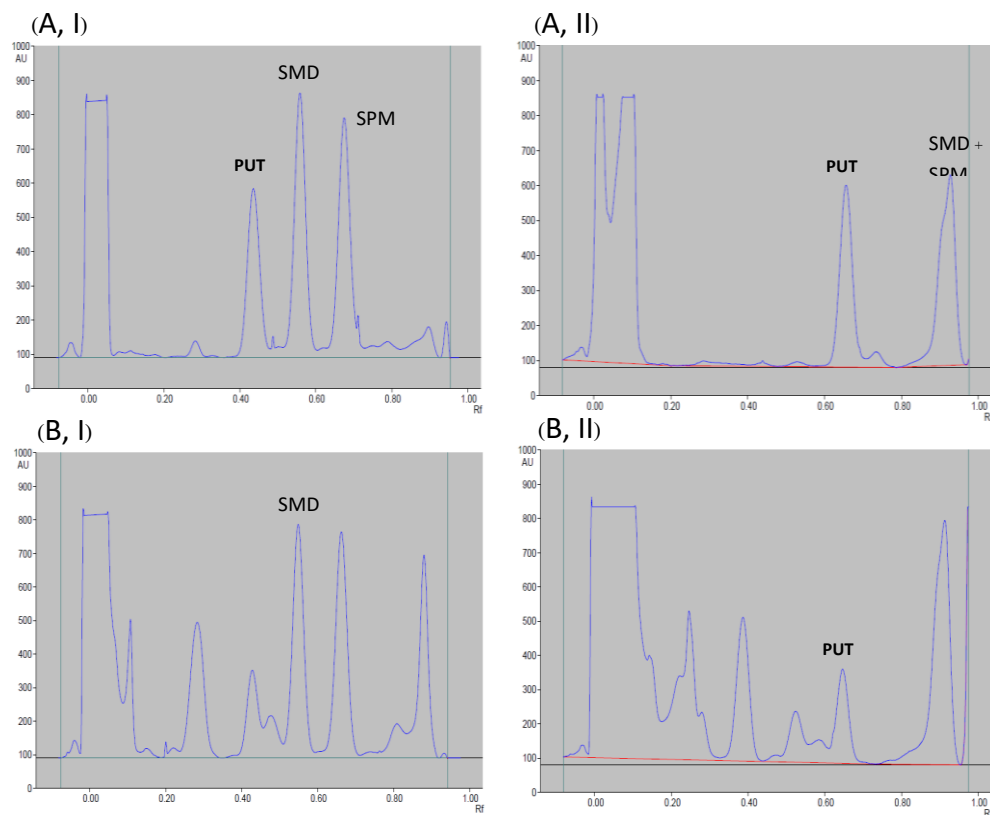


**Fig. 2** TLC of standards PUT, SMD and SPM at 1-20  $\mu\text{g/ml}$  and a Bird pepper using chloroform-diethyl ether-triethylamine (6:4:1,  $v/v/v$ ) (A) and (5:0.5:0.5,  $v/v/v$ ) (B). Lane 1, Bird pepper sample 1; Lane 2, Bird pepper sample 2; Lane 3, 4, 5, 6, 7, PUT, SMD and SPM standards at 1, 2, 5, 10, 20  $\mu\text{g/ml}$ , respectively.

### 3.1 Chromatograms generated by TLC-densitometer



### 3.2 Chromatograms generated by TLC-image analysis (Sorbfil)

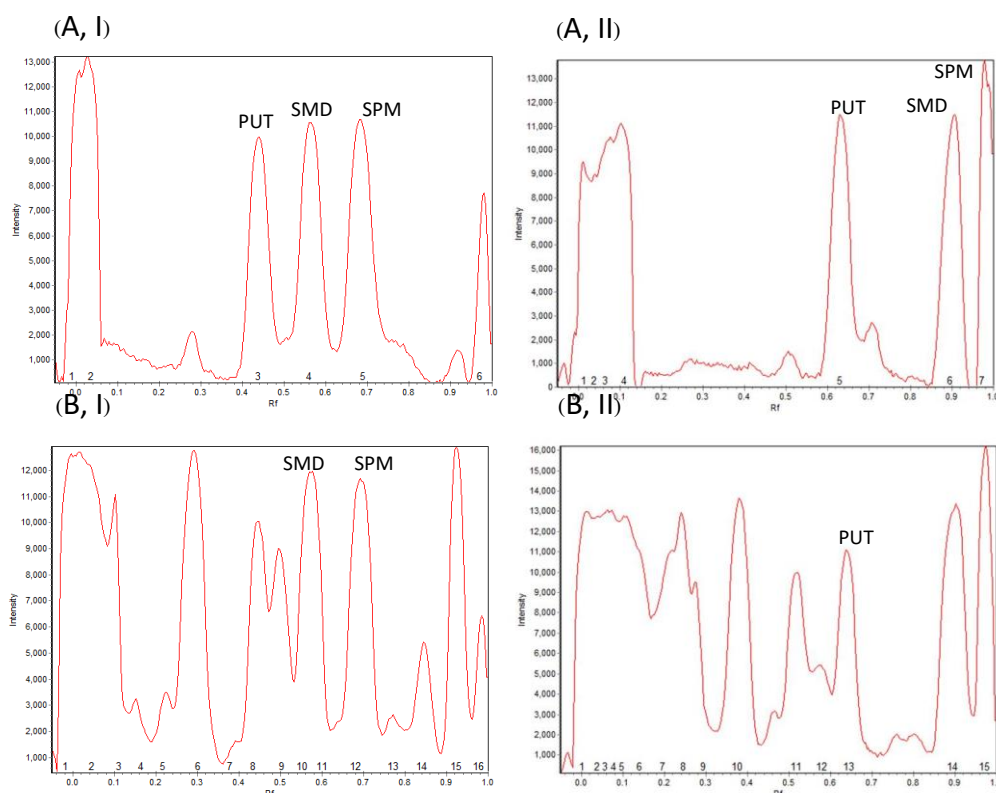


**Fig. 3** Chromatograms generated by TLC-densitometer using wavelength of 360 nm (3.1) and TLC-image analysis (Sorbfil) (3.2) of (A) a standard mixed solution of PUT, SMD, and SPM at a concentration of 10 µg/ml and (B) a Bird pepper solution sample using chloroform-diethyl ether-triethylamine (6:4:1, v/v/v) (I) and (5:0.5:0.5, v/v/v) (II).

**Table 1** The amount of PUT, SMD and SPM (nmol/g of FW ± standard error) of Bird pepper analysed by HPLC and TLC. (\*Significant using ANOVA test at 0.05 level of significance)

Sample	Method			
	HPLC	TLC-Densitometry	TLC-Image Analysis (UNSCAN)	TLC-Image Analysis (SORBFIL)
PUT	327.70 ± 1.94	346.39 ± 5.37	313.34 ± 10.90	325.46 ± 9.95
SPD	405.24* ± 2.92	399.82 ± 5.12	339.97* ± 8.71	302.86* ± 4.20
SPM	371.95* ± 2.15	362.17 ± 6.50	337.23* ± 8.54	320.05* ± 8.87

#### Analysis of dansylated sample by HPLC

The retention times of PUT, SMD and SPM were 6, 14 and 37 min, respectively, as shown in Fig. 4. No peak of matrix in the extracted sample interfered with the polyamine peaks. Standard solutions at five different concentrations ranging from 0.5 to 50 µg/ml were prepared and analyzed in triplicates to prove the linearity of system. Peak area of standard polyamine solution was plotted against their respective concentrations. All calibration curve showed good linearity over the concentration range with a determination coefficient ( $r^2$ ) > 0.995. The amount of PUT, SMD and SPM determined by HPLC was shown in Table 1.

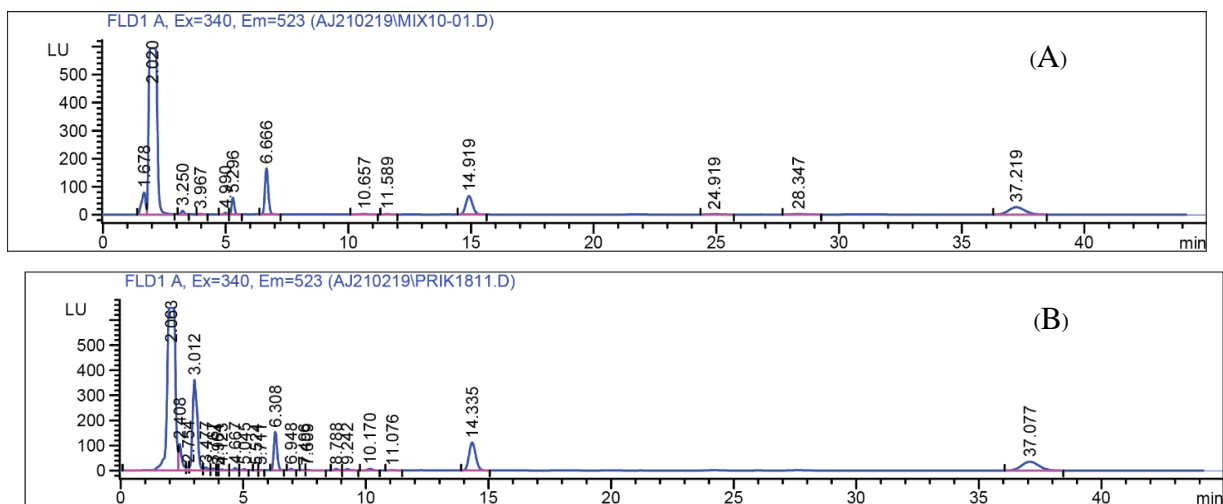


**Fig. 4** Typical HPLC chromatograms of (A) a standard mixed solution of PUT, SMD, and SPM prepared at a concentration of 10  $\mu\text{g}/\text{ml}$  and of (B) a Bird pepper solution sample. Excitation and Emission Wavelength Detection; 340 nm and 523 nm, respectively.

TLC analyzed by image analysis or densitometry gave the content of PUT, SPD, and SPM in Bird pepper sample at concentrations between 302-399 nmol/g of FW, whereas polyamine contents measured by HPLC showed the concentrations between 328-405 nmol/g of FW. Bird pepper exhibited the amount of SPD > PUT > SPM, by both analysis methods. The polyamine contents in Bird pepper is different from other peppers, for example, green pepper has PUT > SPD with no detectable SPM [9]. This finding suggested that different types of pepper might have variable polyamine contents. The decrease of polyamine levels throughout fruit development and maturation or senescence has been previously reported, that is, PUT, SPD and SPM levels in the pericarp of California variety pepper fruit were 2.75 to 1.05, 0.61 to 0.05, and 0.31 to 0.02  $\mu\text{mol}/\text{g}$  of FW, respectively [10]. It indicated that different ripening stages also affect the polyamine contents. The mature green Bird pepper was used in this study. The results showed that polyamine contents in the sample were in the range of 300-400 nmol/g of FW. This result is in agreement with the results reported by Serrano et al. [10]. The amount of PUT analyzed by using the TLC-image analysis method was not significantly different from those determined using the TLC-densitometric and HPLC methods. However, the amount of SPD and SPM obtained by TLC-image analysis were lower than those determined by TLC-densitometric and HPLC methods. This might be because a less well-defined separation at the base of each polyamine peak, especially for SMD and SPM, in the chromatogram generated by image analysis software was obtained, possibly resulting in lower integration area and lower amount of the polyamines analyzed. Nevertheless, TLC-image analysis was considered to be much more simpler, faster and cheaper method as compared to HPLC, it could be used as an alternative method to screen various food samples for the contents of polyamines.

## Conclusion

Bird pepper showed to contain a high level of polyamines (PUT, SPD, and SPM) at a concentration range of 300-405 nmol/g FW by TLC-densitometric, TLC-image and HPLC analysis. Due to several advantages including simplicity and low operating cost, the TLC-image analysis method could be suggested and suitable for screening polyamines in foods.

## Acknowledgement

This research was supported by Faculty of Pharmacy, Silpakorn University (RG 003/2561).

## References

- [1] A.E. Pegg, Polyamine metabolism and its importance in neoplastic growth and a target for chemotherapy. *Cancer Res.* 48 (1988) 759-774.
- [2] N. Buyukuslu, H. Hizli, K. Esin, M. Garipagaoglu, A Cross-Sectional Study: Nutritional polyamines in frequently consumed foods of the Turkish population. *Foods.* 3 (2014) 541-557.
- [3] K. Soda, Y. Dobashi, Y. Kano, S. Tsujinaka, F. Konishi, Polyamine-rich food decreases age-associated pathology and mortality in aged mice. *Exp Gerontol.* 44 (2009) 727-732.
- [4] D.C. Hunter, D. J. Burritt, Polyamines of plant Origin - An Important Dietary Consideration for Human Health, *Phytochemicals as Nutraceuticals - Global Approaches to Their Role in Nutrition and Health*, Venketeshwer Rao, IntechOpen, 2012. DOI: 10.5772/26902. Available from: <https://www.intechopen.com/books/phytochemicals-as-nutraceuticals-global-approaches-to-their-role-in-nutrition-and-health/polyamines-of-plant-origin-an-important-dietary-consideration-for-human-health>.
- [5] K. Nishimura, R. Shiina, K. Kashiwagi, K. Igarashi, Decrease in polyamines with aging and their ingestion from food and drink. *J Biochem.* 139 (2006) 81-90.
- [6] M. Atiya Ali, E. Poortvliet, R. Strömberg, A. Yngve, Polyamines in foods: development of a food database. *Food Nutr Res.* 55 (2011) doi: 10.3402/fnr.v55i0.5572.
- [7] Department of Medical Sciences, Ministry of Public Health, Thai Herbal Pharmacopoeia 2018, The Agricultural Co-operative Federation of Thailand, Bangkok, 2018.
- [8] T.A. Smith, G.R. Best, Polyamines in barley seedlings. *Phytochem.* 16 (1977) 841-843.
- [9] P. Kalač, M. Křížek, T. Pelikánová, M. Langová, O. Veškrna, Contents of polyamines in selected foods. *Food Chem.* 90 (2005) 561-564.
- [10] M. Serrano, M.C. Martínez-Madrid, F. Riquelme, F. Romojaro, Endogenous levels of polyamines and abscisic acid in pepper fruits during growth and ripening. *Physiologia Plantarum.* 95 (1995) 73-76.

# Heavy metals in Thai *Arachis Hypogae* L. determined by inductively coupled plasma mass spectrometry (ICP-MS)

Kritamorn Jitrangsri<sup>1,a</sup>, Amornrut Chaidedgumjorn<sup>1,b</sup>  
and Malai Satiraphan<sup>1,c\*</sup>

<sup>1</sup>Faculty of Pharmacy, Silpakorn University, Sanamchandra Palace Campus,  
Nakhon Pathom 73000, Thailand

<sup>a</sup>jitrangsri\_k@silpakorn.edu, <sup>b</sup>chaidedgumjorn\_a@su.ac.th,

<sup>c</sup>satiraphan\_m@su.ac.th

\*Corresponding author

**Keywords:** Heavy metals, ICP-MS, Peanut

**Abstract.** The contamination of heavy metals in food is primary health concern nowadays. The consumption of heavy metals adulterated food has related to the several serious illnesses. The aim of this study was to determine Ni, As, Cd, Ba and Pb levels in edible peanuts. Raw peanut kernels were digested with nitric acid by Milestone microwave digestion system. The digested solution was diluted and injected on inductively coupled plasma mass spectrometry (ICP-MS). The concentrations of each heavy metal were calculated against multi-element standard solution calibration curves. The results found that the quantity of Ni and As was not significantly different among peanut varieties; Thainan-IV, Kalasin-I and Kalasin-II. Cd and Ba were found significantly high amount in Kalasin-I and Kalasin-II respectively while Pb was detected only in Kalasin-II variety at low level. Overall, heavy metals found in this study were in the limit of contaminated food allowed by the ministry of public health, Thailand.

## Introduction

Peanut (*Arachis Hypogae* L.) is one of common food in Thailand which is usually consumed as boiled or roasted [1]. It is enriched with a variety of nutrients that are beneficial to human health such as amino acids, minerals, vitamins and anti-oxidation compounds [2]. However, growing peanuts in industrially polluted areas may connect with the number of heavy metals entering the plants. Accumulation of lead and cadmium in the root system and fruit shells of peanut has been reported [3]. Pb is an extremely toxic heavy metal. It can disturb the plant physiological processes with no any biological functions [4]. Cd is one of highly toxic and has been ranked number 7 among the top 20 toxins in the world [5]. Arsenic (As) is another highly toxic heavy metal. Chronic exposure of As results in many irreversible changes in the vital organs and potentially lethal toxicity [4]. To ascertain the safety of heavy metals contamination, the ministry of public health of Thailand has allowed the maximum levels of Pb, Cd and As in food at 2.0, 0.3 and 1.0 mg/kg respectively.

Various techniques were reported for analysis of heavy metals in natural matrices. Atomic absorption spectroscopy was used to analyze manganese, cobalt, nickel, copper, zinc, cadmium, and lead in basil (*Ocimum basilicum* L.) [6]. There was a study using inductively coupled plasma optical emission spectrometry (ICP-OES) in the analysis of ten heavy metals (Al, As, Co, Cr, Cu, Fe, Mn, Ni, Pb and Zn) in tropical marine sediments [7]. Inductively coupled plasma mass spectrometry (ICP-MS) was another technique that was reported for quantification of heavy metals in surface water [8] and safflower plant [9]. However, the study of heavy metals contaminated Thai peanuts using ICP-MS analysis has not been established. The objective of this study was to quantify the controlled adulterant heavy metals; Pb, Cd, and As in three daily consumed Thai peanut varieties; Kalasin-I, Kalasin-II and Thainan-IV. Moreover, Barium (Ba) and Nickel (Ni) were also quantified since it has been reported

contamination in peanuts as well [10]. The analysis was carried out using ICP-MS because of its superior robustness and sensitivity [11].

## **Materials and Methods**

### **Materials**

Concentrated nitric acid was purchased from Merck, USA. Ultra-pure water was generated from TKA, UK. Multi-element standard solutions 2A was procured from Agilent, USA.

### **Sample preparation**

Raw peanuts were bought from local market on Phutamonthon Sai 2 Rd in August 2016. The sediments were removed with tap water three times and unpeeled. The raw kernels were blended in high speed blender for 3 minutes and dried at 60°C for 24 hours. The coarse powder was ground into fine powder with mortar and pestle and kept at 2-8°C until analysis.

### **Digestion procedure**

0.3 g of fine sample was transferred into a digestion vessel and digested with 5 ml of concentrated nitric acid by Milestone, Ethos One microwave digestion system. The samples were digested consecutively linear and static mode at 1400W, 180°C for 15 minutes each and then cool down for 30 minutes. The digested samples were adjusted to 25 mL with ultra-pure water and filtered through the Whatman No1 filter papers. The filtrate was collected and kept at 2-8°C until ICP-MS analysis. The samples were prepared triplicate for each peanut varieties.

### **ICP-MS procedure**

Sample solutions were measured by Agilent 7500ce ICP-MS system. The parameters for ICP-MS were power 1500 W, RF matching 1.72 V, make up gas 0.3 L/min, carrier gas 0.85 L/min and nebulizer pump 0.1 rps. The detection mass numbers for Ni, As, Cd, Ba and Pb were set at 60, 75, 111, 137 and 208 respectively. The multi-element standard solutions 2A was diluted to concentration range of 0.1-500 ppb.

### **Statistical analysis**

Statistical significance of heavy metal amount among peanut varieties has been estimated on triplicate samples through one-way ANOVA followed by Tukey's HSD test at  $p < 0.05$  level.



## Results

Analytical performance of ICP-MS was shown in Table 1. Regression equation, correlation coefficient ( $R^2$ ), RSD for repeatability of calibration solutions measurements and detection limit were reported.

**Table 1.** Analytical performance parameters of ICP-MS analysis

Element	Mass number	Regression equation	$R^2$	DL [ppb]	RSD [%]
Ni	60	$y = 7821x + 33220$	0.9980	0.004095	2.6
As	75	$y = 1952x + 3124$	0.9994	0.001565	6.2
Cd	111	$y = 9807x + 44000$	0.9970	0.02977	1.5
Ba	137	$y = 17190x + 104500$	0.9968	0.03772	2.3
Pb	208	$y = 83910x + 777000$	0.9974	0.05075	1.1

\*DL=Detection Limit

Heavy metals were quantitated in this study including Ni, As, Cd, Ba and Pb. The contents of heavy metals found in three peanut varieties were shown in Table 2. The heavy metal found in the highest amount in Thainan-IV and Kalasin-I variety was Ni (2.7354 and 1.8201 mg/kg, respectively) while Ba was the highest in Kalasin-II variety (11.4491 mg/kg). The controlled heavy metals were found in range of 0.0031 - 0.0060 mg/kg for As and 0.0742 – 0.2009 mg/kg for Cd. Lead (Pb) was undetectable in Thainan-IV and Kalasin-I variety but trace amount was found in Kalasin-II variety (0.0680 mg/kg).

**Table 2.** Contents of heavy metals found in Thai peanut varieties

Element	Concentration [mg/kg] $\pm$ SD [n=3]		
	Thainan-IV	Kalasin-I	Kalasin-II
Ni [60]	2.7354 $\pm$ 0.5253	1.8201 $\pm$ 0.1055	2.7022 $\pm$ 0.3711
As [75]	0.0031 $\pm$ 0.0004	0.0060 $\pm$ 0.0037	0.0049 $\pm$ 0.0011
Cd [111]	0.0742 $\pm$ 0.0121	0.2009 $\pm$ 0.0626	0.0905 $\pm$ 0.0316
Ba [137]	1.3153 $\pm$ 0.1399	1.2347 $\pm$ 0.1303	11.4491 $\pm$ 0.1569
Pb [208]	BDL	BDL	0.0680 $\pm$ 0.0501

\*BDL=Below Detection Limit

## Discussion

The analytical method for the determination of heavy metals in this study was simple, robust and reliable. The concentrations and mass counts showed a linear relationship with correlation coefficient ( $R^2$ ) more than 0.99 for all elements. The detection limit of Ba in our study was lower than the study of Naozuka et al. [12] which indicated better sensitivity. The average RSD for repeatability of calibration solutions measurements were in the range of 1.1–6.2%.

Comparative level of heavy metals among peanut varieties was shown in Figure 1. The contents of Ni and As content were not significantly different between varieties ( $p>0.05$ ) while Cd and Ba demonstrated the highest amount in Kalasin-I and Kalasin-II varieties respectively ( $p<0.05$ ). Although average Ni content found in this study was higher than a study of Vineeth

et al. (2.419 vs 0.574 mg/kg), Cd content in our study was lower (0.122 vs 0.290 mg/kg) [10]. Ni and Ba are non-essential metals and have no standard permissible limit contamination in food. However, they have been considered as carcinogenic metals which involved in DNA damage by making base pair mutation, deletion, or oxygen radical attack on DNA [13]. For heavy metal control, As, Cd and Pb, were found only small amount contamination in peanuts and they were less than the permissible limit set by Thai ministry of public health which are 2, 0.3 and 1 mg/kg for As, Cd and Pb respectively. The highest toxic heavy metal found in this study is Cd (0.2009 mg/kg). The WHO recommended tolerable weekly dietary intake for adult females is 7 µg/kg body weight for Cd [14] and we assume that the average weight of an adult Thai female 16-28 years of age is 52.70 kg [15]. This means that it would take over a quarter kilogram of this lot of peanut kernels every day to reach the Cd limit. Pb was undetectable in Kalasin-I and Thainan-IV varieties which was in accordance with the study of Angelova et al [3]. The study found that the accumulation of Pb usually occurs in peanut roots instead of seeds because peanuts create a shallow situated root system at a depth around 30 cm which is not much deep and well developed like other plants rooting system. This makes a suitable environment for heavy metals accumulation [3]. Arithmetic mean arsenic (As) found in this study was 0.0047 mg/kg which was lower than the study of Blair et al. (0.0282 mg/kg) [14]. Low level of arsenic exposure can cause nausea and vomiting, decrease production of erythrocytes and leukocytes, abnormal heart beat, pricking sensation in hands and legs, blood vessels degeneration. Long-term exposure can result in formation of skin lesions, internal cancers, neurological complication, pulmonary disease, peripheral vascular disease, hypertension and cardiovascular disease and diabetes mellitus [4].

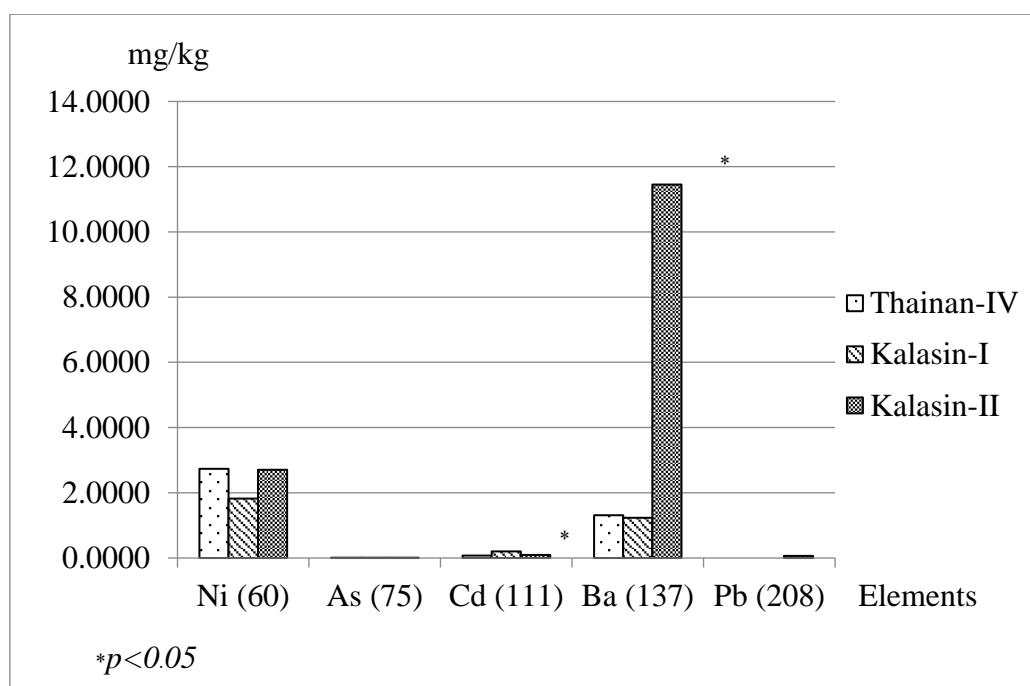


**Figure 1** Comparative heavy metals in three Thai peanuts

Several factors impact the level of heavy metals in plants such as growing area or environmental pollutants [3]. Human activities are also another source of heavy metals creation, for example, the inappropriate waste disposal of paints, soaps, dyes, medications or electrical devices and also the overusing of pesticides or fertilizers in agriculture [4]. However, to prevent the accumulation of heavy metals in human body, the contamination of heavy metals can be decreased by several methods. It has been removed using absorbent materials such as activated carbon or resin. Additionally, the waste biomasses, peanut hulls and chitosan were also effective

to remove heavy metals from peanut extract [16]. Treating soil with specific reagents during planting process was found a significant reduction of heavy metals in plants such as thiuram [6] or calcium hydroxide [10].

### Conclusion

The results of the present study have shown that Ni, As, Cd, Ba and Pb were presented in peanut kernels. The contents of toxic heavy metals including As, Cd and Pb were found less than the permissible limit set by Thai ministry of public health in all three peanut varieties. In conclusion, peanuts that are cropped and marketed in this study were safe to consume.

### Acknowledgment

This study was granted by Silpakorn University Research and Development Institute (grant number SU610109). The authors are also grateful to Faculty of Pharmacy, Silpakorn University for providing instrumental support throughout the study.

### References

- [1] ST Talcott, S Passeretti, CE Duncan, DW Gorbet, Polyphenolic content and sensory properties of normal and high oleic acid peanuts, *Food Chem.* 90 (2005) 379–88.
- [2] VS Settaluri, CVK Kandala, N Puppala, J Sundaram, Peanuts and Their Nutritional Aspects — A Review, *Food Nutr Sci.* 3 (2012) 1644–50.
- [3] V Angelova, R Ivanova, K Ivanov, Heavy metal accumulation and distribution in oil crops, *Commun Soil Sci Plant Anal.* 35 (2004) 2551–66.
- [4] M Jaishankar, T Tseten, N Anbalagan, BB Mathew, KN Beeregowda, Toxicity, mechanism and health effects of some heavy metals, *Interdiscip Toxicol.* 7 (2017) 60–72.
- [5] K Abraham, R Sridevi, B Suresh, T Damodharam, Effect of heavy metals (Cd, Pb, Cu) on seed germination of *Arachis hypogaea*, L. *Asian J Plant Sci Res.* 3 (2013) 10–2.
- [6] D Adamczyk-Szabela, Z Romanowska-Duda, K Lisowska, WM Wolf, Heavy Metal Uptake by Herbs. V. Metal Accumulation and Physiological Effects Induced by Thiuram in *Ocimum basilicum* L, *Water Air Soil Pollut.* 228 (2017) 1–14.
- [7] V Chand, S Prasad, ICP-OES assessment of heavy metal contamination in tropical marine sediments: A comparative study of two digestion techniques, *Microchem J.* 111 (2013) 53–61.
- [8] C Voica, MH Kovacs, A Dehelean, D Ristoiu, A Iordache, ICP-MS determinations of heavy metals in surface waters from Transylvania, *Rom Reports Phys.* 57 (2012) 1184–93.
- [9] LH Jia, Y Liu, YZ Li, Determination of wholesome elements and heavy metals in safflower (*Carthamus tinctorius* L.) from Xinjiang and Henan by ICP-MS/ICP-AES, *J Pharm Anal.* 1 (2011) 100–3.
- [10] D Vineeth, C Venkateshwar, SA Unnisa, Effect of heavy metals in *Arachis Hypogaea* L (groundnut) and its treatment, *World J Pharm Res.* 3 (2014) 533–44.
- [11] L Cid-Barrio, F Calderón-Celis, P Abásolo-Linares, ML Fernández-Sánchez, JM Costa-Fernández, JR Encinar, et al, Advances in absolute protein quantification and quantitative protein mapping using ICP-MS, *TrAC - Trends Anal Chem.* 104 (2018) 148–59.
- [12] J Naozuka, E Carvalho Vieira, AN Nascimento, PV Oliveira, Elemental analysis of nuts and seeds by axially viewed ICP OES, *Food Chem.* 124 (2011) 1667–72.
- [13] PB Tchounwou, CG Yedjou, AK Patlolla, DJ Sutton, *Molecular, Clinical and Environmental Toxicology*, NIH Public Access. 101 (2012) 133–64.
- [14] BF Blair, MC Lamb, Evaluating Concentrations of Pesticides and Heavy Metals in the U.S. Peanut Crop in the Presence of Detection Limits, *Peanut Sci.* 44 (2017) 124–33.
- [15] Information on [http://www.sizethailand.org/region\\_all.html](http://www.sizethailand.org/region_all.html)
- [16] BJ Massie, TH Sanders, LL Dean, Removal of Heavy Metal Contamination from Peanut Skin Extracts by Waste Biomass Adsorption, *J Food Process Eng.* 38 (2015) 555–61.

# Honokiol and magnolol induced DAMPs releases mediated apoptosis induction on human cholangiocarcinoma cells

Worawat Songjang<sup>1, a</sup> and Arunya Jiraviriyakul<sup>1, 2, b \*</sup>

<sup>1</sup>Biomedical Sciences, Faculty of Allied Health Sciences, Naresuan University, Phitsanulok, Thailand 65000

<sup>2</sup>Department of Medical Technology, Faculty of Allied Health Sciences, Naresuan University, Phitsanulok, Thailand 65000

<sup>a</sup>worawats58@email.nu.ac.th, <sup>b</sup>arunyaj@nu.ac.th

**Keywords:** honokiol, magnolol, cholangiocarcinoma, DAMPs

**Abstract.** Introduction and Objectives; Cholangiocarcinoma (CCA) is biliary tract malignancy. Because no specific biomarkers are available, CCA patients frequently present with disseminated tumour that is too late for curative treatment, leading to high mortality rate. Honokiol and magnolol are the hydroxylated biphenyl compounds isolated from *Magnolia officinalis*. Many studies have reported that honokiol and magnolol effectively induced cancer cell death. However, the evidence of the effects of these compounds on CCA has not yet been reported. In this study we aim to study the effect of honokiol and magnolol on human CCA cells. Together with the induction effect of damage-associated molecular patterns expression of these compounds, which is the danger signal for immune system activation. The anti-tumour activity of honokiol and magnolol was determined in context of the cytotoxicity effect, anti-proliferation effect and the mechanism on the induction of cell apoptosis. These compounds exhibited the cytotoxicity on human CCA cells KKU-100 and KKU-213L5. The underlying mechanism was confirmed by Annexin V/PI staining and caspase-3 expression. The results indicated that honokiol and magnolol induce CCA cell death mediated by apoptosis mechanism. Moreover, the effect of honokiol on DAMPs expression from CCA cells also investigated. Interestingly that induction of cell apoptosis by honokiol cause of damage-associated molecular patterns (DAMPs) release including high mobility group box 1 (HMGB1) and heat shock proteins 90 (HSP90). Therefore, in this study we demonstrated that honokiol and magnolol have potential anticancer properties that are promising compounds for alternative CCA treatment. Especially, the induction of DAMPs expression which is fascinated to combine as immunoadjuvant of cancer immunotherapy for CCA treatment.

## Introduction

Cholangiocarcinoma is biliary tract epithelial cell malignancy. It's widely accepted that the development of CCA is associated with *Opisthorchis viverrini* infection and highest incidence rate occur in the northeast of Thailand [1]. Early stages of the disease are asymptomatic and no specific biomarker for clinical diagnosis resulting in poor prognosis, and high mortality rate of CCA patients [2, 3]. Unfortunately, the treatment strategies such as surgical resection, liver transplantation, radiation and other therapeutic approaches are limited causing unsatisfactory treatment efficacy and life quality of CCA patients is low [4]. Therefore, new therapeutic treatments for CCA are urgently required.

Honokiol and magnolol are pharmacological active compounds extracted from plant *Magnolia officinalis*. These compounds have been reported as an agents with multiple pharmacological functions including anti-inflammatory, anti-oxidant, anti-anxiety, anti-depressant, anti-stress, as well as anti-tumour activities [5]. Previous studies reported that honokiol and magnolol can inhibit tumour growth in both of *in vitro* and in animal models. Notably, these compounds have been proven as apoptotic inducer in various cancer type such as colon cancer, breast cancer, glioblastoma, liver cancer and CCA [5, 6]. It's widely known that induction of cell death is cause of immunogenic cell death exposure that capable to activate

the pattern recognition receptor (PRRs) of immune cells. Immunogenic cell death is mainly mediated by expression of DAMPs which release or expose molecules of injured, damaged and apoptotic cells such as calreticulin (CRT), HMGB1 and HSPs [7]. Recently, a DC vaccine based on immunogenic cell death molecules have been demonstrated in both preclinical and clinical studies [8, 9]. Therefore, linking of the anti-tumour activities of honokiol and magnolol and induction of DAMPs expression is fascinating in terms of using these herbal-derived compounds as immunoadjuvant for immunotherapy for CCA treatment.

In this study, for the first time, we report the effect of honokiol and magnolol that induce CCA death mediated-cell apoptosis mechanism. Moreover, honokiol also induced releasing of DAMPs molecules including HMGB1 and HSP90. These findings suggested that honokiol and magnolol are worth to develop as therapeutic agents and recommend using combined with immunotherapy for CCA treatment.

## **Material and Method**

### **Cell culture**

The human bile duct epithelial carcinoma cell lines KKU-213L5 and KKU-100 were kindly provided by Prof. Dr. Sopit Wongkham, Liver Fluke and Cholangiocarcinoma Research Center, Faculty of Medicine, Khon Kaen University, Khon Kaen, Thailand. Cell lines were maintained according to international guidelines on good cell culture practice in Dulbecco's modified Eagle's medium (DMEM) (Thermo Fisher Scientific, MA, USA) supplemented with 5% fetal bovine serum (FBS), 100 units/mL of penicillin, 100 µg/mL of streptomycin, and 0.25 µg/mL of amphotericin B. Cells were grown at 37°C in a humidified atmosphere with 5% CO<sub>2</sub>. Monocytes were isolated following standard protocol. Briefly, the PBMC was first isolated by using Ficoll-Hypaque subsequently by Percoll gradient centrifugation for monocyte enrichment. The monocyte fraction was then plated in cell culture flask for allowing to adhere for 2 h. The non-adherence cell was removed by washing with PBS for 3 times. The adherence monocyte was derived to macrophage by continually culture in RPMI1640 10% FBS supplemented with 50 ng/mL of rhGM-CSF (Miltenyi Biotec, Bergisch Gladbach, Germany). The medium was changed by replacing with fresh medium for every 3 days.

### **Determination of cell viability**

The viability of cells was measured using MTT assay. Briefly, 5×10<sup>3</sup> cells of KKU-213L5, KKU-100 and macrophage were incubated with honokiol and magnolol at indicated concentrations for 24 and 48 h. Then, culture medium was removed followed by adding of working solution of MTT reagent (AMRESCO, OH, USA), and incubated for 4 h at 37°C. Then, DMSO was used to dissolve the formazan dye and gently mixed immediately by autopipette. The light absorbent was measured by microplate spectrophotometer (PerkinElmer, MA, USA) at 540 nm within 30 minutes. The % cell viability was calculated following the formula ((honokiol or magnolol treated Abs<sub>540</sub>)/(control Abs<sub>540</sub>)) × 100 (%).

### **Apoptosis analysis**

Annexin V & Dead Cell were performed utilizing Muse™ Cell Analyzer from Millipore (MA, USA) following manufacturer's instruction. Briefly, after exposed with different concentrations of honokiol and magnolol for indicated time, treated cells were incubated with Annexin V and Dead Cell Reagent (7-AAD) before analyzing. The results were representing by event of live cell, apoptotic cell and dead cell.

### **Western blot analysis**

KKU-213L5 cells were incubated with honokiol at indicated concentrations for 20 h. For the analysis of intracellular proteins, treated cells were washed with ice-cold PBS before cell lysis using RIPA lysis buffer plus protease inhibitor cocktail (AMRESCO, OH, USA).

Then, protein lysates were collected and qualified by using Bradford assay. The secreted protein was collected from conditioned medium, which was concentrated using Amicon® Ultra-2 Centrifugal Filter units (Millipore, MA, USA). The protein was then separated by SDS-PAGE and transferred onto the PVDF membranes. After that, the membranes were blocked with 5% skim milk buffer and then incubated with primary antibody, anti-caspase-3 (Cell Signaling, MA, USA), anti-HMGB1 (ELabScience, TX, USA) and anti-HSP90 (Merck, Darmstadt, Germany) at 4°C overnight. Then, membranes were incubated with horseradish peroxidase (HRP)-linked anti-rabbit antibody (Cell Signaling, MA, USA) before incubated with detection reagent. The image was developed by Chimidoc™ XRS (Bio-rad, CA, USA) and analyzed by Image Lab (Biorad, CA, USA).

## Results

### Honokiol and magnolol induced CCA cells death mediated cell apoptosis

To investigate the cytotoxicity of honokiol and magnolol on human CCA cells. K KU-213L5 and K KU-100 were incubated with compounds for 24 and 48 h. The measuring of cell viability was carried out using MTT assay. The results showed that honokiol and magnolol significantly reduce the viability of K KU-213L5 and K KU-100 in dose- and time-dependent manner (Fig 1A-D). The IC<sub>50</sub> of honokiol with K KU-213L5 at 24 and 48 h were 49.3±0.28 and 26.89±0.54 μM, and with K KU-100 were 47.7±0.77 and 29.16±0.24 μM, respectively. Whereas, the IC<sub>50</sub> of magnolol with K KU-213L5 at 24 and 48 h were 72.21±0.87 and 53.54±0.85 μM, and with K KU-100 were 77.33±2.28 and 37.73±1.40 μM, respectively. In addition, the cytotoxicity of these compound was investigated in human monocytes-derived macrophages. The results showed IC<sub>50</sub> of honokiol at 24 and 48 h were 95.79±5.11 and 92.61±8.41 μM, respectively.

Moreover, the underlying mechanism in induction of cell apoptosis was further investigated using annexin V/PI staining. Honokiol or magnolol treated CCA cells were stained with annexin V and PI before measuring the expression by flow cytometer. The results showed that the percentage of early and late apoptotic cell of K KU-213L5 and K KU-100 after treated with honokiol is distinctly increased in time-dependent manner compared with their control counterpart (Fig 2A). Similarly, magnolol induced CCA cells apoptosis in time-dependent manner at 24 and 48 h (Fig 2B). Together with the morphology changed of K KU-213L5 after incubated with honokiol that show the vacuole, more round shapes and loss of adhesion ability (Fig 3A). In addition, the expression of caspase-3 was measured using immunoblotting. Interestingly, at 25 to 50 μM of honokiol increased the expression level of cleaved caspase-3 (19 kDa) (Fig 3B). Suggesting that honokiol and magnolol induced CCA cells death mediated by cell apoptosis mechanism.

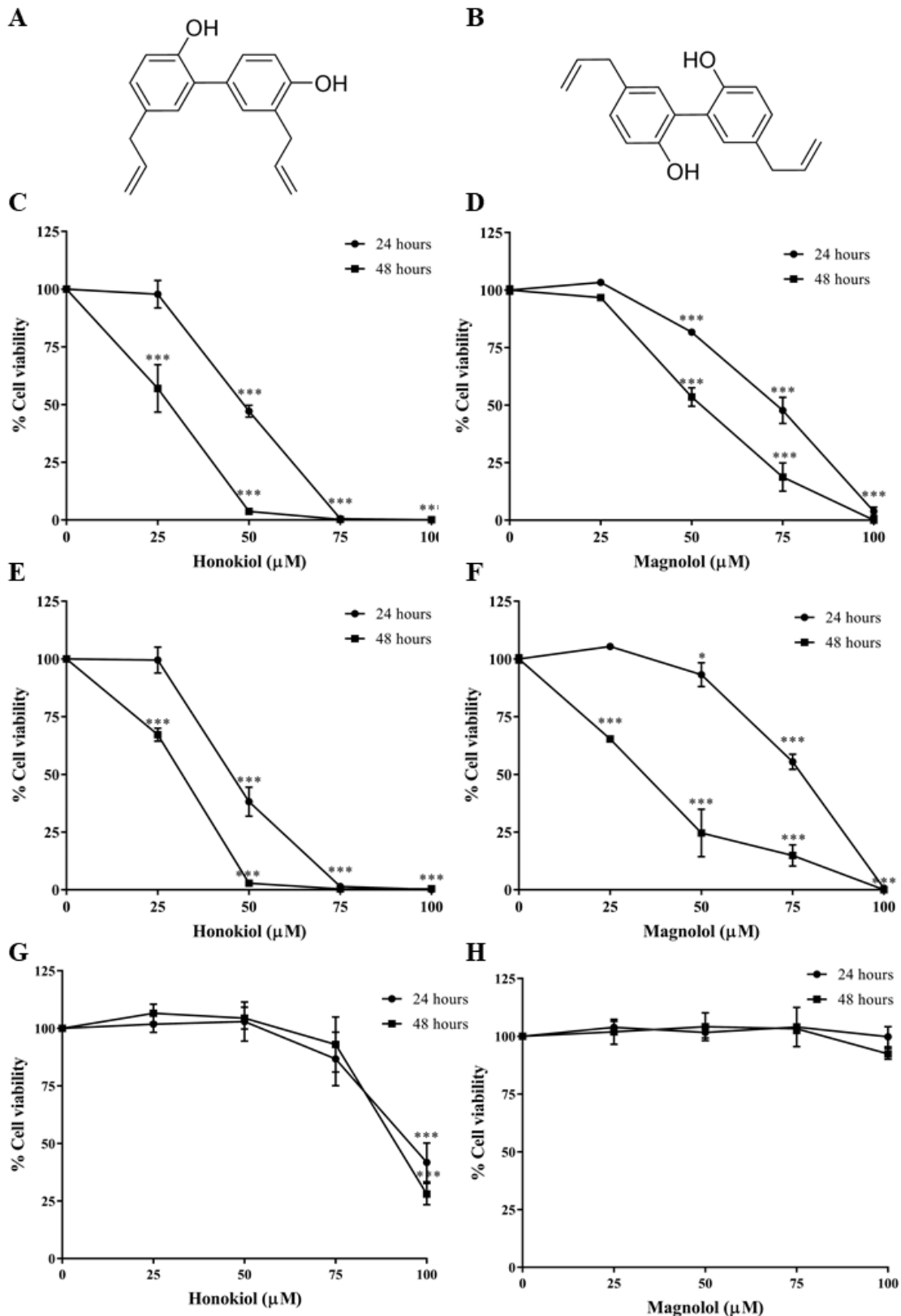


**Fig 1** The cytotoxicity of honokiol and magnolol on CCA cell lines. The chemical structure of (A) honokiol and (B) magnolol. (C-D) KKKU-213L5, (E-F) KKKU-100 and (G-H) human macrophages were treated with honokiol following indicated concentration. After 24 and 48 h, cell viability was determined using MTT assay. Cells were treated with DMSO as negative control, and all groups were normalized with control group. The results presented as mean  $\pm$  SD from three independent experiments. A  $p$ -value  $< 0.05$  was considered statistically significant;  $p$ -value  $< 0.05$  (\*),  $p$ -value  $< 0.01$  (\*\*) and  $p$ -value  $< 0.001$  (\*\*\*).

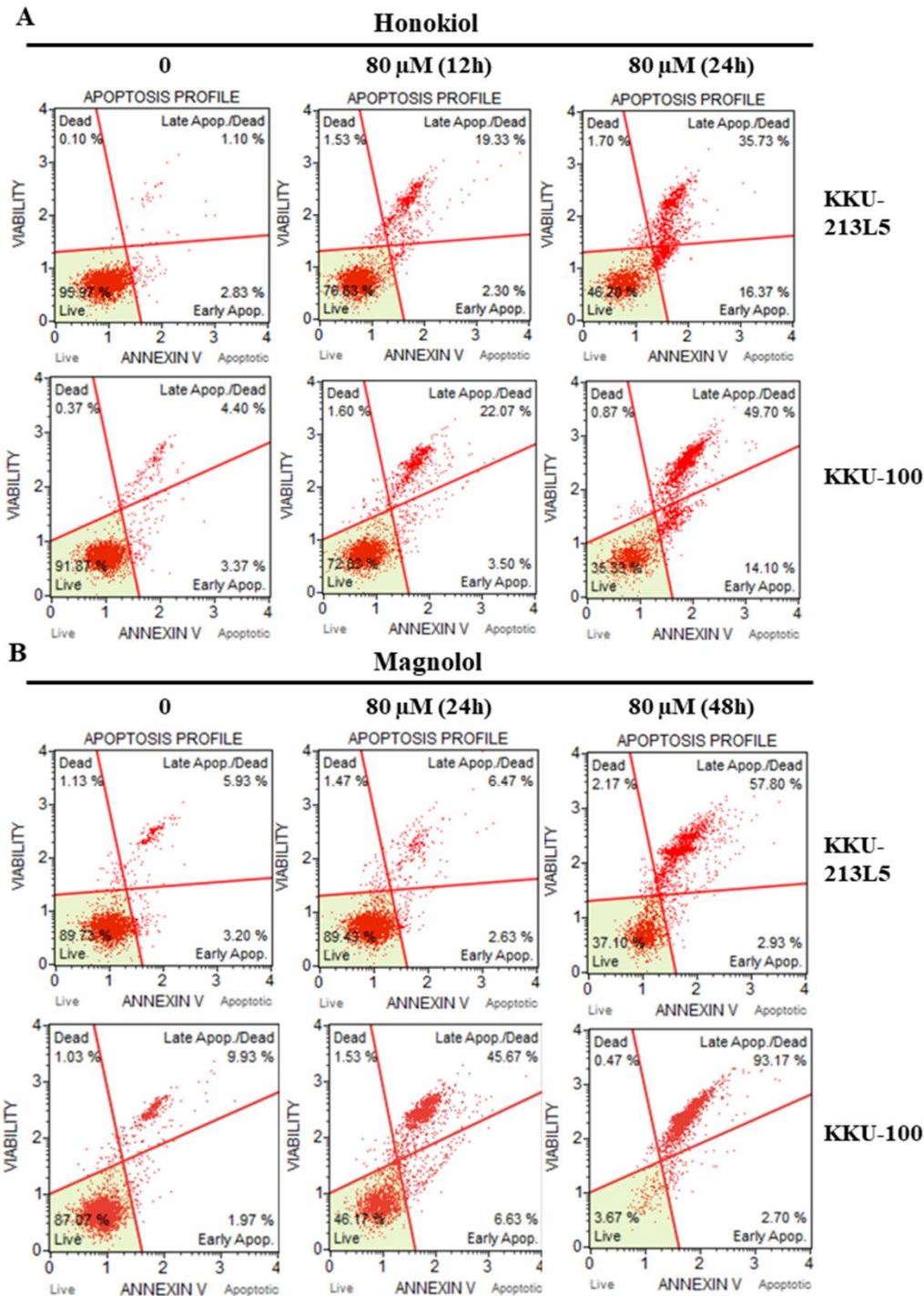


**Fig 2** Honokiol and magnolol induced CCA death mediated cell apoptosis. CCA cells were treated with (A) honokiol and (B) magnolol before analyzing with Muse™ Cell Analyzer. Annexin V/PI from the gated cell showed as percentage of live, early apoptotic, late apoptotic/dead, and dead cell.

### Honokiol induced DAMPs releases from CCA cells

The expression of late DAMPs either intracellular or extracellular proteins were measured using immunoblotting analysis. The results showed that treatment with honokiol at 25 to 50  $\mu$ M concentration for 24 h induced the release of HMGB1 and HSP90 proteins in the conditioned medium in dose-dependent manner. Meanwhile, the levels of intracellular HMGB1 and HSP90 are not dramatically decreased (Fig 3B). Interestingly, at same concentration of honokiol can activate the proteolytic activity of caspase-3 enzyme. These data suggested that honokiol was able to induce CCA apoptosis with secretion of DAMPs.



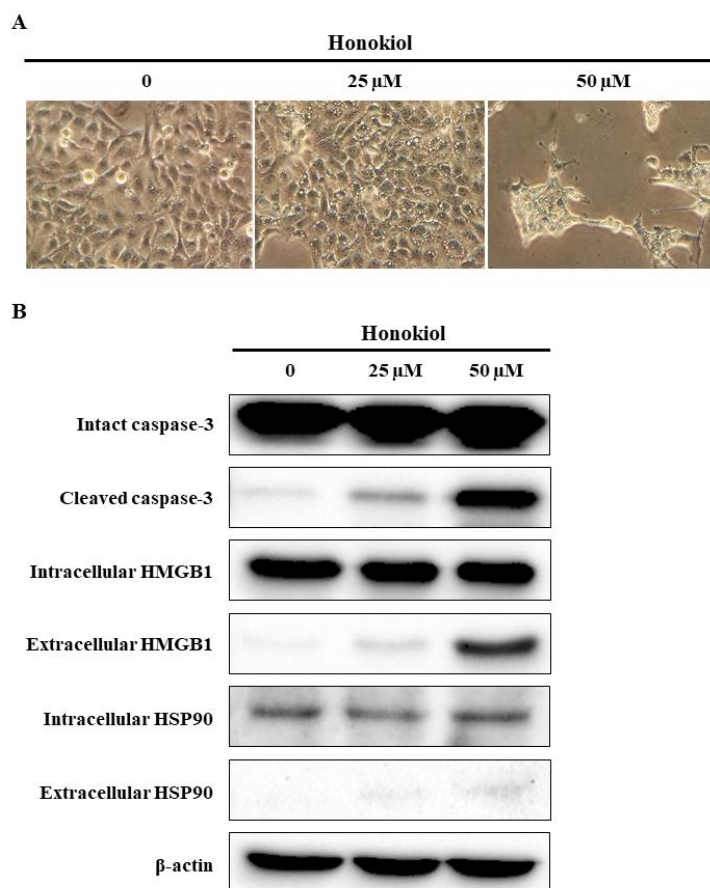


**Fig 3** Honokiol induced DAMPs secretion. KKU-213L5 cells were incubated with honokiol following indicated concentration for 24 h. (A) The cell morphology was observed under inverted microscope at 40x. (B) Protein samples and conditioned medium were analysed using Western blot.

### Discussion and Conclusion

It has been reported that more than seventy percentage of approval anticancer drugs is originate from the herbal-derived compounds or chemical imitations of natural products [10]. According to the efficacy, safety and cost-effectiveness of herbal-derived compound that make them increasing trend used in nowadays. Honokiol and magnolol are the magnolia-derived compounds which exhibit the multiple pharmacological activities. Recently, these compounds were developed and market available for using as supplementation. In this study, for the first time, we showed the anti-tumour activities of honokiol and magnolol on human CCA cells that derived from Thai CCA patients. The results indicated that honokiol and magnolol efficient to induce CCA cell death mediated induction of cell apoptosis. And these phenomenal also associated with the release of DAMPs molecule, HMGB1 and HSP90 from CCA cell to the condition medium.

For the cytotoxicity of these compounds, we also investigated on the human-monocyte-derived macrophages that show highly  $IC_{50}$  more than CCA cells. Meaning that honokiol and magnolol exhibited less cytotoxicity on normal cell less that CCA cells, which is suitable for developing to anticancer drug. Previous studied have reported that the anti-tumour effect of honokiol is stronger than magnolol for various cancer types, such as squamous lung carcinoma and ovarian cancer. This phenomenon may be due to their own isomer structure, which are different by the position of the hydroxyl group that provides distinct properties, such as its solubility and binding pocket on target. Moreover, in this study we also investigated the effects of these compounds on two human CCA cell lines with different metastatic abilities, KKU-213L5 and KKU-100. KKU-213L5, a high-invasive cell line, originated from adenosquamous

CCA with well differentiation and KKU-100, a low-invasive cell line, was isolated from adenocarcinoma CCA with poor differentiation [11]. That the effects of honokiol and magnolol on these CCA cell lines are not different in term of either cytotoxicity or the underlying mechanism.

Immunogenic cell death is mainly mediated by the expression of DAMPs, which release or expose molecules of injured, damaged and apoptotic cells [7]. We examined the expression of two members of DAMPs as secreted HMGB1 and HSP90. The results indicated that both molecules were expressed when CCA cells were treated with honokiol at sub  $IC_{50}$ , while the same concentration caused cell apoptosis. Moreover, these results related to previously reports that demonstrated the induction of cell apoptosis by herbal-derived compound shikonin could induce DAMPs secretion [8]. Therefore, we concluded that honokiol exhibits cytotoxicity against CCA cells by induction of cell apoptosis and causes DAMPs expression in these cells. Similarly to previous report that HSP90 has increasing exposed on cell membrane of cancer cells after treatment with photodynamic therapy [12]. Recently, a DC vaccine based on immunogenic cell death molecules including HMGB1 and HSP90 was shown to elicit danger signals and T-cell activation, resulting in the rejection of high-grade glioma in an animal model [12]. These data suggest that the honokiol-treated tumour antigen may provide maximal efficacy of immunotherapy for CCA treatment.

### **Acknowledgement**

This study was financially supported by Naresuan University research grant (R2557B036).

### **References**

- [1] B. Sripa, S. Kaewkes, P. Sithithaworn, E. Mairiang, T. Laha, M. Smout, C. Pairojkul, V. Bhudhisawasdi, S. Tesana, B. Thinkamrop, Liver fluke induces cholangiocarcinoma, *PLoS. Med.* 4 (2007) e201.
- [2] B. Blechacz, G.J. Gores, Cholangiocarcinoma: advances in pathogenesis, diagnosis, and treatment, *Hepatology* 48 (2008) 308-321.
- [3] J.M. Banales, V. Cardinale, G. Carpino, M. Marzioni, J.B. Andersen, P. Invernizzi, G.E. Lind, T. Folseraas, S.J. Forbes, L. Fouassier, A. Geier, D.F. Calvisi, J.C. Mertens, M. Trauner, A. Benedetti, L. Maroni, J. Vaquero, R.I. Macias, C. Raggi, M.J. Perugorria, E. Gaudio, K.M. Boberg, J.J. Marin, D. Alvaro, Expert consensus document: Cholangiocarcinoma: current knowledge and future perspectives consensus statement from the European Network for the Study of Cholangiocarcinoma (ENS-CCA), *Nat. Rev. Gastroenterol Hepatol*, 13 (2016) 261-280.
- [4] S.B. Reddy, T. Patel, Current approaches to the diagnosis and treatment of cholangiocarcinoma, *Curr. Gastroenterol. Rep.* 8 (2006) 30-37.
- [5] Y.J. Lee, Y.M. Lee, C.K. Lee, J.K. Jung, S.B. Han, J.T. Hong, Therapeutic applications of compounds in the Magnolia family, *Pharmacol. Ther.* 130 (2011) 157-176.
- [6] F.H. Zhang, H.Y. Ren, J.X. Shen, X.Y. Zhang, H.M. Ye, D.Y. Shen, Magnolol suppresses the proliferation and invasion of cholangiocarcinoma cells via inhibiting the NF-kappaB signaling pathway, *Biomed. Pharmacother.* 94 (2017) 474-480.
- [7] D.V. Krysko, A.D. Garg, A. Kaczmarek, O. Krysko, P. Agostinis, P. Vandenabeele, Immunogenic cell death and DAMPs in cancer therapy, *Nat. Rev. Cancer.* 12 (2012) 860-875.
- [8] H.M. Chen, P.H. Wang, S.S. Chen, C.C. Wen, Y.H. Chen, W.C. Yang, N.S. Yang, Shikonin induces immunogenic cell death in tumor cells and enhances dendritic cell-based cancer vaccine, *Cancer. Immunol. Immunother.* 61 (2012) 1989-2002.
- [9] H. Fang, B. Ang, X. Xu, X. Huang, Y. Wu, Y. Sun, W. Wang, N. Li, X. Cao, T. Wan, TLR4 is essential for dendritic cell activation and anti-tumor T-cell response enhancement by DAMPs released from chemically stressed cancer cells, *Cell Mol. Immunol.* 11 (2014) 150-159.

- [10] A. Vickers, C. Zollman, R. Lee, Herbal medicine, *West. J. Med.* 175 (2001) 125-128.
- [11] B. Sripa, S. Leungwattanawanit, T. Nitta, C. Wongkham, V. Bhudhisawasdi, A. Puapairoj, C. Sripa, M. Miwa, Establishment and characterization of an opisthorchiasis-associated cholangiocarcinoma cell line (KKU-100), *World. J. Gastroenterol.* 11 (2005) 3392-3397.
- [12] A.D. Garg, L. Vandenberk, C. Koks, T. Verschuere, L. Boon, S.W. Van Gool, P. Agostinis, Dendritic cell vaccines based on immunogenic cell death elicit danger signals and T cell-driven rejection of high-grade glioma, *Sci. Transl. Med.* 8 (2016) 328ra327.

# Molecular docking study of anthocyanidins and anthocyanins as acetylcholinesterase inhibitors

Phurit Thanarangsarit<sup>1,a\*</sup>, Noppawat Pengkumsri<sup>1,b</sup>, Suthira Yanaso<sup>1,c</sup>,  
Pathamaporn Chuetee<sup>2,d</sup> and Suchanuch Ondee<sup>3,e</sup>

<sup>1</sup>Department of Pharmaceutical Chemistry, Faculty of Pharmaceutical Sciences,  
Huachiew Chalermprakiet University, Thailand

<sup>2</sup>Department of Pharmaceutical Technology, Faculty of Pharmaceutical Sciences,  
Huachiew Chalermprakiet University, Thailand

<sup>3</sup>Section of Experimental Oncotherapy, Research Division, National Cancer Institute,  
Thailand

<sup>a</sup>stamphurit@hotmail.com, <sup>b</sup>Noppawat.pengkumsri@gmail.com,

<sup>c</sup>mim\_sutheera@hotmail.com, <sup>d</sup>pathamaporn.ch@gmail.com, <sup>e</sup>suchanuch@yahoo.com

**Keywords:** anthocyanidins, anthocyanins, acetylcholinesterase inhibitor, molecular docking

**Abstract.** Anthocyanidins and anthocyanins are flavonoid derivatives as known as plant-derived color pigments in many red, purple and blue fruits and vegetables. Anthocyanins are in the form of glycosides, while anthocyanidins are aglycones. Many experiments indicated various health-benefits of these phytochemicals, especially neuroprotective effect *via* acetylcholinesterase (AChE) inhibition. To understand the binding interactions of some anthocyanidins and anthocyanins to the active site of AChE and to predict *in silico* inhibitory activity, molecular docking study was performed using AutoDock 4.2. Docking results showed that pelargonidin-3-glucoside exhibited the best docking profile in terms of good binding affinity and inhibitory activity against human AChE. The binding mode of pelargonidin-3-glucoside was comparable to donepezil, but different to other anthocyanins. The presence of glucose moiety in pelargonidin-3-glucoside structure seemed to play a crucial role for an additional binding interaction nearby the catalytic site (CS) of enzyme, however, enzyme-labile and high polar properties of this functionality may diminish the ability of the compound as a potential inhibitor against AChE.

## Introduction

Anthocyanidins and anthocyanins are the subclasses of polyphenols named flavonoids that found in many fruits (i.e., berries, grape), flowers and leaves, as known as water-soluble color pigments. These two subclasses share a common basic core structure called flavylum cation backbone, but anthocyanins are known as the glycosides which 3-position of the core structure are glycosylated by common sugars, such as glucose (Glc), whereas anthocyanidins are known as the aglycones [1]. Nowadays, many studies have reported various potential health-promoting benefits of anthocyanins due to their antioxidant capacity. Moreover, many scientific studies *in vitro* and *in vivo*, including clinical trials suggested that anthocyanidins and anthocyanins provided antimicrobial, anticarcinogenic, anti-inflammatory activities, chronic disease preventions, such as cardiovascular diseases and diabetes, as well as neuroprotective effects [1, 2]. Interestingly, focusing on the mechanisms of action, anthocyanidins and anthocyanins possess anti-neurodegenerative activities through not only their antioxidative property, but also their acetylcholinesterase (AChE) inhibitory activity as a well-known pathway for the treatment of Alzheimer's disease. Recent *in vitro* studies revealed the inhibitory activity against AChE of these compounds from different sources of plants [3, 4]. Hence, to

understand the binding of anthocyanidins and anthocyanins as AChE inhibitors, molecular docking approach was applied in this study.

## Materials and Methods

### Ligand Preparation

The twelve 3D chemical structures of well-known anthocyanidins and anthocyanins, including donepezil, were retrieved from PubChem Database (<https://pubchem.ncbi.nlm.nih.gov>). For ligand preparation, Gasteiger-Hückel charges were assigned and non-polar hydrogens were merged using AutoDockTools 1.5.6.

### Protein Preparation

All X-ray crystal structures of wild-type ligated human AChE (*hAChE*, PDB code: 4EY5, 4EY6, and 4EY7) with less than 2.5 Å of resolution were retrieved from Brookhaven Protein Data Bank (<https://www.rcsb.org/pdb>). Only one subunit of each dimeric enzymes was selected and the molecule of native ligands, including other nonreceptor atoms, such as water were deleted. The polar hydrogen atoms were added and Gasteiger-Hückel charges were assigned using AutoDockTools 1.5.6. A grid box with the dimensions of 60 × 60 × 60 Å, with a resolution of 0.375 Å was generated and located at the center of the ligand. Corresponding map types were also calculated with AutoGrid.

### Molecular Docking

The prepared ligands were docked on the *hAChE* using AutoDock 4.2 software with the Lamarckian Genetic Algorithm (LGA) method. The following docking parameters were set: a number of GA run was 100, and the maximum of a number of energy evaluations was  $2.5 \times 10^7$ . All other parameters were set as a default setting. One hundred independent docking runs were proceeded of each ligand. The docked poses with less than 2.0 Å of root-mean-square deviations (RMSD) were clustered and the best conformation was chosen to analyze binding orientation, binding energy, and inhibitory constant ( $K_i$ ). The figures of binding interactions, including the length of chemical bonds between the ligand and amino acid residues of *hAChE* were determined using Accelrys Discovery Studio 3.1.

### Validation of Docking Method

To confirm the effectiveness, validity, and reproducibility of docking method, re-docking of each native ligands against their target protein was performed in order to determine the reproducibility of the program. Moreover, cross-docking of each native ligands into the non-native proteins was also conducted. Either re-docking or cross-docking results were accepted when the reference RMSD values from the highest cluster were less than 2.0 Å.

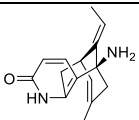
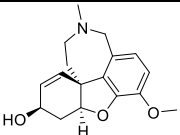
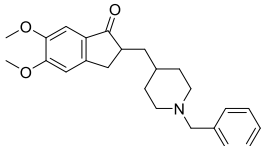
## Results and Discussions

General information of three included X-ray crystal structures of *hAChE* and re-docking results were shown in Table 1. Docking of each native ligands, including huperzine A, galanthamine and donepezil into their target protein exhibited acceptable re-docking validation results, due to the RMSDs obtained from the best cluster were less than 2.0 Å. Thus, cross-docking procedures were conducted to confirm the validity of the docking algorithm. As shown in Table 2, the results revealed that each non-native ligand (huperzine A and galanthamine) produced satisfactory cross-docking outcomes with less than 2.0 Å of the reference RMSD values obtained from the highest cluster. Thus, the *hAChE* (PDB code: 4EY7) was chosen as a template for further molecular docking study.

Molecular docking results of anthocyanidins and anthocyanins against *hAChE*, in comparison with an AChE inhibitor, donepezil were listed in Table 3. In terms of ligand affinity,

the lower binding energy value implies the higher binding affinity, whilst the lower calculated  $K_i$  represents the higher inhibitory activity against the enzyme. The binding energy of anthocyanidins were in the range of -8.32 to -9.21 kcal/mol, whereas anthocyanins exhibited good binding affinity with the binding energy ranging from -8.02 to -10.43 kcal/mol. Intriguingly, pelargonidin-3-glucoside, an anthocyanin derivative displayed a very low binding energy of -10.43 kcal/mol and  $K_i$  of 0.02  $\mu\text{M}$ . In comparison with donepezil, the docking results depicted the binding energy of -11.81 kcal/mol with extremely low  $K_i$  of 0.002  $\mu\text{M}$  (10-fold lower than pelargonidin-3-glucoside).

**Table 1.** General information and re-docking validation results of included *hAChE* PDBs

PDB code	Ligand	Chemical structure	RMS D ( $\text{\AA}$ )	Cluster number	%Member in cluster	Binding energy (kcal/mol)
4EY5	(-)-Huperzine A		0.27	1	100	-10.12
4EY6	(-)-Galanthamine		0.91	1	100	-9.26
4EY7	Donepezil		0.68	8	78	-11.45

**Table 2.** Cross-docking validation results of included *hAChE* PDBs

PDB code	Ligand	RMSD, $\text{\AA}$ (%member in highest cluster)		
		4EY5	4EY6	4EY7
4EY5	(-)-Huperzine A	0.27 (100%)	0.66 (100%)	0.55 (88%)
4EY6	(-)-Galanthamine	2.99 (92%)	0.91 (100%)	1.94 (72%)
4EY7	Donepezil	2.24 (40%)	4.57 (35%)	0.68 (78%)

**Table 3** Molecular docking results of anthocyanidins and anthocyanins against *hAChE* (PDB code: 4EY7)

Compound	CID	Chemical Structure			Binding energy (kcal/mol)	$K_i$ ( $\mu\text{M}$ )
		R <sub>1</sub>	R <sub>2</sub>	R <sub>3</sub>		
<b>Anthocyanidins</b>						
Pelargonidin	44083	H	H	OH	-8.57	0.52
	2					
Cyanidin	12886	OH	H	OH	-9.21	0.18
	1					
Delphinidin	12885	OH	OH	OH	-9.01	0.25
	3					
Peonidin	44177	OCH <sub>3</sub>	H	OH	-8.32	0.79
	3					
Petunidin	44177	OCH <sub>3</sub>	OH	OH	-9.18	0.19
	4					
Malvidin	15928	OCH <sub>3</sub>	OCH <sub>3</sub>	OH	-8.66	0.45
	7					
<b>Anthocyanins</b>						
Pelargonidin-3-glucoside	44364	H	H	OGlc	-10.43	0.02
	8					
Cyanidin-3-glucoside	44166	OH	H	OGlc	-8.90	0.30
	7					
Delphinidin-3-glucoside	44365	OH	OH	OGlc	-8.48	0.61
	0					
Peonidin-3-glucoside	44365	OCH <sub>3</sub>	H	OGlc	-8.47	0.62
	4					
Petunidin-3-glucoside	44365	OCH <sub>3</sub>	OH	OGlc	-8.51	0.58
	1					
Malvidin-3-glucoside	44365	OCH <sub>3</sub>	OCH <sub>3</sub>	OGlc	-8.02	1.33
	2					
Donepezil	3152				-11.81	0.002

In order to understand how the ligand binds to the active site of enzyme, binding orientation and binding interactions between ligands against binding pocket were illustrated (Fig. 1). Emphasizing the best ligand, pelargonidin-3-glucoside aligned in the active site of *hAChE* in the similar pattern like donepezil. Key binding interactions and length of chemical bonds were identified (Fig. 2), the hydroxyl group ( $-\text{OH}$ ) in sugar moiety of pelargonidin-3-glucoside interacted with Trp86 (2.0, 2.2 Å) nearby the catalytic site (CS) of the enzyme, and Tyr124 (3.2 Å) located at the mid gorge site (MGS) *via* hydrogen bond. In addition, the interaction between the  $-\text{OH}$  group of phenol ring (B-ring) and His447 (1.9 Å) located at the CS was hydrogen bond, as well as  $\pi$ - $\pi$  interaction between B-ring and Tyr337 (3.8 Å) at MGS was also indicated. Interestingly, A-ring and C-ring of pelargonidin-3-glucoside core structure

hydrophobically interacted with Trp286 (6.1 Å) and Tyr341 (3.8, 4.2 Å) located at the peripheral anionic site (PAS) of the enzyme *via*  $\pi$ - $\pi$  interactions, whereas the dihydroindenone ring of donepezil also interacted at the same position with Trp286 (4.3, 5.7 Å) and Tyr341 (4.8 Å) *via*  $\pi$ - $\pi$  interactions. Furthermore,  $\sigma$ - $\pi$  interaction between the B-ring of pelargonidin-3-glucoside and Trp86 (3.2 Å) was comparable to  $\pi$ - $\pi$  interaction between the phenyl moiety of donepezil and Trp86 (4.7 Å). These findings suggested the similar structural features between pelargonidin-3-glucoside and donepezil.

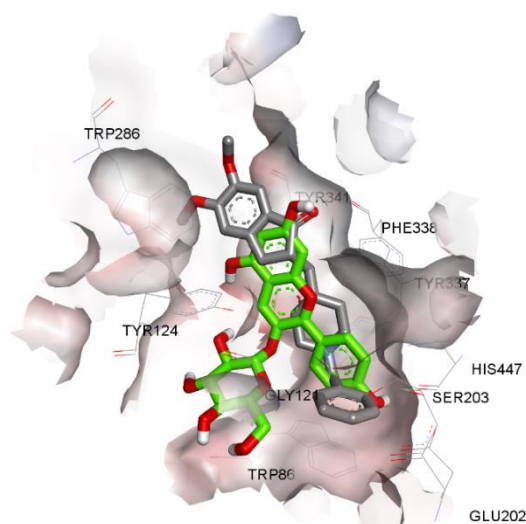


**Figure 1** *In silico*, superimposition of pelargonidin-3-glucoside (green) and donepezil in the active site of *hAChE*. For clarity, only amino acid residues nearby the ligands are shown.

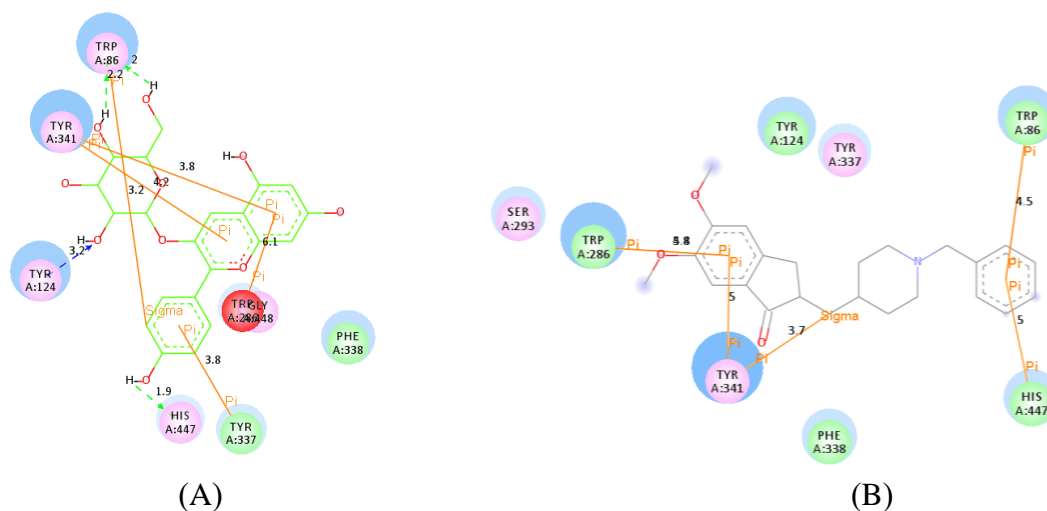


**Figure 2** 2D binding interaction diagrams of pelargonidin-3-glucoside (A), and donepezil (B) in complex with *hAChE*. Hydrogen bonds are showed in green or blue broken lines, and  $\pi$  interactions are showed in orange lines.

According to the outstanding docking profiles of pelargonidin-3-glucoside as mentioned above, 3-*O*-glucose moiety seemed to play an important role for binding to the active site, especially nearby the CS of *hAChE*. In comparison with pelargonidin, an anthocyanin aglycone that contains the same congeners, both determined docking outcomes (binding energy and  $K_i$ ) were inferior to its glucoside derivative. Thus, the binding mode of pelargonidin was considered to gain more information. From the putative binding orientation of pelargonidin (Fig. 3A), the ligand displayed an inverse alignment in the active site of the enzyme. Moreover, the core



structure (A-ring and C-ring) generated only  $\pi$ - $\pi$  interactions with hydrophobic amino acid residues, Trp286 (6.2 Å) and Tyr341 (3.5, 3.7 Å), located at the PAS (Fig. 3B). When compared the binding mode of pelargonidin-3-glucoside to the rest of anthocyanins, the results illustrated that only pelargonidin-3-glucoside showed a unique binding orientation, which all parts of the molecule interacted with the PAS, MGS, including CS of *hAChE*, whereas the other anthocyanins mostly interacted with the PAS and MGS only (Fig. 4). This difference suggested that the sugar moiety in anthocyanin-3-glucosides appeared to be important for additional binding interaction at the CS, but not for all cases. Nevertheless, ligand binding to the PAS also affected enzymatic activities by steric blockade of acetylcholine (ACh) moving through the gorge, and allosteric alteration of the catalytic triad conformation at the CS [5].

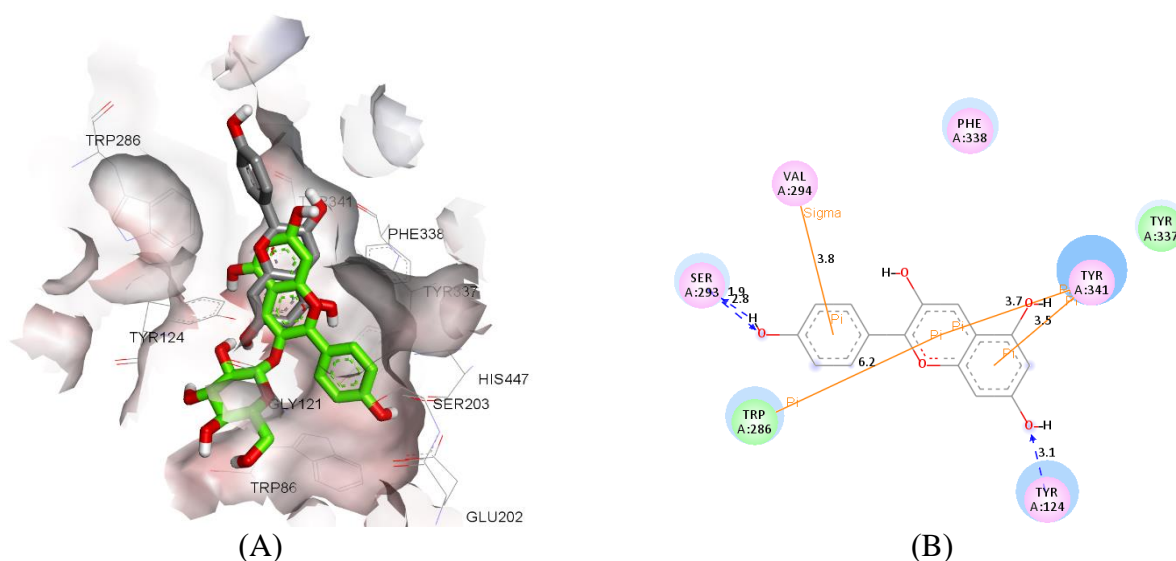


**Figure 3** *In silico*, superimposition of pelargonidin-3-glucoside (green) and pelargonidin (A), and 2D binding interaction diagrams of pelargonidin (B) in the active site of *hAChE*. For clarity, only amino acid residues nearby the ligands are shown. Hydrogen bonds are showed in blue broken lines, and  $\pi$  interactions are showed in orange lines.

Although the presence of sugar moiety in pelargonidin-3-glucoside supposed to be crucial for extra-binding to the active site, particularly at the CS of *hAChE*, instability and hydrophilicity of this functionality cannot be ignored. Pelargonidin-3-glucoside could be absorbed into the gastrointestinal tract, but it can undergo extensive first-pass metabolism and enter the systemic circulation as inactive metabolites, 4-hydroxybenzoic acid and its glucuronide conjugates [6]. Furthermore, glycosylated anthocyanin is highly soluble in water due to the high polarity of additional sugar moiety [2]. This aforementioned property may affect the ability of the molecule to penetrate the blood-brain barrier that required for the inhibition of AChE activity in the brain.

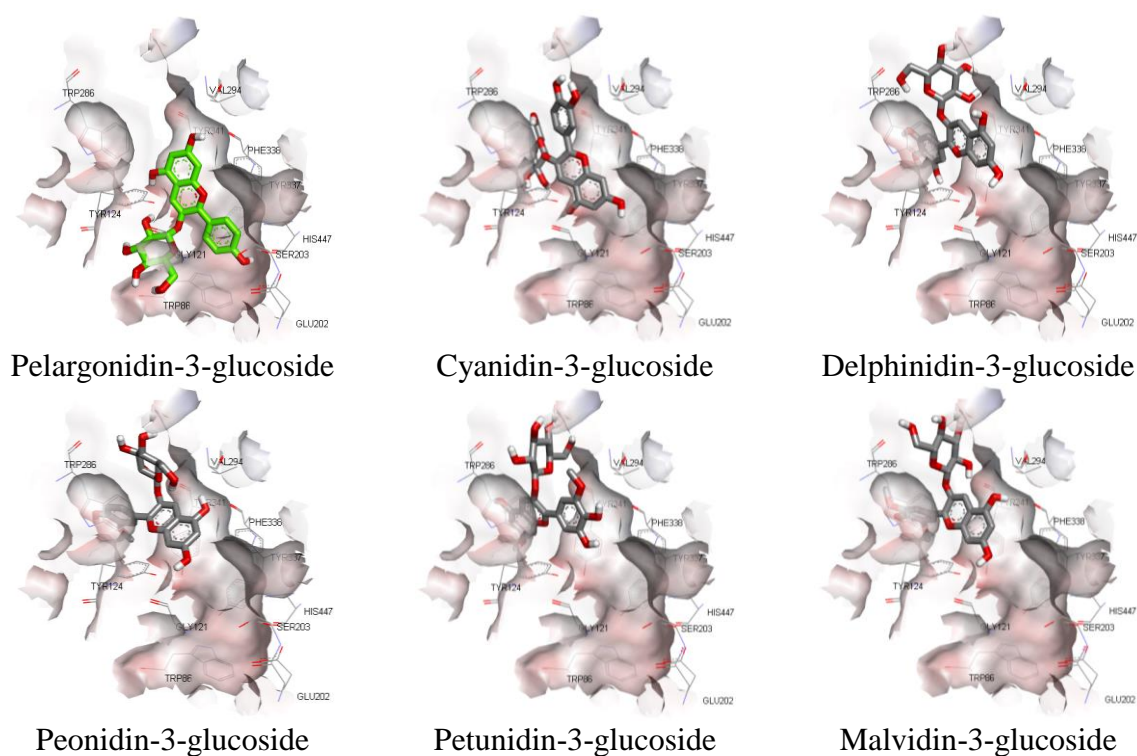


**Figure 4** Binding mode of anthocyanins against the active site of *hAChE*.

## Conclusion

To investigate and to predict the pharmacological effect of anthocyanidins and anthocyanins as AChE inhibitors, twelve molecules of these compounds were docked into the active site of validated *hAChE* using AutoDock. The results indicated that pelargonidin-3-glucoside possessed the highest binding affinity and *in silico* inhibitory activity against *hAChE*. The binding pose of the ligand suggested a unique orientation compared with the other anthocyanins, but similar to donepezil. The presence of glucose moiety seemed to play a crucial role in additional binding interaction with the CS. However, the instability through first-pass metabolism and high polar property of this moiety that may hinder the absorption and brain penetration must be concerned.

## References

- [1] B. Burton-Freeman, A. Sandhu, I. Edirisinghe, Anthocyanins, in: R.C. Gupta (Ed.), *Nutraceuticals: Efficacy, Safety and Toxicity*, Academic Press, Boston, 2016, pp. 489-500.
- [2] H.E. Khoo, A. Azlan, S.T. Tang, S.M. Lim, Anthocyanidins and anthocyanins: colored pigments as food, pharmaceutical ingredients, and the potential health benefits, *Food Nutr. Res.* 61 (2017) 1-21.
- [3] M. Pervin, M.A. Hasnat, Y.M. Lee, D.H. Kim, J.E. Jo, B.O. Lim, Antioxidant activity and acetylcholinesterase inhibition of grape skin anthocyanin (GSA), *Molecules.* 19 (2014) 9403-9418.
- [4] M. Maeda-Yamamoto, T. Saito, A. Nesumi, Y. Tokuda, K. Ema, D. Honma, et al., Chemical analysis and acetylcholinesterase inhibitory effect of anthocyanin-rich red leaf tea (cv. Sunrouge), *J. Sci. Food Agric.* 92 (2012) 2379-2386.
- [5] I. Silman, J.L. Sussman, Acetylcholinesterase: how is structure related to function? *Chem. Biol. Interact.* 175 (2008) 3-10.
- [6] J. Fang, Bioavailability of anthocyanins, *Drug Metab. Rev.* 46 (2014) 508-520.

# Formulation and evaluation of spironolactone anti acne gels

Sunee Channarong<sup>1\*</sup>, Orawan Thammasorn<sup>2</sup>,  
Wisinee Wattanasaringkan<sup>2</sup>, and Pathamaporn Chuetee<sup>1</sup>

<sup>1</sup> Department of Pharmaceutical Technology, Faculty of Pharmaceutical Sciences,  
Huachiew Chalermprakiet University, Bang Phli, Samut Prakan, Thailand.

<sup>2</sup> Undergraduate Student, Faculty of Pharmaceutical Sciences, Huachiew Chalermprakiet University,  
Bang Phli, Samut Prakan, Thailand.

\* Corresponding author: Tel. +66(0)23126300; E-mail address: suneechan555@gmail.com

**Keywords:** Spironolactone, acne gel, antiandrogen, hydroxypropyl methylcellulose

**Abstract.** The objective of this study was to find appropriate compositions to formulate 5% spironolactone topical gel with good stability and physical characteristics for the treatment of hormonal acne. The 5% spironolactone gels were prepared using hydroxypropyl methylcellulose as the gelling agent. The effects of additives (tea tree oil, lactic acid and PEG 400) on the physical characteristics such as clarity, color, pH, viscosity and % drug content, had been investigated after preparing and storing for 1 month at room temperature and under accelerated condition (45°C/75%RH). After preparation, the gels were clear, colorless or yellowish in color in some formulas due to the adding of lactic acid. The pH was in between 3.69 - 5.76, the viscosity was in between  $311.6 \pm 4.2$  to  $676.4 \pm 7.5$  centipoises and the drug content was 89.06% to 95.87%. The formulas containing PEG 400 were found to be higher in the viscosity compared to those without PEG 400. After being stored for 1 month, the formulations containing tea tree oil were found to have less mercaptan-like odor of the drug. The lactic acid containing formulation produced more unacceptable odor. After storage at room temperature and under accelerated condition for 1 month, the assay value decreased from the initial time from 2.2% to 17.7% and 3.3% to 23.9%, respectively. It was found that, tea tree oil can be used as a good odor masking while lactic acid should be avoided. The addition of PEG 400 provided higher viscosity and had no advantage on drug stability.

## Introduction

Acne vulgaris is a common skin disorder of pilosebaceous unit mainly affects childhood and adolescence. It though may present at any age. Acne is also a substantial cutaneous, psychologic and financial burden disease to the patients [1]. The increasing level of circulating androgens of adrenal and gonadal origin seems to trigger the condition. The pathophysiology of acne includes, in a somewhat sequential manner, retention hyperkeratosis, sebaceous gland hyperplasia and increased sebum production, colonization of the follicles by *Propionibacterium acnes*, and perifollicular inflammation [2]. Clinical appearances range from mild comedonal acne to severe nodulocystic acne, which can be permanently defacing. Women with hyperandrogenism usually not respond to conventional topical and systemic antibiotic therapies. Spironolactone is a synthetic 17-spironolactone corticosteroid with potassium-sparing diuretic, antihypertensive, and antiandrogen activities that has a benefit for hormonal therapy in acne. Oral spironolactone has been used for antiandrogenic drug in acne and hirsutism for more than 20 years [3, 4]. These indications are not approved by the FDA, and it should only be considered for the treatment of acne or hirsutism in women in which other treatments have been ineffective. Sato et al. studied the efficacy and safety of oral spironolactone used to treat acne in 139 Japanese patients (116 females and 23 males). Most of female patients exhibited excellent improvement. The efficacy was less in males. Three of them developed gynecomastia and stopped the treatment. They concluded that spironolactone is

effective and safe for the treatment of acne in Asian females and can be good option for severe, recurring and widespread types of the condition [4]. Oral spironolactone is not indicated for women contemplating pregnancy as the drug can cause feminization of the male fetus [3]. Grandhi and Alikhan also reported their study in post adolescent acne patients and found that spironolactone is an effective second-line treatment option with notable side effect of hyperkalemia [6]. Spironolactone has also been studied as a topical formulation [7-9]. In Europe, topical 5% spironolactone lotion and cream have been used to treat grade II acne. Topical spironolactone is not currently available commercially in the United States and as well as in Thailand. A proprietary formulation is not available and the data of topical spironolactone is very limited. Spironolactone is a light, cream-coloured to light-tan crystalline powder with mild mercaptan-like odor. Its melting-point is 198–207 °C, with decomposition. It occasionally shows preliminary melting at about 135 °C, followed by resolidification. Log P of spironolactone is 2.78. It is practically insoluble in water (22 mg/L (at 25 °C)), soluble in ethanol and most organic solvents [10]. These characteristics make it difficult to develop a gel or cream formulation which has good stability, good cosmetic acceptability, and good anti-androgenic activity [9]. Spironolactone is less stable in alkaline conditions with maximum stability at pH 4.5 [11].

In the present study, we formulated a topical 5% spironolactone topical gel for acne purpose. The objective was to find appropriate composition of the gel to obtain the good physical characteristics. The spironolactone gels were evaluated for physical appearance, pH and viscosity. The drug content was also evaluated after storing the gel in an accelerated condition for 1 month.

## **Material and methods**

### **Materials**

#### **Chemicals**

Spironolactone was a gift from Pharmasant Laboratories Co., Ltd., Thailand. Polyethylene glycol 400 (PEG 400) was purchased from Sigma, Germany. Absolute ethyl alcohol was purchased from Carlo Erba. Propylene glycol (PG), lactic acid and tea tree oil were purchased from Namsiang Co., Ltd., Thailand. Hydroxypropyl methylcellulose (HPMC 4000) was purchased from Rama Production, Thailand.

### **Methods**

#### **Preparation of spironolactone acne gel**

Table 1 demonstrates the formulations used to prepare spironolactone gels in various compositions. HPMC was previously hydrated with all of the deionized (DI) water in the formula. Spironolactone was separately dissolved in the mixture of absolute ethyl alcohol and propylene glycol contained in a well closed container using a magnetic stirrer. Then, the resulted clear solution was gradually added into the hydrogel and stirred gently. The gels were evaluated by visual inspection for clarity and texture to select the appropriate amount of the cosolvent used for further optimization.

**Table 1.** The compositions of the formulations (%w/w).

	PF1	PF2	PF3	PF4
Spironolactone	5	5	5	5
Ethyl alcohol	40	45	60	60
Propylene glycol (PG)	10	10	10	10
HPMC 4000	0.5	0.5	0.5	0.5
PEG 400	30	25	15	10
DI water qs to	100	100	100	100

**Table 2** The compositions (%w/w) of the optimized formulations.

Ingredient	Compositions (%w/w)							
	F1	F2	F3	F4	F5	F6	F7	F8
Spironolactone	5	5	5	5	5	5	5	5
Ethyl alcohol	60	60	60	60	60	60	60	60
PG	10	10	10	10	10	10	10	10
HPMC 4000	1	1	1	1	1	1	1	1
PEG 400	10	10	10	10	-	-	-	-
Lactic acid	0.5	0.5	-	-	0.5	0.5	-	-
Tea tree oil	0.5	-	0.5	-	0.5	-	0.5	-
DI water qs to	100	100	100	100	100	100	100	100

Table 2 illustrates the compositions for optimization study. HPMC 4000 was previously hydrated with all of the DI water in the formula. Spironolactone solution was prepared as described above. Then the resulted clear solution was gradually added into the hydrogel and stirred gently. PEG 400, lactic acid and/or tea tree oil (if needed) were added and mixed thoroughly. The gels were kept in glass well-closed containers and stored at room temperature until the time of analysis.

### Drug content analysis

0.5 gram of the spironolactone gel was accurately weighed, dissolved and adjusted to 100 ml with a solvent mixture of ethyl alcohol and water (50:50 v/v). The solution was then diluted by pipetting 0.5 ml of the solution and transferred to a 25 ml-volumetric flask. The volume was adjusted to 25 ml with the solvent mixture. The drug content was analyzed spectrophotometrically at 240 nm using a spectrophotometer (UV 1800, Shimadzu, Japan). The absorbance was transformed to concentration by using a linear regress line from standard solutions ranging from 2.5 – 20 mcg/ml. The placebo gel solution was prepared in the same manner to study the specificity of the analysis.

### Determination of the gel viscosity

The viscosity of the gel preparations was measured using a Brookfield viscometer (DV-II+, USA) with a small sample adaptor. The gels were rotated at 30 rpm using spindle number S34 at a controlled room temperature.

### Determination of the gel pH

One gram of each formulation was dispersed in 5 ml of DI water and mixed well. The pH of each gel preparation was determined using a pH meter (Shott, Model Lab 850, Germany).

### Stability study

The formulations were stored at room temperature (RT) and in an accelerated stability cabinet set at 45°C with 75% relative humidity (45°C/75%RH). The stability was evaluated by visual inspection for the gel appearance, odor and pH. The drug content was determined after storage for 1 month.

## Results and discussion

### Optimization of spironolactone gels

From Table 1, the spironolactone gels with appropriate physical appearance were obtained from PF3 and PF4 which containing high percentage (60%w/w) of ethyl alcohol to dissolve the 5 grams of spironolactone. Therefore, PF3 that contained 10% of PEG 400 was selected for further study as shown in Table 2. Other two additives, lactic acid ( $pK_a = 3.86$ ) and tea tree oil, were used as the pH adjuster and odor masking of the mercaptan-like smell, respectively. Tea tree oil was used because of its antioxidant activity and antibacterial action [12] which may have the benefits to the products.

**Table 3.** The physical properties of the spironolactone gels

	Appearance	pH	Viscosity (cps)	%Drug content (at the initial time)
F1	Pale –yellow, clear gel	4.43	$524.8 \pm 3.1$	95.87
F2	Pale –yellow, clear gel	4.50	$568.2 \pm 3.5$	89.06
F3	Colorless, clear gel	6.40	$529.2 \pm 5.4$	91.56
F4	Colorless, clear gel	6.67	$676.4 \pm 7.5$	93.15
F5	Pale –yellow, clear gel	3.70	$309.6 \pm 3.4$	89.62
F6	Pale –yellow, clear gel	3.69	$322.2 \pm 3.8$	91.54
F7	Colorless, clear gel	5.60	$318.0 \pm 3.1$	91.34
F8	Colorless, clear gel	5.76	$311.6 \pm 4.2$	89.95

The physical properties of the spironolactone gels are listed in Table 3. All of spironolactone gels were clear, smooth and homogeneous at the initial time of preparation. Formulations F1, F2, F5 and F6 had a pale-yellowish gel color due to the nature of lactic acid (Figure 1). The pH of these formulations was in between 3.69-4.50, while of those without lactic acid was in between 5.60-6.67.

The viscosity of the gels varied from  $309.6 \pm 3.4$  to  $676.4 \pm 7.5$  cps depended on the adding of PEG 400 in the formula.

Formulations F3 and F7 which containing only tea tree oil provided camphor-like odor, while F1 and F5 contained both tea tree oil and lactic acid resulted in less acceptable smell.



**Fig. 1.** The appearance of the spironolactone gels after preparation.

### Drug content analysis

Spectrophotometric method for determining spironolactone in gel preparations was developed and validated. Spironolactone showed the maximum absorption wavelength at 240 nm. The linear regression line of calibration curve (2.5 -20 mcg/mL) was  $Abs = 0.0608 \text{ Conc.} + 0.0215$ . The correlation coefficient was found to be 0.9996 which showed good linear relationship between the concentration and absorption.

The % drug contents were examined to be 89.06% to 95.87%. The loss of drug content might be due to improper transferring the drug solution into the gel. However, we used these values as the initial amounts of the drug content for the stability study.

### Stability study

The stability study of all gel formulations was carried out. The physical appearance (color, smell of mercaptan-like odor, pH) and the % drug content reduction were investigated. Table 4 displays the physical properties of the gels after storing for 1 month at room temperature and at 45°C/75%RH. Formulations containing lactic acid (F1, F2, F5 and F6) resulted in the decrease of the drug content upon storage both at room temperature (protect from light) and at 45°C/75%RH. The data was reported as percentage of drug decrease compared to the initial assay value. After storing in the accelerated condition, formulations with lactic acid produced more mercaptan-like smell as well as a darker yellow color.

**Table 4.** Physical stability of the spironolactone gels after 1 month storage

	Appearance		pH		% Drug decrease from the initial assay value	
	RT	45°C/75%RH	RT	45°C/75%RH	RT	45°C/75%RH
F1	Pale –yellow +	Pale –yellow ++	4.41	3.70	8.8	11.2
F2	Pale –yellow++	Pale –yellow+++	4.44	4.41	17.0	20.9
F3	Pale –yellow +	Pale –yellow ++	6.03	5.66	2.2	3.3
F4	Pale –yellow +	Pale –yellow +	6.00	5.39	10.0	19.6
F5	Pale –yellow++	Pale –yellow+++	3.43	3.31	14.9	23.9
F6	Pale –yellow++	Pale –yellow+++	3.53	3.37	3.6	8.4
F7	Colorless	Pale –yellow	4.75	4.10	2.6	4.1
F8	Colorless	Pale –yellow	5.72	3.63	17.7	19.2

From the study, it revealed that spironolactone is susceptible to degradation in all formulations and both storage conditions (at room temperature and at 45°C/75%RH). Formulations F3 and F7 which containing tea tree oil and without lactic acid showed the lowest degradation of the spironolactone as shown in Figure 2.

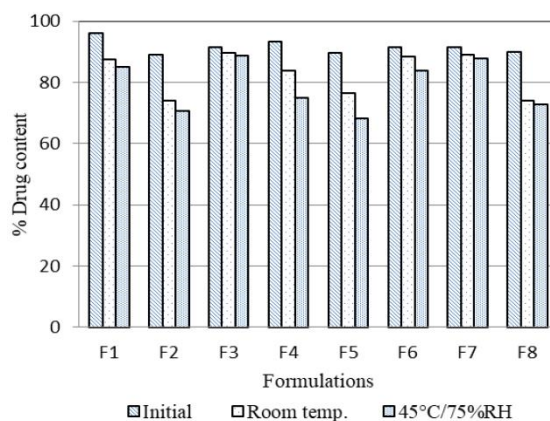


**Fig. 2.** % Drug contents of the optimized formulations after being stored for 1 month at room temperature and at 45°C/75%RH.

For oral administration, spironolactone decreases testosterone biosynthesis by inhibiting steroid 17-alpha-monooxygenase activity. It also performs competitively binding to dihydrotestosterone cytoplasmic receptor, thus decreasing androgenic actions at target tissues [10]. For topical use, spironolactone is expected to affect androgen receptors in the sebaceous glands causing reduced sebum production and thereby causing an improvement in acne symptoms [3]. Spironolactone is soluble in ethyl alcohol thus a very high proportion is needed to dissolve up to 5% of the active ingredient. Propylene glycol was used as cosolvent and as well as drug permeation enhancer. The adding of PEG 400 had no effect on the spironolactone stability or solubility.

### Conclusion

Due to the poor water solubility of spironolactone, it is not easy to formulate a topical gel containing 5% of spironolactone. High percentage of ethyl alcohol is needed as well as a good gelling agent. In this study, HPMC possesses the most desirable in terms of high transparency, good swelling ability and well tolerance in wide range of pH. The solvent system consisting of 60% ethyl alcohol has been proved to be compatible with HPMC. Considering the stability study, tea tree oil can be used as an odor-modulating agent.



## References

- [1] S. Knutesen-Lason, A.L. Dawson, C.A. Dunnick, and R.P. Dellavalle, “Acne vulgaris: pathogenesis, treatment, and needs assessment,” *Dermatologic Clinics*, 2012, vol. 30(1), 99-106.
- [2] W. F. Bergfeld, “The Pathophysiology of Acne Vulgaris in Children and Adolescents, Part 1,” *Cutis*, 2004, vol.74, 92-97. Available online <https://mdedge-files-live.s3.us-east-2.amazonaws.com/files/s3fs-public/Document/September-2017/074020092.pdf> (accessed 29 March 2019)
- [3] G. S. Blair, and N. D. Allie. “Spironolactone use for women with acne or hirsutism,” *Journal of the Dermatology Nurses’ Association*, 2011, vol. 3(6), 374-376. Available online [https://www.nursingcenter.com/pdfjournal?AID=1276102&an=01412499-2011111000-00009&Journal\\_ID=849729&Issue\\_ID=1275755](https://www.nursingcenter.com/pdfjournal?AID=1276102&an=01412499-2011111000-00009&Journal_ID=849729&Issue_ID=1275755) (accessed 29 March 2019)
- [4] T. L. Ebede, E. L. Arch, and D. Berson, “Hormonal treatment of acne in women,” *The Journal of Clinical and Aesthetic Dermatology*, 2009, vol. 2 (12), 16–22.
- [5] K. Sato, D. Matsumoto, F. Iizuka, E. Aiba-Kojima, A. Watanabe-Ono, H. Suga, K. Inoue, K. Gonda, and K. Yoshimura, “Anti-androgenic therapy using oral spironolactone for acne vulgaris in Asians,” *Aesthetic Plastic Surgery*, 2006, vol. 30 (6), 689-694.
- [6] R. Grandhi, and A. Alikhan, “Spironolactone for the treatment of acne: A 4-year retrospective study,” *Dermatology*, 2017, vol. 233(2-3), 141-144.
- [7] H. R. Kelidari, M. Saeedi, Z. Hajheydari, J. Akbari, K. Morteza-Semnani, J. Akhtari, H. Valizadeh, K. Asare-Addo, and A. Nokhodchi, “Spironolactone loaded nanostructured lipid carrier gel for effective treatment of mild and moderate acne vulgaris: A randomized, double-blind, prospective trial,” *Colloids and Surfaces B: Biointerfaces*, 2016, vol. 146:47-53.
- [8] B. M. Afzali, E. Yaghoobi, R. Yaghoobi, N. Bagherani, M. A. Dabbagh, “Comparison of the efficacy of 5% topical spironolactone gel and placebo in the treatment of mild and moderate acne vulgaris: a randomized controlled trial,” *The Journal of Dermatological Treatment*, 2012, vol. 23(1), 21-25.
- [9] C. E. Kim, O. I. Morales, J. J. Pazdur, “Topical spironolactone composition”, Illinois (USA), EP 0410348 A1, 1991. Available online <https://patentimages.storage.googleapis.com/be/2d/4c/110ebac79bd745/EP0410348A1.pdf> (accessed 29 March 2019)
- [10] National Center for Biotechnology Information. PubChem Database. Spironolactone, CID=5833, <https://pubchem.ncbi.nlm.nih.gov/compound/5833> (accessed 29 March 2019)
- [11] Y. Prammar, and V. D. Gupta, “Preformulation studies of spironolactone: Effect of pH, two buffer species, ionic strength, and temperature on stability” *Journal of Pharmaceutical Science*, 1991, vol. 80 (6), 551-553.
- [12] H. J. Kim, F. Chen, C Wu, X. Wang, H.Y. Chung, and Z. Jin, “Evaluation of antioxidant activity of Australian tea tree (*Melaleuca alternifolia*) oil and its components,” *Journal of Agricultural and Food Chemistry*, 2004, vol.52(10), 2849-2854.

# Formulation and characterization of clove oil microemulsions

Panomsuk Suwannee<sup>1, 2, a\*</sup>, Porkar Natcha<sup>1,b</sup>, Meerasen Pornnapa<sup>1,c</sup> and  
Kunrattanaporn Nuttapoj<sup>1, d</sup>

<sup>1</sup>Department of Pharmaceutical Technology, Faculty of Pharmacy, Silpakorn University, Thailand

<sup>2</sup>Pharmaceutical Development of Green Innovations Group (PDGIG), Faculty of Pharmacy,  
Silpakorn University, Thailand

<sup>a</sup>panomsuk\_s@su.ac.th, <sup>b</sup>porkar\_n@silpakorn.edu, <sup>c</sup>meerasen\_p@silpakorn.edu,

<sup>d</sup>kunrattanaporn\_n@silpakorn.edu

**Keywords:** microemulsions, clove oil, Tween 80, ethanol, physico-chemical properties

**Abstract.** The aim of this study was to develop clove oil microemulsions (ME) for topical application. ME containing clove oil as oil phase, Tween 80 as surfactants, ethanol as co-surfactant and water were formulated. The effects of surfactant:co-surfactant ratios (SR), the amount of clove oil and the amount of surfactant mixture (SM) on the physico-chemical properties (pH, conductivity, particle size, zeta potential, and thermodynamic stability) were evaluated.

From pseudo-ternary phase diagrams constructed by using various SR (1:0.5, 1:1 and 1:2), the larger ME zone was found when the ratio was 1:2. The pH values of clove oil ME were 7-7.9. The droplet sizes of all formulations were 15-76 nm. Sizes and conductivities of the system were influenced by SR, the amount of clove oil and the amount of SM. The results revealed that clove oil formulation can be prepared using ME techniques. Topical o/w ME containing 5-20 % clove oil as oil phase with appropriated properties can be formulated using Tween80 and ethanol as surfactant systems.

## Introduction

Clove oil is the volatile essential oil obtained from dried floral buds of clove tree (*Syzygium aromaticum*). The main component (89%) in clove oil is eugenol [1, 2]. Clove oil is used throughout the world for applications ranging from food flavoring to topical analgesic in dentistry. Clove oil is also used in topical products because it has antioxidant, antibacterial, antiviral and antifungal activities [1-3]. The commercial topical products available in the market are cream, lotion, gel toothpaste and mouthwash. Microemulsions (ME) are thermodynamically stable transparent liquids containing oil, mixture of surfactant and co-surfactant, and water [4, 5]. They are stable to phase separation over a wide temperature range. Hydrophilic and lipophilic drugs can be loaded in this system because they contained both water and oil phases. The size of droplet in ME was between 10-100 nm. Among surfactant, Tween 80 is non-ionic surfactant and commonly used in ME and topical products. Ethanol was used as co-surfactant because it is widely used in topical formulations and can be used in high concentration [4, 5].

The objectives of this study are to formulate clove oil using ME techniques for topical applications. ME containing clove oil as oil phase, Tween 80 as surfactant, ethanol as co-surfactant and water were formulated. The effects of surfactant:co-surfactant ratios (SR; 1:0.5, 1:1, 1:2), the amount of clove oil (5-30%) and the amount of surfactant mixture (SM; 60, 70, 80%) on the physico-chemical properties (pH, conductivity, particle size, zeta potential, and thermodynamic stability) were evaluated.

## Materials and Methods

### Materials

Clove oil (Thai-China Flavours and Fragrances Industry Co., Ltd. Thailand), absolute ethanol (Qréc®, New Zealand), Tween 80 (CP drugs Co., Ltd. Thailand) were purchased. All reagents were of analytical grade and were used without further purification.

### Construction of Pseudo-ternary Phase Diagram

Clove oil, an active ingredient, was used as an oil phase. Ethanol at various ratios were used as co-surfactants. The surfactant mixture (SM) of Tween 80 and ethanol at various surfactant:co-surfactant ratios (SR), 1:0.5, 1:1 and 1:2, were used to construct the phase diagram by water titration method [6]. The mixture of clove oil and SM was prepared at weight ratios of 0:10, 1:9, 2:8, 3:7, 4:6, 5:5, 6:4, 7:3, 8:2, 9:1 and 10:0, respectively. The water was slowly added in these mixtures under magnetic stirring. After being equilibrated, the transparent fluid systems were characterized as ME. ME zone in phase diagrams was constructed from the compositions at the equilibrium points.

### Formulation of ME loaded with Clove Oil

The suitable SR was selected from the phase diagram. ME with various amounts of clove oil and SM at the selected ratio were formulated and evaluated for their characteristics.

### Characterization of ME loaded with Clove Oil [4-6].

**Centrifugation.** Thermodynamic stability of the ME was evaluated by ultracentrifugation (Optima L-80, Beckman Instruments, USA) at 40,000 rpm for 30 min at 4°C.

**pH Measurements.** The pH value of the formulation was measured using pH meter (LAQUA twin) at room temperature.

**Conductivity Measurements.** The electrical conductivity of ME was determined using conductivity meter (EC Test 11+, USA) at 25°C.

**Particle Size and Zeta Potential Measurements.** The size and zeta potential of ME was measured using photon correlation spectroscopy (Zetasizer Nano series, Malvern, USA). The measurement was performed using a He-Ne laser at 633 nm with clear disposable zeta cell.

## Results and Discussions

### Pseudo-ternary Phase Diagram.

Figure 1 is the pseudo-ternary phase diagrams constructed from various weight ratios of surfactant and co-surfactant mixture. The shade area represented the ME zone where the mixtures were transparent. ME was mainly formed when the amount of Tween 80 and ethanol was more than 50%. A slightly increase in ME zone was found when the ratio was 1:2. This is similar to the formulation of ME containing curcumin using Tween80 and ethanol as surfactant system where the SR did not efficiently affect the transparent region [7].

### Effects of the Compositions on the Physicochemical Characteristic of ME.

Various ME formulations were prepared mainly using the SR of 1:2. The formulations were designed to study the effect of the amount of SM, the amount of clove oil and SR on physico-chemical characteristics of ME. The compositions and physicochemical properties of ME formulations were shown in Table 1. All formulations are homogeneous and transparent with pH values of 7-7.9 which was suitable for topical application. No phase separation was observed after ultracentrifugation at 25°C, this revealed the thermodynamically stable of all preparations. Zeta potential values of clove oil ME ranged from 0.34 to -0.39 mV. The values between +30 to -30 is acceptable [5]. This reflected the neutral nature of clove oil ME constructed from Tween80, the non-ionic surfactant. The conductivity values depended directly on the amount of water. The conductivity revealed the nature

of the external phase. It was reported that the conductivity of w/o ME was lower than 10  $\mu\text{S}/\text{cm}$  while that of the o/w ME was relatively high with the values about 10–100  $\mu\text{S}/\text{cm}$  [8, 9]. Thus, the results revealed that all formulations could be classified as o/w ME. As the amount of oil increased from 10 to 30% (Rx 1, 4, 5), the conductivity decreased to almost near 10  $\mu\text{S}/\text{cm}$  which was nearly turned to w/o ME.

Figure 2 showed the effects of the amount of SM, clove oil and SR on particle size and polydispersity index (PDI) of ME. The droplet size of clove oil ME ranged in nano-scale, 15-76 nm. PDI values represented the size distribution of the ME system ranged from 0-1. The values near zero revealed the monodispersed particle while the values less than 0.5 indicated narrow size distribution. The droplet size decreased when using the higher amount of SM and clove oil. However, size distribution was higher when increasing the amount of clove oil. Using SR of 1:2 decreased the size of ME (Rx 4, 6, 7). It can be concluded that high amount of ethanol decreased the size and PDI of clove oil ME. Ethanol as co surfactants, with unsaturated bonds, raises the fluidity of the interface between oil and water which results in the decreasing of droplet size [5]. ME containing clove oil:Tween 80:ethanol of 1:2:7 and 1:3:6 were reported for their antimicrobial activity [10]. The sizes were 241.1 and 150.0 nm, respectively, which were larger than 100nm.

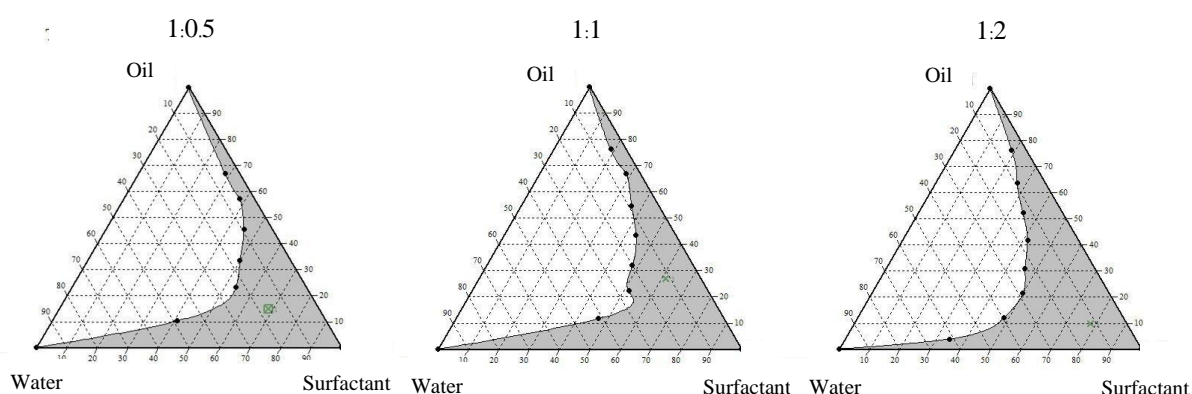


**Figure 1:** Pseudo-ternary phase diagrams of systems composed of clove oil, surfactant (Tween 80 and ethanol) and water at various surfactant:co-surfactant ratios (1:0.5, 1:1, 1:2). The shade area is the ME zone.

**Table 1.** Compositions and physicochemical properties of clove oil ME

Rx No.	ME compositions (%w)				Physicochemical properties of ME [mean $\pm$ SD]		
	Oil	SR	SM	Water	Size [nm]	Zeta potential [mV]	Conductivity [ $\mu\text{S}/\text{cm}$ ]
1	10	1:2	60 (20/40)	30	76.33 $\pm$ 2.78	0.051 $\pm$ 0.193	32.5 $\pm$ 0.21
2	10	1:2	70 (23.2/46.7)	20	30.21 $\pm$ 3.49	-0.092 $\pm$ 0.0727	26.3 $\pm$ 0.21
3	10	1:2	80 (26.7/53.3)	10	33.96 $\pm$ 11.03	-0.386 $\pm$ 0.105	23.5 $\pm$ 0.15
1	10	1:2	60 (20/40)	30	76.33 $\pm$ 2.78	0.051 $\pm$ 0.193	32.5 $\pm$ 0.21
4	20	1:2	60 (20/40)	20	23.74 $\pm$ 3.56	-0.033 $\pm$ 0.238	26.0 $\pm$ 0.62
5	30	1:2	60 (20/40)	10	15.51 $\pm$ 3.45	0.342 $\pm$ 0.081	14.4 $\pm$ 0.92
4	20	1:2	60 (20/40)	20	23.74 $\pm$ 3.56	-0.033 $\pm$ 0.238	26.0 $\pm$ 0.62
6	20	1:1	60 (30/30)	20	33.29 $\pm$ 0.77	-0.112 $\pm$ 0.122	25.6 $\pm$ 0.56
7	20	1:0.5	60 (40/20)	20	56.98 $\pm$ 5.37	0.072 $\pm$ 0.086	27.4 $\pm$ 0.68

SR = Surfactant:co-surfactant ratio

SM = Surfactant mixture

PDI = Polydispersity index

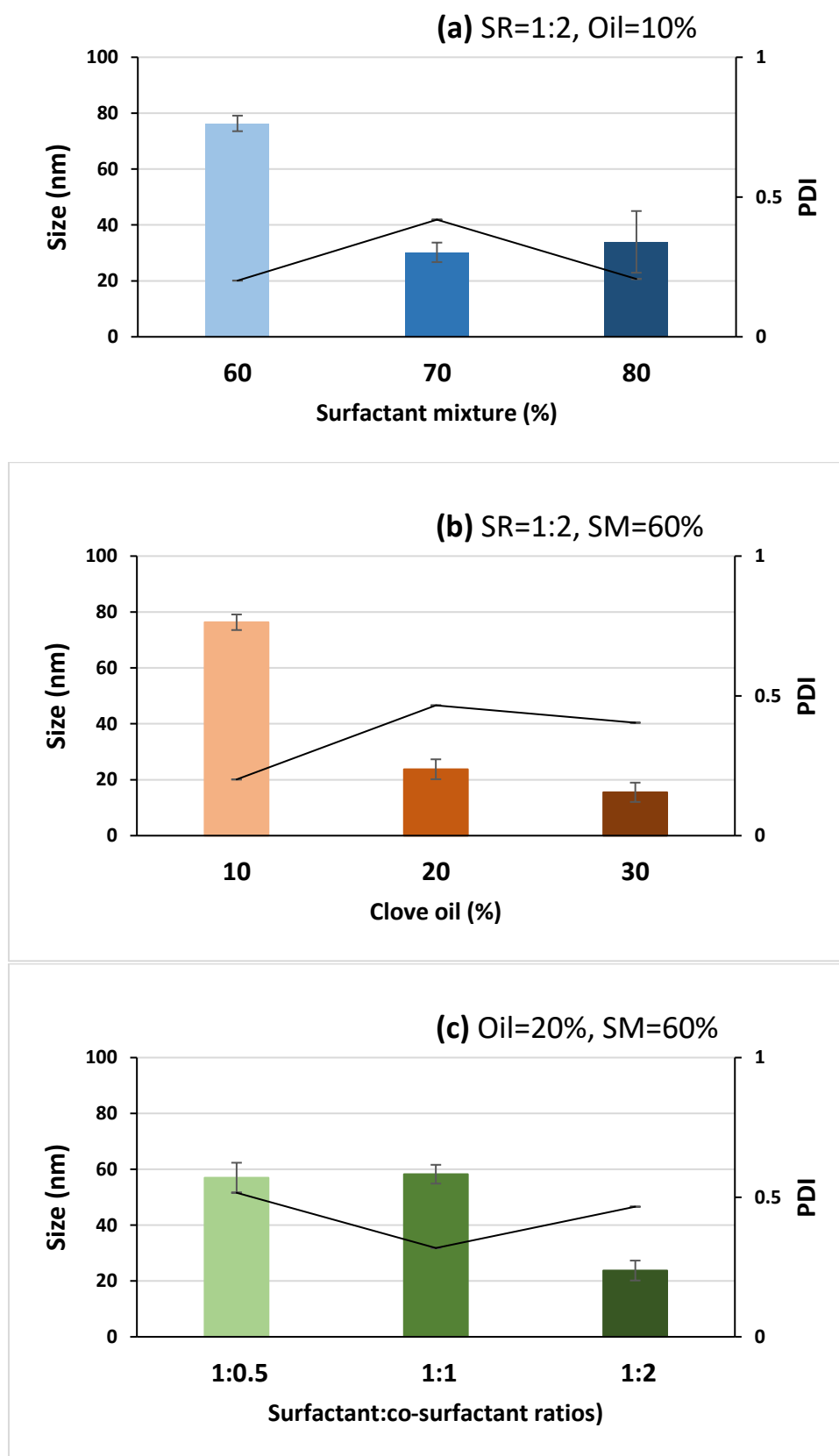


**Figure 2.** Size (bar) and polydispersity index (PDI, line) of clove oil microemulsions: effects of (a) the amount of surfactant mixture, SM (b) the amount of clove oil and (c) surfactant:co-surfactant ratios, SR. (n=3)

## Summary

The construction of pseudo-ternary phase diagram using clove oil as the whole oil phase showed that herbal oil can be formulated using ME techniques. Topical o/w ME containing 10-30 % clove oil as oil phase with appropriated properties can be prepared. The physicochemical characteristic of clove oil ME, especially size and PDI, depended on the amount of oil and ethanol in the system. Ethanol effected directly to the size and PDI of ME droplets. Size and PDI decreased as the amount of ethanol increased. The use of Tween 80 and ethanol produced o/w ME with the size range within 100 nm.

## Acknowledgements

The authors would like to thanks Faculty of Pharmacy, Silpakorn University for the financial support.

## References

- [1] D.F. Cortés-Rojas, C.R. Fernandes de Souza and W.P. Oliveira, Clove (*Syzygium aromaticum*): a precious spice, *Asian Pac J Trop Biomed.* 4(2) (2014) 90-96.
- [2] K. Chaieb, H. Hafedh Hajlaoui, T. Zmantar, A.B. Kahla-Nakbi, M. Rouabhia, K. Mahdouani and A. Bakhrouf, The chemical composition and biological activity of clove essential oil, *Eugenia caryophyllata (Syzygium aromaticum L. Myrtaceae): a short review*, *Phytother. Res.* 21 (2007) 501–506.
- [3] I Gülçin, M Elmastaş, H.Y. Aboul-Enein, Antioxidant activity of clove oil, A powerful antioxidant source. *Arab. J. Chem.* 5 (2012) 489–499.
- [4] S.P. Callender, J.A. Mathews, K. Kobernyk, S.D. Wettig, Microemulsion utility in pharmaceuticals: implications for multi-drug delivery, *Int. J. Pharm.* 526 (2017) 425–442.
- [5] S.N. Kale1, S.L. Deore, Emulsion micro emulsion and nano emulsion: a review, *Sys Rev Pharm.* 8(1) (2017) 39-47.
- [6] T. Ngawhirunput, N. Worachun, P. Opanasopit, T. Rojanarata and S. Panomsuk, Cremophor RH40-PEG 400 microemulsions, *Pharm Dev Tech.* 18(4) (2013) 798–803.
- [7] C.H. Liu and F.Y. Chang, Development and characterization of eucalyptol microemulsions for topical delivery of curcumin, *Chem. Pharm. Bull.* 59(2) (2011) 172—178.
- [8] B. Baroli, M.A. López-Quintela, M.B. Delgado-Charro, A.M. Fadda and J. Blanco-Médez, Microemulsions for topical delivery of 8-methoxsalen, *J Control Release.* 69 (2000) 209–218.
- [9] E.S. Park, Y. Cui, B.J. Yun, I.J. Ko and S.C. Chi, Transdermal delivery of piroxicam using microemulsions, *Arch Pharm Res.* 28 (2005) 243–248.
- [10] S. He, X. Ren, Y. Lu, Y. Zhang, Y. Wang\*, L. Sun, Microemulsification of clove essential oil improves its *in vitro* and *in vivo* control of *Penicillium digitatum*, *Food Control.* 65 (2016) 106-111.

# Effect of mucoadhesive substances on physico-chemical properties of in situ gels for buccal applications

Panomsuk Suwannee<sup>1, 2, a\*</sup>, Keawsri Kunyakorn<sup>1, b</sup>, Limsatjapanit Chanapa<sup>1, c</sup>  
Asneesantiwong Nutcha<sup>1, d</sup> and Chomto Parichat<sup>1, e</sup>

<sup>1</sup>Department of Pharmaceutical Technology, Faculty of Pharmacy, Silpakorn University, Nakhon Pathom 73000, Thailand

<sup>2</sup>Pharmaceutical Development of Green Innovations Group (PDGIG), Faculty of Pharmacy, Silpakorn University, Nakhon Pathom 73000, Thailand

<sup>a</sup>panomsuk\_s@su.ac.th, <sup>b</sup>kunyakorn.keawsri@gmail.com, <sup>c</sup>chanapa.limsatjapanit@gmail.com, <sup>d</sup>nutcha.asneesantiwong@gmail.com, <sup>e</sup>chomto\_p@su.ac.th

**Keywords:** In situ gels, buccal mucoadhesive, benzalkonium chloride, povidone iodine.

**Abstract.** In situ gels for oral mucoadhesive applications using benzalkonium chloride (BZK) and povidone iodine (PI) as active pharmaceutical ingredients were formulated using Poloxamer 407, a thermo-sensitive sol-gel polymer. Xanthan gum (XAN) and sodium carboxymethylcellulose (SCMC) were added to study the effect of mucoadhesive polymer on the physico-chemical properties of gels. The formulations were evaluated for the viscosity (25 and 37 °C), pH, gel strength in artificial saliva at 37 °C and adhesion to porcine buccal mucosa. At 37 °C, the viscosity of all preparations increased ( $p < 0.05$ ). They turned to gels in buccal conditions with good gel strength and dissolution time were more than 45 min. PI reduced the viscosity of the gel ( $p < 0.05$ ). For Poloxamer 407-PI formulation, only SCMC promoted the mucoadhesive property. In situ gels prepared from Poloxamer 407-BZK showed suitable properties for buccal applications. XAN and SCMC did promote the gel properties by increase the viscosity at 37 °C.

## Introduction [1-3]

Buccal drug delivery systems can avoid the first pass effect and side effect of drugs. However, in application for local effect, the difficulty of applying due to high viscosity of semisolid preparations or the ease of removing due to low viscosity of solutions does affect the therapeutic efficacy. To overcome these disadvantages, the in situ gel (the liquid preparation turns to gel after applying on buccal mucosa) was developed using thermo-sensitive sol-gel polymers. Poloxamer, polyethylen oxide-polypropylene oxide-polyethylen oxide (PEO-PPO-PEO), is triblock copolymers with relatively low toxicity and ability to form clear gels in aqueous media, have been commonly used in pharmaceutical delivery system. Benzalkonium chloride (BZK) and povidone iodine (PI) are common antiseptics and wound healing applications. BZK is classified as a quaternary ammonium compound. It is a common use as preservative and antimicrobial. PI demonstrates broad spectrum of activity, be able to penetrate biofilms, exhibit anti-inflammatory properties, low cytotoxicity and good tolerability and lack of associated resistance. The objectives of this research were to study the effect of mucoadhesive substances on the physico-chemical properties, gel strength and buccal mucoadhesive properties of in situ gels for buccal applications.

## Materials and Methods

### Materials

Poloxamer 407 (P, BASF SE, Germany), benzalkonium chloride (BZK, Acros organics, Denmark), povidone iodine (PI, CP drugs Co., Ltd., Thailand), xanthan gum (XAN, CP drugs Co.Ltd.,

Thailand), sodium carboxymethylcellulose (SCMC, CP drugs Co., Ltd. Thailand) were purchased from various suppliers and used as received. All reagents were of analytical grade and were used without further purification.

### **Formulation of mucoadhesive in situ gels**

In situ gel bases were formulated using 20% w/w P. BZK 0.1% and PI 0.45% w/w were incorporated as active pharmaceutical ingredients. XAN and SCMC were added to study the effect of mucoadhesive polymer on the physico-chemical properties of gels. The compositions of various gel formulations were shown in Table 1.

### **Evaluations of in situ gels**

The formulations were evaluated for the physical appearance, pH (pH meter, METTLER TOLEDO SCL12020109), viscosity at 25 and 37°C (Rheometer, Malvern Instrument limited KNX2100), gel strength in artificial saliva at 37 °C and buccal mucoadhesive (adhesion to porcine buccal mucosa). Good formulations should be transparent and quickly turn to gel at buccal conditions with high buccal mucoadhesive force and maintain gel integrity for a period of time. Gel strength was measured through gelling capacity by placing a drop of formulations into artificial saliva at oral conditions (pH 6.7, 37°C), the gel formation time and gel dissolved time were measured [4]. The buccal mucoadhesive to porcine buccal mucosa test, modified from the reported method, was performed [5]. The surface of buccal mucosa (5x5 cm<sup>2</sup>) was slowly soaked by 10 ml of PBS pH 7.4 at 37°C. The formulation (0.3 ml) at 25°C was dropped on the buccal mucosa and waited for 10 second. The mucosa was then put upright until the surface of the mucosa was 45° degree from the first position as shown in Fig. 1. After one minute, the formulation that did not move or flow downward was defined as good buccal mucoadhesive property. Porcine buccal mucosa was used within 24 hours after it was separated from the animal and kept in Krebs's buffer at 10°C prior to use.

### **Results and Discussions**

All preparations were homogeneous and transparent at both 25 and 37°C. Figure 2 showed that the viscosity of all formulations (Rx 1-9) at 37°C was higher than at 25°C,  $p < 0.05$ . This was from the properties of a thermo-sensitive sol-gel polymer, Poloxamer 407. The effect of API (BZK and PI) and mucoadhesive substances (XAN and SCMC) on viscosity of gels at 37 °C was shown in Fig. 3. PI reduced the viscosity of the gel ( $p < 0.05$ ). As free iodine can liberate from the PI complex in solution to promote the antimicrobial activity, this free iodine might affect the sol-gel formation of poloxamer thus reduced the viscosity of the formulation. The free iodine might form hydroiodic (HI) acid thus caused the decreased of pH values as shown in Table 1. The influence of API added in in situ gel containing poloxamer was also reported, diclofenac sodium significantly increased the gelation temperature and weakened the gel strength and bioadhesive force, while sodium chloride did the opposite [6]. The incorporation of XAN and SCMC increased the viscosity of Poloxamer 407 gel at both 25 and 37°C.

As shown in Table 1, all formulations exhibited gelling capacity at 37°C, they immediately turned to gel after dropping into the artificial saliva and had dissolution time of more than 45 min. Formulation containing PI did not show mucoadhesive effect as shown in Table 1. However, adding SCMC to the formulation did promote the mucoadhesive property of the P-PI formulation.

### **Summary**

In situ gels prepared from Poloxamer 407, BZK showed suitable properties for buccal applications. XAN and SCMC did promote the gel properties by increase the viscosity at 37 °C. For formulation P-PI, only SCMC increased the mucoadhesive property.



**Table 1.** Compositions and properties of in situ gels.

Rx No.	Compositions (%w/w)					Properties		
	P407	BZK	PI	XAN	SCMC	pH	Mucoadhesive	Gel strength, Dissolving time [min]
1	20	-	-	-	-	5.2	✓	> 45
2	20	0.1	-	-	-	5.2	✓	> 45
3	20	-	0.45	-	-	3.2	✗	> 45
4	20	-	-	0.3	-	5.2	✓	> 45
5	20	0.1	-	0.3	-	5.2	✓	> 45
6	20	-	0.45	0.3	-	3.2	✗	> 45
7	20	-	-	-	0.4	5.2	✓	> 45
8	20	0.1	-	-	0.4	5.2	✓	> 45
9	20	-	0.45	-	0.4	4.4	✓	> 45

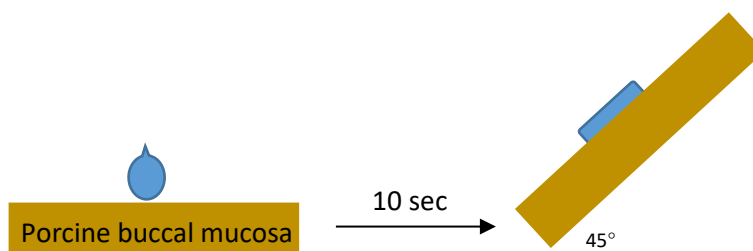


**Figure 1.** The position of mucoadhesive to porcine buccal mucosa test after 0.3 ml of formulation at 25°C was dropped on the surface of mucosa.

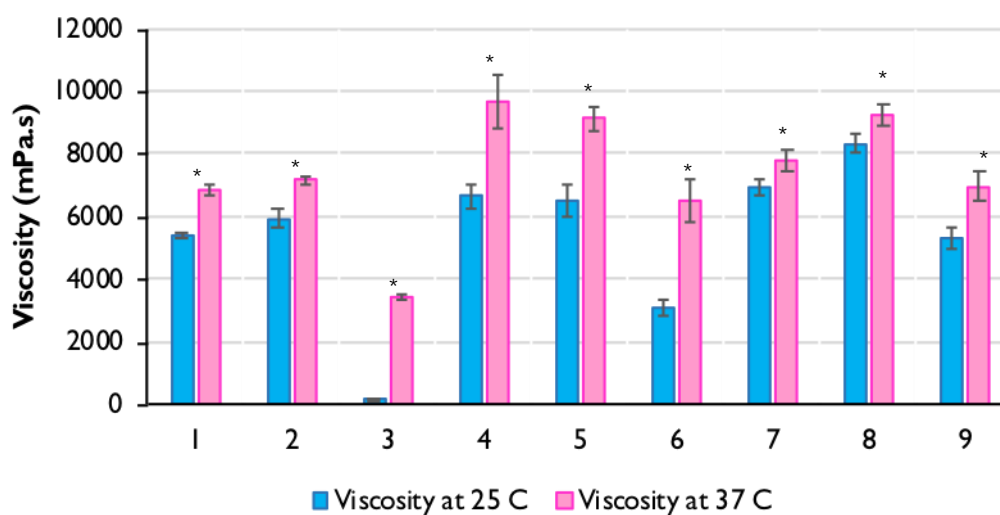


**Figure 2.** Viscosity of various in situ gel formulations at 25 and 37 °C.  
\* = significant different from viscosity at 25 °C,  $p < 0.05$ .

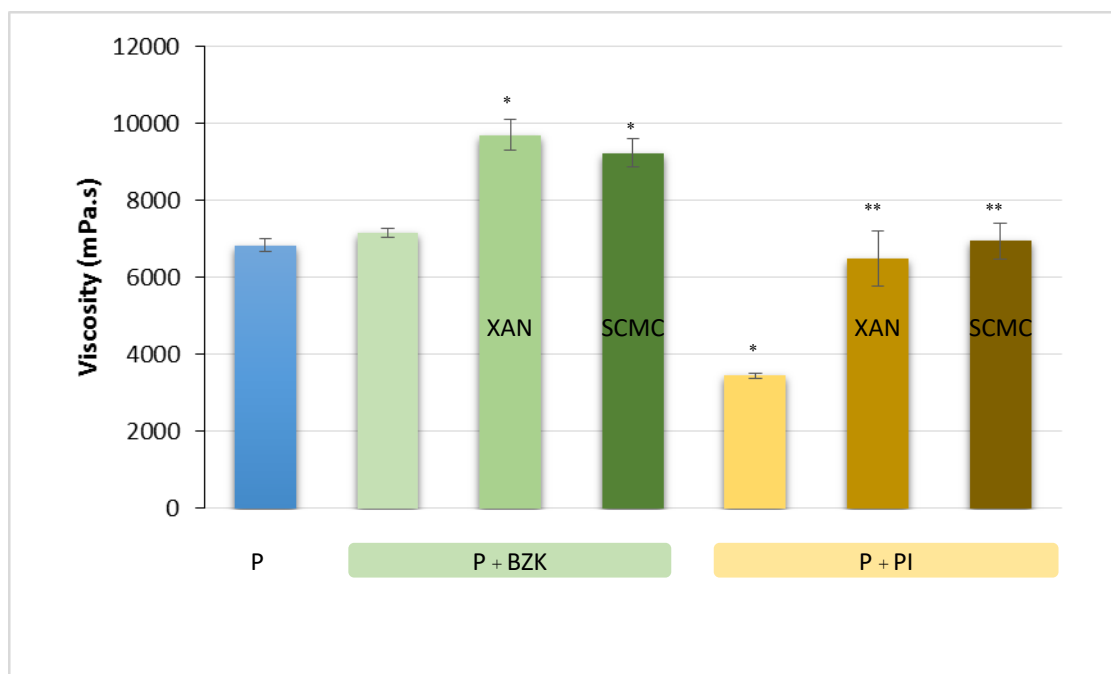


**Figure 3.** Effect of API (BZK and PI) and mucoadhesive substances (XAN and SCMC) on viscosity of gels containing 20% P407 at 37 °C. (n=3)

\* = significant different from viscosity of formulation P,  $p < 0.05$ .

\*\* = significant different from viscosity of formulation P+PI,  $p < 0.05$ .

### Acknowledgements

The authors would like to thanks Faculty of Pharmacy, Silpakorn University for the financial support.

### References

- [1] J. Byeongmoon, W.K. Sung and H.B. You, Thermosensitive sol–gel reversible hydrogels. *Adv Drug Del Rev.* 54 (2002) 37-51.
- [2] N.M. Hrisah, P. Prabhu, R.N. Charyulu, A. Gulzar and E.V.S. Subrahmanyam, Formulation and evaluation of in situ gels containing clotrimazole for oral candidiasis. *Indian J Pharm Sci.* 71(4) (2009) 421-427.
- [3] R.I. Burks, Povidone-iodine solution in wound treatment. *Phys Ther.* 78(2) (1998) 212-218.
- [4] K. Nagahama, Y. Imai, T. Nakayama, J. Ohmura, T. Ouchi and Y. Ohya, Thermo-sensitive sol-gel transition of poly(depsipeptide-co-lactide)-g-PEG copolymers in aqueous solution. *Polymers.* 50 (2009) 3547-55.
- [5] K. Małolepsza-Jarmołowska, The effect of poloxamer 407 on the properties of hydrophilic gels containing lactic acid complexed with chitosan, *Progress in Chemistry and Application of Chitin and its Derivatives (PCACD).* 15 (2010) 143-148.
- [6] C.S. Yong, J.S. Choi, Q.Z. Quan, J.D. Rhee, C.K. Kim, S.J. Lim, K.M. Kim, P.S. Oh, H.G. Choi, Effect of sodium chloride on the gelation temperature, gel strength and bioadhesive force of poloxamer gels containing diclofenac sodium. *Int J Pharm.* 2261(1-2) (2001) 195-205.

## Development of topical vitamin E nanoemulsion

Nadhikan Niamprasert<sup>1,a</sup>, Tuangpond Siriwat<sup>1,b</sup>,  
Thanaton Kunlaphongthada<sup>1,c</sup>, Surawut Watana<sup>2,d</sup>, Somlak Kongmuang<sup>1,e</sup>  
and Gaysorn Chansiri<sup>1,f\*</sup>

<sup>1</sup>Department of Pharmaceutical Technology, Faculty of Pharmacy, Silpakorn University, Thailand  
<sup>2</sup>Department of Pharmacology and Toxicology, Faculty of Pharmacy, Silpakorn University, Thailand

<sup>a</sup>niamprasert\_n@silpakorn.edu, <sup>b</sup>siriwat\_t@silpakorn.edu, <sup>c</sup>kunlaphongthada\_t@silpakorn.edu,  
<sup>d</sup>watana\_s@su.ac.th, <sup>e</sup>kongmuang\_s@su.ac.th, <sup>f</sup>chansiri\_g@su.ac.th

**Keywords:** Vitamin E, Nanoemulsion

**Abstract.** The objective of this research was to study the appropriated conditions for topical vitamin E nanoemulsion formulations such as types of instrument (Homogenizer and Ultrasonicator), power, mixing time, oil phase volume ratio, type and percentage of emulsifier in preparations. Nanoemulsion of higher percentage of oil phase, lower energy consumption and good physical appearance were selected for physical properties test. From the results of homogenizer method, particle size was reduced as increasing mixing time meanwhile ultrasonicator method exhibited more rapidly reduced particle size and produced more constant nanosize than homogenizer. The formulations with lower percentage of oil phase exhibited smaller size. The appropriated method was 75% amplitude of ultrasonicator with 40% v/v of oil phase mixed for 10 minutes. Types and percentages of emulsifier were varied as follow: span 80 : tween 80 (ratio 7:3) at 5, 10, 15, 20% v/v; transcutool CG : tween 80 (ratio 7:3) at 5, 10, 15% v/v and sodium cholate at 0.5, 1, 2, 3, 5% w/v. Only formulations with span 80:tween 80 showed good physical properties without oil drop on the surface of emulsion. Stability studies were performed and interpreted by paired t-test with PSPP version 0.10.4. Nanoemulsion containing 5, 10 and 15% v/v of span 80:tween 80 were stable after 1 week storage at room temperature. The droplet size, zeta potential, pH and viscosity did not change significantly ( $p \geq 0.05$ ).

### Introduction

Nanoemulsion is a thermodynamically unstable system in which internal liquid phase dispersed as droplets of size about 100-500 nm in another immiscible liquid. Nanoemulsion has been proved to be useful for various applications in pharmaceutical and medical aspects such as parenteral nutrition through intravenous infusion, solubilization of sparingly soluble drugs, drug delivery system to reduce side effect of many drugs and improvement of drug absorption especially through skin. Nanoemulsion also has some applications in vaccine and biomaterial delivery system. It is additionally very popular for various cosmetic products [1]. There are generally two methods for producing nanoemulsion which are high pressure homogenization and low pressure method through phase inversion temperature. The high pressure method provides better control of droplet size of nanoemulsion than the lower pressure method and allows a lot of production choices to utilize [2]. Vitamin E or tocopherols is a lipid soluble vitamin commonly found in egg yolk and vegetable oil such as sunflower oil, peanut oil and olive oil [3]. Natural vitamin E can be existed in 8 forms:  $\alpha$ -,  $\beta$ -,  $\gamma$ -,  $\sigma$ -tocopherol and  $\alpha$ -,  $\beta$ -,  $\gamma$ -,  $\sigma$ -tocotrienol.  $\alpha$ -tocopherol is usually found in human tissue and serum. Vitamin E was shown to provide anticancer effect and protection of skin from light [4]. The antioxidant action of vitamin E is related to the neutralization of lipid peroxide radical to produce lipid peroxide which then inhibits lipid peroxidation and prevents DNA or cells damage [5]. Vitamin E which is mostly and widely used as antioxidant and antiaging for skin cosmetics is  $\alpha$ -tocopherol or its synthetic ester or ether derivatives. General concentration of  $\alpha$ -tocopherol or tocopherol acetate in topical preparations is 1-5% [6]. However, preparations containing  $\alpha$ -tocopherol are more sensitive

to oxidation than those containing tocopherol acetate. Therefore, it is recommended that vitamin E be protected from light and kept at low temperature or refrigerator [7]. Vitamin E acetate was reported to transform to free  $\alpha$ -tocopherol by bioconversion during passing through human skin [8]. The important concern of topical vitamin E preparation is the skin absorption of vitamin E. Comparison studies on skin penetration revealed that lipophilic drugs exhibited better skin penetration than hydrophilic drugs and small particle size tended to show higher penetration through skin. Therefore, a potential strategy for development of topical drug delivery system is to produce small vesicles or particles and one of those small particle systems is nanoparticles [9]. It is then our objectives for this research to formulate topical vitamin E nanoemulsion using vitamin E acetate as active ingredient and mixture of coconut oil and sesame oil as oil phase. Many factors involving production of nanoemulsion including types of instrument, power, mixing time, oil phase volume ratio, types and concentration of emulsifiers are investigated.

## Method

### 1. Chemicals

Vitamin E acetate, coconut oil, sesame oil, tween 80, span 80, benzalkonium chloride, EDTA, BHT, sodium cholate and transcutool CG (diethylene glycol monoethyl ether) were purchased from P.C.Drug Center Co. Ltd. (Bangkok, Thailand) and were used as received.

### 2. General Formula of Vitamin E Nanoemulsion

Topical vitamin E nanoemulsion contained 1% v/v vitamin E acetate as active ingredient, 9-39% v/v mixture of coconut oil and sesame oil (ratio 1:1) as emollient and oil phase, 0.1% v/v benzalkonium chloride as preservative, 0.1% w/v BHT as antioxidant, 0.1% w/v EDTA as chelating agent, emulsifiers (various types and concentrations) and ultrapure water to make 100 ml emulsion.

### 3. Studies The Effect of Instrument Types, Power and Mixing Time for Production of Nanoemulsion at Various Oil Phase Volume Ratio

The formula of nanoemulsion was consisted of ingredients as described in 2. The emulsifier composed of span 80 and tween 80 at ratio of 7:3 to produce required HLB of 7.4 and the concentration was fixed at 10% v/v. The oil phase volume ratio was varied at 10, 20, 30 and 40% v/v. The oil phase referred to a combination of vitamin E acetate and mixture of coconut oil and sesame oil. The effect of types of instruments, power and mixing time was studied as follow:

3.1 Homogenizer (Homogenizer.IKA.model T25D, Germany) at three speeds (13,500 rpm; 17,000 rpm and 20,000 rpm) was used to produce nanoemulsion in the environment of ice bath to maintain temperature of nanoemulsion about 30-50°C. The mixing time at each speed was done at 5, 10, 15, 20, 30 and 40 minutes. Three samples from each speed and mixing time were drawn to evaluate for physical appearance, size and size distribution.

3.2 Ultrasonicator (Ultrasound, sonicator probe, UP400S, Hielscher, Germany) at three amplitudes (75%, 85% and 95%) was used to produce nanoemulsion in the environment of ice bath to maintain temperature of nanoemulsion at 30-50°C. The mixing time at each speed was done at 3, 6, 9, 12, 15, 18, 21, 24, 27 and 30 minutes. Three samples from each amplitude and mixing time were drawn to evaluate for physical appearance, size and size distribution.

### 4. Studies The Effect of Types and Concentrations of Emulsifier for Production of Nanoemulsion

The appropriate condition to produce good nanoemulsion from 3 was selected to investigate for the effect of types and concentrations of emulsifier as follow:

- 4.1 span 80 : tween 80 (ratio 7:3) at 5, 10, 15 and 20% v/v
- 4.2 transcutool CG : tween 80 (ratio 7:3) at 5, 10 and 15% v/v
- 4.3 sodium cholate at 0.5, 1, 2, 3 and 5% w/v

Three samples from each type and concentration of emulsifier were drawn to evaluate for physical appearance, size and size distribution, zeta potential, pH and viscosity.

#### **5. Preliminary Stability Study**

Nanoemulsion with good physical properties from 4 were chosen for preliminary stability study. These nanoemulsions were kept at room temperature for one week and the physical properties both before and after one week storage were evaluated and compared by using paired t-test (PSPP version 0.10.4).

#### **6. Particle size and size distribution**

Tested samples (n=3) were measured for their particle sizes and size distributions using laser scattering particle size and size distribution analyzer LA-950 (Horiba®). The mean volume particle size (nm) and standard deviation were analyzed.

#### **7. Zeta potential**

Measurement of zeta potential for each tested nanoemulsion (n=3) was performed using zeta potential analyzer (Brookhavan ZetaPlus). The mean zeta potential (mV) and standard deviation were calculated.

#### **8. Viscosity**

Samples of nanoemulsion were determined for their viscosity by using rheology analyzer (Brookfield DV-III ULTRA programmable rheometer). The mean viscosity (mPa·s or cps) and standard deviation were calculated from three samples of each interested nanoemulsion.

#### **9. pH**

The pH of nanoemulsion samples (n=3) was measured using pH meter (Professional Meter Sartorius) and calculated for mean pH and standard deviation.

#### **10. Physical appearance**

Nanoemulsion was visually observed for external appearance such as color and texture. The sign of cracking or the present of oil droplets on the surface of nanoemulsion was also investigated.

### **Results and Discussion**

Experimental results showed that both homogenizer and ultrasonicator were capable of producing vitamin E liquid nanoemulsion of the indicated formula. However, the speed, time of mixing and oil phase volume ratio exhibited combined influence on the nature of nanoemulsion. At 10% v/v of oil phase, homogenizer at all three speeds (13,500 rpm, 17,000 rpm and 20,000 rpm) could produce nanoemulsion of about 200-400 nm within 15 minutes. Particle size remained relatively constant even with longer mixing time up to 40 minutes. Nevertheless, formula with higher oil volume ratio (20, 30 and 40% v/v) could not be prepared as nanoemulsion by homogenizer at those three speeds within 40 minutes. However, the particle size seemed to decrease slightly with mixing time.

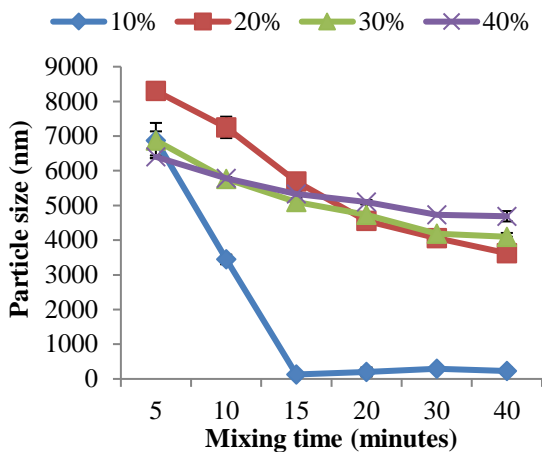


**Fig. 1** Particle size reduction of emulsions containing oil phase volume ratio of 10, 20, 30 and 40% v/v using homogenizer at 13,500 rpm.

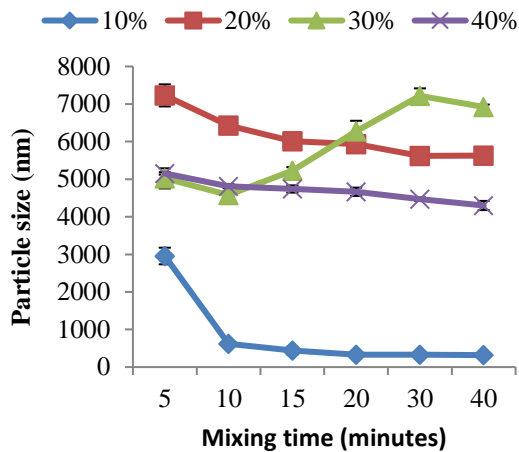


**Fig. 2** Particle size reduction of emulsions containing oil phase volume ratio of 10, 20, 30 and 40% v/v using homogenizer at 17,000 rpm.

In case of ultrasonicator, it was effective to produce nanoemulsion of particle size around 200–270 nm within 3 minutes from formula containing 10, 20, 30 and 40% v/v oil phase and at all three amplitudes (75%, 85% and 95%). Higher oil volume ratio showed slightly larger particle size. However, longer mixing time than 5-10 minutes did not show any significant reduction of particle size except that the heat generation was evidence. In our study, cooling system using ice bath was effective to control temperature of nanoemulsion within 30-50°C. This could prevent degradation of vitamin E since it was reported that 6.4 percentage loss of vitamin E would occur at 215°C [10].

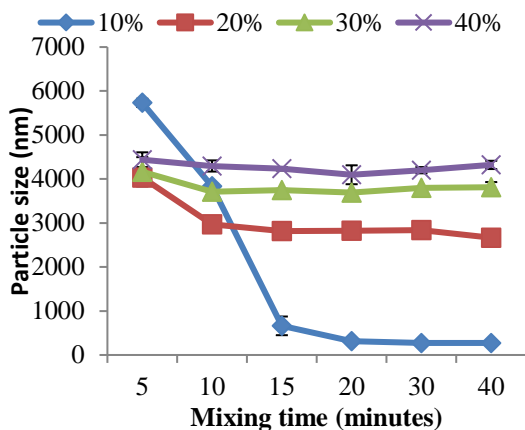


**Fig. 3** Particle size reduction of emulsions containing oil phase volume ratio of 10, 20, 30 and 40% v/v using homogenizer at 20,000 rpm.

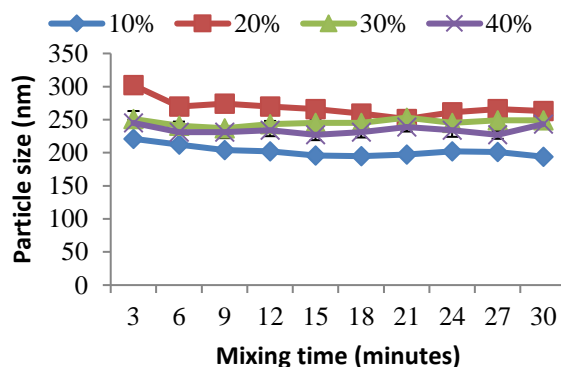


**Fig. 4** Particle size reduction of emulsions containing oil phase volume ratio of 10, 20, 30 and 40% v/v using ultrasonicator at 75% amplitude.

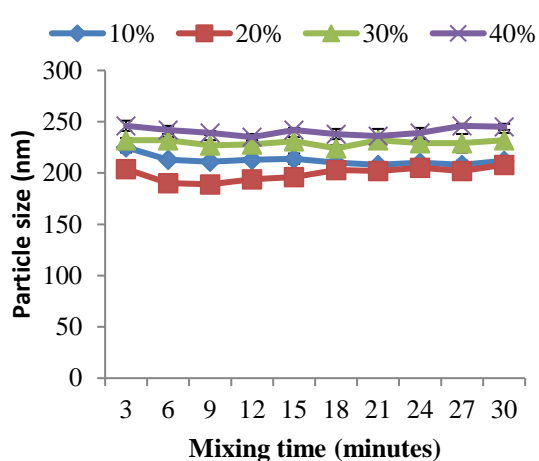


**Fig. 5** Particle size reduction of emulsions containing oil phase volume ratio of 10, 20, 30 and 40% v/v using ultrasonicator at 85% amplitude.

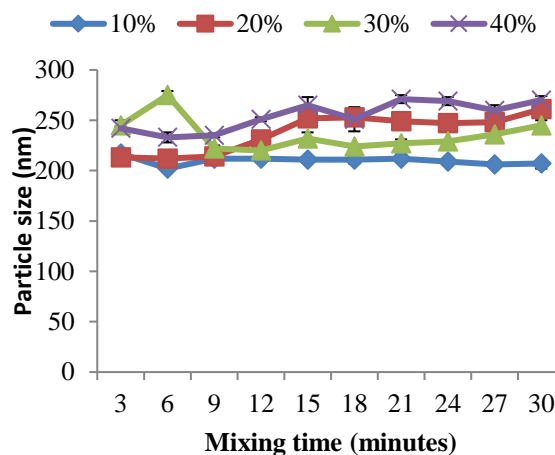


**Fig. 6** Particle size reduction of emulsions containing oil phase volume ratio of 10, 20, 30 and 40% v/v using ultrasonicator at 95% amplitude.

Then, the production method selected for investigating effect of emulsifier was the usage of ultrasonicator at 75% amplitude with 10 minutes mixing time and the formula contained 40% v/v oil phase to maximize emollient effect on skin. Examination for suitable type and concentration of emulsifier for production of vitamin E nanoemulsion was performed using span 80: tween 80 (ratio 7:3), transcutool CG: tween 80 (ratio 7:3) and sodium cholate at various concentrations. The combination of span 80 and tween 80 at ratio 7:3 with concentration of 5, 10 and 15% v/v exhibited stable nanoemulsion during one week storage at room temperature. The droplet size, zeta potential, pH and viscosity did not change significantly ( $p \geq 0.05$ ). P-value of droplet size, zeta potential, pH and viscosity for 5%v/v emulsifier preparation was 0.548, 0.865, 0.059 and 0.261 respectively and those for 10%v/v emulsifier preparation was 0.060, 0.479, 0.061 and 0.052 respectively. The p-value for 15%v/v emulsifier preparation was 0.128, 0.150, 0.129 and 0.177 respectively. Nanoemulsion containing transcutool CG: tween 80 (ratio 7:3) at 5, 10 and 15% v/v or sodium cholate at 0.5, 1, 2, 3 and 5% w/v as emulsifier failed to obtain stable nanoemulsion after one week storage at room temperature. Nanoemulsion containing transcutool CG: tween 80 (ratio 7:3) or sodium cholate as emulsifier cracked during short time storage as they exhibited oil droplets on the surface of emulsion. Combination of transcutool CG and tween 80 at ratio 7:3 provided HLB of 7.4 which was equal to the required HLB of preparation. However, it produced unstable nanoemulsion. This might be due to a low possibility of the emulsifiers to produce complex film on the surface of oil droplets since their chemical structures were not similar.

**Table 1** Physical properties (before and after one week storage at room temperature) of vitamin E nanoemulsions containing a mixture of span 80 and tween 80 (ratio 7:3) at various concentrations as emulsifier. Nanoemulsions were prepared using ultrasonicator at 75% amplitude for 10 minutes.

Concentration of emulsifier [% v/v]	Investigation before or after 1 week storage	Physical appearance	Particle size [nm] (SD)	Zeta potential [mV] (SD)	pH (SD)	Viscosity [mPa·s] (SD)
5	before	milky white	443(70)	-4.71(0.78)	4.32(0.02)	6.35(0.07)
	after	milky white	422(30)	-4.59(0.33)	4.26(0.01)	6.97(0.33)
10	before	milky white	246(0)	-13.74(0.53)	5.03(0.04)	13.32(0.20)
	after	milky white	241(0)	-12.10(3.22)	4.98(0.02)	14.60(0.71)
15	before	milky white	225(0)	-8.38(1.39)	5.30(0.08)	38.26(1.83)
	after	milky white	221(0)	-7.47(0.76)	5.19(0.01)	43.16(3.26)
20	before	milky white	297(0)	-17.19(3.45)	5.13(0.01)	79.43(1.58)
	after	milky white	281(0)	-11.50(4.05)	5.08(1.58)	106.50(5.48)

**Table 2.** Physical properties (before and after one week storage at room temperature) of vitamin E nanoemulsions containing a mixture of transcutool CG and tween 80 (ratio 7:3) at various concentrations as emulsifier. Nanoemulsions were prepared using ultrasonicator at 75% amplitude for 10 minutes.

Concentration of emulsifier [% v/v]	Investigation before or after 1 week storage	Physical appearance	Particle size [nm] (SD)	Zeta potential [mV] (SD)	pH (SD)	Viscosity [mPa·s] (SD)
5	before	milky white	150(10)	-26.34(7.38)	3.37(0.19)	6.26(0.06)
	after	cracking	-	-	-	-
10	before	milky white	340(10)	-52.94(1.61)	3.04(0.01)	8.57(0.07)
	after	cracking	-	-	-	-
15	before	milky white	228(0)	-36.11(8.87)	3.09(0.12)	18.26(0.25)
	after	cracking	-	-	-	-

**Table 3.** Physical properties (before and after one week storage at room temperature) of vitamin E nanoemulsions containing sodium cholate at various concentrations as emulsifier. Nanoemulsions were prepared using ultrasonicator at 75% amplitude for 10 minutes.

Concentration of emulsifier [% w/v]	Investigation before or after 1 week storage	Physical appearance	Particle size [nm] (SD)	Zeta potential [mV] (SD)	pH (SD)	Viscosity [mPa·s] (SD)
0.5	before	milky white	4182(2.49)	-18.17(3.97)	6.40(0.02)	3.92(0.01)
	after	cracking	-	-	-	-
1	before	milky white	313(0)	-24.63(2.96)	6.78(0.08)	4.95(0.03)
	after	cracking	-	-	-	-
2	before	milky white	205(0)	-63.27(1.78)	7.05(0.02)	10.13(0.06)
	after	cracking	-	-	-	-
3	before	milky white	116(0)	-54.68(0.76)	7.33(0.07)	22.13(0.36)
	after	cracking	-	-	-	-
5	before	milky white	104(0)	-55.85(0.74)	6.83(0.06)	13.95(0.03)
	after	cracking	-	-	-	-

For nanoemulsion containing sodium cholate as emulsifier, deterioration of nanoemulsion might be a combination of various causes such as the difference between HLB of sodium cholate and the required HLB, chemical structure of sodium cholate which formed an unstable film on the surface of oil droplets, and its preferential to migrate from surface into bulk medium. Therefore, sodium cholate might not appropriate for using as single emulsifier [11].

## Conclusion

It could be summarized from the experiments that factors influencing on the production of nanoemulsion included type of instrument, power or speed of mixing, mixing time and internal (oil) phase volume ratio. Homogenizer and ultrasonicator were effective for reducing particle size of oil droplets in emulsion to nanosize. Droplet size reduction by homogenizer required longer mixing time than ultrasonicator. Formula containing lower oil phase volume ratio tended to exhibit smaller oil droplet size than those containing higher oil phase volume ratio for the same instrument, mixing speed and mixing time. Vitamin E topical nanoemulsion composed of 40% v/v of a 1:1 mixture of coconut oil and sesame oil (also including 1% v/v vitamin E acetate) and a combination of span 80 and tween 80 (ratio7:3) at 5, 10, 15 and 20% v/v as emulsifier could be obtained by using ultrasonicator at 75% amplitude for 10 minutes mixing time. Nanoemulsions containing 5, 10 and 15% v/v emulsifier were stable during one week storage at room temperature.



## Acknowledgement

We would like to convey our special thanks to the Faculty of Pharmacy, Silpakorn University for its financial support and all necessary facilities.

## References

- [1] A. Gupta, H.B. Eral, T.A. Hatton, P.S. Doyle, Nanoemulsions: formation, properties and applications, *Soft Matter* 12 (2016) 2826-2841.
- [2] P. Izquierdo, J. Feng, J. Esquina, T. Tadros, J. Dederen, M. Garcia, The influence of surfactant mixing ratio on nano-emulsion formation by PIT method, *J. Colloid Interface Sci.* 285 (2005) 388-394.
- [3] M.L. Colombo, An update for vitamin E, tocopherol and tocotrienol-perspectives, *Molecules* 15 (2010) 2103-2113.
- [4] M.A. Keen, I. Hassan, Vitamin E in dermatology, *Indian Dermatol online J.* 7 (2016) 311-315.
- [5] H. Verhagen, B. Buijsse, E. Jansen, B. Bueno-de-Mesquita, The state of antioxidant affair, *Nutr Today* 41 (2006) 244-250.
- [6] M. Manela-Azulay, E. Bagatin, Cosmeceutical vitamins. *Clin. Dermatol.* 27 (2009) 469-474.
- [7] A.H. Nada, A. Zaghloul, M. Hedaya, Stability of vitamin E and vitamin E acetate containing cosmetic preparations, *J. Glob. Pharm. Technol.* 4 (2012) 1-8.
- [8] W. Baschong, C. Artmann, D. Hueglin, J. Roeding, Direct evidence for bioconversion of vitamin E acetate into vitamin E: an ex vivo study in viable human skin, *J. Cosmet. Sci.* 52 (2001) 155-161.
- [9] M. Kong, X.G. Chen, D.K. Kweon, H.J. Park, Investigations on skin permeation of hyaluronic acid based nanoemulsion as transdermal carrier, *Carbohydr. Polym.* 86 (2011) 837-843.
- [10] N Kuppithayanant, P. Hosap, N. Chinnawong, The effect of heating on vitamin E decomposition in edible palm oil, *I.J.E.R.D.* 5 (2014) 121-125.
- [11] E.S. Mahdi, M.H.F. Sakeena, Effect of surfactant and surfactant blends on pseudoternary phase diagram behavior of newly synthesized palm kernel oil esters, *Drug Des. Dev. Ther.* 5 (2011) 311-332.

# Development of indomethacin and lidocaine sonophoresis gel

Somlak kongmuang<sup>1, a \*</sup>, Kwanputtha Arunprasert<sup>1</sup>, Jarukit Ongarjwasinkul<sup>1</sup>,  
and Napon Kasemmongkolchai<sup>1</sup>

<sup>1</sup>Pharmaceutical Technology Department, Faculty of Pharmacy, Silpakorn University, Thailand

\*<sup>a</sup>somlak.kongmuang@gmail.com, kwanputthaarunprasert@gmail.com, jarukittop@gmail.com,  
kasemmongkolcha\_n@silpakorn.edu

**Keywords:** indomethacin, lidocaine, sonophoresis, gel, formulation

**Abstract.** A transparent ultrasound gel of Indomethacin (IDM) combined with Lidocaine (L) was formulated to avoid gastrointestinal (GI) side effect from oral administration. Heat, co-solvent, eutectic mixture and solid dispersion (SD) methods were tested in order to circumvent IDM's aqueous insolubility in the transparent gel. The best method for this system was the solid dispersion method (IDM: polyethene glycol 4000, 1:20) together with co-solvent containing of isopropyl alcohol (IPA) and water. 15% Hydroxypropylmethylcellulose 5- 9 cps (HPMC) was selected as a gelling agent. There was a chemical interaction between IDM and L from FTIR spectrogram. IDM was shown to be in an amorphous form in SD formulation from X ray diffractogram. After stability test, gel separation was noted when the gel was subjected to 4 cycles of temperature cycling at 4°C for 24 hours and 45°C for 24 hours. No significant change in physical appearance was found after the gel was kept at room temperature (30°C) for 4 days. However, the IR spectrum showed that the amount of IDM was significantly increased. This may be due to the interaction between some components in the formulation and/or vapor evaporation of the gel.

## Introduction

Non-Steroidal anti-inflammatory drugs (NSAIDs) are widely used in relieving inflammation of various bone and joint disorders. The use of oral NSAIDs has been associated with side effects in the digestive tract and the coronary arteries. Sonophoresis or phonophoresis implies application of ultrasound energy to drive molecules into and across skin, thereby bypassing the GI tracts and reducing the GI side effect [1]. The exact mechanism behind enhancement of transdermal delivery by sonophoresis is not yet known [1]. The medium for sonophoresis is an UG with drug. An interesting issue in this drug development is the combination of IDM and L into sonophoresis gel or UG, which can help relieve inflammation of patients from the effects of NSAIDs and relieve pain from the effects of anaesthetic drugs [2]. IDM is a widely used NSAIDs. Its low aqueous solubility (0.5 mg/ml) makes it difficult for preparation of a transparent UG [3]. Therefore, several methods have been introduced to overcome this problem. Thus, this research interest was to develop a stable transparent sonophoresis gel with the anti-inflammation and pain releaser for patients who suffer from pain, and especially those susceptible to GI side effects from oral NSAIDs.

## Material and Method

### Materials

Indomethacin (IDM) (lot # 175080) and lidocaine HCl (L) (lot # TL/LD/017) were purchased from Sigma. Carbopol 940 (C), carbopol Ultrez 21(CU), hydroxypropylmethylcellulose 5-9 cps (HPMC), methylcellulose 4000 (MC), sodium carboxymethylcellulose (CMC), sodium hydroxide (NaOH), ethyl alcohol (EA), isopropyl alcohol (IPA), polyethylene glycol 400 (PEG400), propylene glycol (PG) also purchased from P C drug center co., ltd. as pharmaceutical grade.

Polyvinylpyrrolidone K 90 (PVP K90) and polyethylene glycol 4000 (PEG 4000) were purchased from BASF. All other chemical were of analytical grade. The commercial ultrasound gel (UG) was a gift from Nakhon Pathom Hospital (Ultrasound gel® from MC-Gel company, Bangkok, lot number 17P0911).

## Methods

### I. Gel preparation

Several gel formulations containing five different types and various amount of polymer; HPMC, C, CU, MC or CMC were prepared. The optimum gel physical properties were compared with a commercial UG. The interesting properties of the commercial UG are conductivity (S) of 0.414, pH of 6.75 and viscosity (cP) of 37851 (data from in-house measurement). Gels were prepared by using various concentrations of each polymer to achieve similar properties as the commercial one. The dispersion of powder with water was the method for obtaining gel from CMC (concentration range of 4-6%) and HPMC (concentration range of 2-10%). The hot and cold water method was used for preparation of MC gel (concentration range of 2-4%). The dispersion with water and addition of triethanolamine was a method for C (concentration range of 0.5-2%) and CU (concentration range of 0.5-2%) gel. The optimum concentration of each polymer was identified according the similarity properties of a commercial UG.

### Viscosity Measurement

Brookfield viscometer (model DV III ultra, USA) was used to measure the viscosity all formulations at  $25\pm 2^\circ\text{C}$  using spindle. The 250 ml beaker was filled with the gel sample, and then spindle was inserted into the center of sample. The spindle was rotated, and viscosity measurements were recorded in triplicates.

### Clarity Evaluation

All prepared UG formulations were inspected visually for their clarity, appearance, color, and consistency against a black and white background.

### The pH and conductivity determination

The pH and conductivity of all gel preparations were directly measured by a digital pH meter model HANNA HI4522 for triplicate data collection.

## II. The techniques for enhancement of aqueous solubility of IDM

- A. Heat method:** Dissolve 1% W/V of IDM in water or EA at  $40^\circ\text{C}$  on the water bath for 15 minutes. The solution was tested for clarity by optical observation.
- B. Cosolvent method:** The dielectric constant of Indomethacin was 25.62 [4]. PG, EA, G, IPA, PEG400 and water were used as solvents in this study. All ratios of solvent mixtures were calculated and prepared by mixing each solvent into cosolvent as following, PG:EA, G:EA, IPA:G, IPA:PG, IPA:Water, IPA:PEG400:water with a ratio of (%W/W) 28:72, 13:87, 70:30, 47:53, 88:12, 66:20:14, respectively. One gram of IDM was dissolved in 10 g of each cosolvent system. The clarity of solution was observed. The suitable cosolvent system was selected for the next experiment.
- C. Eutectic mixture:** The ratio of 1:1 (IDM: L) was directly heat to  $170^\circ\text{C}$  [5] on hot plate. The eutectic mixture was obtained. After cooling this system, all powder was incorporated into gel with a selected polymer. The gel clarity was examined.
- D. Solid dispersion method:** The two ratios of IDM: polymer (PVP K 90 or PEG 4000) as 1:10 and 1:20 (w:w) were studied. The physical mixture of IDM and each polymer at specific ratio was obtained in a beaker. The solution of mixture was obtained by addition of EA. The

solution was heated over the water bath until dry. The lump of solid dispersion was ground into powder by mortar and pestle, and passed through sieve number 200. This powder was used for incorporation into UG. The chemical interactions were determined by FTIR and XRDP (sec 4.1 and 4.2).

### III. The preparation of lidocaine and IDM UG

After using all different techniques for increasing solubility of IDM, UG with IDM and L were prepared from selected formula. The amount of IDM and L in formulation were 1 and 10% W/W, respectively. There were three methods for making gel: UG with a selected cosolvent system, UG with a selected solid dispersion and UG with a selected SD together with a selected cosolvent system. Both physical and chemical properties of each system were evaluated.

### IV. Chemical evaluation

#### 4.1 Fourier-transform infrared spectroscopy (FT-IR)

The FT-IR spectra (range 650–4000  $\text{cm}^{-1}$ ) of all tested powder were recorded using an FT-IR spectrophotometer (Thermo Electron corporation, model Nicolet 4700). The sample was mounted on the sample stage and pressure applied by turning the top of the arm of the sample stage to create a flat surface and maintain intimate contact between the sample and the stage. The spectra obtained were the average of 4 scans at 1  $\text{cm}^{-1}$  resolution.

#### 4.2 X-ray powder diffraction (XRPD)

XRPD was performed with an X-ray diffractometer (Miniflex, Japan). The diffraction pattern was recorded in the interval  $3^\circ < 2\theta < 40^\circ$  in a step scan mode of  $0.02^\circ$  per step every second. The powder samples were ground in an agate mortar and side loaded in the sample holder. The amount of 1% w/w of IDM and 10% w/w of L were incorporated in the formula both with SD and physical mixture. The ambient temperature was maintained at  $25 \pm 1^\circ\text{C}$ .

### V. Stability

The temperature cycling method was used for the stability study (4 cycles,  $4^\circ\text{C}$  for 24 hour /  $45^\circ\text{C}$  for 24 hour). Moreover, the samples were also kept at the room temperature for 4 days. The physical tests were pH, conductivity, viscosity, clarity. The contents of drugs were analyzed using UV-Visible Spectrophotometer (T60) at a wavelength of 280 nm only for IDM, however, the concentration of L was below detection limit.

### VI. Statistical evaluation






The SPSS program was used for statistical analyses. The pair T-test was chosen for comparing data with the 95 % confidential interval.

## Result and Discussion

### I. Gel preparation:

The various amount of different types of gelling agents were evaluated in comparison with marketed UG. The specific amount of each polymer were shown in Table 1. It was found that all of polymers could be shown to have similar physical properties as the commercial one in different concentrations.

**Table 1** The physical properties of UG from different polymers

Gelling agent	Concentration (%)	Viscosity (cP)	pH	Physical appearance
CMC	4.00	37000 ± 1500	6.5 ± 0.1	
HPMC	5.00	36500 ± 1250	6.9 ± 0.1	
MC	3.00	37800 ± 1480	6.8 ± 0.1	
C	0.65	37600 ± 1100	7.2 ± 0.1	
CU	0.65	36800 ± 1800	7.3 ± 0.1	

## II. The method to increase IDM solubility

**Heat method:** 1g of IDM was dissolved in either water or EA to make 100 ml. After heating at 40°C for 15 minutes. The IDM solution with EA was shown to be clear while the formulation made by water was still turbid. Thus, the system of heating IDM in aqueous system could not be used to make a clear gel.

**Cosolvent:** The dielectric constant of IDM was 25.62 [4]. The solution of various type of cosolvent systems with the same dielectric constant were all clear. However, caution was made not to use high amount of ethanol for incorporation with gel base which may cause gel separation [4]. The suitable system for mixing with IDM solid dispersion was IPA: water.

**The eutectic mixture:** It was found that the eutectic mixture of IDM: L was the same as reported from Y. Shimada et al at 170°C [6]. The eutectic mixture at 170°C was shown to be yellowish, liquid-like substance. The liquid was solidified into a yellowish glassy state when left at room temperature. This material could not be easily dissolved in water as shown in Fig. 2. Even this eutectic mixture was claimed to have a complex with two drugs. The complex in the rubber state took on a clathrate-like structure, in which the mobility of IDM and L were limited, to minimize the decrease in entropy [7]. Thus the application of eutectic mixture for enhancing IDM solubility was not applied in this study.

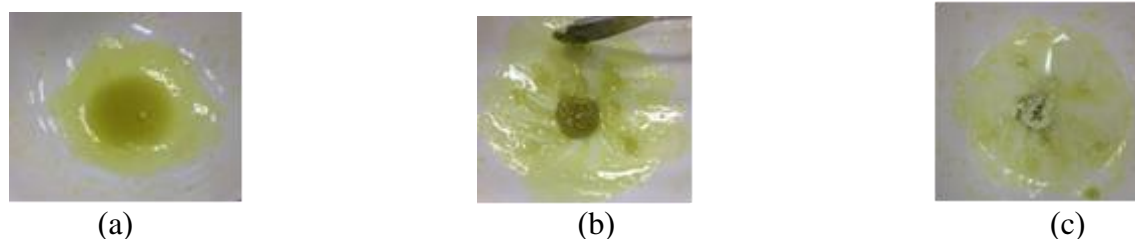


**Fig. 2.** The eutectic mixture of IDM: L, a) IDM: L at 1:1 by weight was heated at 170°C for 5 minutes, b) The eutectic mixture was at room temperature, c) The eutectic mixture was dissolved in an aqueous system

**Solid dispersion method :** The solid dispersion of 1 % W/W of IDM with either PEG 4000 or PVP K 90 was obtained by solvent evaporation method. It was found that the solid dispersion of PVP K90 could not be ground into powder according to its glassy-rubber state. Only IDM with PEG 4000 at both ratios were further studied. The solid dispersion of IDM with PEG 4000 was mixed with all UG gel. All of UG with solid dispersion appeared to be opaque which may result from low solubility of IDM in SD.

To improve the clarity of the system, combination of SD and cosolvent methods was then applied. After mixing all ingredients from both methods, the viscosity of the formula was decreased. The amount of 10, 15 or 18 % HPMC added into system were studied for enhancement of viscosity of the system. Only 15% of HPMC gave the system viscosity similar to commercial UG. Then, the optimum system for a transparent UG was the formulation of 1 g indomethacin (from SD with PEG 4000, ratio 1:20), lidocaine 10 g, HPMC 15 g, IPA 16.2 g and water 37.8 g (Fig.3). This formula was selected for stability study.



**Fig. 3** the optimum IDM: L transparent ultrasound gel

### The stability study

The content of only IDM was determined at a wavelength of 280 since there were no peaks of L available after scanning UV spectrum from 200-400 nm, shown in Fig. 4. There was an interference from gel component in the spectrum even after using UG as blank. After 4 temperature cycles, the gel was separated. Thus, some more ingredient might be added to improve its stability. However, when the gel was kept at room temperature for 4 days, there were some changes in physical appearance. The pH, viscosity and conductivity of the gel after 4 days at room temperature were not statistically significantly decreased using the pair T test analysis ( $p < 0.5$ ). However, the content of IDM was found to be higher than the added amount at day 0 and after 4 days (138 and 153%, respectively). The reason for this might be contributed to the chemical interaction of IDM with L forming complex [6] and/or evaporation of IPA.

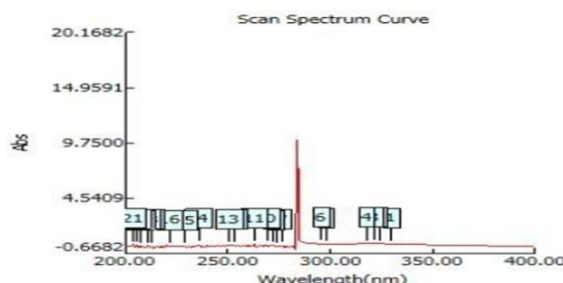


**Fig. 4** The scanning of UV absorbance of IDM-L in ultrasound gel from 200-400nm

### The chemical interaction in the system

The chemical interaction of IDM in gel was investigated by using FTIR. It was found that the IDM peak disappeared. However, a new peak at  $2484.8 \text{ cm}^{-1}$  occurred due to aromatic C-H stretch carboxylic acid shown in Fig 5 (b) top and (c) bottom. This might be contributed to the interaction between an acid group of IDM interaction with a basic group of L [5] (Fig. 5).

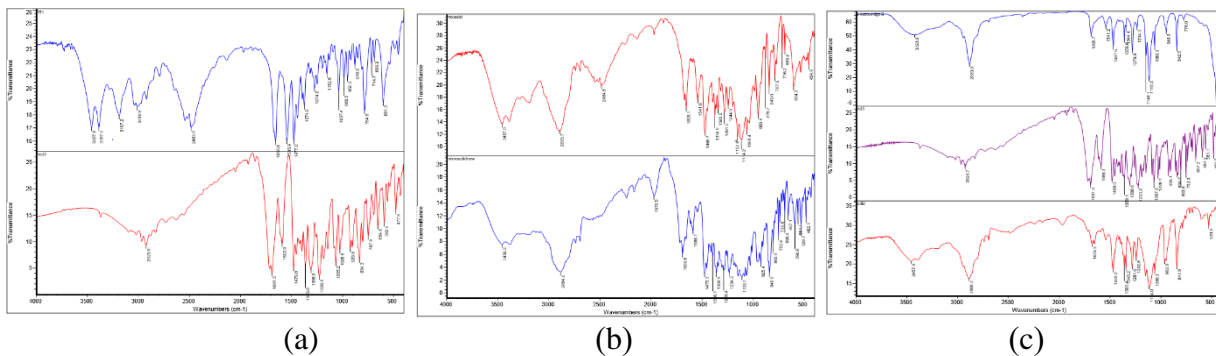


**Fig. 5** (a) IR spectrum of L (top) and IDM (bottom), (b) IR spectrum of the gel made by mixing with solid dispersion (top), a physical mixture (bottom), (c) IR spectrum of blank ultrasound gel (top) and physical mixture gel (middle) and solid dispersion gel (bottom)

The crystallinity of IDM also appeared to be amorphous in SD. This amorphous part of IDM could be facilitated for enhancing its aqueous solubility [7]. This phenomenon would make a transparent gel (Fig. 6).

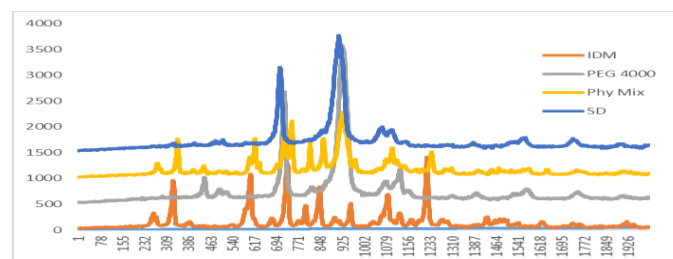


**Fig.6** X-ray diffractogram of IDM, PEG4000, Phy Mix (Physical mixture), SD

## Conclusion

The transparent ultrasound gel of IDM and L was formulated. The suitable method for enhancement aqueous solubility of IDM was SD together with cosolvent method. However, more improvement in stability of system could be explored to obtain the better formula to help ease the patients who suffer from pain.

## References

- [1] A. Pahade, V.M.Jadhav, V.J. Kadam, Sonophoresis an overview., *IJPS*. 2 (2010) 24-32
- [2] M.F. Powell, Stability of lidocaine in aqueous solution: effect of temperature, pH, buffer, and metal ions on amide hydrolysis, *Pharm. Res.* 1(1987) 42-5
- [3] X. Wang, H. Novoa de Armas, N. Blaton, A. Michoel, G. Van den Mooter, Phase characterization of indomethacin in binary solid dispersions with PVP VA64 or Myrj 52, *Int. J. of Pharm.* 345 (2007) 95–100
- [4] F. Shakeel, F.K. Alanazi, I.A. Alsarra, N. Haq, Solubility prediction of indomethacin in PEG 400 and water mixtures at various temperatures, *J. Mol. Liq.* 188 (2013) 28-32.
- [5] Y. Shimada, S. Goto, H. Uchiro, H. Hirabayashi, K. Yamaguchi, Features of heat-induced amorphous complex between indomethacin and lidocaine, *Colloids and Surfaces B: Biointerfaces.* 102 (2013) 590–596
- [6] Y. Shimada, R. Tateuchi, H. Chatani, S. Goto, Mechanisms underlying changes in indomethacin solubility with local anesthetics and related basic additives, *J. of Mol. Structure.* 1155 (2018) 165-170
- [7] Y. Ben Osman, T. Liavitskaya, S. Vyazovkin, Polyvinylpyrrolidone affects thermal stability of drugs in solid dispersions, *Int. J. of Pharm.* 551 (2018) 111–120

# Development and characterizations of amphotericin B nanoemulsion containing cyclodextrin

Phyo Darli Maw<sup>1,a</sup>, and Phatsawee Jansook<sup>1,b\*</sup>

<sup>1</sup>Faculty of Pharmaceutical Sciences, Chulalongkorn University, Bangkok, Thailand

<sup>a</sup>phyodarlimaw1994@gmail.com, <sup>b</sup>phatsawee.j@chula.ac.th

**Keywords:** amphotericin B, cyclodextrin, nanoemulsion, fungal keratitis

**Abstract.** Fungal keratitis, a corneal fungal infection of the eyes caused mainly by *Candida*, *Fusarium* and *Aspergillus* species, has become the leading cause of blindness from corneal disease. Amphotericin B (AmB) is considered as the drug of choice for fungal infections. However, its use in ophthalmic drug delivery is limited by low corneal residence at ocular surface as a result of blinking reflex, tear turnover and nasopharyngeal drainage. The aim of this study was to demonstrate AmB/cyclodextrin (CD) complex loaded nanoemulsion for the improvement of targeted delivery of AmB to the ocular surface. AmB/CD loaded nanoemulsion was prepared by using MCT as lipid phase and lecithin as emulsifier with high pressure homogenizer. The pH, osmolality, viscosity, particle size, zeta potential, drug content and the entrapment efficiency, the aggregation behavior of AmB and the stability index were evaluated. The prepared nanoemulsions exhibited a measured size range of 181-425 nm, zeta potential of 30-32mV and entrapment efficiency of 75-80%. All formulations exhibited AmB in moderate aggregated form. Thus, it supported that AmB nanoemulsion could be a promising system for effective ocular drug delivery of AmB for targeted fungal keratitis therapy.

## Introduction

Keratitis is an inflammation of the layers of the cornea. It is most commonly associated with bacterial, viral or fungal microorganisms that invade into the corneal stroma, resulting in inflammation and ultimately destruction of these structures [1]. Filamentous fungi, such as *Fusarium* and *Aspergillus* and yeast-like fungi, such as *Candida*, are most commonly associated with keratitis. Moreover, nowadays the use of contact lenses has become more popular risk factor for fungal keratitis.

Amphotericin B (AmB) belongs to the family of polyene macrolide antibiotics and was the first broad-spectrum antifungal agent to be discovered. In ophthalmology, systemic administration has poor AmB penetration into ocular tissues and does not reach to the therapeutic levels in the cornea, aqueous or vitreous humor [2, 3]. The conventional topical eye drop is the main route of administration, but the relatively low amount of drug attained resulted in low bioavailability.

Nanoemulsion is a thermodynamically stable carrier and has been become potential vehicle for ocular drug delivery system because of high drug loading efficiency and cost-effective formulation [4]. Also, it is well-known that drug-cyclodextrin inclusion complexes can substantially increase the bioavailability of poorly soluble drugs. According to the literatures, AmB solubility can be enhanced by  $\gamma$ CD and HP $\gamma$ CD [5,6]. Thus, in this present study,  $\gamma$ CD and HP $\gamma$ CD were used to increase the solubility of AmB and consequently to increase the drug loading. AmB loaded nanoemulsion containing CDs was developed and physicochemical properties of the formulation were evaluated.



## Materials and Methods

### Materials

Amphotericin B (AmB) was purchased from Shanghai 21CEC Pharmaceutical, Ltd. (Shanghai, China), gamma cyclodextrin ( $\gamma$ CD), hydroxypropyl gamma cyclodextrin (HP $\gamma$ CD) from Wacker Chemie (Munich, Germany), lecithin and benzalkonium chloride (BAC) from Sigma (St. Louis, MO), medium chain triglyceride (MCT) from Mead Johnson (Evansville, IN), glycerol,  $\alpha$ -tocopherol, castor oil, isopropyl myristate, labrasol, tween 80, olive oil and oleic acid from Srichand United Dispensary, Co. Ltd (Bangkok, Thailand), miglyol 812 from Sasol (Witten, Germany) and Lutrol-F 127 (Poloxamer 407; P407) from BASF (Ludwigshafen, Germany). All other chemicals used were of analytical reagent grade purity. Milli-Q (Millipore, Billerica, MA) water was used for the preparation of all solutions.

### Methods

#### Solubility determination of AmB in oils and surfactants

For the determination of solubility of AmB, two types of oil were selected; long chain oils (castor oil, isopropyl myristate, olive oil and oleic acid) and medium chain oils (MCT and miglyol). Solubility of AmB in various surfactants (tween 80, poloxamer 407, labrasol and lecithin) was also determined. The excess amount of AmB was added to 2-ml of various oils and surfactants in screw capped glass vials. After vortex mixing, the mixtures were kept at ambient temperature for 7 days for equilibration. The equilibrated samples were centrifuged at 4000 rpm for 10 min to remove the undissolved AmB. The supernatant was taken and diluted with methanol. The amount of AmB in methanolic solutions was quantified by HPLC analysis.

#### Preparation of AmB nanoemulsions

To increase the drug loading, two types of cyclodextrin ( $\gamma$ CD and HP $\gamma$ CD) were used to enhance the solubility of AmB by the formation of inclusion complexes. AmB has the affinity for  $\gamma$ CD and HP $\gamma$ CD with the complexation efficiency (CE) between 0.04 and 0.07 and indicating that every 15-27 molecules of CD formed complex with 1 molecule of AmB [5,6]. Table 1 shows the composition of AmB nanoemulsions.

Firstly, 2/3 of amount of AmB was dissolved in Milli-Q water containing  $\gamma$ CD or HP $\gamma$ CD as the aqueous phase. Lecithin and BAC were then added into aqueous phase. The rest of AmB was added into vial with MCT oil and  $\alpha$ -tocopherol as the oily phase. Then, the emulsion was prepared by adding the oily phase into aqueous phase and the resulted mixture was homogenized with probe sonicator for 3min to form coarse emulsion. After that, the osmolality of the formulations was adjusted with glycerol. Finally, the obtained emulsion was passed through high pressure homogenizer (Microfluider LM 20, Westwood, MA) at 20000 psi with 20 cycles.

#### Physical and chemical characterizations of AmB nanoemulsions

The pH value and osmolality of formulations were measured with pH meter (METTLER TOLEDO TM, SevenCompact, Germany) and Gonotec (OSMOMAT 3000 basic, Germany) at room temperature, respectively. The viscosity measurement of each formulation was conducted by using the viscometer (Brookfield LVDV-II+, USA) at 25°C and 37°C. All measurement samples in triplicate were performed. The average particle size, polydispersity index and zeta potential of all formulations were determined by dynamic light scattering (DLS) using Zetasizer (Nano-ZS, Malvern, UK).

**Table 1.** Composition of AmB nanoemulsions

Ingredients	F1	F2	F3	F4
AmB	0.12	0.12	0.18	0.18
$\gamma$ CD	7.5	-	7.5	-
HP $\gamma$ CD	-	7.5	-	7.5
MCT	10	10	10	10
LC	1	1	3	3
$\alpha$ -tocopherol	0.01	0.01	0.01	0.01
BAC	0.02	0.02	0.02	0.02
Glycerol	2.5	2.5	1.5	1.5
Milli-Q water to (ml)	100	100	100	100

Total drug content and entrapment efficiency (%EE) of the formulations were quantified by HPLC analysis. For the determination of total drug content, after appropriately diluting 100  $\mu$ l formulations with methanol (80%), the samples were analyzed by HPLC. For the determination of entrapment efficiency, the sample was centrifuged at 5000 rpm for 45 min and the supernatant was diluted with methanol 80% and analyzed by HPLC.

$$EE\% = \frac{(Dt - Ds)}{Dt} \times 100$$

Where Dt is total drug content and Ds is drug content in supernatant.

### Degree of AmB aggregation

Initially, AmB was solubilized in DMSO:methanol (1:999 v/v). Then, 10 $\mu$ g/ml of AmB solution, and nanoemulsions were prepared in isotonic simulated tear fluid (STF), pH 7.4 by serial dilution. The reference formulations which related to the AmB formulations but not contained CD were also performed. UV/VIS spectra of AmB preparations were recorded from 300 nm to 500 nm with UV-VIS spectrophotometer (Model UV-1601, Shimadzu, Japan). The ratio of the absorbance at 348 nm (peak I) and the absorbance at 409 nm (peak IV) of AmB was calculated to assess the degree of aggregation of AmB in STF, pH 7.4.

### Stability index

The emulsion stability index was calculated by taking the ratio between the volume of the emulsion at the time of assessment (six weeks) and the total volume of the mixture.

## Results and discussions

### Solubility of AmB in oils and surfactants

The solubility of AmB in various oils and surfactants are shown in Fig. 1. MCT oil showed the highest solubility of AmB among the other oils. It was agreed with other reported that long-chain glycerides showed lower drug solubility than medium-chain glycerides [7-9]. Lecithin was selected as an emulsifier based on its highest solubility of AmB. HLB value of lecithin was lower than other surfactants. The lower the HLB values, the higher lipophilicity and it therefore can cause more solubility of lipophilic drug.

### Physical and chemical characterizations of AmB nanoemulsions

The AmB loaded nanoemulsions showed the yellowish solution. The pH value, the osmolality, the viscosity, mean particle size, polydispersity index and zeta potential of each formulation was shown in the Table 2.

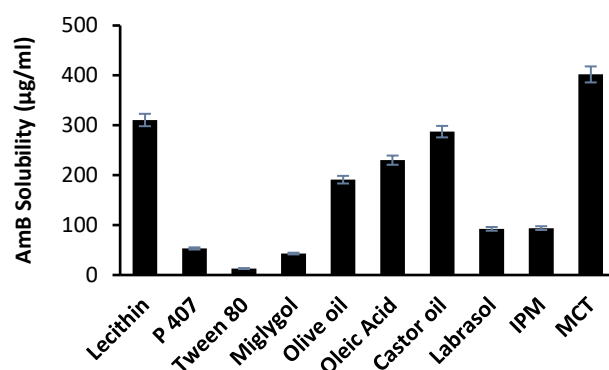


**Fig. 1.** Solubility of AmB in various oils and surfactants

**Table 2.** pH value, osmolality, viscosity, mean particle size, polydispersity index and zeta potential of the formulations (n=3, ±SD)

F	pH	Osmolality (mOsmol/kg)	Viscosity (cP)		Mean particle size (nm)	PDI	Zeta Potential (mV)
			25°C	37°C			
F1	4.88±0.04	291.33±4.73	2.58±0.26	2.37±0.12	181.03±1.98	0.487±0.01	31.03±0.83
F2	4.67±0.06	292.33±10.79	2.34±0.17	2.09±0.18	159.37±3.33	0.438±0.02	30.27±0.74
F3	4.90±0.07	296.90±7.66	20.64±1.04	19.66±0.70	425.60±4.92	0.654±0.05	31.37±0.31
F4	4.82±0.07	307.20±6.14	3.07±0.28	2.58±0.52	301.90±8.08	0.572±0.03	32.67±0.21

Although the ideal pH value of the lachrymal fluid is 7.4, the eyes can be tolerated with the pH range of 3.5-8.5 due to its natural buffering system [10]. The osmolality of all formulations ranged from 291.33 to 307.3 mOsmol/kg which was within the acceptable range (260-330 mOsmol/kg). The viscosity that measured at 25°C was higher than that measured at 37°C because increasing in temperature resulted in reduction in viscosity. The viscosity of F3 was significantly higher than that of other formulations.

DLS measurement of these formulations gave 3 size populations (data not shown) and the mean diameter was 181-425 nm based on the intensity distribution (Table 2). PDI values of all formulations was lower than 0.7 therefore it indicated that the formulations had narrow particle size distribution. The zeta potential of all formulations was observed in the range of about 30-32 mV. Therefore, the zeta potential of all formulations showed the good values for the stability.

The total drug content and the %EE were exhibited in the Table 3. It was shown that higher amount of lecithin in the formulation result in slightly lower amount of EE. This is due to fact that increase in stabilizer concentration leads to stabilization of small droplets and results in smaller microspheres. The researchers pointed the reason for the decrease of the EE is that micelle formation of lecithin because it has an amphiphilic property and tend to form the inclusion complexes itself [11].

### Degree of AmB aggregation behavior

AmB self-associates in aqueous media, forming supramolecular aggregates. The spectra of AmB in DMSO solution demonstrated non-aggregated state of AmB. The degree of aggregation behavior of AmB in all formulations was in the range of 1.04 to 1.07. This indicated that the moderate degree of aggregated form and it can be interpreted that it acts as the reservoir of monomeric form of AmB [12]. It can be observed that the degree of aggregation of reference formulations without CD was higher than that of all formulations. It was suggested that AmB/CD complexes provided the monomeric form of AmB.

**Table 3.** Total drug content and entrapment efficiency of all formulations (n=3,  $\pm$ SD)

Formulation	Total Drug Content (%)	Entrapment Efficiency (%)
F1	97.47 $\pm$ 1.39	80.07 $\pm$ 4.01
F2	97.7 $\pm$ 0.43	78.77 $\pm$ 4.31
F3	97.63 $\pm$ 0.86	76.73 $\pm$ 6.12
F4	98.77 $\pm$ 0.85	75.68 $\pm$ 4.7

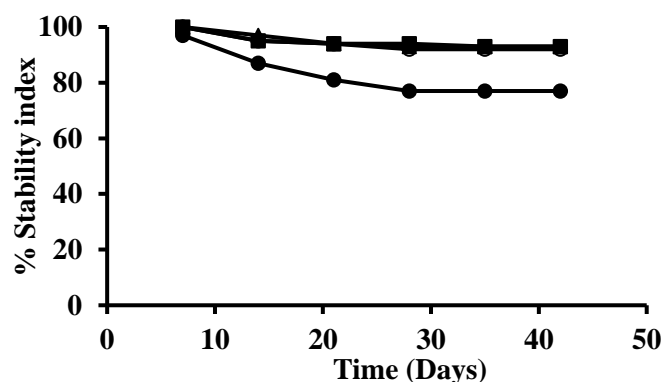
**Table 4.** Peak ratio of AmB in DMSO and all formulation in simulated tear fluid (STF)

Formulations	Diluents	Peak (I/IV) ratio
Pure AmB	DMSO	0.25
F1	STF	1.04
F2		1.07
F3		1.06
F4		1.07
Ref. 1 <sup>a</sup>		1.56
Ref. 2 <sup>b</sup>		1.88

CD-free AmBnanoemulsion prepared with <sup>a</sup>1% w/v lecithin or <sup>b</sup>3% w/v lecithin.

### Stability index

The stability index of all formulation was presented in the Fig 2. The phase separation of F3 was found, which represented to nanoemulsion instability. It was due to the presence of highest intensity distribution of larger particles in F3 (data not shown) than other formulations that can lead to some coalescence of large particle. After the physicochemical characterization, F3 was excluded from further studies due to its low stability index.

**Fig. 2.** The stability index (%) of AmBnanoemulsions after storage at the room temperature

(○) F1; (■) F2; (●) F3; (▲) F4.

### Conclusion

AmB has poor aqueous solubility and permeability which limits clinical therapeutic efficacy. AmB loaded nanoemulsion containing CDs were developed and evaluated. The AmB/ $\gamma$ CD and AmB/HP $\gamma$ CD complexes loaded into the nanoemulsion was less aggregated that it indicated less toxicity. Thus, these formulations represented a promising strategy for fungal keratitis therapy.

## References

- [1] Z. Ansari, D. Miller, A. Galor, Current thoughts in fungal keratitis: Diagnosis and treatment, *Current fungal infection reports*, 7 (2013) 209-218.
- [2] D. Goldblum, B.E. Frueh, S. Zimmerli, M. Bohnke, Treatment of postkeratitis fusarium endophthalmitis with amphotericin B lipid complex, *Cornea*, 19 (2000) 853-856.
- [3] I.P. Kaur, C. Rana, H. Singh, Development of effective ocular preparations of antifungal agents, *Journal of ocular pharmacology and therapeutics : the official journal of the Association for Ocular Pharmacology and Therapeutics*, 24 (2008) 481-493.
- [4] H.O. Ammar, H.A. Salama, M. Ghorab, A.A. Mahmoud, Nanoemulsion as a potential ophthalmic delivery system for dorzolamide hydrochloride, *AAPS PharmSciTech*, 10 (2009) 808-819.
- [5] P. Jansook, S.V. Kurkov, T. Loftsson, Cyclodextrins as solubilizers: formation of complex aggregates, *Journal of pharmaceutical sciences*, 99 (2010) 719-729.
- [6] P. Jansook, T. Loftsson, CDs as solubilizers: Effects of excipients and competing drugs, *International journal of pharmaceutics*, 379 (2009) 32-40.
- [7] J. Cannon, M. Long, *Emulsions, Microemulsions, and Lipid-Based Drug Delivery Systems for Drug Solubilization and Delivery, Part II*, 2008.
- [8] P. Li, S.R. Hynes, T.F. Haeefe, M. Pudipeddi, A.E. Royce, A.T. Serajuddin, Development of clinical dosage forms for a poorly water-soluble drug II: formulation and characterization of a novel solid microemulsion concentrate system for oral delivery of a poorly water-soluble drug, *Journal of pharmaceutical sciences*, 98 (2009) 1750-1764.
- [9] H.N. Prajapati, D.P. Patel, N.G. Patel, D.D. Dalrymple, A.T.M. Serajuddin, Effect of difference in fatty acid chain lengths of medium-chain lipids on lipid-surfactant-water phase diagrams and drug solubility, *Journal of excipients and food chemicals*, (2011) 73-88%V 72.
- [10] M.M. Ibrahim, A.-E.H. Abd-Elgawad, O.A.-E. Soliman, M.M. Jablonski, Natural bioadhesive biodegradable nanoparticle-based topical ophthalmic formulations for management of glaucoma, *Translational vision science & technology*, 4 (2015) 12-12.
- [11] C.-M. Lee, M.-H. Kim, H.-S. Na, J. Kim, K.-Y. Lee, The effect of caseinate on inclusion complexes of  $\gamma$ -cyclodextrin for oxidative stabilization of fish oil, *Biotechnology and Bioprocess Engineering*, 18 (2013) 507-513.
- [12] P. Jansook, W. Pichayakorn, G.C. Ritthidej, Amphotericin B-loaded solid lipid nanoparticles (SLNs) and nanostructured lipid carrier (NLCs): effect of drug loading and biopharmaceutical characterizations, *Drug development and industrial pharmacy*, 44 (2018) 1693-1700.

# Comparative study of oryzanol- and rice bran oil-load niosomes for anti-aging cosmetics

Sureewan Duangjit<sup>1, a</sup> \* Chudanut Akarachinwanit<sup>1, b</sup>, Warisada Sila-On<sup>1, c</sup>,  
Sureewan Bumrungthai<sup>2, d</sup> and Tanasait Ngawhirunpat<sup>3, e</sup>

<sup>1</sup>Faculty of Pharmaceutical Sciences, Ubon Ratchathani University, Ubon Ratchathani 34190, Thailand

<sup>2</sup>Department of Microbiology and Parasitology, School of Medical Sciences, University of Phayao, Phayao 56000 Thailand

<sup>3</sup>Faculty of Pharmacy, Silpakorn University, Nakhon Pathom 73000 Thailand

<sup>a</sup>sureewan.d@ubu.ac.th, <sup>b</sup>akarachinwanit.c@gmail.com, <sup>c</sup>warasida.s@ubu.ac.th,

<sup>d</sup>sureewan.b@windowslive.com, <sup>e</sup>ngawhirunpat\_t@su.ac.th

\* corresponding author

**Keywords:** Rice bran oil, Oryzanol, Anti-aging, Nanovesicles, Niosomes

**Abstract.** Oryzanol (OZ) is one of such a phytochemical purified from rice bran oil (RBO). Tocopherols, tocotrinols, sterols, fatty acids, vitamin A, vitamin B and lecithin are also ingredients having the potential to be used as emollient and antioxidant in pharmaceutical, nutraceutical and cosmoceutical products. Recently, the nanotechnology focused on the production of OZ loaded niosomes. The simultaneous incorporation of various components of RBO into niosomes was compared to pure OZ formulation. The aim of this study was to develop the oryzanol- and rice bran oil-load niosomes for anti-aging cosmetics. The of niosome formulation from rice (OZ and RBO) was conducted by sonication method. The physicochemical properties and stability of the formulation were the parameters that indicated the production ability of niosome formulation. The vesicle size, polydispersity index, zeta potential and entrapment efficiency were investigated. The results indicated that OZ- and RBO-loaded niosome were in the nanosize range 83 to 203 nm. The polydispersity index was 0.22 to 0.44. The zeta potential was negative between 8 to 32 mV. The entrapment efficiency was 4.2 to 52.7%. The OZ- and RBO-loaded niosome were stable under 5 and 25 °C for 90 days. The finding suggests that physicochemical properties of the RBO-loaded niosomes were close to the OZ-loaded niosomes. The skin permeation and antioxidant activity are necessary to be conducted in further study.

## Introduction

Rice bran oil (RBO) is extracted from the germ and inner husk of rice. RBO was used as the potential active ingredient and excipient as antioxidant and emollient, respectively in pharmaceutical, nutraceutical and cosmoceutical products.  $\gamma$ -oryzanol (OZ) is an ester mixture of ferulic acid and phytic acid. RBO products have been reported to prevent several symptoms e. g., inhibiting platelet aggregation, gastric secretion, modulating pituitary secretion, antioxidant [ 1 ], decreasing hyperlipidemia [ 1-3 ], type 2 diabetes [ 4 ], reducing menopausal symptoms [ 5 ], osteoporosis [ 6, 7 ]. Several health care properties of RBO are review. OZ has been extensively used as antioxidants in numerous skin care products. Tocopherols, tocotrinols, sterols, fatty acids, vitamin A, vitamin B and lecithin are also doing the same as components having the potential to be used in products. There are several steps during the refining process from crude to refined rice bran oil. Numerous studied investigated the oxidative stability of RBO at different stages of refining process [ 8, 9 ]. It remarked that the percentage of the oryzanols were lost during the process [ 10 ]. Moreover, the primary problem of OZ is the degradation of its activity due to the exposure to environment (air and light). Niosomes have been utilized to overcome the degradation of active ingredients by entrapment. The stability and

efficacy of drug-loaded niosome were improved [11]. To improve the efficacy of rice byproduct, RBO product as a rich source OZ and other potential compounds was developed in this study. The various components in RBO were incorporated into niosomes and compared to pure OZ loaded niosome formulation. The aim of this study was to develop the oryzanol- and rice bran oil-load niosomes for anti-aging cosmetics. The niosome formulation from rice (OZ and RBO) was conducted by sonication method. The vesicle size, polydispersity index, zeta potential and entrapment efficiency were investigated. The physicochemical properties and stability of the formulation were compared.

## Materials

Rice bran oil (O-RBO) obtained from the agriculture cooperative Ltd. Ubon Ratchathani province. Oryzanol (OZ) and oleic acid were supplied by Sigma-Aldrich (Buchs, Switzerland). Phosphatidylcholine (PC) was generously gifted by Lipoid GmbH (Ludwigshafen, Germany). Tween 60 (T60) and cholesterol (Chol) was purchased from Wako Pure Chemical Industries (Osaka, Japan). All other chemicals used were of reagent grade and were purchased from Wako Pure Chemical Industries.

## Methods

**RBO-loaded niosomes preparation.** RBO-loaded niosomes were formulated by sonication method. The niosome formulations contained an optimal ratio of T60: CHOL: oleic acid (OA) (1: 1: 0.1) (Table 1). The RBO was various among 2.73 mg/mL as low level, 10.30 mg/mL as medium level and 27.30 mg/mL as high level, depended on their extraction method. Each component was dissolved in chloroform: methanol (2: 1) and evaporated by using nitrogen stream. The dried film loaded OZ and RBO was hydrated with a phosphate buffer saline (PBS) at pH 7.4. All niosomes were subsequently sonicated for two cycles. The OZ in different extraction method was an investigated parameter and pure OZ was a control. The RBO loaded niosomes were freshly prepared and stored in airtight containers at 4°C prior to use.

**Physicochemical Characterization.** The vesicle size, polydispersity index and zeta potential of the OZ- and RBO-loaded niosomes were determined by photon correlation spectroscopy (PCS) (Zetasizer Nano series, Malvern Instruments, U.K.). The measures were taken at room temperature (25°C). At least three independent measurements were recorded. The OZ content in the RBO loaded niosome formulation was determined after niosome disruption with Triton<sup>®</sup> X-100 (0.1% w/v) at a 1:1 volume ratio, and then appropriated dilution with PBS. The niosomes/Triton<sup>®</sup> X-100 solution was centrifuged at 10,000 rpm at 4°C for 10 min. The supernatant was filtered through a 0.45 µm nylon syringe filter, and then analyzed by HPLC.

**Stability Evaluation.** The stability of RBO loaded niosomes was evaluated by monitoring the formulations for at least 90 days after their initial preparation. The niosome formulations were kept in glass bottles with plastic plugs at incubation period. The physicochemical stability of RBO-loaded niosomes was evaluated under the intermediated stability. The stability condition was conducted under 5±2°C, 25±2°C and 45±2°C, for 90 days. The physicochemical characteristics of niosomes including vesicle size, polydispersity index, zeta potential and drug remaining were determined.

**HPLC analysis.** The concentration of OZ in RBO loaded niosome formulation was determined using the HPLC (Thermo Scientific<sup>™</sup> UltiMate 3000 UHPLC System). A C18 reversed-phase column (Symmetry<sup>®</sup>, VertiSep<sup>™</sup>, Vertical, Thailand) with dimensions of 5 µm, 4.6×150 mm was used. The mobile phase composed of methanol, acetonitrile and acetic acid (52:45:3) was mixed. A UV-VIS detector used was 330 nm at 25°C. The flow rate was 1.0 ml/min and the injection volume was 20 µL. The calibration curves for CUR were in the range of 10-250 µg/ml with a correlation coefficient of 0.999.

**Data analysis.** The data were reported as the means ± standard deviation (SD) (n=3). A *p*-value of less than 0.05 was considered to be significant.

**Table 1.** Compositions of RBO loaded niosomes

Code	T60 (mg)	CHOL (mg)	OA (mg)	RBO/OZ (mg)	PBS pH 7.4 (mL)
RBO-L	386.5	386.5	-	2.73	100
RBO-M	386.5	386.5	309	10.30	100
RBO-H	386.5	386.5	-	27.30	100
OZ	386.5	386.5	309	0.61	100

Abbreviation; RBO-L; rice bran oil at low level, RBO-M; rice bran oil at medium level, RBO-H; rice bran oil at high level, T60; tween 60, CHOL; cholesterol, OA; oleic acid, RBO; rice bran oil, OZ; oryzanol, PBS; phosphate buffer saline

## Results and Discussion

### Physicochemical Characterization

Rice bran oil is unique among eatable oil because its rich source of commercially and nutritionally important compounds e. g. , oryzanol, tocopherols, tocotrinols, sterols, lecithin, vitamin A and vitamin B [1]. However, most of these compounds are removed from the rice bran oil as waste byproducts during the refining process. OZ occurs in RBO at 1 to 2 percent depended on their extraction method. To improve the efficacy of natural antioxidant products from rice byproduct, RBO were used in this study. The physicochemical characteristics of OZ- and RBO-loaded niosomes were prepared and characterized. The different extraction method affected the different physicochemical characteristics. The goal physicochemical characteristics of niosomes were the minimum vesicle size under 600 nm, the minimum PDI under 0.5, the zeta potential between  $\pm 30$  mV and maximum entrapment efficiency not less than 20%. The appropriate physicochemical characteristics of RBO-loaded nanovesicles have mentioned in previous studies [12, 13].

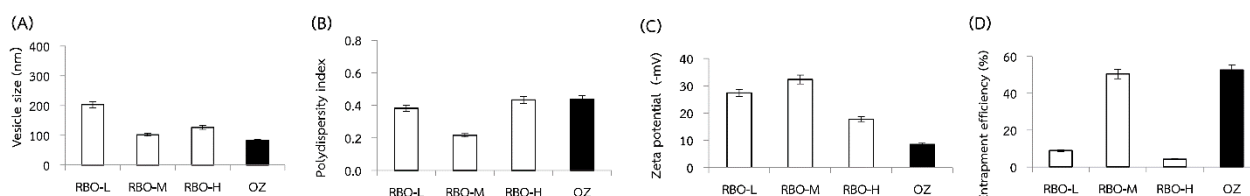


**Figure 1.** The physicochemical characteristics of OZ- and RBO-loaded niosomes (A) vesicle size (B) polydispersity index (C) zeta potential and (D) entrapment efficiency. The white bars represent RBO-loaded niosomes and the solid bars represent OZ-loaded niosomes (control).

Considering the physicochemical characteristics of OZ- and RBO-loaded niosomes indicated that the vesicle size, the polydispersity index and the zeta potential of all RBO-loaded niosomes were within the criteria. The vesicle smaller than 600 nm was able to penetrate into deep skin [14, 15]. The entrapment efficiency RBO-M was close to the control. These results indicated that the RBO from the different extraction method significantly affected the entrapment efficiency. The physicochemical characteristics was a latent factor that may affect the skin permeation and antioxidant activity of niosome formulation. Therefore, the RBO-M was chosen for further study.

### Stability Evaluation.

The previous studies reported that the antioxidant activity of RBO is decreased and not sufficient for anti-aging cosmetic due to its low stability to air and light. RBO-loaded niosomes were nonionic-surfactant based nanovesicles with more advantageous physicochemical characteristics including higher stability, smaller particle sizes and lower cost than the phospholipid vesicles as well as the ethosomes and transfersomes [13]. Niosomes have the advantages for topical delivery of several



drugs and cosmetics. Thus, niosome formulations were prepared in this study. Niosomes were used to entrap the RBO and evaluated for their stability for 90 days.

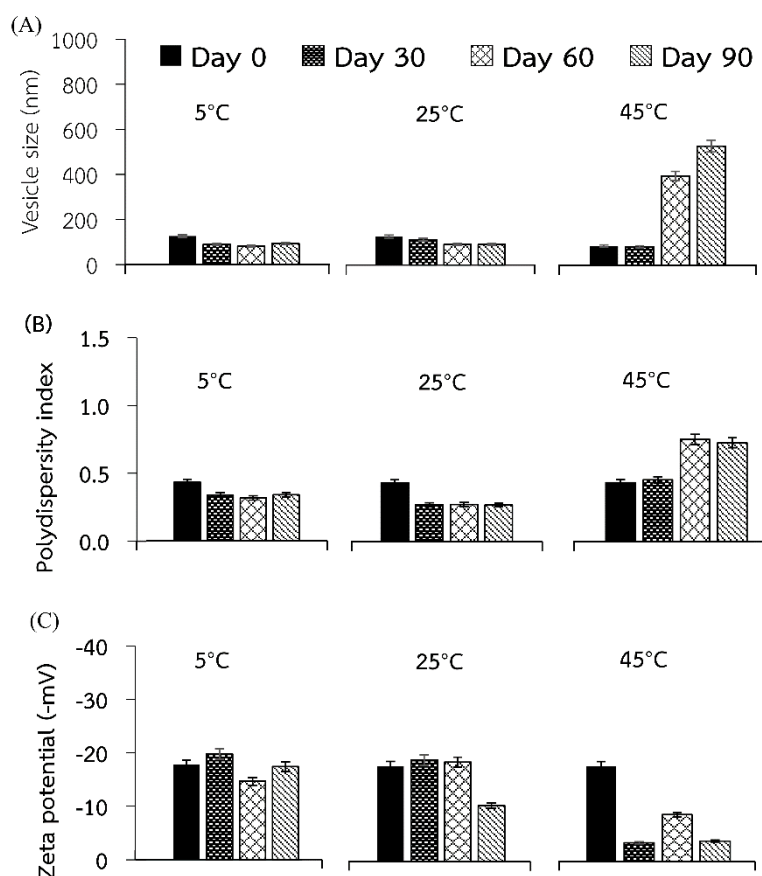


**Figure 2.** The physicochemical characteristics of OZ- and RBO-loaded niosomes (A) vesicle size (B) polydispersity index (C) zeta potential.

Considering the criteria of physicochemical characteristics that mentioned above, the vesicle size of BRO-M fell within the limit of a 600 nm. While the polydispersity index at 45°C was significantly increased at day 60 and 90. The zeta potential at 45°C of day 30, 60 and 90 was significantly decreased. It could be suggested that RBO-M have a good physical stability at storage temperature of 5 and 25°C at least 60 days. Previous studies reported that the niosomes storage at 4°C showed an initial burst release possibly due to the ruptured membrane of niosome [12]. Thus, the recommended storage condition for RBO-M was 25°C for 60 days. Vitamin D3-loaded niosomes prepared using a supercritical carbon dioxide based method have a good physical stability for 21 days at 20°C [16]. The physical stability of niosome formulation was affected not only by the formulation factor, but also the method of preparation.

## Summary

The optimal formulation (RBO-M), defined as the formulation with appropriate physicochemical characteristics, was prepared by sonication method. Comparing the physicochemical characteristics between OZ- and RBO-loaded niosome formulation, we were successful in showing the feasibility of nanovesicles for anti-aging cosmetics. To approach the high value added of rice from organic agriculture cooperative Ltd. Ubon Ratchathani province, niosomes can be the candidate choice. However, the efficacy, the safety and the stability of the cosmetics should be concerned as the primary factors. The further study is required to perform the RBO-M loaded serum, gel or cream formulation.

## Acknowledgement

The authors gratefully acknowledge Thailand Research Fund through the Royal Golden Jubilee Advanced Program (Grant No. RAP59K0019) and the National Research Council of Thailand (NRCT) for the financial support. Grateful thanks also go to Faculty of Pharmaceutical Sciences, Ubon Ratchathani University for supporting facilities and equipment. In addition, the authors would like to thank the the Queen Saovabha Memorial Institute, Thai Red Cross Society, Bangkok, Thailand for kindly providing the shed snake skin used in the pre-formulation study.

## References

- [1] Cicero AF, Gaddi A, Rice bran oil and gamma-oryzanol in the treatment of hyperlipoproteinaemias and other conditions. *Phytother Res*, 15, 277-289 (2001).
- [2] Bumrungrert A, Chongsuwat R, Phosat C, Butacnum A, Rice Bran Oil Containing Gamma-Oryzanol Improves Lipid Profiles and Antioxidant Status in Hyperlipidemic Subjects: A Randomized Double-Blind Controlled Trial. *J Altern Complement Med*, 25, 353-358 (2019).
- [3] Wilson TA, Nicolosi RJ, Woolfrey B, Kritchevsky D, Rice bran oil and oryzanol reduce plasma lipid and lipoprotein cholesterol concentrations and aortic cholesterol ester accumulation to a greater extent than ferulic acid in hypercholesterolemic hamsters. *J Nutr Biochem*, 18, 105-112 (2007).
- [4] Lai M-H, Chen Y-T, Chen Y-Y, Chang J-H, Cheng H-H, Effects of rice bran oil on the blood lipids profiles and insulin resistance in type 2 diabetes patients. *J Clin Biochem Nutr*, 51, 15-18 (2012).
- [5] Tamura M, Hori S, Hoshi C, Nakagawa H, Effects of rice bran oil on the intestinal microbiota and metabolism of isoflavones in adult mice. *Int J Mol Sci*, 13, 10336-10349 (2012).
- [6] Ishimi Y, Dietary equol and bone metabolism in postmenopausal Japanese women and osteoporotic mice. *J Nutr*, 140, 1373s-1376s (2010).
- [7] Wang JF, Effect of Acupuncture Combined With TDP on Estrogen and Bone Metabolism in Postmenopausal Patients With Deficiency of Liver and Kidney Syndrome. *Zhongguo Zhen Jiu*, 29, 623-625 (2009).
- [8] Mezouari S, Eichner K, Comparative study on the stability of crude and refined rice bran oil during long-term storage at room temperature. *Eur J Lipid Sci Technol*, 109, 198-205 (2007).
- [9] Latha RB, Nasirullah DR, Physico-chemical changes in rice bran oil during heating at frying temperature. *J Food Sci Technol*, 51, 335-340 (2014).
- [10] Srisaipet A, Nuddagul M, Influence of Temperature on Gamma-Oryzanol Stability of Edible Rice Bran Oil during Heating. *IJCEA*, 5, 303-306 (2015).
- [11] Manosroi A, Chutoprapat R, Sato Y, Miyamoto K, Hsueh K, Abe M, Manosroi W, Manosroi J, Antioxidant activities and skin hydration effects of rice bran bioactive compounds entrapped in niosomes. *J Nanosci Nanotechnol*, 11, 2269-2277 (2011).
- [12] Manosroi A, Chutoprapat R, Abe M, Manosroi W, Manosroi J, Transdermal absorption enhancement of rice bran bioactive compounds entrapped in niosomes. *AAPS PharmSciTech*, 13, 323-335 (2012).
- [13] Manosroi A, Chutoprapat R, Abe M, Manosroi W, Manosroi J, Anti-aging efficacy of topical formulations containing niosomes entrapped with rice bran bioactive compounds. *Pharm Biol*, 50, 208-224 (2012).
- [14] Jennings V, Gysler A, Schafer-Korting M, Gohla SH, Vitamin A loaded solid lipid nanoparticles for topical use: occlusive properties and drug targeting to the upper skin. *Eur J Pharm Biopharm*, 49, 211-218 (2000).
- [15] Abdel-Mottaleb MM, Mortada ND, El-Shamy AA, Awad GA, Physically cross-linked polyvinyl alcohol for the topical delivery of fluconazole. *Drug Dev Ind Pharm*, 35, 311-320 (2009).
- [16] Wagner ME, Spoth KA, Kourkoutis LF, Rizvi SS, Stability of niosomes with encapsulated vitamin D3 and ferrous sulfate generated using a novel supercritical carbon dioxide method. *J Liposome Res*, 26, 261-268 (2016).

# A comparison of antioxidant capacity and total polyphenols quantity between imported olive oils and edible vegetable oils in Thailand

Saowapak Vchirawongkwin<sup>1,2,a\*</sup>, Piyanut Thongphasuk<sup>1,3,b</sup>,  
Chadatan Jangkitkul<sup>1,c</sup>, Benjamas Khemsuk<sup>1,d</sup> and Chulaluck Niruntasook<sup>1,e</sup>

<sup>1</sup>College of Pharmacy, Rangsit University, Thailand

<sup>2</sup>Department of Pharmaceutical Chemistry, College of Pharmacy, Rangsit University, Thailand

<sup>3</sup>Department of Pharmacognosy, College of Pharmacy, Rangsit University, Thailand

<sup>a</sup>saowapak.k@rsu.ac.th, <sup>b</sup>piyanut.t@rsu.ac.th, <sup>c</sup>chadatan.j57@rsu.ac.th, <sup>d</sup>i\_q100@hotmail.com,

<sup>e</sup>chulaluck\_jane@hotmail.com

**Keywords:** olive oils, edible vegetable oils, DPPH, total polyphenols, antioxidant activity

**Abstract.** This study aimed to compare the total polyphenols and antioxidant capacity between imported extra virgin olive oil (Evo) and seven types of edible vegetable oils in Thailand. Seven types of edible vegetable oils produced and marketed in Thailand, was coconut oil (Co), palm oil (Po), olive oil (Oo), soybean oil (Sbo), sesame oil (Seo), rice bran oil (Rio), and sunflower oil (Suo), were evaluated the level of total polyphenols content and antioxidant capacity. Two brands of each seven types of edible vegetable oils marketed in Thailand were compared to three brands of imported extra virgin olive oil (Evo) for every test. Folin-Ciocalteu method proceeded to quantify the total polyphenols in eight edible vegetable oils. DPPH radical scavenging assay used to provide IC<sub>50</sub> values of the samples. Considering the results from this study, we found that the methanolic extracts of brand E of Evo allowed the highest average amount of total polyphenols of 9.26 mg GAE/g crude extract and IC<sub>50</sub> values of 24 ppm. These comparisons indicate that the difference of gallic acid equivalent content and IC<sub>50</sub> values connected to the types of edible vegetable oils whereas no correlation between gallic acid equivalent content and IC<sub>50</sub> values, with statistically significant (*p-value* < 0.05).

## Introduction

Most of the food industries in Asian countries have used edible oils extracted from plant sources. Edible vegetable oil has classified into two groups by the type of fatty acid containing i.e. unsaturated fatty acids and saturated fatty acids [1]. High contained saturated fats oils are coconut oil, palm oil, and palm kernel oil. Unsaturated fats oil, which is generally triglycerides, include olive oil, peanut oil, safflower oil, sunflower oil, soybean oil, corn oil, canola oil, mustard oil, and cottonseed oils. Coconut oil mainly contains caproic acid, caprylic acid, capric acid, and lauric acid as saturated fatty acids. Phenolic compounds in virgin coconut oil were present as vanillic acid, syringic acid, ferulic acid and *p*-coumaric acid, since coconut oil contains mainly medium-chain triglycerides requiring carbon chain between C-6 to C-12, coconut fatty acids are health beneficial saturated fatty oil [2]. Sesame oil includes essential, unique components of sesamin and sesamol, which encourage the inherent higher stability of sesame oil. The rice bran oil is a rich source of dietary antioxidants such as  $\alpha$ -,  $\beta$ -,  $\gamma$ - and  $\delta$ -tocopherol and  $\gamma$ -oryzanol. The phenolic compounds of olive oil have established enlarged consideration for their health-promoting benefits, especially against cardiovascular disorder. Extra virgin olive oil is the most widely everyday use as a edible vegetable oil produced in the Mediterranean region, being the leading olive oil producing countries e.g. Spain (44.83%), Italy (12.64%), Greece (12.54%), Tunisia (10.87%), Turkey (7.94%), and Morocco (4.60%). Extra virgin olive oil (Evo) contains a predominant of monounsaturated fatty acid, oleic acid, with antioxidant and anti-inflammatory properties [3]. Some of the main phenolic markers found

in olive oil with biological activities are oleocanthal, oleacein, oleic acid, oleuropein and its derivatives, tyrosol, and hydroxytyrosol [4].

Oxidation is the reaction of electron transfer from one atom to another and displays an essential part of both aerobic life and our metabolism since oxygen is the most electron acceptor producing energy in the form of ATP. Free radicals are generated when the electron flow becomes uncoupled, known as reactive oxygen species (ROS), including superoxide, peroxy, alkoxy, hydroxy, and nitric oxide [5]. Oxidative stress is a state of raised levels of ROS from a variety of conditions that refer to stimulate either ROS production or a decline in antioxidant defenses. During oxidative stress, the dysregulation of ROS levels in a variety of tissues has been associated to disease states, including inflammation, macular degeneration, muscular dystrophy, and type 2 diabetes with insulin resistance [6]. Phenolic compounds, widespread in plants, are the compounds range structurally from a simple phenolic molecule to complex high-molecular-weight polymers. These compounds are an essential part of human nutrition and are of substantial interest due to their antioxidant properties and potential advantageous health effects. Presently, there is increasing evidence that consumption of a variety of phenolic compounds present in foods may lower the risk of health disorders where their antioxidant activity [7]. Edible vegetable oils contain many phenolic compounds, which encourage oxidative stability and may serve to reduce the stress of oxidation on human health as antioxidants. DPPH radical scavenging activity and Folin-Ciocalteu methods are both the most usual procedure used to quantify the antioxidant activity and total phenolic compounds, respectively [8-10].

Indeed, there is no research of correlation between imported extra virgin olive oil and edible vegetable oils from Thailand to compare the number of total polyphenols and antioxidant activity. Therefore, the objective of the present study was to examine the antioxidant potential of imported extra virgin olive oil (Evo) and seven types of edible vegetable oils used from a convenient shop in Thailand using DPPH assay, which may be correlated with total polyphenols using Folin-Ciocalteu method.

## Materials and Methods

Chemicals were acquired for DPPH assay and total phenolic content including ascorbic acid (Ajax Finechem, Australia), 2,2-diphenyl-1-picrylhydrazyl (Sigma-Aldrich, Germany), sodium carbonate (Ajax Finechem, Australia), gallic acid (Sigma-Aldrich, Germany) and Folin-Ciocalteu reagent (Merck, Germany). Solvents for the extraction were the purified water (TKA, Germany), absolute ethanol (Darmstadt, Germany) and acetonitrile (Burdick & Jackson, Korea). Eight vegetable oils which are brand A (CoA) and brand B (CoB) of Co, brand C (EvoC), brand D (EvoD), and brand E (EvoE) of Evo, brand F (OoF) and brand G (OoG) of Oo, brand H (PoH), and brand I (PoI) of Po, brand J (RioJ), and brand K (RioK) of Rio, brand L (SeoL), and brand M (SeoM) of Seo, brand N (SboN), and brand P (SboP) of Sbo, and brand Q (SuoQ), and brand R (SuoR) of Suo were purchased from convenient shops in Thailand. Extraction of phenolic compounds from vegetable oil was a modified method by Garcia and co-worker [11]. Accurately 14 g of vegetable oils were weighed into a centrifuge tube containing 14 mL of 80% methanol in purified water, mixed well with vortex for 1 min, and centrifuged with 3200 rpm for 10 min. Repeated the extraction method for three more times and accumulate the methanol phase to dry. Re-extraction the dried methanol residue with 10 mL of acetonitrile and washing with 15 mL of hexane in a separator for three times. Dry the acetonitrile extracts under speed vacuum and re-dissolved with methanol prior testing.

Total polyphenols contents of the edible oil extracts were determined with some modified of Folin-Ciocalteu method [12]. The applied concentration for the test of Evo and Seo extracts were 0.05 mg/mL, Oo and Co extracts were 1.0 mg/mL, and Po, Rio, Sbo and Suo extracts were 0.5 mg/mL in methanol. The calibration graph was prepared in the range of 0.1 to 100.0 µg/mL using gallic acid as a standard. Concisely, 20 µL of sample was added into 100 µL of a 10-fold dilution of 2N Folin-Ciocalteu reagent, mixed well, stand for 5 min and then added 80 µL of 7.5% sodium carbonate prior keeping for 2 hours. The measurement of phenolic compounds was done under UV-Vis

spectrophotometer at 760 nm (n=3). The linear equation was obtained by plotting the absorbance values (y-axis) versus the concentration of gallic acid (x-axis) with  $r^2 = 0.9998$  as shown in Fig. 1.

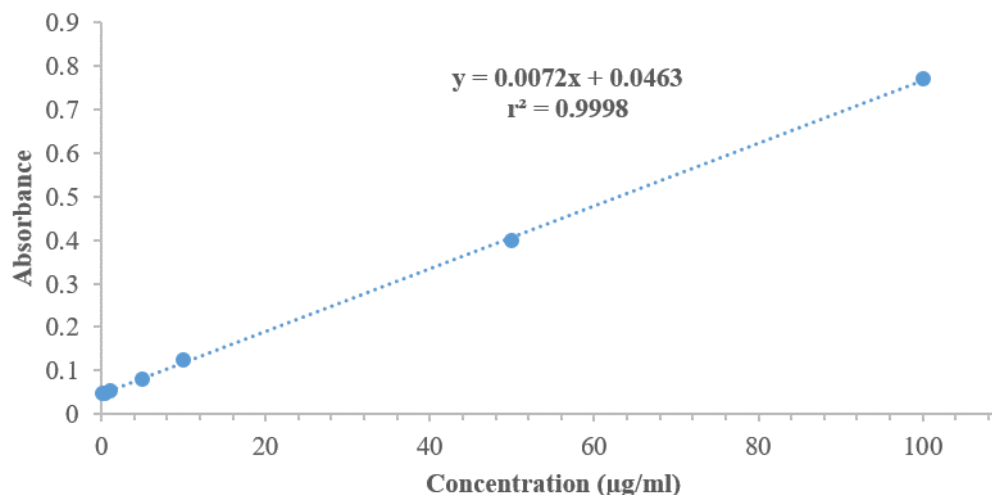


**Figure 1.** Gallic acid calibration curve for total polyphenols determination.

DPPH assay was used to monitor the antioxidant capacity with minor changing from the previous research [13]. The extract solutions were arranged in three different concentration of 100 ppm, 10 ppm, and 1 ppm. Methanol was applied to calibrate the spectrophotometer before the measurement. The reaction mixture was a sample extract added to 0.1 mM DPPH solution and used L-ascorbic acid in the same concentration as a positive control. For the negative control, 100 µL of methanol was mixed with 100 µL of DPPH solution. The reaction mixture was allowed to stand for 20 min before measuring at 517 nm. The following equation calculated the ability to scavenge DPPH radicals in percentage (%):

$$\% \text{ of DPPH radical scavenging activity} = [1 - ((\text{Abs}_{\text{sample}} - \text{Abs}_{\text{blank}}) / \text{Abs}_{\text{control}})] \times 100$$

Where  $\text{Abs}_{\text{sample}}$  is the absorbance of the reaction solution,  $\text{Abs}_{\text{blank}}$  is the absorbance of oil extracts, and  $\text{Abs}_{\text{control}}$  is the absorbance of DPPH solution. This assay presented as the  $\text{IC}_{50}$  values indicate the concentration in ppm of the sample, which is required to inhibit 50% of DPPH free radicals.

## Results and Discussion

Total polyphenols contents have expressed as milligrams per gram of crude extract as mean  $\pm$  SD for at least triplicates analysis. The determination of total polyphenols is an initial step for antioxidant capacity assay. The calculated total phenolic content has presented in Table 1. The average highest amount of total polyphenols is  $9.26 \pm 0.24$  mg GAE/g of olive oil of EvooE, followed by  $7.41 \pm 0.29$  of SeoL,  $7.27 \pm 0.29$  of EvooD,  $7.00 \pm 0.16$  of EvooC,  $5.65 \pm 0.14$  of SuoR,  $5.56 \pm 0.21$  of SuoQ,  $5.24 \pm 0.14$  of SboP,  $4.77 \pm 0.16$  of RioK,  $4.40 \pm 0.24$  of PoH,  $4.40 \pm 0.14$  of CoA,  $4.36 \pm 0.08$  of PoI,  $4.36 \pm 0.21$  of CoB,  $4.31 \pm 0.16$  of OoG,  $4.26 \pm 0.14$  of SboN,  $4.26 \pm 0.14$  of RioJ and the lowest average amount is  $4.03 \pm 0.32$  of OoF edible vegetable oils. We could not measure the total phenolic content from SeoM due to the brown color of the sesame extract (brand M) disturbing the UV absorption using spectrophotometry. According to the extraction technique, most of the phenolic compounds were separated into the methanolic solvent with a very small extracts amount due to edible oil process from industrial production. The extracts were re-separated using acetonitrile solvent and removing the non-polar part by hexane. The final extract contained especially phenolic compounds. As previous results, the imported extra virgin olive oil provided the highest capacity of total polyphenols compared to edible vegetable oils marketed in Thailand.

**Table 1** The average amount of total polyphenols contents in methanolic edible vegetable oil extracts presented in mg of gallic acid equivalent per g of crude extract (mean  $\pm$  SD, n = 3).

Total phenolic compounds (mg GAE/g of crude extract)							
CoA	CoB	OoF	OoG	PoH	PoI	RioJ	RioK
4.40 $\pm$ 0.14	4.36 $\pm$ 0.21	4.03 $\pm$ 0.32	4.31 $\pm$ 0.16	4.40 $\pm$ 0.24	4.36 $\pm$ 0.08	4.26 $\pm$ 0.14	4.77 $\pm$ 0.16
EvooC	EvooD	EvooE	SeoL	SboN	SboP	SuoQ	SuoR
7.00 $\pm$ 0.16	7.27 $\pm$ 0.29	9.26 $\pm$ 0.24	7.41 $\pm$ 0.29	4.26 $\pm$ 0.14	5.24 $\pm$ 0.14	5.56 $\pm$ 0.21	5.65 $\pm$ 0.14

**Note:** Coconut oils brand A (CoA) and brand B (CoB), Extra virgin olive oils brand C (EvooC), brand D (EvooD), and brand E (EvooE), Olive oils brand F (OoF) and brand G (OoG), Palm oils brand H (PoH) and brand I (PoI), Rice bran oils brand J (RioJ) and brand K (RioK), Sesame oils brand L (SeoL) and brand M (SeoM), Soy bean oils brand N (SboN) and brand P (SboP), and Sunflower oils brand Q (SuoQ) and brand R (SuoR)

This study evaluated the antioxidant activities of the edible vegetable oils using DPPH test. The decreasing agent scavenges the DPPH radical through the proton donation with changing of color from purple to yellow after reduction. This reaction can be measured by its reduce of absorbance at 517 nm. The methanolic oil extracts showed radical scavenging activity against DPPH and compared to ascorbic acid standard with an IC<sub>50</sub> value of 0.0016 mg/mL. The antioxidant potential of vegetable edible olive oil has reported as the IC<sub>50</sub>, the concentration of olive oil extracts necessary to inhibit 50% of radical scavenging DPPH. The radical scavenging activity followed by order EvooE > EvooD > EvooC > SeoL > PaH > RioJ > PaI > CoB > RioH > OoF > CoA > OoG as shown in Fig. 2., with brand E extra virgin olive oil providing the highest radical scavenging activity with an IC<sub>50</sub> value of 0.024 mg/mL.

One-way ANOVA generating by the Data Analysis of Microsoft Excel program provided comparisons of the types of edible oils correlated to total phenolic content and antioxidant capacity. Pearson's correlation delivered the correlation coefficient (*r*) between the amount of gallic acid equivalent and IC<sub>50</sub> values. Due to the concentration of crude extract solution of soybean oils (SboN and SboP) and sunflower oils (SuoQ and SuoR) were not enough concentration for DPPH measurement and brown solution of SeoM, therefore six types of edible vegetable oils (number of brand, n = 12) were evaluated the correlation with gallic acid equivalent content and IC<sub>50</sub> values by one-way ANOVA analysis. The comparisons indicated that the difference of gallic acid equivalent content and IC<sub>50</sub> values connected to the brands of edible vegetable oils with statistically significant (*p-value* < 0.05) as the results were shown in Table 2. Whereas no correlation between gallic acid equivalent content and IC<sub>50</sub> values (*r* = -0.4847) with statistically significant (*p-value* < 0.05).

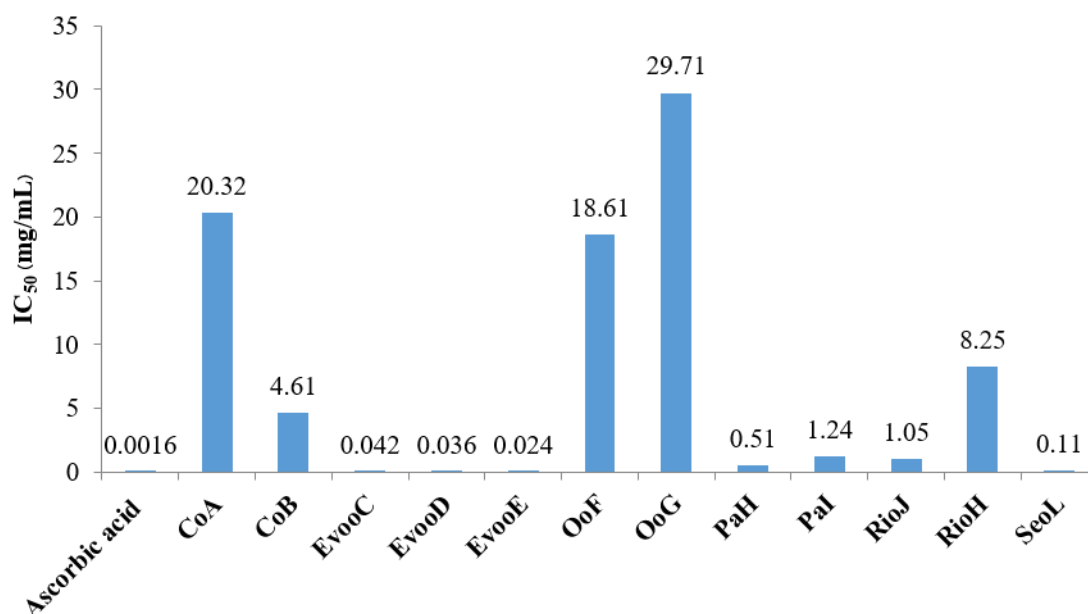


**Figure 2.** DPPH assay for antioxidant capacity used to determine as IC<sub>50</sub> values in eight different kinds of vegetable oil and duplicate of each type for testing. Ascorbic acid was a standard used as a positive control.

Therefore, imported extra virgin olive oil (EVOO) seems to be a very valuable edible oil with the highest presence of total polyphenols and antioxidant activity in the methanolic extracts while olive oil and coconut oil contributed the least quantity of total phenolic compounds and scavenging activity in hydrophilic extracted part. The oil production process of the extra virgin olive oil usually produces under the cold extraction but for the other oils commonly produce by refine processing with high temperature that might be the main reason related to the results of decreasing the yield of total phenolic compounds and the corresponding antioxidant activity. Moreover, the minor reason as described by A. Bajoub and co-workers, the crop season, geographic localization and climatic conditions might be the causes of the reduction of total phenolic content and various phenolic compound types and others [3].

**Table 2** One-way ANOVA analysis parameters of brands of edible vegetable oil (n=12), total phenolic contents, and IC<sub>50</sub> values.

Source of Variation	SS	df	MS	F	P-value	F crit
Within groups	550.44	11	50.04	0.93	0.54	2.82
Between groups	274.31	1	274.31	5.11	0.04	4.84
<b>Total</b>	1414.73	23				

## Summary

In conclusion, a new contribution of this research is a comparison of gallic acid equivalent content and IC<sub>50</sub> values between imported extra virgin olive oil (EVOO) and seven types of edible vegetable oils produced and marketed in Thailand. According to the results informed in this work, it is possible to confirm that imported extra virgin olive oil seems to be a very promising and valuable vegetable oil for consumption with the highest presence of total polyphenols and antioxidant activity in the methanolic extracts of edible vegetable oil. From our point of view, our results should encourage further studies to extend the experiments also to determine the total polyphenols and antioxidant activity in the oil phase extracts and evaluate the content of specific compounds in edible

vegetable oils by high performance liquid chromatography. Furthermore, this research could stand for useful information for the consumers.

## References

- [1] T.D. Xuan, G. Gangqiang, T.N. Minh, T.N. Quy and T.D. Khanh, An overview of chemical profiles, antioxidant and antimicrobial activities of commercial vegetable edible oils marketed in Japan, *Foods*. 7 (2018) 21-34.
- [2] C. Janu, D.R. S. Kumar, M.V. Reshma, P. Jayamurthy, A. Sundaresan and P. Nisha, Comparative study on the total phenolic content and radical scavenging activity of common edible vegetable oils, *J. Food Biochem.* (2013) 1-7.
- [3] A. Bajoub, S. Medina-Rdrigues, E. Hurtado-Fernandez, E.A. Ajal, N. Ouazzani, A. Fernandez-Gutierrez and A. Carrasco-Pancorbo, A first approach towards the development of geographical origin tracing models for North Moroccan olive oils based on triacylcerols profiles, *Eur. J. Lipid Sci. Technol.* 117 (2015) 1-13.
- [4] P. Kouka, A. Priftis, D. Stagos, A. Angelis, P. Stathopoulos, N. Xinios, A-L. Skaltsounis, C. Mamoulakis, A.M. Tsatsakis, D.A. Spandidos and D. Kouretas, Assessment of the antioxidant activity of an olive oil total polyphenolic fraction and hydroxytyrosol from a Greek *Olea europea* variety in endothelial cells and myoblasts, *Int. J. Mol. Med.* 40 (2017) 703-712.
- [5] P-G. Pietta, Reviews: Flavonoids as antioxidants, *J. Nat. Prod.* 63 (2000) 1035-1042.
- [6] PA. Grimsrud, H. Xie, T.J. Griffin and D.A. Bernlohr, Oxidative stress and covalent modification of protein with bioactive aldehydes, *J. Biol. Chem.* Vol. 283 No. 32 (2008) 21837-21841.
- [7] F. Shahidi and P. Ambigaipalan, Phenolics and polyphenolics in foods, beverages and spices: Antioxidant activity and health effects: A review, *J Funct Foods*. Vol. 18 part B (2015) 820-897.
- [8] T-I. Lafka, A.E. Lazou, V.J. Sinanoglou and E.S. Lazos, Phenolic extracts from wild olive leaves and their potential as edible oils antioxidants, *Foods*. 2 (2013) 18-31.
- [9] A. Bouyahya, N. Dakka, A. Talbaoui, N. El Moussaoui, J. Abrini and Y. Bakri, Phenolic contents and antiradical capacity of vegetable oil from *Pistacia lentiscus* (L), *J. Mater. Environ. Sci.* Vol. 9 Issue 5 (2018) 1518-1524.
- [10] Y. Yang, X. Song, X. Sui, B. Qi, Z. Wang, Y. Li and L. Jiang, Rosemary extract can be used as a synthetic antioxidant to improve vegetable oil oxidative stability, *Ind Crops Prod.* 80 (2016) 141-147.
- [11] A. Garcia, E. Rodriguez-Juan, G. Rodriguez-Gutierrez, J.J. Rios and J. Fernandez-Bolanos, Extraction of phenolic compounds from virgin olive oil by deep eutectic solvent (DESs), *Food chem.* 197 (2016) 554-561.
- [12] X. Chen, Y. Zhang, Y. Zu, L. Yang, Q. Lu and W. Wang, Antioxidant effects of rosemary extracts on sunflower oil compared with synthetic antioxidant, *J. Food Sci. Technol.* Vol. 49 Issue 2 (2013) 1-7.
- [13] A.F.K. Gonçalves, R.B. Friedrich, A.A. Boligon, M. Piana, R.C.R. Beck and M.L. Athayde, Anti-oxidant capacity, total phenolic contents and HPLC determination of rutin in *Viola tricolor* (L) flowers, *Free Rad. Antiox.* Vol. 2 Issue 4 (2012) 32-36.



# ***In vivo* toxicity testing and clearance of gold nanoparticles in whole blood and urine samples of animal models**

Sarinya Wongsanit<sup>1, a\*</sup>, Thunyatorn Yimsoo<sup>2, b</sup>, Werayut Yingmema<sup>2, c</sup>  
and Pattra Lertsarawut<sup>1, d</sup>

<sup>1</sup> Research and Development Division,

Thailand Institute of Nuclear Technology (Public Organization), Nakorn-Nayok, Thailand

<sup>2</sup>Laboratory Animal Center, Advanced Science and Technology, Thammasat University, Thailand

<sup>a</sup>sariyaw@tint.or.th, <sup>b</sup>Tyimsoo@tu.ac.th, <sup>c</sup>Werayut@tu.ac.th, <sup>d</sup>pattra.lert@hotmail.com

**Keywords:** Gold nanoparticles, Animal models, ICP-MS analysis, Diagnostic and Therapeutic

**Abstract.** Gold nanoparticles (AuNPs) are a promising candidate for *in vivo* applications given their low immunogenicity, clearance times, and biocompatibility. AuNPs have been widely employed for diagnostics, and have seen increasing use in the area of therapeutics. Before applying AuNPs to the clinical level requires rigorous testing and inspection in order to reduce toxicity and unnecessary impact. Animal studies using ICP-MS analysis of blood and urine have shown that gold nanoparticles cause no morbidity at any concentration up to  $1 \times 10^{13}$  particles/injection. Urine analysis showed a significant percentage of particles are cleared through renal filtration within 1 h, continues for up to 24 h and returns to baseline concentrations within 1 week. Whole blood analysis showed particle circulation within the bloodstream up to 24 hours post-injection. This was consistent with the primary clearance pathway of the particles being by excretion in urine. Gold nanoparticles also targeted primary organs although providing gradual dissipation and clearance over time. In summary of all study, mice injected with gold nanoparticles did not experience any clinical signs of illness, stress, or discomfort, nor did any expire over the course of the entire 6-week study. Therefore, gold nanoparticles presumably did not cause any toxic effects and undetectable stress to the mice. This study suggests that gold nanoparticles may be as promising materials to construct nanoscale diagnostic and therapeutic delivery systems.

## **Introduction**

Many metal nanoparticle formulations have progressed recently from the design and synthesis phase to *in vitro* testing with encouraging results. Gold-nanoparticles (AuNPs) is one of the metal nanoparticle that have an important role on medical, particularly in drug delivery system and molecular imaging [1]. AuNPs are small gold particles with a diameter of 1 to 100 nm which, once dispersed in water, are also known as colloidal gold. Gold nanostructures and nano-complexes have attracted much attention in different research areas because of their unique qualities. With its excellent catalysis activity and optical characteristics and biocompatibility, gold could efficiently facilitate both biomolecular imaging and the multifunctional treatment of targeted disease cells/tissues, acknowledging sensitive and specific disease diagnostics and reducing side effects and toxicity of relevant agents [2]. AuNPs also have been widely employed in bionanotechnology based on their unique properties and multiple surface functionalities. The ease of AuNPs functionalization provides a versatile platform for nanobiological assemblies with oligonucleotides, antibodies, and proteins. Bioconjugates of AuNPs have also become promising candidates in the design of novel biomaterials for the investigation of biological systems [3]. By combination with ultrasonic diagnostics and photothermal therapy, integration of the multimodal detection and therapeutic capabilities of AuNPs could be realized, highlighting its potential for cell identification, bioimaging and therapeutics for difficult-to-treat diseases like cancers [4].

The need to investigate toxicity, biodistribution, and clearance of nanoparticles *in vivo* is thus becoming increasingly important to their translation into clinical settings. Pharmacologic profiles, routes of administration, biodistribution patterns, and dosage are all important considerations that are only beginning to be addressed in detail. The AuNPs could label with radioisotope in order to form the AuNPs-radiopharmaceutical targeted Somatostatin receptor (SSTRs). The SSTRs, especially SSTR subtype 2, are found expressed at relatively higher levels in many tumor cells and in tumoral blood vessels relative to normal tissues[5]. Moreover, AuNPs have attracted much interest in targeted delivery as research has shown that the particles are able to permeate out of the blood stream to accumulate at tumor sites. In addition, their prolonged circulation time in blood enhances their efficiency in both diagnostic and therapeutic applications. Prior to clinical use, the profiles of *in vivo* toxicity, biodistribution and clearance of AuNPs is necessary to be done [6]. Moreover, the pre-clinical testing profile can determine whether these AuNPs could be used as a platform for the treatment of cancer and infectious diseases.

## Materials and Methods

The study of *in vivo* cytotoxicity of AuNPs (AuPEGCOOH) in urine and blood circulation system was performed by using Inductivity coupled plasma mass spectrometry (ICP-MS). All animal experiments were approved by the Laboratory Animal Center, Advanced Science and Technology, Thammasat University, Thailand. and carried out in compliance with the Thailand laws relating to the conduct of animal experimentation. The animal prototype used in this experiment was 4 weeks ICR-mice. Animals were purchased from National laboratory animal center, Mahidol University and were housed in a Laboratory animal center, Thammasat University. The facilities, were fully certified by the Institute of Animals for Scientific Purpose Development (IAD, NRCT) and the Association for Assessment and Accreditation of Laboratory Animal Care (AAALAC). All animals were allowed 1 week for acclimation before experimentation.

Nanoparticles were prepared in sterile phosphate-buffered saline (n=3 mice/concentration group) and injected subcutaneously. Dosage concentrations were 0, 1x10E8, 1x10E9, 1x10E10, 1x10E11, 1x10E12 and 1x10E13 particles in a 200  $\mu$ L total volume of phosphate-buffered saline (PBS). Blood was drawn via submandibular bleeding techniques, in compliance with our protocol and guideline for blood collection (bleeding amount in mL per kg body weight per week). Urine was collected on cellophane with special precaution to avoid fecal contamination. Blood and Urine samples were collected once a week until 4 week. During the experiment, mice were observed the clinical signs of illness such as fever, nausea and vomiting, signs of stress such as attempts to bite, lethargy and weight loss and also any signs of discomfort. Mice were euthanized via CO<sub>2</sub> asphyxiation, followed by cervical dislocation at the end of experiment.

Because of limitations in fluid collection, A 10  $\mu$ L of blood/urine sample was used. The fluid sample was added to a 4.5 mL solution of distilled water and then added 0.5 mL of hydrochloric acid (10% HCl dilution, HPLC grade). All samples were then analyzed in duplicate by ICP-MS (Agilent 7900, USA) for gold content using a standard calibration as well as the addition of an internal standard. The calibration curve covered the interval from 0 to 100 ppb of AuNPs (AuPEGCOOH, 5,000 Da, 12 nm, NITPARTICLES) diluted in ultrapure water to ensure that concentration of all the samples fits the chosen range. A standard check was made using a 10, 40 and 70 ppb AuNPs standard. A 45-second rinse with 4% HCl was used between every standard and sample.

## Results and discussion

The results of *in vivo* toxicity of AuNPs (AuPEGCOOH) in urine as determined by ICP-MS is shown in Fig. 1. The results showed that a large percentage of AuNPs, more than 35%, were voided through the renal system within 1 hour and more than 70% were excreted within 24 hours. There is no dysfunction of the excreted urine. The trend of urine excretion rates varies by concentrations and decreased with in time of excretion. At the 2<sup>nd</sup> week of experiment, the low range of injected concentration, (1x10E9 and 1x10E10 particles) showed excretion rate higher than high range of

injected concentration, ( $1 \times 10^{11}$ - $1 \times 10^{13}$ ). When compare to the content of AuNPs in blood in Fig. 2, the reason of this phenomenon maybe involved to the absorption of AuNPs into blood stream of mice. At high concentration, the amount of AuNPs can be more absorbed, transferred to blood stream and excreted than lower rang of concentration. The AuNPs concentration in the urine returned to baseline levels within 4 weeks.

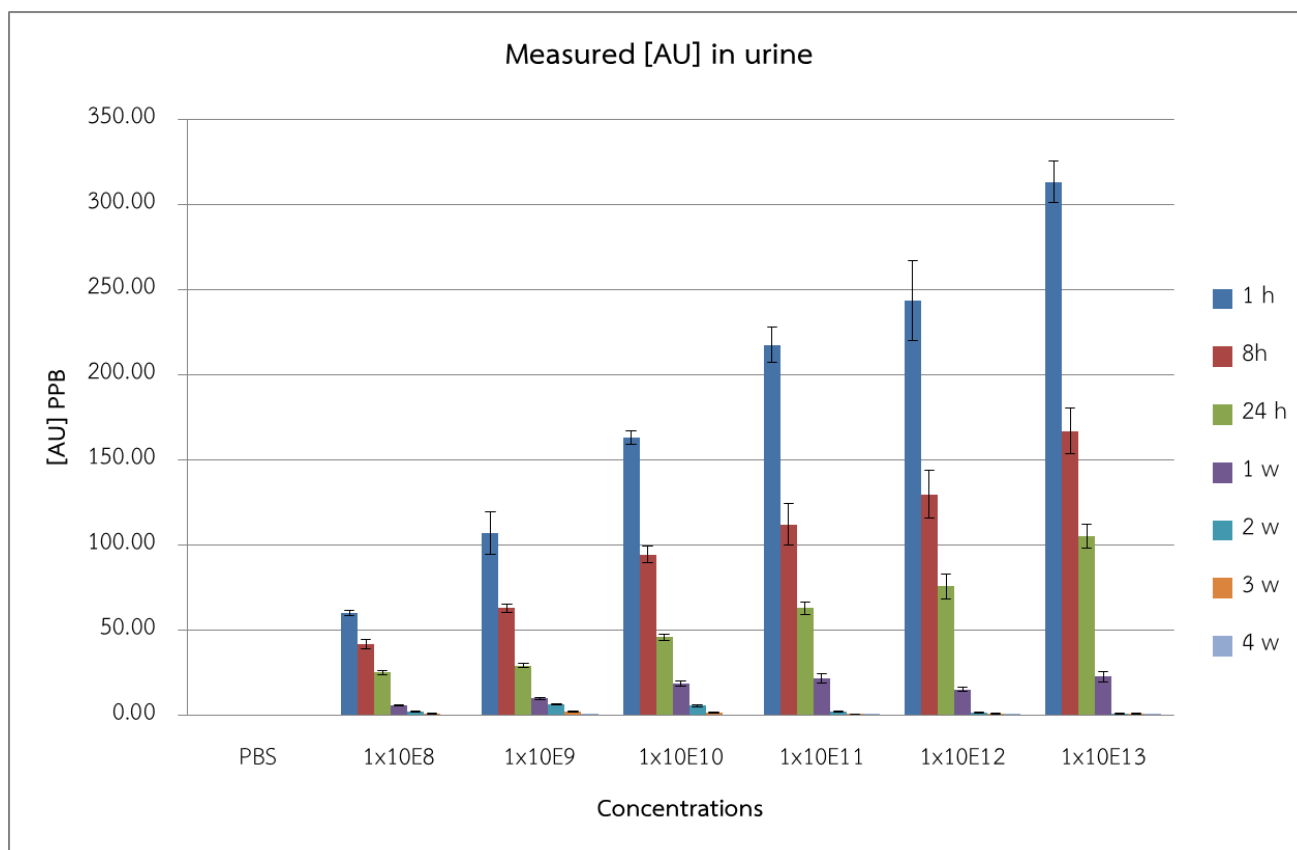


**Fig. 1** AuNPs (AuPEGCOOH) content analysis of urine samples (n = 3 for each time point)

In the monitoring of whole blood samples is shown in Fig. 2, the highest content of AuNPs was found at 8 h of experiment. It can be assumed that the AuNPs content that not being excreted in the excretory system can be absorbed to circulatory system. In every concentration of AuNPs, the Au nanoparticles showed high excretion rate at 8-24 h and almost particles would be nearly completed clearance within 1-2 week. However AuNPs in high concentration range of  $1 \times 10^{11}$ - $1 \times 10^{13}$  particles found particles accumulation until 4 weeks of sampling

Moreover, an interesting case has been observed in a series of high concentrations of AuNPs, at the amount of  $1 \times 10^{12}$  and  $1 \times 10^{13}$  particles. That is, at the 3<sup>rd</sup> week of experiment, there're no AuNPs detected in the blood circulatory system, but can detected again at the 4<sup>th</sup> week of experiment. The detected AuNPs may come from the accumulation of AuNPs at the mice organs and slowly transfer into the circulatory system due to the reason of the metabolism process and the excretions process of the animal model.

These results indicate that AuNPs were capable of rapid passage into the kidneys and bladder and had good circulation and clearance in bloodstream. Moreover, mice injected with AuNPs did not show any clinical signs of illness, stress or discomfort, nor did any expire over the course of the entire 4-week study.

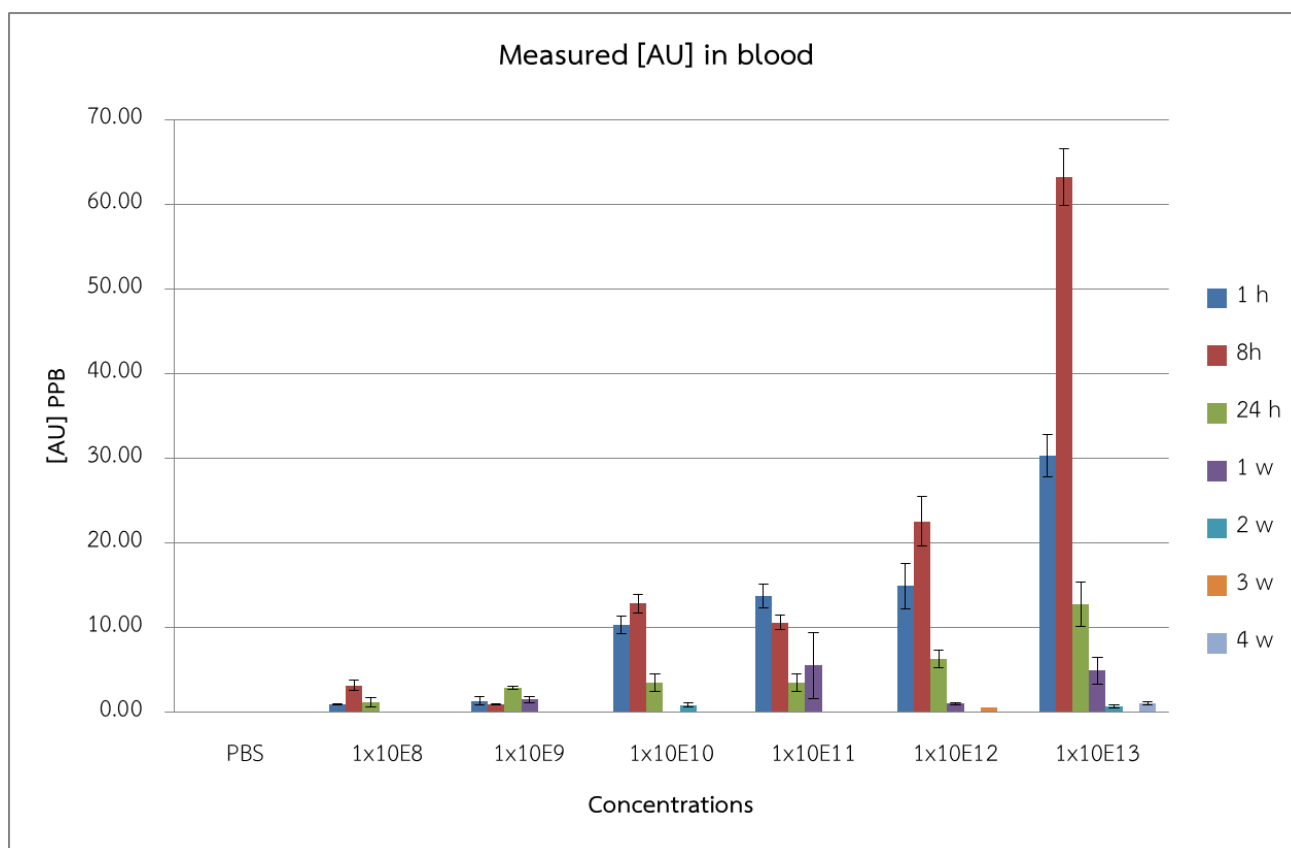


Fig. 2 AuNPs (AuPEGCOOH) content analysis of blood samples (n = 3 for each time point)

## Conclusions

The preclinical study of this research showed that AuNPs concentrations in the range of  $1 \times 10^8$ - $1 \times 10^{10}$  particles (represented low level) may be suitable for the radiolabeling with diagnostic isotopes such as F-18, TC-99m or Ga-68. And the AuNPs concentrations in the range of  $1 \times 10^{11}$ - $1 \times 10^{13}$  particles (represented high level) may be suitable for the radiolabeling with therapeutic isotopes such as Re-188, Lu-177, or Y-90. The results of preclinical study obtained from this research also showed a good tendency to form AuNPs-radiopharmaceutical. Those can be used in order to target diagnostic, therapeutic or theranostic via molecular imaging technique such as SPECT/CT, PET/CT, MRI and computed tomography (CT). This research has planned the future study by labeling AuNPs with 1,4,7,10-tetraazacyclododecane-1,4,7,10-tetraacetic acid-1-Na<sub>3</sub> - octreotide (DOTANOC) in animal model.

## References

- [1] N. Baltzer, T. Copponex, Precious metals for biomedical applications, first ed., Elsevier, USA, 2014.
- [2] Y.-C. Yeh, B. Creran, V.M. Rotello, Gold nanoparticles: preparation, properties, and applications in bionanotechnology, *Nanoscale* 4(6) (2012) 1871-1880.
- [3] S.K. Sahoo, Applications of nanomedicine, *Asia Pac Biotech News* 9(20) (2005) 1048-1050.
- [4] H. Xie, Z.J. Wang, A. Bao, B. Goins, W.T. Phillips, In vivo PET imaging and biodistribution of radiolabeled gold nanoshells in rats with tumor xenografts, *Int. J. Pharm.* 395(1-2) (2010) 324-330.
- [5] M. Díaz, P. Vivas-Mejia, Nanoparticles as drug delivery systems in cancer medicine: emphasis on RNAi-containing nanoliposomes, *Pharmaceuticals* 6(11) (2013) 1361-1380.
- [6] C.A. Simpson, K.J. Salleng, D.E. Cliffler, D.L. Feldheim, In vivo toxicity, biodistribution, and clearance of glutathione-coated gold nanoparticles, *Nanomedicine: NBM* 9(2) (2013) 257-263.

# Physicochemical characteristics and antioxidant activity of mak mao berry loaded nanovesicles for cosmetics

Sureewan Duangjit<sup>1,a\*</sup>, Kittiyarat Phimphong<sup>1,b</sup>, Weerawut Kacha<sup>1,c</sup>,  
Natthaporn Janjarasjitt<sup>1,d</sup>, Kusuma Jitsaeng<sup>1,e</sup>, Bancha Yingngam<sup>1,f</sup>,  
Sasipong Tiphatchdaporn<sup>2,g</sup>, and Sureewan Bumrunghai<sup>3,h</sup>

<sup>1</sup>Faculty of Pharmaceutical Sciences, Ubon Ratchathani University, Ubon Ratchathani 34190, Thailand

<sup>2</sup>Pra-Arjarn-Fhan-Arjaro Hospital, Sakon Nakhon 47130, Thailand

<sup>3</sup>Department of Microbiology and Parasitology, School of Medical Sciences, University of Phayao, Phayao 56000 Thailand

<sup>a</sup>sureewan.d@ubu.ac.th, <sup>b</sup>kittiyarat.p@ubu.ac.th, <sup>c</sup>weerawut.k@ubu.ac.th, <sup>d</sup>natthaporn.j@ubu.ac.th,

<sup>e</sup>kusuma.j@ubu.ac.th <sup>f</sup>bancha.y@ubu.ac.th <sup>g</sup>champharmact@hotmail.com,

<sup>h</sup>sureewan.b@windowslive.com

\* corresponding author

**Keywords:** Mak Mao berry, Berry Extract, Liposome, Niosome, Total Phenolic

**Abstract.** Currently, nanotechnology is continuously utilized to improve the therapeutic effect of a natural antioxidant. The objective of this study was to design and develop the natural antioxidant loaded nanovesicle (liposomes and niosomes). *Antidesma puncticulatum* extract or maoberry (MM) was used as an active ingredient. MM obtained from Pra-Arjarn-Fhan-Arjaro Hospital, Sakon Nakhon. MM loaded nanovesicle was prepared by sonication method. The vesicle size, size distribution, zeta potential and total organic acids was investigated. Moreover, the antioxidant activity and total phenolic content were evaluated by radical scavenging assay (DPPH) and Folin Ciocalteu method, respectively. The vesicle size of MM loaded liposomes and niosomes was 94-550 and 116-687 nm, respectively. The width of size distribution was 0.27-0.81 and 0.46-0.93. While the zeta potential was 2-21 and 6-24 (-mV). The ascorbic acid was an antioxidant that determined by the HPLC analysis. The oxalic acid, malic acid, citric acid and tartaric acid were organic acid presented in MM loaded nanovesicles. The inhibition was liposomes and niosomes was 23-62 and 23-42%, respectively. The total phenolic compound was 70-132 and 88-182 mg gallic acid equivalent/mg (or mg GAE/g). The finding could be concluded that the source of natural antioxidant as MM can be incorporated in the nanovesicles as liposomes and niosomes. To improve the market value of the MM extraction from Pra-Arjarn-Fhan-Arjaro Hospital, further study is required to incorporate MM loaded nanovesicle into serum base.

## Introduction

Recently the consumers around the world are more concerned about their health, beauty and their appearance. This trend has created an enormous demand for natural health care products including cosmetic products. The efficacy, safety and stability are the primary concern by the pharmacists and/or scientists. Nanotechnology is continuously utilized to improve the efficacy of various natural extractions. Natural antioxidant are the active ingredient that provided several health and beauty, ageing-benefits such as anti-oxidant, wrinkle and skin lightening properties that make them widely used in health care and cosmetic products. The natural product with antioxidant activity becomes an interesting active compound. Moreover, the approach of nanotechnology with the natural product is attention to the design and development of health care and cosmetic products. Nanotechnology is one of the most extensive technologies utilized in novel delivery systems for

.pharmaceutical and natural productsThe application of nanotechnology for drug and cosmetic delivery was absolute unique, potential and versatile delivery systems.

*Antidesma puncticulatum* fruit or maoberry (MM) is an indigenous fruit in Southeast Asia especially in the dipterocarp forest of the Phupan Valley in the northeast area of Thailand [1]. The ripe of MM is of purplish-red or dark-purple depending on the level of ripeness that occurs from August to October. Various phenolic compounds have been found in MM extract as fruit-based wine including gallic acid, caffeic acid, catechin, and monogalloyl glucoside. The MM wine also contained anthocyanin pigments e.g. cyanidin-3-sophoroside, delphinin-3-sambubioside and pelargonidin-3-malonyl glucoside [2]. Not only the antioxidant activity of MM has been reported, the  $\alpha$ -glucosidase inhibitory activity, the anti-apoptosis and the anti-inflammatory activity of MM are also recommended for health-promoting benefit [1].

The objective of this study was to design and develop the natural antioxidant loaded nanovesicle (liposomes and niosomes). The vesicle size, size distribution, zeta potential and total organic acids were investigated. Moreover, the antioxidant activity and total phenolic content was evaluated by radical scavenging assay (DPPH) and Folin Ciocalteu method, respectively.

## Materials and Methods

**Materials.** Mak Mao berry extract (MM) obtained from Pra-Arjarn-Fhan-Arjaro Hospital, Sakon Nakhon. Phosphatidylcholine (PC, 90H) was generously supported by Lipoid GmbH (Ludwigshafen, Germany). Cholesterol (Chol) was expended from Wako Pure Chemical Industries (Osaka, Japan). All chemicals used were of reagent grade and were purchased from Wako Pure Chemical Industries.

**Liposomes and Niosomes Preparation.** Two types of nanovesicles (liposomes and niosomes) were prepared according to the proper ratio obtained from our previous studies [3, 4]. Table 1 shows the nanovesicle formulations prepared from the sonication method. Briefly, the mixtures of PC, Chol, and various penetration enhancers including fatty acid, ethanol, nonionic surfactant and terpene were dissolved in chloroform/methanol (2:1 ratio). The solvent was evaporated under a nitrogen gas stream and dried in a desiccator for 6 hours. The dried film was hydrated with MM extraction. The nanovesicles were subsequently sonicated for 30 minutes using a bath-type sonicator. The excess composition was removed by centrifugation at 4°C and 15,000 rpm for 15 minutes, and the supernatant was collected. All formulations were freshly prepared or stored in air-tight containers at 4°C prior to further studies.

**Table 1** The composition of each nanovesicle formulation

PE	Liposome formulation	PC	Chol	Niosome formulation	Tween 60	Chol
Control	CLP	10 mM	4 mM	NS	7 mM	7 mM
Surfactant	TFS	10 mM	4 mM	TNS	7 mM	7 mM
Ethanol	ETS	10 mM	4 mM	ENS	7 mM	7 mM
Nonionic surfactant	FXS	10 mM	4 mM	FNS	7 mM	7 mM
Terpene	IVS	10 mM	4 mM	INS	7 mM	7 mM

Abbreviation: penetration enhancer (PE), phosphatidylcholine (PC), cholesterol (Chol), conventional liposomes (CLP), transfersomes (TFS), ethosomes (ETS), flexosomes (FXS), invasomes (IVS), niosomes (NS), transfersomes-niosomes (TNS), ethosomes-niosomes (ENS), flexosomes-niosomes (FNS), invasomes-niosomes (INS)

**Physicochemical Characterization.** The vesicle size, size distribution and zeta potential of the nanovesicles (liposomes and niosomes) were measured by photon correlation spectroscopy (Zetasizer Nano series; Malvern Instruments, Malvern, UK). Twenty microliters of sample were diluted with the optimal ration of deionized water. All samples were determined at room temperature, at least three independent samples were collected.

**Free Radical Scavenging Activity Assay.** The antioxidant activity of MM extract was measured using DPPH assay according to the method previously described [5]. The antioxidant activity of the MM extract was calculated from the standard curve of Trolox and the results are expressed as millimolar Trolox equivalent per gram of dry plant powder (mM TE/g).

**Phenolic Compounds Determination by Folin–Ciocalteu reagent.** The stock solutions of gallic acid at 20 µg/mL was prepared in distilled water. Thirty milliliters of each sample was transferred to a 5 mL volumetric flask containing deionized water (470 µL) and Folin-Ciocalteu reagent (250 µL) [9]. The volume was completed with 10.75% anhydrous sodium carbonate (w/v), resulting in final concentrations of 1 µg/mL of standard. The samples were scanned in a UV/Vis spectrophotometer (Shimadzu PC-1650, Japan) 10 to 30 min after the addition of the sodium-carbonate solution, and scanning from 400 to 800 nm. Deionized water was used as a blank, with a quartz cell (1 cm path length).

**Quantitation of Organic Acids.** Five organic acids including L-ascorbic acid, oxalic acid, L-malic acid, citric acid and L-(+)-tartaric acid were used as the standard substance. The HPLC instruments of Thermo™ comprised of a degasser, quaternary pump, automated sample injector, column oven and a diode array detector. The Vertical column C18 (4.5 mm × 250 mm i.d., 4.5 µm particle size) was used. Fifty mM of phosphate buffer solution was the mobile phase. The flow rate was set at 0.7 mL/min at 35°C. The detection wavelength of each organic acid was set at 214 nm, except for L-ascorbic acid (254 nm).

**Data analysis.** The data are reported as the means ± standard error (n=3–9), and statistical analysis of the data was carried out using one-way analysis of variance. A *P*-value of less than 0.05 was considered to be statistically significant.

## Results and Discussion

### Physicochemical Characteristics

The physicochemical characteristics of all nanovesicles are in Figure 1. The average vesicle of MM loaded nanovesicles depended on the penetration enhancers incorporated. The ionic-surfactant incorporated results in increased vesicle size of nanovesicles because of the electrostatic repulsion at the polar head group of the single chain surfactant. At high concentration of surfactant, the vesicle may transform to nanostructure because the release of the curvature disruption may increase the curvature of the bilayer. While the nonionic-surfactant led to decrease and increase the vesicle size of liposomes and niosomes, respectively. It was known that the lipophilicity tail packing of nonionic-surfactant differed from ionic-surfactant. Thus the packing of the bilayer was tight and more rigid than a monolayer. The previous study revealed that the overall influence of the organization is not absolutely predicted [6]. This result suggested that the electrostatic repulsion was not more enough to alter the CPP value. Contradictory, it has been reported the electrostatic forces may increase the distance of the monolayer and lead to an increase in the size of vesicles. The ethanol added led to an increase in the vesicle size of nanovesicles. The previous study discussed the thickness of the bilayer increased when the concentration of ethanol increase [7]. The terpene incorporation decreased the vesicle size of the liposome. It is well known that the conductivity related to the size of vesicles. The incorporation of 1 to 3 µM (but not more than 200 µM) of terpene increased the conductance of bilayer [8]. The conductivity of vesicular bilayer was not only affected by the concentration of terpene, but the types of terpene also do the same. The vesicle size of the liposomes after the stability test was not significantly different, except IVS. The vesicle size stability of niosomes was lower than that of liposomes (Figure 2A).

The width of size distribution was 0.27-0.81 and 0.46-0.93 for liposomes and niosomes, respectively. The formulation factor and the method of preparation were the major roles that affected the size distribution of the nanovesicles (liposomes and niosomes). The zeta potential of all vesicle was negative charge with 2-21 (-mV) in liposomes and 6-24 (-mV) in niosomes. The zeta potential depended on the total net charge of all compositions in the formulations. The Helmholtz–

Smoluchowski equation may not be appropriate for the calculation of the zeta potential of the liposomes. The magnitude and sign of the zeta potential were calculated by net charge accumulated on the vesicle surface. The zeta potential over 20 mV can stabilize and protect the nanovesicles from the aggregation [9].

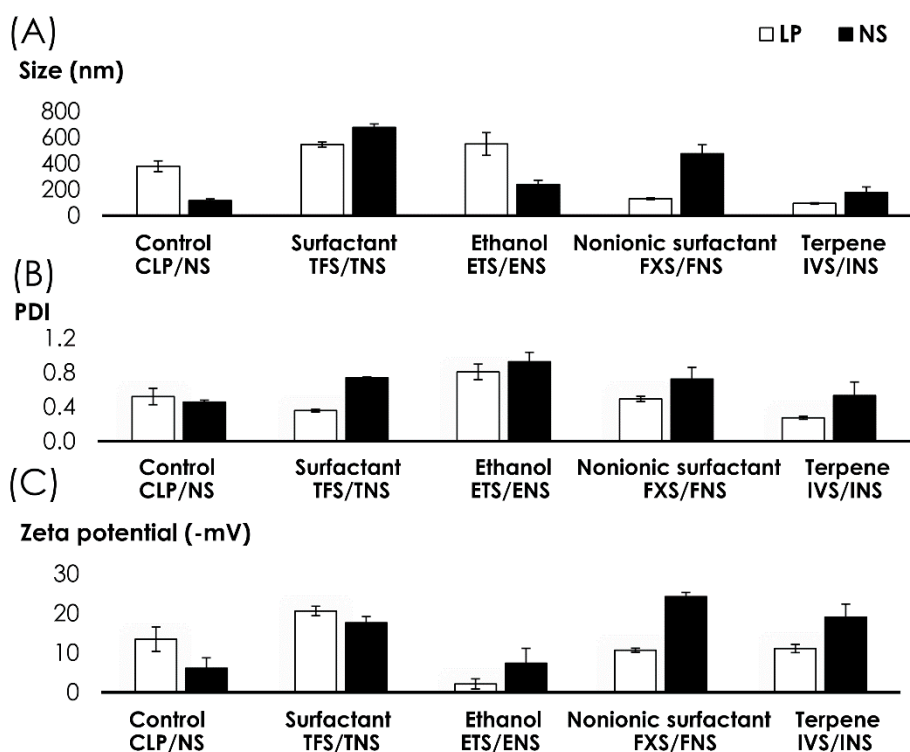


**Figure 1.** The physicochemical properties of all nanovesicles: (A) vesicle size (B) size distribution and (C) zeta potential

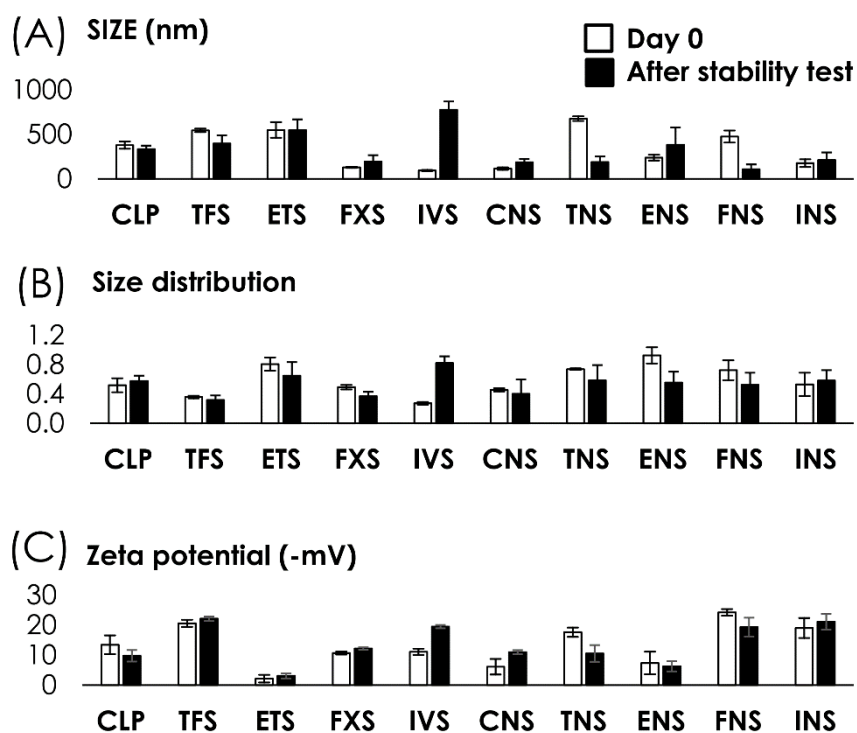


**Figure 2.** The physicochemical stability of all nanovesicles: (A) vesicle size (B) size distribution and (C) zeta potential



Considering the qualitative analysis, ascorbic acid was an antioxidant that determined by the HPLC analysis. The oxalic acid, malic acid, citric acid and tartaric acid were organic acids presented in MM loaded nanovesicles. Further study, we suggest determining the content of organic acid in each formulation.

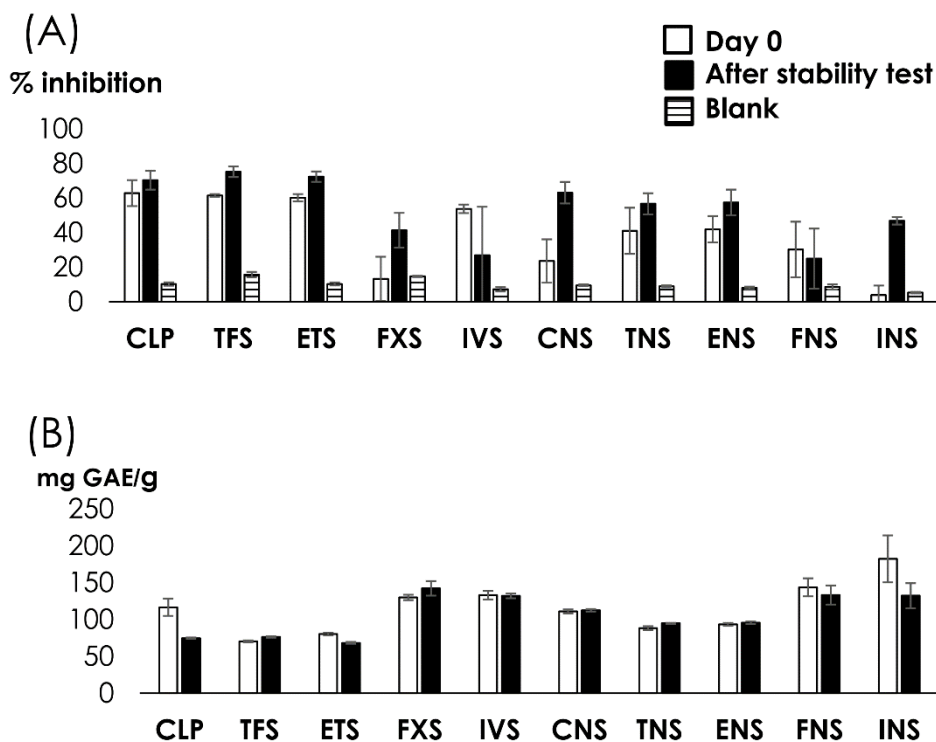


**Figure 3.** The comparison of the initiation and after stability test of nanovesicles: (A) antioxidant activity and (B) total phenolic compounds content

### Antioxidant Activity

The antioxidant activity of all nanovesicles at the initial and after the stability test is demonstrated in Figure 3A. The percent inhibition of liposomes and niosomes was 23-62 and 23-42%, respectively. The antioxidant activity of MM loaded liposomes was significantly stronger than the MM loaded niosomes. The inhibition decreased due to the incorporation of the nonionic surfactant and terpene. The terpene may be a competitor to provide an antioxidant activity due to its hydroxyl moiety as reported in the literature [10]. Thus, the terpene may rapidly interact with DPPH free radical before the MM. The activity of the antioxidant after incorporation in the nanovesicles did not only correlated to its chemical activity, but also to its entrapment efficiency into the bilayer and modifying effect on the bilayer characteristics [10]. It could be summarized that MM loaded liposomes have stronger antioxidant activity than MM loaded niosomes. The antioxidant activity of the nanovesicle after the stability test was greater than the initial. This may be attributed to the conversion of conjugated glycosides into more potent aglycones [11]. This result indicated that the nanovesicle can be used to protect the antioxidant activity of MM extraction.

### Total Phenolic Compounds

The total phenolic compound of the formulation of liposomes and niosomes was compared (Figure 3B). The different penetration enhancer incorporation affected the total phenolic compound found in the formulation, which depended on their intrinsic properties. The total phenolic compound in liposomes and niosomes was 70-132 and 88-182 mg gallic acid equivalent/g (or mg GAE/g), respectively. Considering the stability test, the total phenolic compound of the formulation after the

incubation time was very close to the initiation. The result revealed that nanovesicles can protect the phenolic compounds in the herbal product formulation from degradation.

### Summary

The finding could be concluded that the source of natural antioxidant of such MM can be incorporated in the nanovesicles as liposomes and niosomes. The liposomes are the proper nanovesicle in our study. To increase the value-added MM extract from Pra-Arjarn-Fhan-Arjaro Hospital, further study is required to incorporate MM loaded nanovesicle into serum base as anti-aging cosmetics.

### Acknowledgements

The authors gratefully acknowledge Thailand Research Fund through the Research Team Promotion Grant (RTA6180003), the Silpakorn University Research and Development Institute (SURDI610110), the Faculty of Pharmacy, Silpakorn University and Faculty of Pharmaceutical Sciences, Ubon Ratchathani University for financial and facilities support. In addition, the authors would like to thank the Queen Saovabha Memorial Institute, Thai Red Cross Society, Bangkok, Thailand and Pra-Arjarn-Fhan-Arjaro Hospital, Sakon Nakhon, Thailand for kindly providing the shed snake skin and MM, respectively. We also give special thanks to the staffs in the laboratory for their assistance in this research.

### References

- [1] Yingngam B, Monschein M, Brantner AH, Application of ultrasonic assisted extraction of bioactive compounds from the fruits of *antidesma puncticulatum* Miq. and evaluation of its antityrosinase activity. *Chiang Mai J Sci*, 43, 518-533 (2016).
- [2] Nuengchamnong N, Ingkaninan K, On-line HPLC–MS–DPPH assay for the analysis of phenolic antioxidant compounds in fruit wine: *Antidesma thwaitesianum* Muell. *Food Chem*, 118, 147-152 (2010).
- [3] Duangjit S, Nimcharoenwan T, Chomya N, Locharoenrat N, Ngawhirunpat T, Computational design strategy: an approach to enhancing the transdermal delivery of optimal capsaicin-loaded transinvasomes. *Drug Dev Ind Pharm*, 43, 98-107 (2017).
- [4] Duangjit S, Opanasopit P, Rojanarata T, Takayama J, Takayama K, Ngawhirunpat T, Bootstrap resampling technique to evaluate the reliability of the optimal liposome formulation: skin permeability and stability response variables. *Biol Pharm Bull*, 37, 1543-1549 (2014).
- [5] Kedare SB, Singh RP, Genesis and development of DPPH method of antioxidant assay. *J Food Sci Technol*, 48, 412-422 (2011).
- [6] Yagmur A, Laggner P, Zhang S, Rappolt M, Tuning curvature and stability of monoolein bilayers by designer lipid-like peptide surfactants. *PloS One*, 2, e479-e479 (2007).
- [7] Patra M, Salonen E, Terama E, Vattulainen I, Faller R, Lee BW, Holopainen J, Karttunen M, Under the influence of alcohol: the effect of ethanol and methanol on lipid bilayers. *Biophys J*, 90, 1121-1135 (2006).
- [8] Abramov AY, Zamaraeva MV, Hagelgans AI, Azimov RR, Krasilnikov OV, Influence of plant terpenoids on the permeability of mitochondria and lipid bilayers. *Biochim Biophys Acta*, 1512, 98-110 (2001).
- [9] Chibowski E, Szczes A, Zeta potential and surface charge of DPPC and DOPC liposomes in the presence of PLC enzyme. *Adsorption*, 22, 755–765 (2016).
- [10] Gonzalez-Burgos E, Gomez-Serranillos MP, Terpene compounds in nature: a review of their potential antioxidant activity. *Curr Med Chem*, 19, 5319-5341 (2012).
- [11] Komori RHYKT, Thermal degradation of glycosides, I. Degradation of typical Triterpenoid and steroid glycosides. *EurJOC*, 1985, 638-646 (1986).

## Development of coated tablets using polymer blend technique

Nattapol Panyaprapakorn<sup>a\*</sup>, Pattarapol Latchanon<sup>b</sup>, Sujimon Tunvichien<sup>c</sup> and Duangratana Shuwisitkul<sup>d\*</sup>

Department of pharmaceutical technology, Srinakharinwirot University, Thailand.

<sup>a</sup> patchdeb128@gmail.com, <sup>b</sup> pz\_of\_nagas@hotmail.com, <sup>d</sup> sujimon@g.swu.ac.th, <sup>e\*</sup> duangrats@g.swu.ac.th

**Keywords:** Coated tablet, polymer blend, rheological properties, viscoelasticity, controlled release

**Abstract.** Polymer blend is a technique to achieve desired drug release profiles with many advantages compared to single polymer coating. The study aimed to develop controlled-release coated tablets with acid resistant properties and ability of sustained release under the condition of small intestine by polymer blend technique and to compare rheological, disintegration and drug release of coating polymer between using single polymer and polymer blends. Theophylline and CPM were used as model drugs. The core tablets were coated with hydroxypropyl methylcellulose (HPMC), Eudragit L, ethylcellulose (EC), and their blends. 10% Triethyl citrate (TEC) was used as a plasticizer. The result showed that the polymer blend solutions had lower viscosity than HPMC solution. However, the rheological properties when performed temperature sweep test had no difference between the polymer solution and polymer blend solutions. The temperature of changing from viscous to elastic properties of the polymer blend solutions between Eudragit L and HPMC was increased in comparison to Eudragit L alone. Polymer blends coated tablet showed slower disintegration time in both medium. Theophylline from the polymer blends coated tablets released slower drug release than the single polymer coated tablets in both medium. The polymer blends between HPMC and EC in the ratio of 1:1 resulted in no drug release in 0.1 M HCl and slow release in phosphate buffer pH 6.8. It can be concluded that the polymer blend in the appropriate ratio can achieve controlled-release tablets and provide better rheological properties.

### Introduction

The coating process is the critical step in the tablet production. The coating process was used to mask the odor, taste or color of the drug, to provide physical and chemical protection for the drug, to increase in drug stability in gastric environment of stomach. Generally, hydrophobic and/or hydrophilic polymers were used as coating materials, such as Eudragit L, EC or HPMC [1].

Polymer blends technique is a technique which used different properties of the two polymers to form suitable materials. The polymer blends for tablet coating have many advantages, such as modified or controlled drug release and improving gastric stability for oral tablets [2].

This research aimed to develop controlled-release coated tablets using polymer blend technique and to compare rheological, disintegration and drug release of coating polymer between using single polymer and polymer blends. Hydroxypropyl methylcellulose (HPMC), copolymer of methacrylic acid and ethyl acrylate (Eudragit L) and ethylcellulose (EC) and their blends were used as coating materials to obtain controlled-release with acid resistant properties and ability of sustained release under the condition of small intestine from coated tablets.

## Materials and method

### Materials

Eudragit® L100 was obtained from Evonik Industry AG (Darmstadt, Germany). Ethyl cellulose T10 (EC) (Aqualon™) was received from Ashland™ (Kentucky, USA). Hydroxypropyl methylcellulose E15 (HPMC) (Methocel E15) was purchased from Samsung Fine Chemicals Co., Ltd. (Seoul, Korea). Triethyl citrate (TEC) was purchased Merck (Darmstadt, Germany). The model drugs were theophylline (Jilin shulan synthetic pharmaceutical Co., Ltd., China) and chlorpheniramine malate (CPM) (Vankatara chemicals Ltd., India).

### Preparation of core tablet and film coated tablets

The core tablets containing the model drug were prepared by wet granulation. The model drug of 100 mg was added into each core tablet (300 mg). Lactose was used as a filler. Magnesium stearate was used as a lubricant and corn starch was used as a disintegrant. The core tablets with the hardness higher than 8 kg were required.

Film coating solutions (table 1) were prepared for 2000 g per formula. All components were mixed and stirred not less than 6 hours. The core tablets were coated using Thai coater under the following condition: rotation speed of 7-8 rpm, inlet air temperature at 55°C and outlet air at 40 °C.

**Table 1.** The composition of the film coating solution.

Ingredient	F 1 HPMC	F 2 EC	F 3 Eudragit L 100	F 4 HPMC : Eudragit L 100 (1 : 1)	F 5 HPMC : Eudragit L 100 (1 : 2)	F 6 EC : Eudragit L 100 (1 : 1)
HPMC	2%	-	-	1%	0.6%	-
EC	-	2%	-	-	-	1%
Eudragit L 100	-	-	2%	1%	1.4%	1%
TEC	0.2%	0.2%	0.2%	0.2%	0.2%	0.2%
IPA: H <sub>2</sub> O (8:2)	q.s. to 100%					

After the mixing solution, rheological properties were investigated by the rheometer.

### Rheological studies

Viscosity and viscoelasticity of coating solutions were measured by rheometer (HAAKE Rheostress I, Thermo Fisher Scientific, Germany). The method with constant shear rate of 50 s<sup>-1</sup> was used to determine viscosity. Amplitude, frequency and temperature sweep methods were used for viscoelasticity behavior of coating solutions. Amplitude at 5 Pa was used in frequency sweep test. Frequency from 0.1-10 Hz was applied. The temperatures from 20-80°C were measured for the temperature sweep test.

### Dissolution test

Dissolution or drug releases from the coated tablets were studied using USP dissolution apparatus 2. (Varian VK7010 Dissolution Apparatus, USA). 900 ml of 0.1 N HCl or phosphate buffer pH 6.8 at 37°C ± 0.5 was used. The coated tablets (n=3) was studied drug dissolution in 0.1 N HCl for first two hours and then, in phosphate buffer pH 6.8 for four hours. The sample concentration

was determined using an UV-VIS Spectrophotometer (Agilent Technologies, Varian Cary® 50 UV-Vis Spectrophotometer, USA) at 272 nm and 265 nm for Theophylline and CPM, respectively.

## Results and discussion

The prepared film coating with HPMC (F1) showed the highest viscosity at  $19.575 \pm 2.253$  cP, while the Eudragit L 100 (F3) showed the lowest viscosity at  $4.039 \pm 0.610$  (Table 2). After the mixed polymers as a polymer blend, the viscosity of the film coating was decreased caused by losing of the adhesive ability [3].

**Table 2.** Viscosity of the film coating solutions at shear rate  $50 \text{ s}^{-1}$

Formula	viscosity (cP)
F1 (HPMC)	$19.575 \pm 2.253$
F2 (EC)	$8.008 \pm 0.085$
F3 (Eudragit L 100)	$4.039 \pm 0.610$
F4 (HPMC : Eudragit L, 1:1)	$9.387 \pm 1.149$
F5 (HPMC : Eudragit L, 1:2)	$6.147 \pm 0.0251$
F6 (EC : HPMC, 1:1)	$5.249 \pm 0.212$

The study of viscoelasticity by frequency sweep method was shown in Figure 1. The result indicated that  $G''$  value higher than  $G'$  at the lower frequency. It means the dominant viscous properties of the polymer solution. [4] At the higher frequency above approximately 10 Hz, the dominant properties began to fluctuate. The results showed in the same trend of viscoelasticity in all formula. The polymer blends had no effect on the rheological properties from frequency sweep testing.

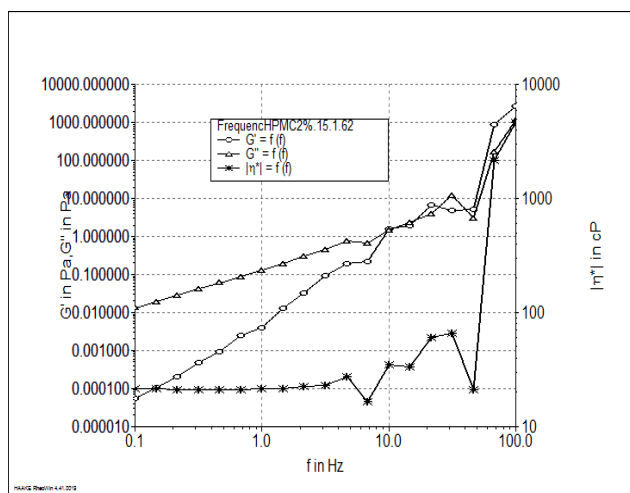


**Figure 1** Viscoelasticity behavior from frequency sweep of the HPMC.

From the temperature sweep technique, it could be found that  $G''$  was above  $G'$  for HPMC (Figure 2a) and EC (data not shown) and there was no intersection between  $G''$  and  $G'$ . It indicated the dominant viscous properties at all measuring temperatures. Eudragit L coating solution alone

showed the inversion of viscoelasticity properties from viscous to elastic properties at the approximate temperature of 70°C (Figure 2b). The temperature of changing from viscous to elastic properties of polymer blend solutions between Eudragit L and HPMC was increased in comparison to Eudragit L alone (Figure 2c).

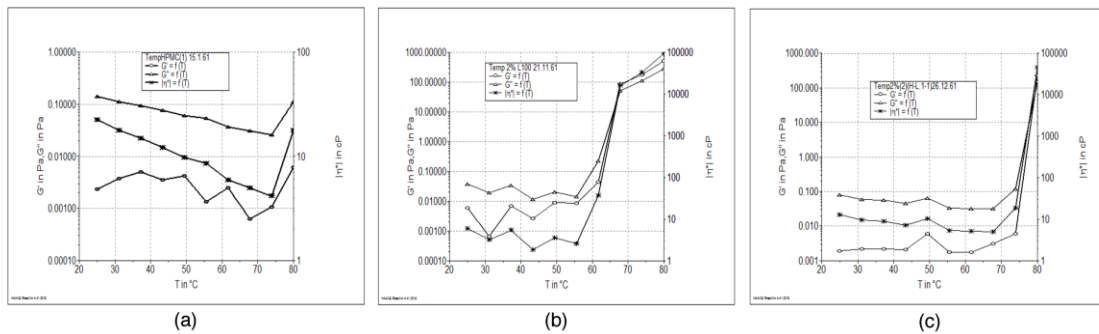


**Figure 2** Viscoelasticity behavior from temperature sweep of the (a) HPMC, (b) Eudragit L 100, and (c) their blend (1:1), respectively.

The study of theophylline dissolution from the film coated tablets demonstrated that the polymer blend between Eudragit L and HPMC could retard theophylline release (Figure 3a). The drug release was slower than that from the tablets coated by either Eudragit L or HPMC alone.

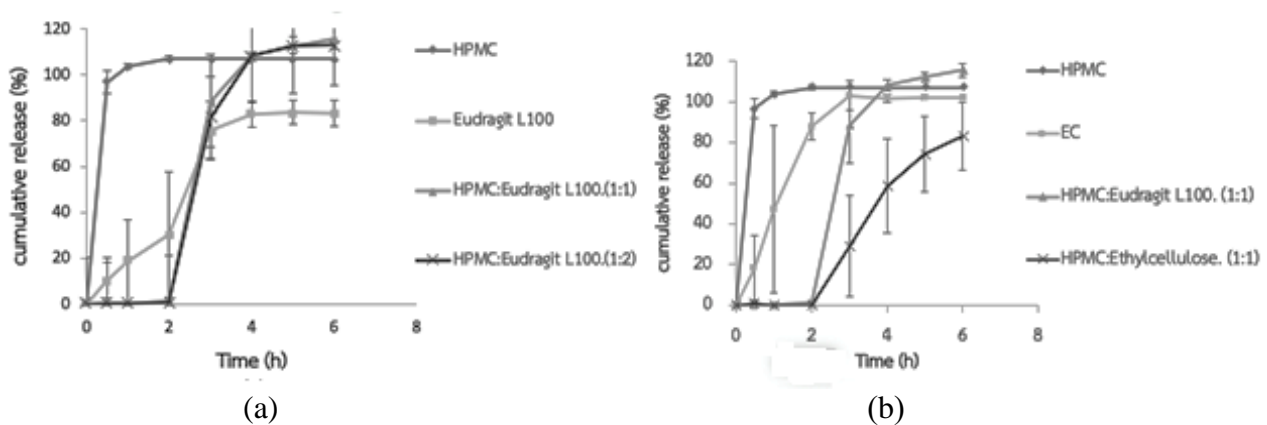


**Figure 3** Comparison of theophylline dissolution profiles between the single polymers and polymer blends; (a) HPMC, Eudragit L and their blends (1:1, 1:2); (b) HPMC, EC, HPMC:Eudragit L (1:1) and HPMC:EC (1:1).

Theophylline release could be more control in phosphate buffer pH 6.8 when using EC instead of Eudragit L for the polymer blends (Figure 3b). The controlled release up to 4 hours was achieved in in phosphate buffer pH 6.8 after no release in 0.1N HCl for 2 hours.

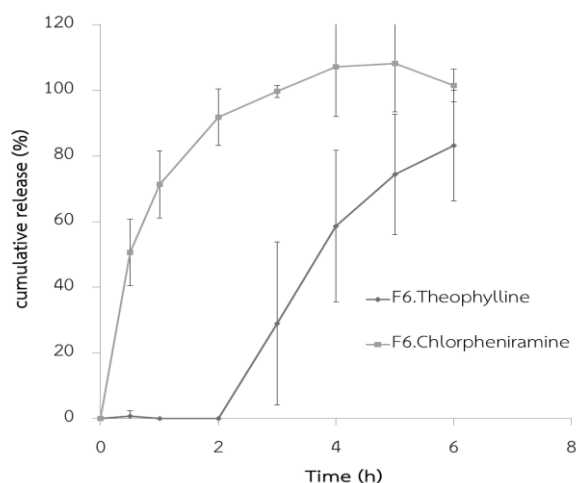


**Figure 4** Comparison of theophylline and CPM release from the tablets coated by HPMC:EC blend in the ration of 1:1 (F6).

CPM release from the tablets coated by HPMC:EC blend in the ration of 1:1 could not be retarded in comparison to theophylline (Figure 4). The higher solubility of CPM in 0.1N HCl and phosphate buffer pH 6.8 led to faster release in 0.1N HCl. Therefore, with the higher water-soluble drug this polymer blend was not successful for controlling drug release.

## Conclusion

The polymer blend between the hydrophobic and hydrophilic polymers in the appropriate ratio can achieve controlled-release tablets in comparison to the single polymers. Moreover, the polymer could help improve rheological properties. The lower viscosity form the polymer blends contributed to easily tablet coating and the temperature of changing elasticity could be modified.

## References

- [1] Z-Z Piao, L.Kyoung-Ho, K.Dong-Jin.Comparison of Release-Controlling Efficiency of Polymeric Coating Materials Using Matrix-type Casted Films and Diffusion-Controlled Coated Tablet.AAPS PharmSciTech.2010 Jun; 11(2) : 630-636
- [2] F.Siepmann, J.Siepmann, M. Walther .Polymer blends for Controlled Release Coatings.J control Release 2008 Jan 4; 125(1):1-15.
- [3] C- M Chan, J. Feng Mechanisms for viscosity reduction of polymer blends: Blends of fluoroelastomer and high-density polyethylene. Journal of Rheology .1997. 319-33 .
- [4] S.Gupta, N.Solanki and A.Serajuddin. Investigation of Thermal and Viscoelastic Properties of Polymers Relevant to Hot Melt Extrusion, IV: Affinisol™ HPMC HME Polymers. AAPS PharmSciTech. 2016 Feb; 17(1): 148–157.